

# UC Santa Barbara

## UC Santa Barbara Electronic Theses and Dissertations

### Title

Characterization of the Type VI Secretion System in Enterobacter cloacae

### Permalink

<https://escholarship.org/uc/item/1bd616wx>

### Author

Donato, Sonya Lisa

### Publication Date

2019

Peer reviewed|Thesis/dissertation

UNIVERSITY OF CALIFORNIA

Santa Barbara

Characterization of the Type VI Secretion System in *Enterobacter cloacae*

A dissertation submitted in partial satisfaction of the  
requirements for the degree Doctor of Philosophy  
in Molecular, Cellular, and Developmental Biology

by

Sonya Lisa Donato

Committee in charge:

Professor Christopher S. Hayes, Chair

Professor Emeritus Eduardo Orias

Professor David Low

Professor Kathleen Foltz

September 2019

The dissertation of Sonya Lisa Donato is approved.

---

Kathleen Foltz

---

David Low

---

Eduardo Orias

---

Christopher S. Hayes, Committee Chair

September 2019

Characterization of the Type VI Secretion System in *Enterobacter cloacae*

Copyright © 2019

by

Sonya Lisa Donato

## ACKNOWLEDGEMENTS

This dissertation would not be possible without a number of people supporting me in this endeavor. I must firstly thank Chris Hayes for being paramount to my success in grad school. It's hard to imagine what grad school would have been like in another lab, so I am incredibly grateful for getting the opportunity to work in his lab, where I was able to grow as both a scientist and a person. I am also grateful to have had an advisor that allows me enough guidance to not feel lost or directionless, while simultaneously giving me freedom to pursue my own experiments and grow confidence in my ability to work independently as a scientist. His intellect and enthusiasm for science sets a high bar for the rest of the lab to aspire to.

I must also thank our collaborators in other labs. David Low's enthusiasm and broad-picture thinking has often been a welcome counterpoint to Chris' more pointed perspectives. Zach Ruhe's technical expertise and scientific creativity has generally been relied upon by every member of the Hayes lab. Steve Poole, Rick Dahlquist, and Nick Bartelli have been welcome additions to group meetings, and I am grateful to have had their combined expertise and intelligence helping me with my research.

The Hayes lab is my work family, and I would be remiss were I to not thank all those who were down in the metaphorical scientific trenches with me. While everyone in the lab contributed to that sense of community, and I am therefore quite grateful for all of them, I want to specially thank Christina Beck and Julia Willett for mentoring me; they are both incredible scientists and gave me very concrete

examples of what grad student excellence looks like. Additionally, I need to thank my two undergraduate researchers, Ian Singleton and Jensen Abascal, who were both dedicated and hardworking individuals and gave a lot of their time to help me out, even with my bossy and strict tendencies. Their perseverance and dedication are greatly appreciated, which I never said to them often enough.

My other friends helped keep me sane during the mental marathon that is grad school, and I am so grateful for all of them and their support and commiseration over the years. And finally and most importantly, I must thank my family, whose support has always been unwavering. My success is entirely dependent on their encouragement and love.

Thank you all.

## VITA OF SONYA LISA DONATO

### Education

- 2012-Present: University of California, Santa Barbara  
Ph.D. student  
*Molecular, Cellular, and Developmental Biology*
- 2007-2011: University of California, San Diego  
*B.S., summa cum laude, Molecular Biology*

### Research Experience

- 2012 – Present: Ph.D. student; University of California, Santa Barbara  
Advisor: Christopher S. Hayes  
*Characterization of the Type VI Secretion System in Enterobacter cloacae*
- 2012: Research Technician at City of Hope, Duarte  
Supervisor: Susan Kane  
*PCR-genotyping of transgenic mice, analyzing t-Darpp expression in human breast tumor samples*
- 2011: Research Internship at City of Hope, Duarte.  
Supervisor: Susan Kane  
*PCR-genotyping of transgenic mice*

### Teaching Experience

- 2014-2018:  
(once per year) Teaching Assistant for Microbiology Lab  
*Led weekly laboratory instruction in common microbiology techniques. I also helped devise curriculum and wrote approximately half the student lab manual, including experimental designs and protocols, for 2017 and future terms.*
- 2014: Teaching Assistant for Eukaryotic Genetics  
*Led weekly discussion sections and helped students solve genetics problem sets.*
- 2012: Teaching Assistant for Introductory Biology Lab  
*Led weekly lab instruction in basic laboratory techniques.*

## **Laboratory Mentoring**

### Graduate Student Mentor (laboratory rotation projects)

Steven Jensen (Winter 2016), *Genetic screen for Rhs receptors in E. cloacae*

Shane Nourizadeh (Winter 2014), *Validation of putative T6SS effectors in E. cloacae*

### Undergraduate Student Mentor

Jensen Abascal (2015-2017), *Determination of the binding specificity of Hcp-linked effectors in E. cloacae*

Ian Singleton (2014-2015), *Characterization of E. cloacae's T6SS-1 locus*

## **Conference Presentations**

### Oral presentations

**Donato, S.L.** and Hayes, C.S. Molecular Genetics of Bacteria and Phages Meeting. *Forging the spike: how Rhs proteins help assemble the Type VI Secretion System nano-weapon in Enterobacter cloacae*, 2018.

**Donato, S.L.** and Hayes, C.S. West Coast Bacterial Physiologists Meeting. *The Enterobacter cloacae Type VI Secretion System (T6SS) requires Rhs*, 2014.

### Poster presentations

**Donato, S.L.** and Hayes, C.S. Molecular Genetics of Bacteria and Phages Meeting. *Rhs proteins aid in the assembly of the trimeric VgrG spike of the Type VI Secretion System in Enterobacter cloacae*, 2017.

**Donato, S.L.** and Hayes, C.S. Molecular Genetics of Bacteria and Phages Meeting. *Rhs proteins are a required component of Type VI Secretion System-1 (T6SS-1) in Enterobacter cloacae*, 2016.

**Donato, S.L.**, Beck C.M., and Hayes C.S. Molecular Genetics of Bacteria and Phages Meeting. *Characterization of type VI secretion system-1 (T6SS-1) in Enterobacter cloacae*, 2014.

## **Publications**

**Donato, S.L. et al.**, Rearrangement hotspot (Rhs) proteins stabilize trimeric VgrG and are required for type VI secretion system activity in *Enterobacter cloacae*. (In preparation)

## **Awards**

2018: Doreen J. Putrah Cancer Research Foundation Conference Fellowship  
(for conference travel)

2017: Academic Senate Doctoral Student Travel Grant (for conference travel)

2016: Ellen Schamberg Burley Award (for conference travel)

2016: Yzurdiaga Fellowship (for conference travel)

2014: Doreen J. Putrah Cancer Research Foundation Conference Fellowship  
(for conference travel)

2014: Jean Devlin Fellowship, awarded for excellent performance in the preliminary qualifying exam

2012: Wilcox Fellowship, Rathmann Fellowship; both awarded for outstanding academic record and personal interview during graduate school recruitment

## ABSTRACT

Characterization of the Type VI Secretion System in *Enterobacter cloacae*

by

Sonya Lisa Donato

Bacteria live in complex communities and must compete with their neighbors for resources. They have therefore evolved multiple different competition systems in order to improve their fitness in dense, complex environments. The type VI secretion system (T6SS) is a Gram-negative weapon used to inhibit the growth of neighboring cells. It does this by delivering toxic effector proteins directly into neighbors using a speargun-like apparatus. A spear-shaped protein complex is propelled out of the T6SS-expressing cell, and this spear punctures a neighboring cell to deliver its toxic payload. Toxic effector proteins are bound either covalently or non-covalently to this secreted complex, and these toxins can target both periplasmic or cytoplasmic substrates, as well as membranes. Kin protect themselves from these effectors by expressing cognate immunity proteins to block effector activity.

This thesis explores several aspects of the T6SS in *Enterobacter cloacae* ATCC 13047. In Chapter 1, I provide a general introduction to the T6SS and covers topics such as the structure and assembly of the apparatus, regulation of T6SS loci and effectors, and effector diversity. I then describe the genetics of the T6SS in *E. cloacae* and explore what effectors are deployed in this system in Chapter 2. In Chapter 3, I focus on one particular effector deployed by this system, the type VI secretion system lipase effector, Tle, and investigate its intriguing reliance on its cognate immunity protein, Tli, for toxicity. Next, Chapter 4 discusses the role of rearrangement hotspot

(Rhs) proteins in the assembly of the T6SS apparatus. Chapter 5 then looks at the role of the Rhs accessory protein effector-associated gene with Rhs (EagR). Finally, I summarize my findings and discuss open questions in the field in Chapter 6.

## TABLE OF CONTENTS

I. Introduction .....	1
A. Structure of the T6SS apparatus.....	2
B. Assembly and firing of the T6SS apparatus.....	3
C. T6SS effector activities.....	6
D. Mechanism of T6SS effector delivery.....	9
E. T6SS acquisition and modularity.....	11
F. T6SS regulation.....	14
G. Thesis overview.....	16
H. Figures.....	17
II. T6SS activity in <i>E. cloacae</i> is mediated by the T6SS-1 locus.....	19
A. Introduction.....	21
B. Results.....	22
C. Discussion.....	34
D. Materials and methods.....	38
E. Figures and tables.....	45
III. The effector Tle requires its cognate immunity for delivery in <i>E. cloacae</i> .....	73
A. Introduction.....	75
B. Results.....	76
C. Discussion.....	80
D. Materials and methods.....	82
E. Figures and tables.....	90

IV. Formation of the VgrG $\beta$ -spike is dependent on Rhs in <i>E. cloacae</i> .....	103
A. Introduction.....	105
B. Results.....	107
C. Discussion.....	116
D. Materials and methods.....	120
E. Figures and tables.....	128
V. EagR is required for Rhs-dependent T6SS activity but not for Rhs-CT processing.....	146
A. Introduction.....	147
B. Results.....	149
C. Discussion.....	155
D. Materials and methods.....	160
E. Figures and tables.....	168
VI. Concluding Remarks.....	185
References.....	197

## **Chapter 1: Introduction**

Bacteria are found in a variety of diverse habitats across the planet, and in many of these environmental niches resources are limited. As a consequence, bacteria have evolved a variety of competition systems used to inhibit the growth of other cells in order to acquire additional space or nutrients. One such competition system, found in Gram-negative bacteria, is the type VI secretion system (T6SS), discovered in *Vibrio cholerae* in 2006 (1, 2). The T6SS can be used for both intra- and inter-species competition against other Gram-negative cells or even eukaryotic organisms (2-6).

The dysbiosis, or imbalance of microorganisms, in human microbiomes has been implicated in wide-ranging human diseases such as obesity, chronic fatigue syndrome, inflammatory bowel disease, and even cancer (7-13). Therefore, a proper understanding of the bacterial interactions that take place in the human host has wide-ranging health implications. Moreover, the T6SS has been directly implicated in bacterial pathogenesis of humans and other vertebrates (14-20). Additionally, many phytobacteria possess T6SSs, and T6SS activity has been implicated in plant virulence for multiple plant pathogens (21-24). Therefore, a firm grasp of the molecular basis of the T6SS may inspire new treatment or preventative care approaches to animal or plant diseases.

This introduction will provide a review of the genetic and molecular basis of the T6SS across different Gram-negative species. First, I will discuss the structure and mechanism of the T6SS apparatus. Next, I review the kinds of protein cargo known to be secreted by this apparatus, as well as how these cargo are first loaded

onto the apparatus. I then explore the acquisition of T6SS loci and effector-immunity gene pairs, and discuss the modularity of T6SS factors. Finally, I discuss the known regulatory signals involved in T6SS activation or repression.

### *Structure of the T6SS apparatus*

The T6SS consists of a large, speargun-like apparatus that ejects protein toxins directly into neighboring cells. Understanding of this apparatus was developed via its structural and functional homology to contractile bacteriophage tails (4, 25, 26, 27). Thus far, 14 core components of the apparatus have been identified: nomenclature of these components can vary between research groups and the bacterial species under investigation, but a common naming scheme recognizes type VI secretion proteins A-M (TssA-M) as 13 of the core T6SS elements, as well as an additional 14<sup>th</sup> component, PAAR (proline-alanine-alanine-arginine), that is described as an essential component of the T6SS in at least some organisms (28, 29). Figure 1.1 presents a schematic summary of the T6SS apparatus.

The apparatus assembles at the cell membrane (Figure 1.1A) and is anchored to the membranes and cell wall through 3 proteins: TssJ, TssL, and TssM (30-35). Attached to this membrane anchor is an assembly platform, referred to as the baseplate complex, composed of 4 proteins: TssE, TssF, TssG, and TssK (36, 37). A contractile sheath, composed of TssB and TssC, is attached to this baseplate, and this sheath is capped by TssA (39, 40, 41, 43). The TssEFGK baseplate complex is thought to coordinate the contraction of the TssBC sheath (42; Zachary Ruhe, Hayes lab, unpublished). The sheath surrounds a hollow filament composed of TssD, which

is more commonly referred to as hemolysin-coregulated protein (Hcp). Hcp forms hexameric rings that stack to form a long, hollow tube (25, 43, 44, 45). The Hcp tube connects to the membrane-puncturing spike complex, composed of TssI and PAAR. TssI is more commonly referred to as valine-glycine repeat protein G (VgrG). VgrG forms a trimer that binds a single PAAR polypeptide, and together this tube and spike complex makes up the secreted “spear” complex that is propelled out of the cell following contraction of the sheath (Figure 1.1B) (25, 28). Finally, the ATPase TssH, more commonly referred to as caseino-lytic protease (virulent strain) (ClpV), disassembles the TssBC sheath after use in order to allow for successive assembly of a new apparatus using recycled components (46, 47). It is worth noting that ClpV is not absolutely required for T6SS activity if there is sufficient cell growth and de novo synthesis of sheath components (48, 49).

### *Assembly and firing of the T6SS apparatus*

The order of assembly of the T6SS apparatus (Figure 1.1A) can be broadly inferred from protein-protein interaction data and live-imaging microscopy. First, the membrane-spanning complex, composed of TssJLM, assembles at the membrane. TssJ seeds formation of the membrane-complex at the outer-membrane, sequentially recruiting TssM and TssL into the eventual 1.7-megadalton complex that has five-fold symmetry of each of its 3 components (51). TssM extends into the periplasm and binds both TssJ and the peptidoglycan cell wall to anchor this complex to the membrane (52). TssL spans the inner-membrane, but the bulk of the protein resides in the cytoplasm; TssL may be involved in both stabilization of the

membrane-spanning complex, as well as subsequent apparatus assembly in the cytoplasm (53-55).

Following assembly of the membrane-spanning complex, the baseplate complex must next assemble and properly dock onto the membrane complex (Figure 1.1A). Brunet *et. al.* have prepared the most comprehensive analysis of T6SS apparatus assembly (36). They demonstrate that the baseplate components TssF and TssG interact and stabilize each other in the absence of other T6SS factors, suggesting baseplate assembly can initiate independent of the rest of the apparatus. Subsequently, the baseplate appears to be recruited to the cell envelope via association with TssM. Hcp assembly is dependent on formation of the baseplate and VgrG-spike complex, and sheath assembly is dependent on Hcp assembly.

Thus, Brunet *et. al.* propose that the membrane-spanning complex initiates T6SS assembly, and subsequently recruits and promotes full baseplate assembly. The partial baseplate complex TssFG can be seeded in the cell cytoplasm, and is then recruited to the membrane-spanning complex, likely through contacts between TssK and TssM. Once the full baseplate has docked onto the membrane-complex, polymerization of the Hcp tube and subsequent TssBC sheath polymerization around Hcp can occur. Figure 1.1A presents this model of the assembly of the T6SS apparatus. At this time it is unclear when the VgrG-PAAR spike complex assembles onto the apparatus: does it assemble before, concomitant with, or after baseplate assembly? This thesis seeks to give insight on that question in Chapter 4.

The TssBC sheath polymerizes in about one minute to a length spanning approximately the full width of the cell (39, 48). The sheath will then contract, where

rings of sheath proteins sequentially rotate to form a wider, more compact structure that spans roughly half of its original length (48). This contraction, or firing event, is believed to occur in less than 5 ms (48). Subsequently, ClpV-dependent sheath disassembly is thought to take 10s of seconds (39, 48). This T6SS duty-cycle is presented in Figure 1.1B.

Basler (50) calculates that the amount of energy released during T6SS contraction could be approximately 18,000 kcal mol<sup>-1</sup>, or the equivalent of 1,600 molecules of ATP hydrolyzed. This amount of energy is thought to be enough to physically puncture the target cell membrane in the absence of any specific lipid-disrupting structure, allowing for fewer evolutionary constraints on the structure of these translocated proteins. There is currently no evidence that the T6SS-dependent puncturing of cell membranes induces cell toxicity independent from effector activity (50). This is in contrast to R-type pyocins, which puncture the bacterial cell via another contractile injection system, but leaves a stable tube inserted in the cell membrane that allows for ion leakage and eventual cell death (78-80).

There is some contention about whether the T6SS apparatus can puncture all the way through to the Gram-negative bacterial cytoplasm, or whether effectors are only delivered into the periplasm. Reports studying the T6SS in *V. cholerae* suggest that the VgrG-PAAR spike complex does get delivered into the target cell cytoplasm, and that periplasmic-acting effectors can encode periplasmic-trafficking-signals to facilitate transport back to the periplasm (76, 77). However, the majority of T6SS toxins appear to be periplasmic-acting, not cytoplasmic-acting, (see next section, entitled “T6SS effector activities”), and heterologous expression of many of these

periplasmic-acting T6SS toxins in laboratory *Escherichia coli* requires the addition of a periplasmic-trafficking sequence for intoxication, suggesting they must be delivered directly to the periplasm in order for activity to occur (59, 65, 87). Additionally, the majority of identified cytoplasmic-acting toxins have putative N-terminal transmembrane domains that may be present to facilitate translocation from the target cell periplasm across the inner-membrane (67, 69, 71, 73, 74). Finally, it has been demonstrated that T4 bacteriophage contractile tails do not penetrate through the inner-membrane (181). Taken together, the preferred model of T6SS delivery is that it does not pierce through to the cytoplasm.

#### *T6SS effector activities*

There are a variety of cargo proteins secreted by the T6SS. While the majority of identified cargo function as effectors to induce toxicity in target cells, some bacteria use the T6SS to secrete metal-acquisition proteins in order to promote metal uptake (56-58). However, this appears to be a more recent evolutionary function of this secretion system; it is largely accepted that the T6SS evolved to deliver toxic effectors into target cells. The first T6SS effector discovered cross-links actin in eukaryotic targets to impair the cell's cytoskeleton (3, 4). Since then, other families of anti-eukaryotic factors have been discovered (52, 53, 141). However, the focus of this thesis is on anti-bacterial toxins. These anti-bacterial toxins are consistently found encoded in effector-immunity gene pairs, where the downstream-encoded immunity protein blocks the activity of the toxin.

The first inter-bacterial toxin discovered degrades the Gram-negative bacterial cell wall (59). Following that discovery, many other cell-wall degrading enzymes have been identified as toxic T6SS effectors (60-62). Of particular relevance to my thesis work, the T6SS amidase effector (Tae) in *Enterobacter cloacae* is described as a toxic effector in Chapter 2, and is predicted to hydrolyze cell-wall peptide crosslinks at  $\gamma$ -D-glutamyl-*m*DAP DL-bonds (60).

Additionally, many membrane-disrupting effectors have been identified. A diverse group of T6SS (phospho)lipase effector (Tle) proteins have been reported, and have varying catalytic activities (63-65). Chapter 3 will focus on one such Tle effector found in *E. cloacae*, and explores its unique reliance on its cognate immunity for proper activation and delivery. Intriguingly, because phospholipid bilayers are a shared hallmark of both bacterial and eukaryotic membranes, these Tle toxins can be used to inhibit both bacterial and eukaryotic targets (65). Effectors with membrane pore-forming-activity have also been reported, whose activities result in increased cell permeability and dissipation of the proton-motive force (66). In Chapter 2 I discuss one such putative pore-forming effector in *E. cloacae*, named T6SS effector protein 1 (Tep1).

A variety of T6SS effectors target nucleic acids. For example, T6SS-dependent DNases have been discovered in *Dickeya dadantii*, *Agrobacterium tumefaciens*, *Serratia marcescens*, Shiga toxin-producing *E. coli*, and *Pseudomonas aeruginosa* (67, 68, 69, 95, 186). Additionally, *P. aeruginosa* type VI secretion effector 2 (Tse2) is predicted to have RNase activity (70). *E. cloacae*'s RhsB has also been shown to

have DNase activity (71). A T6SS nuclease used to inhibit eukaryotic cells has not been discovered to date, although the possibility does exist.

Notably, the majority of these confirmed DNases are all encoded in Rhs proteins (67, 69, 71). It is currently unclear if Rhs proteins do indeed have a propensity for encoding nucleases over other toxins, and what the biological significance of such a correlation would be. Interestingly, Rhs proteins are predicted to form a hollow, shell-like structure that encapsulates the toxin domain (72). Rhs proteins may therefore represent a specialized translocation system for nucleases or other cytoplasmic-acting effectors. The role of *E. cloacae*'s Rhs proteins in the T6SS is the central theme of Chapter 4.

More recently, the Mougous lab has identified 2 novel T6SS anti-bacterial effector activities. In 2015, they published that *P. aeruginosa*'s Tse6 is an NAD(P)<sup>+</sup> glycohydrolase that breaks down the essential metabolite NAD(P)<sup>+</sup> into nicotinamide and ADP-ribose (73). NAD(P)<sup>+</sup> is an essential metabolite across all forms of life, so it remains to be seen whether any bacteria deploy a similar T6SS effector to intoxicate eukaryotes or even archaea. Additionally, their lab published in 2018 that *Serratia proteamaculans* deploys an ADP-ribosylating toxin that modifies the essential bacterial cell-division protein FtsZ (74). FtsZ is also found in chloroplasts, mitochondria, and archaea, and may represent another substrate that could be targeted by T6SS effectors in order to theoretically inhibit a broad range of organisms.

However, many T6SS-dependent effectors have unknown functions with no readily predictable activities. Of note, *E. cloacae*'s RhsA effector, discussed at length

in Chapters 4 and 5, has no known function (71, 81). This implies the diversity of T6SS effectors has not yet been fully realized, and suggests novel cellular substrates exist.

### *Mechanism of T6SS effector delivery*

In the previous section, T6SS effectors were grouped together based on their activities. However, these effectors can also be categorized based on their mechanism of assembly onto the T6SS apparatus. The first T6SS effector discovered is encoded at the C-terminal end of VgrG (4). Since that discovery, numerous other VgrG-fusion effectors have been characterized (62, 64, 82, 83). These so-called “evolved” VgrGs represent a class of effectors where the toxin is covalently linked to a structural component of the secretion complex. Similarly, “evolved” Hcp and PAAR proteins also exist (28, 69, 81, 84, 85, 86, 93, 186). *E. cloacae*’s RhsA and RhsB effectors, explored in Chapters 4 and 5 of this thesis, both encode PAAR domains, for example. Given that these structural components are required for the T6SS, this category of covalently-linked effectors may represent a mechanism to prevent wasteful secretion of assemblies lacking effectors.

In addition to covalently-linked effectors, many effectors have been shown to interact with the Hcp or VgrG structural components directly. For example, some effectors have been shown to bind directly to VgrG (64, 87). Curiously, one example of this interaction involves the effector binding to the C-terminal transthyretin-like (TTR) extension domain of VgrG (87). This is an example of an “evolved” VgrG that encodes an adaptor domain, rather than an effector domain. Similarly, many PAAR

proteins have been bio-informatically identified that possess this TTR adaptor domain (28). Other effectors have been shown to directly interact with Hcp instead (19, 88). Notably, Hcp forms a hollow tube, and effectors have been shown to situate within the lumen of this tube (88). In Chapter 2, I describe experiments that reveal *E. cloacae*'s Tae protein interacts directly with Hcp.

Other effectors are known to interact indirectly with VgrG. For example, *V. cholerae*'s lipase effector TseL uses its upstream accessory gene as an adaptor to mediate the interaction between TseL and VgrG; this phenomenon appears to be a genetically conserved mechanism that is distributed throughout Proteobacteria (89, 90). Another example of an adaptor-dependent toxin assembly is the *A. tumefaciens* DNase toxin Tde1, which uses a different adaptor to bind to VgrG (97). In many cases, while an effector interaction to VgrG has not yet been experimentally demonstrated, the interaction can be inferred through genetic interactions. For example, some effectors have a genetic dependency on a specific VgrG paralog for secretion, suggesting a molecular interaction between effector and VgrG (81, 86). There also appears to be a strong genetic association with Tle effectors and VgrG, again suggesting some molecular interaction between Tle and VgrG (63). Chapter 3 addresses this point with *E. cloacae*'s Tle protein. The N-terminal domain of the VgrG trimer forms a hollow cup that is wide enough to accommodate small proteins; it is therefore plausible that Tle and other small effectors could be loaded onto the N-terminus of VgrG (92).

While the majority of cytoplasmic-acting T6SS effectors with confirmed substrates are covalently linked to a PAAR domain, the known exceptions are the 2

DNases in *A. tumefaciens*, which are genetically linked to VgrG, and the DNase in STEC004 *E. coli*, which is covalently linked to Hcp (68, 95). As discussed previously, cytoplasmic-acting toxins may require additional translocation mechanisms to get past the target cell inner-membrane; it may therefore be significant that the majority of these cytoplasmic-acting toxins are loaded onto the VgrG-PAAR membrane-puncturing spike complex. For example, it is possible that the association with the spike complex promotes effector delivery as proximal to the inner-membrane as possible.

While the unadorned spike complex forms a sharp tip that is thought to promote membrane puncturing, this is seemingly contradicted by the fact that many effectors are predicted to simply hang off the sharp PAAR tip (28). Indeed, Rhs proteins, which often encode PAAR domains, form structures around ~4 nm wide, which is approximately half the width of the Hcp tube itself (1, 72). It is currently unclear where these VgrG-encoding or PAAR-encoding effectors sit on or in the apparatus during either assembly or delivery.

### *T6SS acquisition and modularity*

Given the diversity of effector assembly onto the T6SS apparatus, it appears as though bacteria can deploy an arsenal of multiple toxins in a single T6SS firing event. Given that most of the T6SS-expressing strains studied encode multiple effectors, this brings into question how and why these bacteria evolved multiple effectors. In many cases, horizontal gene transfer appears to facilitate effector acquisition. For example, highly related effector-immunity gene pairs can appear

across different species and genera while “skipping” more closely-related kin (60, 63, 98). More directly, some T6SS effector-immunity modules are encoded on known horizontally-transferred genomic islands (99, 100). A recent report suggests *V. cholerae* will replace old effectors with new, horizontally-transferred, effector-immunity gene pairs while retaining the old immunity, allowing the recombinant strain to deploy new toxins while maintaining immunity against its old toxins (101). There is even evidence that entire T6SS loci can be acquired via horizontal gene transfer (102, 103). This is perhaps not surprising in light of the fact that many bacteria carry multiple T6SS loci, with the highest known number being 6 T6SS loci in *Yersinia pestis* and *Burkholderia pseudomallei* (21).

In addition to acquiring complete genes via horizontal gene transfer, T6SS effectors can also be internally diversified via more modular mechanisms. For example, the covalently-linked effectors, described in the previous section of this chapter, represent examples of polymorphic toxins, where the N-terminal structural domain (*e. g.* PAAR) often stays conserved while the C-terminal toxin domain is variable. In other words, nature has evolved examples of modular effector swapping between these “evolved” structural proteins. One example of this is with *E. cloacae*’s RhsA protein, which shares strong sequence identity with Rhs proteins from other genera, but which encodes a different C-terminal toxin domain compared to related Rhs alleles (Figure 1.2). Chapter 5 addresses the results of engineering different Rhs toxins onto *E. cloacae*’s RhsA in order to create viable chimeric proteins. An engineered chimeric VgrG has also been shown to successfully intoxicate its parental strain by replacing the original effector domain with one from a different species (77).

Additionally, many of these “evolved” structural proteins have associated orphan effector-immunity pairs, encoded downstream of the full-length gene, which are believed to be capable of recombining onto the full-length gene in order to deploy different effectors (93-95). In a broader context, some T6SS toxins are closely related to toxins deployed via other growth inhibition systems, such as CDI or colicins (93, 95, 96, Figure 5.8B). Therefore, many T6SS toxins can be interchanged between different T6SS structural components, and can even be interchanged by different toxin translocation systems entirely.

Another means of diversifying the T6SS is through the use of redundant components to make new combinations of pre-existing factors. For example, many bacteria encode multiple Hcp, VgrG, or PAAR alleles, even though only one of each is required for T6SS activity. While these paralogs are often redundant for supporting T6SS activity, they frequently represent distinct effector export pathways. For example, *A. tumefaciens* can use either VgrG1 or VgrG2 for T6SS activity, but secretion of its DNase effectors Tde1 or Tde2 is dependent on their specific cognate VgrG (97). A similar story occurs with *P. aeruginosa*'s Tse5 and Tse6 effectors, and with *E. cloacae*'s RhsA and RhsB effectors (81). Notably, *E. cloacae*'s RhsA and RhsB proteins also encode PAAR, and either can support T6SS activity if its cognate VgrG is also expressed (Chapter 4). *S. marcescens* uses 2 different VgrGs and 3 different PAARs for T6SS activity; while only one of each is sufficient for T6SS activity, PAAR1 specifically utilizes VgrG1, whereas both PAAR-encoding Rhs1 and Rhs2 must utilize VgrG2 (29). Altogether, this shows that while there is a common theme of bacteria expressing redundant T6SS factors, these bacteria will utilize their different T6SS assemblies to specify which toxins get secreted. While the experiments described

above were performed under laboratory conditions, it is important to remember that bacteria might regulate expression of these different assemblies under different growth conditions in order to control which effectors are secreted at a given time in natural environments.

### *T6SS regulation*

The T6SS is prevalent across diverse Gram-negative bacteria, and as such, the regulatory mechanisms governing T6SS expression can vary widely between species and strains. Many bacteria will respond to environmental cues in order to transcriptionally control T6SS gene expression. For example, pathogens that utilize the T6SS against eukaryotic cells have been observed to upregulate T6SS expression when provided with signals promoting infection of a host. These signals include quorum-sensing cell density signals, iron limitation, phagocytosis, and other signals of host contact (38, 75, 91, 104-109). Other external signals, not necessarily related to eukaryotic infection, include biofilm development and changes in temperature, pH, or salinity (110-114).

The molecular mechanism of T6SS regulation has arguably been most comprehensively studied in *P. aeruginosa*'s bacterial-targeting H1-T6SS locus. Interestingly, this locus is stringently controlled through 2 layers of regulation. One layer involves the Gac/Rsm pathway, where the sensor kinase RetS represses the Gac/Rsm pathway and therefore H1-T6SS expression (1, 115, 116). *P. aeruginosa* *retS* mutants therefore have upregulated T6SS activity and have been commonly used as a model system to study the T6SS. The Gac/Rsm pathway is a global regulatory pathway that is known to induce expression of antibiotics and virulence

factors (117, 118). This pathway has recently been described as a danger-sensing pathway in *P. aeruginosa*, as it is activated by the lysis of neighboring *P. aeruginosa* cells in order to turn on these various offensive systems, including the T6SS (119).

A second layer of regulation involves the post-translational threonine phosphorylation pathway (TPP), in which the H1-T6SS-encoded kinase PpkA and phosphatase PppA oppose each other to differentially activate or inactivate the T6SS scaffolding protein Fha (120). TPP regulation controls rapid changes to protein localization and induces T6SS apparatus assembly, and appears to allow cells to spatially control T6SS firing (121). Membrane perturbation has been proposed as a trigger for TPP activation due to the intriguing observation that *P. aeruginosa* appears to deploy its T6SS as a counter-attack against inter-bacterial T6SS activity or even conjugation (47, 121, 122). However, those studies were carried out in a *retS* mutant background, and a counter-argument has more recently been proposed that this counter-attack phenomenon, also called T6SS dueling, is dependent on the Gac/Rsm pathway, rather than TPP-dependent activation of H1-T6SS (119). As such, the trigger for TPP is currently unclear.

A number of bacteria do not appear to need any activating signal in order for T6SS activity to occur. Many strains have been shown to utilize constitutively active T6SSs when grown under typical laboratory conditions, including the *E. cloacae* strain under investigation in this thesis (2, 16, 19, 81, 109, 123-125). There is a current trend in the literature that these organisms with constitutively active T6SSs inhibit other bacteria, rather than eukaryotes (126). However, the evolutionary and ecological implications governing regulated versus constitutive T6SS loci have yet to be properly explored.

## *Thesis overview*

The type VI secretion system is a widespread bacterial growth-inhibition system, but most of the seminal work describing this system has been performed in *Pseudomonas aeruginosa* and *Vibrio cholerae*. This thesis seeks to introduce *Enterobacter cloacae* (ECL) as a new model organism in which to study the T6SS. Chapter 2 introduces basic information about the 2 T6SS loci in ECL and the 4 known effectors it deploys, then explores other T6SS-associated effectors not deployed by ECL under laboratory conditions. Additionally, Chapter 2 seeks to investigate why ECL encodes 2 T6SS loci but 5 separate *hcp* alleles. Chapter 3 discusses a collaborative work-in-progress project regarding ECL's lipase toxin. This toxin is unique in that delivery of this toxic effector requires its downstream immunity protein. This is the first known example of a bacterial effector that requires its immunity for activation. In Chapter 4, I explore the impact of Rhs proteins on ECL's T6SS. Notably, I find Rhs is required for T6SS activity in ECL because it stabilizes the  $\beta$ -spike of trimeric VgrG. Moreover, our findings suggest Rhs promotes VgrG trimerization prior to docking with the T6SS baseplate. Chapter 5 next addresses the role of the Rhs chaperone protein, effector-associated gene with Rhs (EagR). I show that EagR is required for Rhs and T6SS activity in ECL. Furthermore, Chapter 5 explores the proteolytic cleavage event of the polymorphic RhsA toxin and its subsequent retention within the Rhs  $\beta$ -encapsulation structure. Finally, Chapter 6 concludes with a summary of my findings and a review of some of the remaining questions left in the field.

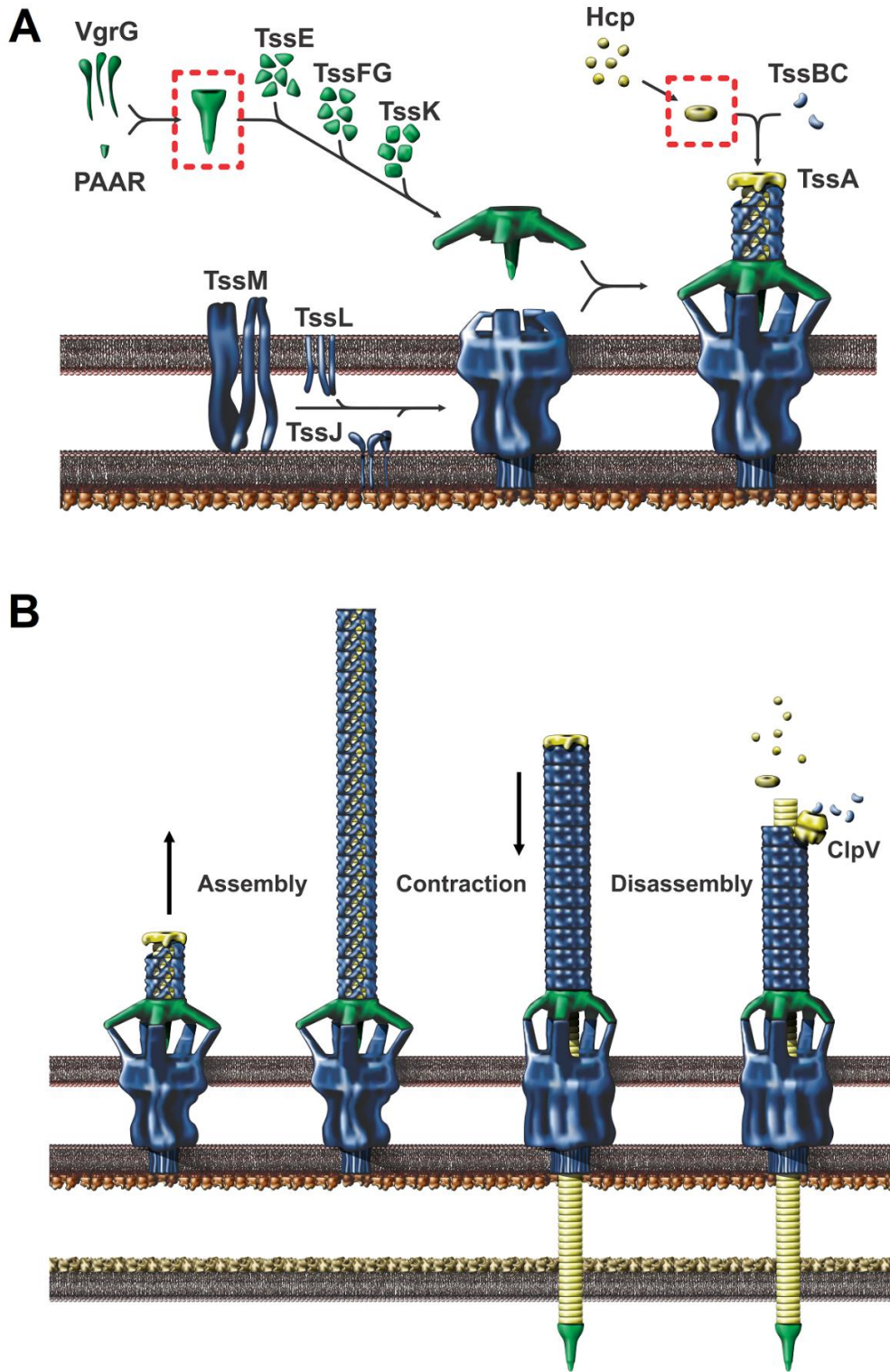


**Figure 1.1. Schematic of the type VI secretion system (T6SS).** (A) Schematic of the T6SS apparatus assembly. Boxed components represent the protein factors secreted by the apparatus. (B) Schematic of the T6SS duty-cycle. Figures are reproduced with permission from Zachary Ruhe (unpublished).

```

ECL_01567 1 MSDNNAARQDEIITHSSIFADITSIVAEQAAAYVIGAAVLAATAAABLIGAGAAAAGVA
A3780_13225 1 MSKQAAARQDEIITHSSIFADITSIVAEQAAAYVIGAAVLAATAAABLIGAGAAAAGVA
B1H58_04015 1 MSDNNAARQDEIITHSSIFADITSIVAEQAAAYVIGAAVLAATAAABLIGAGAAAAGVA
CTU_00940 1 -----TDDISNMFQCGHAFPPSPAGKLTGSSNVLNLSLPA

ECL_01567 61 AVGSSCLLSGIIIGGLANVAGITDDISNAANTGCAFPSPAGKLTGSSNVLNLSLPA
A3780_13225 61 AVGSSCLLSGIIIGGLANVAGITDDISNAANTGCAFPSPAGKLTGSSNVLNLSLPA
B1H58_04015 61 AVGSSCLLSGIIIGGLANVAGITDDISNAANTGCAFPSPAGKLTGSSNVLNLSLPA
CTU_00940 1 -----TDDISNMFQCGHAFPPSPAGKLTGSSNVLNLSLPA

ECL_01567 121 ARAAGTITATDTPPEFPOSFADYHGMLLSAAQFGSEMNOPTVAAAGSPLDEEK
A3780_13225 121 ARAAGTITATDTPPEFPOSFADYHGMLLSAAQFGSEMNOPTVAAAGSPLDEEK
B1H58_04015 121 ARAAGTITATDTPPEFPOSFADYHGMLLSAAQFGSEMNOPTVAAAGSPLDEEK
CTU_00940 40 ARAAGTITATDTPPEFPOSFADYHGMLLSAAQFGSEMNOPTVAAAGSPLDEEK

ECL_01567 181 VACDKHSGFOYLAEGSKSVFINGQPAVRARDKTTCETVSDVSENVLIIGETLIVRDIK
A3780_13225 181 VACDKHSGFOYLAEGSKSVFINGQPAVRARDKTTCETVSDVSENVLIIGETLIVRDIK
B1H58_04015 181 VACDKHSGFOYLAEGSKSVFINGQPAVRARDKTTCETVSDVSENVLIIGETLIVRDIK
CTU_00940 100 VACDKHSGFOYLAEGSKSVFINGQPAVRARDKTTCETVSDVSENVLIIGETLIVRDIK

ECL_01567 241 SGKTLGLAVAMIALSLIRGPRGKILKMPICALAAAGGMLADMAVNAVFPSSHPVHAATG
A3780_13225 241 SGKTLGLAVAMIALSLIRGPRGKILKMPICALAAAGGMLADMAVNAVFPSSHPVHAATG
B1H58_04015 241 SGKTLGLAVAMIALSLIRGPRGKILKMPICALAAAGGMLADMAVNAVFPSSHPVHAATG
CTU_00940 160 SGKTLGLAVAMIALSLIRGPRGKILKMPICALAAAGGMLADMAVNAVFPSSHPVHAATG

ECL_01567 301 VKVLNDNELDFSLPGRFPLRWORSYNSLITREGFLGWAIFDSYLTLEENNAWFDE
A3780_13225 301 VKVLNDNELDFSLPGRFPLRWORSYNSLITREGFLGWAIFDSYLTLEENNAWFDE
B1H58_04015 301 VKVLNDNELDFSLPGRFPLRWORSYNSLITREGFLGWAIFDSYLTLEENNAWFDE
CTU_00940 220 VKVLNDNELDFSLPGRFPLRWORSYNSLITREGFLGWAIFDSYLTLEENNAWFDE

ECL_01567 361 TGRELRTLPFPPVDAAGVYSISEGITVRRNESGDVALDDDDGAVWRLEKFRANPSVLRLAS
A3780_13225 361 TGRELRTLPFPPVDAAGVYSISEGITVRRNESGDVALDDDDGAVWRLEKFRANPSVLRLAS
B1H58_04015 361 TGRELRTLPFPPVDAAGVYSISEGITVRRNESGDVALDDDDGAVWRLEKFRANPSVLRLAS
CTU_00940 280 TGRELRTLPFPPVDAAGVYSISEGITVRRNESGDVALDDDDGAVWRLEKFRANPSVLRLAS

ECL_01567 421 LSEYGNALTEGWDEHGRVLRHDPFAIDVTIYFEDERFPPQVTSASHFDGSRWELMT
A3780_13225 421 LSEYGNALTEGWDEHGRVLRHDPFAIDVTIYFEDERFPPQVTSASHFDGSRWELMT
B1H58_04015 421 LSEYGNALTEGWDEHGRVLRHDPFAIDVTIYFEDERFPPQVTSASHFDGSRWELMT
CTU_00940 340 LSEYGNALTEGWDEHGRVLRHDPFAIDVTIYFEDERFPPQVTSASHFDGSRWELMT

ECL_01567 481 WVDARGOIAASADAEQVVTREYRNYGLMWHRLGGLESEYRWKFDHWRVVENRIS
A3780_13225 481 WVDARGOIAASADAEQVVTREYRNYGLMWHRLGGLESEYRWKFDHWRVVENRIS
B1H58_04015 481 WVDARGOIAASADAEQVVTREYRNYGLMWHRLGGLESEYRWKFDHWRVVENRIS
CTU_00940 400 WVDARGOIAASADAEQVVTREYRNYGLMWHRLGGLESEYRWKFDHWRVVENRIS

ECL_01567 541 TGDGCRFTYDLAGLITVEHYDQTRQHYWNAQGLIYRFVDERGENWRYENDELTIR
A3780_13225 541 TGDGCRFTYDLAGLITVEHYDQTRQHYWNAQGLIYRFVDERGENWRYENDELTIR
B1H58_04015 541 TGDGCRFTYDLAGLITVEHYDQTRQHYWNAQGLIYRFVDERGENWRYENDELTIR
CTU_00940 460 TGDGCRFTYDLAGLITVEHYDQTRQHYWNAQGLIYRFVDERGENWRYENDELTIR

ECL_01567 601 IDPLGNVTFVYDIMGNRVQETDAGNRPQWLEHRLPAITAEADGATTFYDDEHG
A3780_13225 601 IDPLGNVTFVYDIMGNRVQETDAGNRPQWLEHRLPAITAEADGATTFYDDEHG
B1H58_04015 601 IDPLGNVTFVYDIMGNRVQETDAGNRPQWLEHRLPAITAEADGATTFYDDEHG
CTU_00940 520 IDPLGNVTFVYDIMGNRVQETDAGNRPQWLEHRLPAITAEADGATTFYDDEHG

ECL_01567 661 LKRVYDLAGLITVEHYDQTRQHYWNAQGLIYRFVDERGENWRYENDELTIR
A3780_13225 661 LKRVYDLAGLITVEHYDQTRQHYWNAQGLIYRFVDERGENWRYENDELTIR
B1H58_04015 661 LKRVYDLAGLITVEHYDQTRQHYWNAQGLIYRFVDERGENWRYENDELTIR
CTU_00940 580 LKRVYDLAGLITVEHYDQTRQHYWNAQGLIYRFVDERGENWRYENDELTIR

ECL_01567 721 LGWLVTFVYDIMGNRVQETDAGNRPQWLEHRLPAITAEADGATTFYDDEHG
A3780_13225 721 LGWLVTFVYDIMGNRVQETDAGNRPQWLEHRLPAITAEADGATTFYDDEHG
B1H58_04015 721 LGWLVTFVYDIMGNRVQETDAGNRPQWLEHRLPAITAEADGATTFYDDEHG
CTU_00940 640 LGWLVTFVYDIMGNRVQETDAGNRPQWLEHRLPAITAEADGATTFYDDEHG

ECL_01567 781 YDAAGRLVTRNSMGEVRRRSDRSRGLIALNENGEAYFRWGDSSLLEEFGLDGVAS
A3780_13225 781 YDAAGRLVTRNSMGEVRRRSDRSRGLIALNENGEAYFRWGDSSLLEEFGLDGVAS
B1H58_04015 781 YDAAGRLVTRNSMGEVRRRSDRSRGLIALNENGEAYFRWGDSSLLEEFGLDGVAS
CTU_00940 700 YDAAGRLVTRNSMGEVRRRSDRSRGLIALNENGEAYFRWGDSSLLEEFGLDGVAS

ECL_01567 841 RYGYDACGRTIISRTFAAGHEPAITHTFWSAAGQLARTTPEGGTRHRYTSPGTRHRL
A3780_13225 841 RYGYDACGRTIISRTFAAGHEPAITHTFWSAAGQLARTTPEGGTRHRYTSPGTRHRL
B1H58_04015 841 RYGYDACGRTIISRTFAAGHEPAITHTFWSAAGQLARTTPEGGTRHRYTSPGTRHRL
CTU_00940 760 RYGYDACGRTIISRTFAAGHEPAITHTFWSAAGQLARTTPEGGTRHRYTSPGTRHRL

ECL_01567 901 PPLSADAVSFAEQELFEYDALGRVTEGEGNGALGWYDALGNRTSVLPDGRKLC
A3780_13225 901 PPLSADAVSFAEQELFEYDALGRVTEGEGNGALGWYDALGNRTSVLPDGRKLC
B1H58_04015 901 PPLSADAVSFAEQELFEYDALGRVTEGEGNGALGWYDALGNRTSVLPDGRKLC
CTU_00940 820 PPLSADAVSFAEQELFEYDALGRVTEGEGNGALGWYDALGNRTSVLPDGRKLC

ECL_01567 961 LYVYSGHLLSIALNLFVSDFTDELHRESRTOGLLITRSEYDRGLRHRDVFETGNAQ
A3780_13225 961 LYVYSGHLLSIALNLFVSDFTDELHRESRTOGLLITRSEYDRGLRHRDVFETGNAQ
B1H58_04015 961 LYVYSGHLLSIALNLFVSDFTDELHRESRTOGLLITRSEYDRGLRHRDVFETGNAQ
CTU_00940 880 LYVYSGHLLSIALNLFVSDFTDELHRESRTOGLLITRSEYDRGLRHRDVFETGNAQ

ECL_01567 1021 RPSRWSRWDYDYNRLREERDDNPFVYRWYDYSAGRLITQDGLPQEQWRWDA
A3780_13225 1021 RPSRWSRWDYDYNRLREERDDNPFVYRWYDYSAGRLITQDGLPQEQWRWDA
B1H58_04015 1021 RPSRWSRWDYDYNRLREERDDNPFVYRWYDYSAGRLITQDGLPQEQWRWDA
CTU_00940 940 RPSRWSRWDYDYNRLREERDDNPFVYRWYDYSAGRLITQDGLPQEQWRWDA

ECL_01567 1081 GNELDSAP-KIHNRLTOLNGIRWYDGHGRTVEKMGOTRWRYDGEHRLTEVISQF
A3780_13225 1081 GNELDSAP-KIHNRLTOLNGIRWYDGHGRTVEKMGOTRWRYDGEHRLTEVISQF
B1H58_04015 1079 GNELDSAP-KIHNRLTOLNGIRWYDGHGRTVEKMGOTRWRYDGEHRLTEVISQF
CTU_00940 1000 GNELDSAP-KIHNRLTOLNGIRWYDGHGRTVEKMGOTRWRYDGEHRLTEVISQF

ECL_01567 1140 RDRNKPQVYSFRYDPLGRISRTKRLGAGQPTKAVITRFRVWGRFLLQIHDVPLT
A3780_13225 1140 RDRNKPQVYSFRYDPLGRISRTKRLGAGQPTKAVITRFRVWGRFLLQIHDVPLT
B1H58_04015 1138 RDRNKPQVYSFRYDPLGRISRTKRLGAGQPTKAVITRFRVWGRFLLQIHDVPLT
CTU_00940 1060 RDRNKPQVYSFRYDPLGRISRTKRLGAGQPTKAVITRFRVWGRFLLQIHDVPLT

ECL_01567 1200 VVYSDQSYFLARIDGQAPETIYWFQDNGTPERLIDAEGEREONSANGKLLRE
A3780_13225 1200 VVYSDQSYFLARIDGQAPETIYWFQDNGTPERLIDAEGEREONSANGKLLRE
B1H58_04015 1198 VVYSDQSYFLARIDGQAPETIYWFQDNGTPERLIDAEGEREONSANGKLLRE
CTU_00940 1120 VVYSDQSYFLARIDGQAPETIYWFQDNGTPERLIDAEGEREONSANGKLLRE

ECL_01567 1260 FTLGSGVGNLRMQGYLDRRETGLHYNLFRVYDPCGRFTQDDPIGLAGINLYOYAPNA
A3780_13225 1261 FTLGSGVGNLRMQGYLDRRETGLHYNLFRVYDPCGRFTQDDPIGLAGINLYOYAPNA
B1H58_04015 1258 FTLGSGVGNLRMQGYLDRRETGLHYNLFRVYDPCGRFTQDDPIGLAGINLYOYAPNA
CTU_00940 1180 FTLGSGVGNLRMQGYLDRRETGLHYNLFRVYDPCGRFTQDDPIGLAGINLYOYAPNA

ECL_01567 1320 LTRNDLGLKQEEVIYMRKDEAASAAEAGS-----GSG-----LYPNRQD
A3780_13225 1321 LTRNDLGLKQEEVIYMRKDEAASAAEAGS-----GSG-----LYPNRQD
B1H58_04015 1318 LTRNDLGLKQEEVIYMRKDEAASAAEAGS-----GSG-----LYPNRQD
CTU_00940 1240 LTRNDLGLKQEEVIYMRKDEAASAAEAGS-----GSG-----LYPNRQD

ECL_01567 1363 KALVYDLAGLITVEHYDQTRQHYWNAQGLIYRFVDERGENWRYENDELTIR
A3780_13225 1366 KALVYDLAGLITVEHYDQTRQHYWNAQGLIYRFVDERGENWRYENDELTIR
B1H58_04015 1368 KALVYDLAGLITVEHYDQTRQHYWNAQGLIYRFVDERGENWRYENDELTIR
CTU_00940 1291 KALVYDLAGLITVEHYDQTRQHYWNAQGLIYRFVDERGENWRYENDELTIR

ECL_01567 1399 ---LQKSKV---DYRTEK-----LQKSKV-----LQKSKV-----
A3780_13225 1411 LKRVYDLAGLITVEHYDQTRQHYWNAQGLIYRFVDERGENWRYENDELTIR
B1H58_04015 1410 ---LQKSKV---DYRTEK-----LQKSKV-----LQKSKV-----
CTU_00940 1319 ---LQKSKV---DYRTEK-----LQKSKV-----LQKSKV-----

ECL_01567 1422 ---EPGAGTIGKILARNDKITSFQKRDKAGNMKSGRIT
A3780_13225 1463 ---EPGAGTIGKILARNDKITSFQKRDKAGNMKSGRIT
B1H58_04015 1463 PNYKGVYDLAGLITVEHYDQTRQHYWNAQGLIYRFVDERGENWRYENDELTIR
CTU_00940 1363 ---EPGAGTIGKILARNDKITSFQKRDKAGNMKSGRIT

```

**Figure 1.2. *Enterobacter cloacae*'s RhsA is an example of a T6SS effector with a polymorphic toxin domain.** Multiple sequence alignment of Rhs proteins from different bacterial genera. While the bulk of the primary sequence is conserved, the C-terminal toxin domain is polymorphic in nature. ECL=*Enterobacter cloacae*, A3780=*Kosakonia radicinicans*, B1H58=*Pantoea alhagi*, CTU=*Cronobacter turicensis*.

## **Chapter 2: T6SS activity in *E. cloacae* is mediated by the T6SS-1 locus**

Note: other members of the Hayes lab participated on this project. Former graduate student Christina Beck and former undergraduate Ian Singleton contributed to the work presented in Figure 2.2. Ian also contributed to the work presented in Figure 2.10. Former undergraduate Jensen Abascal was largely responsible for the work presented in Figure 2.9. All above participants also helped with plasmid construction for this work. Former rotation student Shane Nourizadeh contributed to plasmid construction for the work presented in Figure 2.4. Fellow graduate student Steven Jensen contributed to the work presented in Figure 2.8B.

## Abstract

*Enterobacter cloacae* ATCC 13047 effectively outcompetes many enterobacterial species during co-culture on solid media. This competitive fitness advantage depends on the type VI secretion system-1 (T6SS-1) locus, which is constitutively expressed under laboratory conditions. It was previously determined that RhsA and RhsB proteins, which carry C-terminal toxin domains, are potent T6SS-dependent toxins deployed by *E. cloacae*. Here, I examine 10 additional predicted *E. cloacae* effector proteins to determine whether they are secreted via T6SS-1. In addition to the 2 Rhs proteins, murein-amidase and phospholipase toxins, encoded within T6SS-1, are also used to inhibit target bacteria. In contrast, other predicted effectors encoded in operons with hemolysin co-regulated proteins (Hcp) do not appear to be delivered. Moreover, additional PAAR-domain containing toxins are also not deployed under laboratory conditions. Deletion of *hcp3* (which is the only *hcp* gene within the T6SS-1 locus) abrogates all T6SS activity, suggesting it is the only *hcp* paralog utilized under laboratory conditions. However, I have determined that at least 2 of the other Hcp-linked predicted effectors still encode toxic proteins. Bioinformatic analyses suggest these other effectors may be employed by the inactive T6SS-2 locus.

## Introduction

*Enterobacter cloacae* is a Gram-negative opportunistic pathogen that can infect a variety of human tissues and organs. In 2003, *Enterobacter* species were found to be one of the primary causes of nosocomial Gram-negative pneumonia and surgical site infections in the United States (127). While *Enterobacter* species are diverse and widespread in nature, *E. cloacae* and *E. hormaechei* are the species most commonly associated with human isolates (128). In particular, the *E. cloacae* species has been observed to be multi-drug-resistant, and worryingly, multiple *E. cloacae* isolates have recently emerged that are resistant to the “last resort” carbapenem antibiotic family (129, 130). As such, *E. cloacae* is the type strain for this genus, and *E. cloacae* subsp. *cloacae* ATCC 13047 is the type strain for this species. *E. cloacae* ATCC 13047 (hereafter simply referred to as *E. cloacae*) was originally isolated from human cerebrospinal fluid in 1890 (131). This isolate is nevertheless classified as a BSL-1 organism, and is a convenient model system for the *Enterobacteriaceae*. In particular, it is a genetically tractable organism that has been fully sequenced, and (as this thesis work demonstrates) it is amenable to genetic and molecular biology techniques tailored for *Escherichia coli*. In this thesis, I present *E. cloacae* as a model system to study the molecular biology of the type VI secretion system (T6SS).

The Hayes lab has previously shown that *E. cloacae* deploys a constitutive T6SS system that is capable of inhibiting *E. coli* on solid media. (81, 132, 133). Subsequent work has demonstrated that *E. cloacae* is also able to inhibit a variety of Gram-negative bacteria, including *Enterobacter aerogenes*, *Salmonella enterica*, *Serratia marcescens*, *Alcaligenes faecalis*, and *Citrobacter freundii* (71). Here, I

show that this inter-bacterial inhibition ability is mediated by the T6SS-1 locus, which deploys 4 identified effectors. I next demonstrate that other, unidentified, factors must contribute to the inhibition of *E. coli*. Using a candidate-based approach, I tested 8 putative T6SS effector-immunity gene pairs for their involvement in bacterial inhibition. While none of the 8 tested effectors appear to be toxins deployed by the T6SS-1 apparatus, I did validate that 2 of these gene pairs function as bona-fide effector-immunity pairs. Finally, I investigate the possibility that many of these other putative effectors maybe be deployed via the T6SS-2 apparatus, which is not active under laboratory conditions.

## **Results**

### *Enterobacter cloacae* ATCC 13047 deploys 4 known effectors via T6SS-1

It has previously been demonstrated that *E. cloacae* inhibits multiple species of bacteria on solid media under laboratory conditions using the T6SS (71). *E. cloacae* encodes 2 distinct T6SS loci, T6SS-1 and T6SS-2 (Figure 2.1A and 2.1C). T6SS-1 encodes a cluster of core T6SS genes, as well as a variable set of effectors and accessory ORFs. Re-arrangement hotspot protein A (RhsA) is encoded at the end of T6SS-1, followed by a cluster of putative orphan immunity genes. T6SS-2 encodes many of the same core T6SS genes, although the homologs between the 2 loci are genetically distinct from one another. T6SS-2 lacks any *rhs* genes, though a second *rhs* gene, *rhsB*, is encoded outside either T6SS locus (Figure 2.1B). The RhsB protein has been shown to have a toxic C-terminal domain that functions as an anti-bacterial

DNase; however, the function of the RhsA C-terminal toxin domain has not been determined (71.)

Both Rhs proteins *in E. cloacae* are toxic to susceptible *E. cloacae* target cells lacking the Rhs immunity ( $\Delta rhsI$  cells), and both these Rhs proteins are deployed via T6SS-1 (81). Here I show that only T6SS-1 mediates interspecies killing of *E. coli* under laboratory conditions: deletion of *tssM* in T6SS-1 (*tssM1*) abrogates inhibition, whereas deletion of *tssM* in T6SS-2 (*tssM2*) does not (Figure 2.2A). Additionally, I identify 2 other T6SS effectors deployed in *E. cloacae*: a putative class 4 amidase effector, Tae4 (Figure 2.2B), and a putative lipase effector, Tle (Figure 2.2C), both encoded within T6SS-1 (Figure 2.1A). For all 4 identified effectors, *E. cloacae* susceptible targets (*i.e.* *E. cloacae* strains with a deletion of the respective effector-immunity gene pair) can be protected from the toxin through plasmid-borne expression of the cognate immunity gene. These results demonstrate that 4 effectors have been identified as toxic cargo deployed by the *E. cloacae* T6SS-1 apparatus, and that intra-species inhibition of susceptible target strains can be blocked through the expression of the cognate immunity gene.

*E. cloacae* deploys additional unidentified effector(s) using T6SS-1; candidate-based experiments did not identify any new effectors

Intra-species competitions with targets lacking a particular effector-immunity pair allow for the study of individual effector activities at a time. However, *E. cloacae* can deliver multiple effectors with each firing of the T6SS apparatus. While

individually each of the 4 plasmid-borne immunities were able to protect the susceptible *E. cloacae* target cells, *E. coli*, lacking all of *E. cloacae*'s immunity genes, cannot be protected from these effectors through plasmid-borne expression of the immunity genes. *E. cloacae* inhibitors lacking 2 of the known effectors (*E. cloacae*  $\Delta tae4 \Delta rhsA$  or  $\Delta tae4 \Delta rhsB$  mutants) are still able to inhibit *E. coli* targets carrying *tli* and *rhsI* (Figure 2.3A). This suggests either additional, unidentified, effectors exist in the *E. cloacae* genome and are deployed under laboratory conditions, or that the T6SS apparatus itself somehow has toxic activity against *E. coli*. Across over a decade of T6SS literature the latter model has never been described or noticed in any T6SS-expressing bacteria; this suggests there are likely additional effectors yet to be identified in *E. cloacae*. However, even though at least 4 unique effectors (and likely more) are deployed via T6SS-1, co-deletion of both *E. cloacae* *rhs* effectors abrogated *E. coli* inhibition, even though the inhibitor strain still expressed Tle and Tae4 (Figure 2.3A). This result is discussed more thoroughly in Chapter 4.

I next investigated 8 other putative effector-immunity gene-pairs as possible toxic effectors deployed by T6SS-1. These 8 effectors were chosen due to their genetic association with known T6SS elements. The effectors investigated in this study are presented in Table 2.1. Upon analysis of the *E. cloacae* genome, 4 additional *hcp* genes are found encoded outside either of the T6SS loci. Interestingly, all 5 *hcps* are encoded immediately adjacent to 2 hypothetical proteins. These were considered as potential effector-immunity pairs, and were named type VI effector proteins (Tep1-5) and type VI immunity proteins (Tip1-5), respectively. Tep3, associated with Hcp3, is encoded within T6SS-1 and has been previously designated as Tae4 (Figure 2.2B). Thus, 4 candidate effectors were chosen based on genetic linkage to *hcp* genes.

Additionally, a search of the *E. cloacae* genome reveals additional PAAR-containing genes not encoded in either of the T6SS loci. ECL\_02217 and ECL\_04194, both PAAR-containing proteins with a C-terminal extension, share sequence similarity, and their downstream open-reading-frames are also similar (Figure 2.3C and 2.3D). The C-terminal extensions are annotated as S-type pyocins, which are known DNase toxins. I considered these C-terminal extensions to be the same potential effector and therefore acknowledged the possibility of these putative immunities cross-protecting against the non-cognate, but highly similar, effector. A third PAAR-containing gene with a C-terminal extension, ECL\_03144, was also identified; intriguingly, it is encoded upstream of RhsB, though transcribed in the opposite direction as RhsB. This C-terminal extension was previously annotated as homologous to a known pore-forming toxin but that annotation has since been removed; as of the writing of this document the C-terminus is currently not annotated.

Finally, a pair of hypothetical proteins is encoded within T6SS-1, and were considered as a possible effector-immunity gene pair. When this investigation was started this putative effector, ECL\_01556, was annotated as a putative Cas9 nuclease; however, that annotation has since been removed and is now annotated as homologous to a known T6SS immunity protein in *Pseudomonas aeruginosa*. I nevertheless include ECL\_01556 in this analysis.

For all 8 candidate effector-immunity pairs, deletion strains of both putative effector and downstream immunity were generated and competed against both wild-type *E. cloacae* and a T6SS-null mutant ( $\Delta$ tssM1). A quadruple-deletion mutant of

ECL\_02217, ECL\_04194, and their respective immunities was generated to negate the possibility of immunity cross-protection. In all cases, the deletion strains do not suffer any T6SS-dependent fitness defect against parental strain inhibitors (Figure 2.3B). This suggests none of the 8 candidates tested are effectors deployed by *E. cloacae* under laboratory conditions.

*Each of E. cloacae's hcp genes are genetically linked to putative effector-immunity gene pairs*

Of the *hcp*-linked effectors, only *tae4*, associated with *hcp3* and encoded within T6SS-1, is deployed under laboratory conditions (Figure 2.2B and 2.3B). Next, I investigated whether these other *hcp*-linked putative effectors encode actual toxic proteins. The activity of a toxin is dependent on its ability to interact with its substrate; accordingly, these putative toxins must be expressed in the correct cellular compartment in order to assess any toxic effect. Periplasmically-acting T6SS effectors do not need to encode signal sequences in order to reach the periplasm of target cells because the T6SS apparatus is able to deliver effectors directly to the periplasm. However, the cognate immunity proteins for these toxins must be trafficked to the correct compartment in the inhibitor cell, so bioinformatic analyses of immunity genes can reveal the likely compartment a toxin functions in. Transmembrane prediction analyses were performed using the TMHMM and TMPred servers, and signal sequence analyses were performed with the SignalP-5.0 and Signal-BLAST servers (134-137).

Bioinformatic analysis reveals that Tip1 is strongly predicted to encode at least 1 transmembrane helix, suggesting its cognate effector Tep1 acts in the periplasm of cells. Similarly, Tip2 is strongly predicted to encode at least 1 transmembrane helix, suggesting Tep2 is also periplasmically-acting. Tae4 is predicted to be a class 4 murein amidase, and is therefore expected to be periplasmically-acting. Investigation by another group confirms this to be the case (138). Consistent with this finding, the Tai4 immunity is found to encode a signal sequence. Neither Tip4 nor Tip5 are found to encode signal sequences. Tip4 was predicted by the TMPred server to have 1 transmembrane helix, whereas the TMHMM server did not predict Tip4 to be a transmembrane protein. Thus, Tep4 is only weakly predicted to be periplasmically-acting. In contrast, Tip5 was not predicted to be a transmembrane protein by either server, suggesting it is cytoplasmically-acting.

#### *Validation of E. cloacae's hcp-linked putative effectors and immunities*

In order to validate whether these putative effectors are indeed toxic, I cloned the putative *hcp*-linked effectors both with and without a (co-translational *dsbA*) signal sequence in order to test the ability of these genes to produce products toxic to *E. coli* in either the cytosol or periplasm. I did not test *tep4* due to the presence of an internal restriction endonuclease cut site within the gene. Somewhat surprisingly, given the bioinformatic predictions, I find that Tep1 is toxic to *E. coli* when expressed in the cytosol (Figure 2.4A). Attempts to clone Tep1 with a signal sequence were only viable when the cells already expressed the cognate immunity, Tip1.

Expression of periplasmically-expressed Tep1 is also toxic to *E. coli*, even when Tip1 is present (Figure 2.4A). Tip1 is encoded on a separate plasmid under the *lac* promoter, and simultaneous induction of ss-Tep1 and Tip1 is still toxic (Figure 2.4A, IPTG sample). Thus, *tep1* does encode a toxic effector protein that is toxic in both the cytosol and periplasm, but is more toxic when expressed in the periplasm.

Next, I tested whether Tep2 is toxic to *E. coli*. I find that Tep2 is not toxic in either the cytosol or the periplasm (Figure 2.4B). *Tae4*, the predicted murein amidase, is confirmed to be toxic in the periplasm but not in the cytosol (Figure 2.4C). Finally, Tep5 is shown to be toxic in the periplasm but not in the cytosol (Figure 2.4D). This was surprising given that the bioinformatic analyses predicted the putative immunity, Tip5, would not traffic to the periplasm.

After *tep1*, *tae4*, and *tep5* were confirmed to encode genuine toxins, I next investigated the possible function of these toxins. *Tae4* is strongly predicted to have amidase activity, but bioinformatic analyses were unsuccessful in predicting the function of Tep1 and Tep5. Because both Tep1 and Tep5 appear to function in the periplasm, periplasmic substrates like the cell wall or lipid membranes are likely targets of these toxins. Another possible activity is the formation of membrane pores that dissipate the cell's proton-motive force (pmf). Loss of pmf can be easily assayed with an ethidium bromide (EtBr) efflux experiment: EtBr will readily permeate bacteria and stain internal nucleic acids, but *E. coli* normally exports the EtBr back out through the use pmf-dependent efflux pumps; retention of the EtBr stain is therefore an indicator of loss of pmf.

I induced expression of ss-Tep1, ss-Tep5, and control constructs in *E. coli*, then stained live cultures with EtBr. After multiple washes, un-intoxicated *E. coli* do not retain the EtBr stain, indicating pmf is not disrupted in the control strain (Figure 2.5). Conversely, intoxication with the known pmf-dissipating toxin CdiA-CT<sub>EC93</sub> leads to high retention of EtBr (179, 180). I find that intoxication with ss-Tep1 similarly disrupts EtBr efflux. However, neither intoxication with ss-Tep5, nor with the predicted cell-wall-degrading toxin YbfO, appears to significantly disrupt pmf (Figure 2.5). Taken together, this suggests that Tep1 functions to dissipate pmf; the activity of Tep5 still remains unknown.

Given that *tep1*, *tae4*, and *tep5* are confirmed to encode genuine toxins, I next tested whether the downstream putative immunity will protect against activity of the cognate toxin. I find that with all 3 toxins, the downstream putative immunity does indeed function to protect cells against the cognate toxin (Figure 2.6). This confirms the hypothesis that these *hcp*-linked gene pairs encode functional effector-immunity gene pairs.

I next wished to investigate whether the plasmid-expressed Teps were still toxic to wild-type *E. cloacae*, given that this parental strain encodes all the immunity genes in question. While Tep1 and Tep5 do not appear to be deployed by T6SS-1 under laboratory conditions, it still remains to be seen whether these effectors and immunities are even expressed in the cell under laboratory conditions. Somewhat surprisingly, cytoplasmically-expressed Tep1 is not very toxic to *E. cloacae* (Figure 2.7A), as compared to the toxicity seen with this same construct in *E. coli* (Figure 2.4A). This lower amount of inhibition does not appear to be dependent on

expression of chromosomally-encoded *tip1*, as a deletion strain of  $\Delta\text{tep1} \Delta\text{tip1}$  expressing Tep1 has more robust growth than Tep1-expressing *E. coli* (Figure 2.8). This may suggest that this pmf-dissipating toxin has a diminished ability to integrate into the *E. cloacae* inner-membrane, as least from the cytoplasmic leaflet. This species-dependent difference in cytoplasmic inhibition may suggest that there are host factors that facilitate Tep1 activity or membrane integration, and that these factors differ between *E. cloacae* and *E. coli*. In contrast, I find that Tep1 is very toxic to *E. cloacae* when expressed from the periplasm (Figure 2.7B), which is consistent with the previous findings in *E. coli* (Figure 2.4A).

Tep2 was not toxic to *E. coli* (Figure 2.4B), but it is possible *E. coli* lacks the correct substrate for this toxin, therefore; I also tested whether periplasmically-expressed Tep2 is toxic to *E. cloacae*. Again, I find Tep2 is non-toxic (Figure 2.7C). Tae4, which is naturally deployed by *E. cloacae*, is not toxic to *E. cloacae*, presumably due to constitutive expression of the cognate Tai4 immunity (Figure 2.7D). Finally, periplasmically-expressed Tep5 is toxic to *E. cloacae* (Figure 2.7E). Together, these data suggest that not only is Tae4 the only effector deployed by *E. cloacae* under laboratory conditions, but that these other *hcp*-linked effectors and immunities are likely not even expressed under laboratory conditions.

#### *Only Hcp3 has specificity to T6SS-1-encoded factors*

Some T6SS system effectors have been shown to interact directly with Hcp, and are stabilized by this interaction (88). Thus, I sought to test the ability for the

T6SS-1-encoded Tae4 to interact with any of the 5 Hcps in *E. cloacae*. Plasmid-borne Hcp-H6 constructs were co-expressed with plasmid-borne-FLAG-Tae4 in *E. coli*, and Ni-NTA affinity purification was performed to test which, if any, of the Hcps Tae4 will stably interact with. I find that Tae4 is only able to stably associate with its cognate Hcp3, which is the only Hcp encoded within the T6SS-1 locus (Figure 2.9). Next, I asked which Hcps support T6SS-1 activity. I individually deleted each *hcp* in the genome to test which, if any, Hcp is required for T6SS activity. I find that only *hcp3*, encoded within T6SS-1, is required for T6SS activity under laboratory conditions (Figure 2.10A). It is very plausible that the *hcp*-linked immunity genes outside T6SS-1 are not expressed under laboratory conditions (Figure 2.7); therefore, it is plausible that these other *hcp* genes are not expressed either. Thus, I forced on the expression of these *hcps* on plasmids, and asked which *hcps* will complement a *hcp3* deletion. I find that again, only Hcp3 supports T6SS activity under laboratory conditions (Figure 2.10B). This suggests that there is binding specificity between the T6SS-1 apparatus and Hcp3, and that the other Hcps cannot assemble onto the T6SS-1 apparatus.

Given that these Hcps and their linked effector-immunity pairs, encoded outside T6SS-1, do not appear to be used by T6SS-1, it seems likely that these other Hcps might be specific to the T6SS-2 apparatus. However, T6SS-2 confers no competitive advantage to *E. cloacae* under laboratory conditions (Figure 2.2A). Notably, the T6SS-2 locus does not encode its own *hcp* gene. Genetic analyses to the related bacterium *Enterobacter hormaechei* show a similar T6SS-2 locus to that of *E. cloacae*'s. I acquired 2 *E. hormaechei* strains: a mouse intestinal isolate donated

from the lab of Naohiro Inohara, termed isolate NI1077, and an ATCC strain, isolated from human sputum, termed ATCC 49162.

Interestingly, both strains of *E. hormaechei* encode a *hcp* gene in its T6SS-2 locus, and multiple sequence alignment analyses reveal that both *E. hormaechei* T6SS-2 Hcps share strong sequence similarity. Moreover, the *E. cloacae* Hcps encoded outside T6SS-1 also have strong sequence similarity to the T6SS-2 Hcps (Figure 2.11A). Pairwise sequence alignment reveals that *E. cloacae*'s Hcp3, encoded within T6SS-1, is most dissimilar to the other Hcps under investigation, with sequence identity ranging from 16% (against Hcp1) to 22% (against Hcp2 and Hcp4) (Figure 2.11B). Conversely, the other *E. cloacae* Hcps are more similar to each other, and to the *E. hormaechei* Hcps, with sequence identity ranging from 46% (Hcp1 against Hcp4) to 71% (Hcp2 against *E. hormaechei* Hcps) (Figure 2.11B). Together, this suggests these unused Hcps in *E. cloacae* might be specific to the T6SS-2 apparatus, and cannot therefore complement a *hcp3* deletion.

#### *E. hormaechei*'s T6SS-2 is not active under laboratory conditions

I have previously shown that *E. cloacae*'s T6SS-2 locus is not active under laboratory conditions (Figure 2.2A). Multiple sequence alignment analyses demonstrate that *E. cloacae*'s T6SS-2 contains multiple genetic lesions. In addition to lacking any *hcp* gene, as mentioned previously, the locus also contains truncations of multiple structural components. TssF2 has an N-terminal truncation compared to the TssF2 proteins in *E. hormaechei* (Figure 2.12A). The T6SS-2 PAAR protein in *E.*

*hormaechei* has a large C-terminal extension, likely encoding an effector, but *E. cloacae*'s T6SS-2 PAAR protein is truncated from the C-terminal end (Figure 2.12B). It still remains possible *E. cloacae*'s truncated PAAR is only missing the effector domain, and could still support PAAR function given no other genetic lesions of the T6SS-2 locus. But additionally, the disassembly ATPase ClpV is truncated at the N-terminus (Figure 2.12C), and the structural component VgrG is pseudogenic (Figure 2.12D). Given these multiple genetic issues, it is likely that *E. cloacae*'s T6SS-2 locus is un-useable and no amount of induction or regulatory control would produce a competitive advantage from T6SS-2.

Both strains of *E. hormaechei* under investigation, NI1077 and ATCC 49162, appear to have intact T6SS-2 loci. Thus, I sought to test whether T6SS-2 is active under laboratory conditions in *E. hormaechei*. Inter-species competition experiments against *E. coli* reveal all competitive advantage comes from T6SS-1 under laboratory conditions in both strains (Figure 2.13A). Additionally, Hcp secretion of *E. hormaechei* NI1077 was monitored by Coomassie stain of cell supernatants. The results suggest that if Hcp is at all secreted from T6SS-2, it is secreted at levels below the detection limit of this experiment (Figure 2.13B). Thus, the T6SS-2 loci in both *E. hormaechei* strains tested are not active under laboratory conditions. It remains to be seen whether T6SS-2 genes are at all expressed in the cell under laboratory conditions, and whether altering growth conditions can induce T6SS-2 expression in *E. hormaechei* and activate a competitive advantage from this locus.

## Discussion

The work presented here demonstrates that *E. cloacae* is a feasible model system to study the T6SS. Here, I find that *E. cloacae* deploys 4 different toxic effectors via T6SS-1. Two of these effectors are Rhs proteins, both of which contain a PAAR domain and are therefore predicted to directly interact with VgrG to help form the membrane-puncturing spike of the apparatus (28; see also Figure 1.1A). The Rhs C-terminally-encoded toxins are therefore fused to the apparatus via the N-terminal PAAR domain. In contrast, Tae and Tle are small effectors that do not contribute to the structure of the T6SS apparatus. I find that Tae is genetically linked to Hcp3 and interacts with Hcp3 in the absence of other T6SS factors. This supports the model that Tae resides in the Hcp lumen during T6SS biogenesis (88). While the work presented in this chapter does not explore the mechanism of Tle recruitment to the T6SS apparatus, the work presented in Chapter 3 suggests Tle interacts with the N-terminal region of VgrG.

My findings also suggest that *E. cloacae* deploys other T6SS effectors yet to be identified. Using a candidate-based approach, 8 putative T6SS effector-immunity gene pairs were tested, but all failed to elicit *in vivo* T6SS inhibition. However, after testing 3 of the 8 putative effectors for toxic activity, I find that 2 out of 3 tested do represent bona-fide effector-immunity gene pairs. It remains to be seen why these validated toxins, Tep1 and Tep5, as well as the other candidate effectors, are not deployed by *E. cloacae* under laboratory conditions. One explanation is that these genes are simply not expressed under laboratory conditions, and may be regulated

via environmental signals not provided by the culture conditions used. Another explanation is that these effectors have specificity to the T6SS-2 locus.

While *E. cloacae* clearly encodes 2 distinct T6SS loci, I find that only T6SS-1 is used. Consistent with this finding, further analysis revealed that the T6SS-2 locus contains multiple genetic mutations that would likely abrogate function of multiple structural components of the apparatus. Bioinformatic analyses suggest that at least some of the candidate effectors are likely to have specificity to the T6SS-2-encoded apparatus.

*E. cloacae* encodes 5 unique *hcp* alleles, with *hcp3* encoded within T6SS-1. Strikingly, T6SS-2 does not encode *hcp* at all. Upon analysis of 2 distinct strains of the related bacteria *E. hormaechei*, both encoding closely related and seemingly intact T6SS-2 loci, I find that the T6SS-2 *hcp* alleles in *E. hormaechei* have strong sequence similarity to the 4 *hcp* alleles encoded outside *E. cloacae*'s T6SS-1 locus (*i.e.* *hcp1*, *hcp2*, *hcp4*, and *hcp5*). All 5 *hcp* alleles are encoded immediately adjacent to either confirmed (*tep1*, *tae*, *tep5*) or candidate (*tep2*, *tep4*) effector-immunity gene pairs.

Taken together, these data would suggest Tep1, Tep2, Tep4, and Tep5 are effectors that evolved to be deployed via T6SS-2. The additional finding that only Hcp3 supports T6SS-1 activity strengthens the hypothesis that these other Hcps, and their cognate effector-immunity pairs, are specific to T6SS-2. It remains to be seen whether these other Hcps could be used by *E. hormaechei*'s T6SS-2, and what the biological significance of having multiple *hcp* alleles, all specific to the same T6SS apparatus, would be. Given that all the *hcps* are genetically associated with their own

particular effector-immunity pair, this could be a method for differential regulation and subsequent selective effector deployment to tailor the toxic payload to particular external signals whilst maintaining the same foundational T6SS apparatus.

It is currently unclear why *E. hormaechei* has 2 T6SS loci but only expresses 1, or why *E. cloacae* lost functionality of its T6SS-2 locus. The presence of putative effectors with putative immunity genes suggests T6SS-2 would have anti-bacterial rather than anti-eukaryotic function; therefore, tight regulation of T6SS-2 would not seem to be necessary. Given that the regulation of T6SS-2 is currently unknown, this question will likely persist until it is understood what conditions turn on T6SS-2. And if the multiple *hcp*-linked effectors described above do indeed utilize the T6SS-2 apparatus, then T6SS-2 activity would likely be very finely modulated and adjusted.

Another remaining question in the T6SS field is the significance of gene position for T6SS effectors. While many effectors are encoded within their respective T6SS locus, there is clearly precedent for effectors encoded elsewhere in the genome. For example, *E. cloacae*'s RhsB is not encoded within or next to either the T6SS-1 or T6SS-2 locus, yet it is the most potent effector deployed by T6SS-1. Given that these externally-encoded effectors must necessarily be transcribed by a different promoter than the T6SS locus, these effectors may be regulated differently than the T6SS locus. A simple explanation for RhsB's potency may be that it is simply expressed at higher levels than the T6SS-1 encoded effectors. The external location of these effectors may also be an indication that these effectors were acquired via horizontal gene transfer.

The existence of externally-encoded effectors complicates bioinformatic identification of new T6SS cargo. While secretome proteomics approaches have been successful in the past in identifying T6SS substrates, these experiments have often failed to identify known effectors (5, 81, 69, 139). Whether this is because some effectors are not deployed under conditions amenable to secretome preparation, or simply that these effectors are not secreted at high enough levels to reach the detection limit, it is clear that bioinformatic approaches have been a very important complement to secretome approaches. A different proteomics approach has been successfully utilized by the Mougous lab in order to detect effectors stabilized through interaction with Hcp: they compared cellular proteomes of *hcp+* versus *hcp-* strains to identify effectors enriched in the *hcp+* strain (81). Given that *E. cloacae* appears to deploy at least one additional effector as yet un-identified, the Mougous lab graciously performed this Hcp-dependent cellular proteomics approach with *E. cloacae*; unfortunately, this experiment failed to generate any reasonable candidates (data not shown). Thus far, no one has published a similar cellular proteomics approach for identification of VgrG- or PAAR-stabilized effectors; this seems like a logical follow-up to the Hcp proteomics assay.

Another remaining fundamental question about T6SSs is the basic value of deploying multiple effectors through a single apparatus, rather than a single, potent toxin. The number of effectors deployed by any given T6SS apparatus varies from system to system, so there is no set “rule” regarding the breadth of the toxic payload: for example, the entero-aggregative *E. coli* (EAEC) T6SS-1 locus appears to deploy only a single effector, whereas *E. cloacae*’s T6SS-1 deploys at least 4, and *P.*

*aeruginosa* has 7 identified effectors deployed via H1-T6SS (81, 87, 186). Moreover, there does not appear to be overlap in the function of *E. cloacae*'s effectors, nor in *P. aeruginosa*'s. One reason for deploying such a wide arsenal may be to prepare for any change in environmental conditions that would influence the efficacy of a given toxin. For example, a recent report demonstrates that some *P. aeruginosa* effectors are affected by temperature, pH, salinity, or oxygen levels (140). A simpler explanation may simply be to maximize the chances of inhibiting neighboring cells and to prevent the evolution of a resistant population.

## **Materials and Methods**

### *Bacterial growth and conditions*

Bacteria were cultured in shaking lysogeny broth (LB) or on LB-agar at 37°C unless indicated otherwise. Bacteria were supplemented with antibiotics at the following concentrations: 150 µg/mL ampicillin (Amp), 66 µg/mL chloramphenicol (Cm), 50 µg/mL kanamycin (Kan), 100 µg/mL spectinomycin (Spc), 200 µg/mL rifampicin (Rif), 25 µg/mL tetracycline (Tet), and 100 µg/mL trimethoprim (Tp).

### *Strain construction*

All bacterial strains, plasmids, and oligonucleotides used in this study are listed in Tables 2.2, 2.3, and 2.4. Gene-deletion constructs for *E. cloacae* were generated using overlap-extension PCR (OE-PCR) or via the plasmids pKAN or

pSPM as described previously (67, 142, 143). Briefly, OE-PCR constructs were made with upstream and downstream homology PCR fragments overlapped to the CH2952/CH2953 PCR product amplified from either pKAN or pSPM. pKAN or pSPM plasmid constructs were generated by restriction cloning PCR fragments from upstream and downstream of the target gene into pKAN or pSPM to flank the antibiotic-resistance cassette. Restriction enzymes used are specified in the oligonucleotide names listed in Table 2.4.

Resulting constructs were PCR-amplified, DpnI-digested to remove methylated template DNA, then directly electroporated into *E. cloacae* cells expressing phage  $\lambda$ -Red recombinase proteins as described (144). Transformants were selected on LB-agar supplemented with either Kan or Spc. All chromosomal deletions were confirmed by whole-cell PCR analysis. Kan or Spc cassettes were cured as necessary via pCP20 (145).

Gene deletions for *E. hormaechei* were introduced via allele-exchange (146). Deletion constructs were generated via either OE-PCR or restriction cloning, then the deletion constructs were restriction cloned using SacI/KpnI into the pRE118-derivative pRE118-pheS\*. The resulting plasmid was then transformed into MFD $\pi$  donors and mated into *E. hormaechei* recipients (147). Integrants were selected on LB-agar supplemented with kanamycin, then 3 rounds of chloro-phenylalanine counter-selection was performed on 1x M9 minimal media supplemented with .5% glucose and 10 mM d/l-*p*-chlorophenylalanine. Clones were screened for Kan-sensitivity, and Kan-sensitive clones were screened via whole-cell PCR analysis.

### *Plasmid construction*

All plasmids and oligonucleotides used in this study are listed in Tables 2.3 and 2.4. All PCR products were purified, digested with the restriction enzymes indicated in the oligonucleotide names (Table 2.4), and ligated to a vector treated with the same enzymes. Plasmids were confirmed by DNA sequencing (University of California, Berkeley). Plasmid transformations were performed by making strains TSS competent (148). Constructs were cloned directly into the final vector in one cloning step, with exceptions or complications described below.

For generation of DsbA(ss)-Tep constructs, PCR products were cloned into pCH10626 using NcoI/HindIII in order to fuse the signal sequence to the gene. All 5 Hcp-His6 constructs were initially restriction cloned into pET21P using NcoI/XhoI or into pET21P-K using KpnI/XhoI, then all 5 constructs were subsequently subcloned into pET24db using XbaI/XhoI. For generation of pKAN or pSPM constructs, upstream and downstream homology regions were sequentially restriction cloned into either pKAN or pSPM, or the construct was made via OE-PCR then cloned into pKAN/pSPM using SacI/KpnI. For immunity deletion constructs, the upstream homology region used was the same region used for the cognate effector deletion construct. For *tep1*, *tep2*, and *tep5* deletion constructs, the downstream reverse oligonucleotide used was the same oligonucleotide used for the downstream reverse cognate immunity deletion.

For generation of pCH13252, the deletion construct was initially cloned into pSPM as described above, then the resulting construct was subcloned into pDL6480 using SacI/KpnI. For generation of pCH14675, the deletion construct was initially

cloned into pBluescript II SK+ in the same manner described for pKAN/pSPM constructs, then the resulting construct was subcloned into pDL6480 using SacI/KpnI.

### *Competitions*

*Enterobacter* strains were used as inhibitor cells during LB-agar co-cultures against either *E. cloacae* derivatives or X90 *E. coli* targets. Cells were grown in LB-medium to log phase, then collected by centrifugation and resuspended in 1x M9 salts. Inhibitors and targets were mixed 1:1 at OD 17 (200 uL total volume), then 100 ul of the mixture was spread on LB-agar without antibiotics and incubated at 37°C for 4 h. Culture aliquots were taken at the beginning of the co-culture and after 4 h to quantify viable inhibitor and target cells as colony forming units (CFU). After 4 h, co-cultures were harvested in 1.5 mL of 1x M9 salts. For competitions with plasmid-expressed Hcp, inhibitors were grown in LB-medium supplemented with 0.4% L-arabinose and Tet. Co-cultures were then performed as above on LB-agar supplemented with 0.4% L-arabinose.

For all competitions, cell suspensions were serially diluted into 1x M9 salts and plated onto LB-agar supplemented with appropriate antibiotics to separately enumerate inhibitor and target cells. Competitive indices were calculated as the ratio of inhibitor to target CFUs at 4 h divided by the initial inhibitor to target CFU ratio.

### *Growth curves*

Plasmid-bearing strains were plated on LB-agar supplemented with 0.4% glucose and appropriate antibiotics. The following day, strains were inoculated off plates into LB-medium supplemented with 0.4% glucose and appropriate antibiotics and grown to log phase, then collected by centrifugation and resuspended in 1x Mg salts. Cells were then diluted to an OD<sub>600</sub> of .05 in fresh LB-medium supplemented with appropriate antibiotics and either 0.4% L-arabinose or 0.4% glucose (as indicated). Cell growth was monitored by measuring the OD<sub>600</sub> every 30 min for 5 h.

### *Tae4 pulldown assay*

*E. coli* strains were grown in LB-medium supplemented with Amp and Kan to log phase and protein expression was induced with 1.5 mM Isopropyl-beta-D-thiogalactoside (IPTG) for 1.5 h. Cells were then collected by centrifugation and resuspended in extraction buffer [20 mM sodium phosphate (pH 7.0), 150 mM NaCl, 0.05% Triton X-100]. Each cell suspension was broken by 2 passages through a French press, then insoluble debris was removed via centrifugation at 23,000 *xg* for 10 min at 4°C. The clarified lysate was added to Ni<sup>2+</sup>-NTA agarose resin and incubated on a rotisserie for 1 h at 4°C. Following incubation, the beads were washed extensively in wash buffer [20 mM sodium phosphate (pH 7.0), 500 mM NaCl, 0.05% Triton X-100, 50 mM imidazole], then eluted in elution buffer [8M urea, 10 mM Tris-HCl (pH 8.0), 300 mM NaCl, 250 mM imidazole].

Samples were analyzed by SDS-PAGE on Tris-tricine 10% polyacrylamide gels run at 110 V (constant) for 1 h. For visualization of Hcp, gels were stained with Coomassie brilliant blue dye. For visualization of Tae4-FLAG, gels were soaked for 10 min in transfer buffer [25 mM Tris, 192 mM glycine (pH 8.6), 20% methanol], then electroblotted to nitrocellulose membranes using a semi-dry transfer apparatus at 17 V (constant) for 30 min. Membranes were blocked with 4% non-fat milk in PBS for 30 min at room temperature, then incubated with primary antibody in 0.1% non-fat milk in PBS overnight at 4°C. Mouse anti-FLAG (Sigma) was used at a 1:25,000 dilution. Blots were incubated with 680LT-conjugated goat anti-mouse IgG (1:125,000 dilution, LICOR) in PBS, then visualized with a LI-COR Odyssey infrared imager.

#### *Hcp secretion assay*

*E. hormaechei* strains were cultured in LB-medium overnight. The following day, cells were collected by centrifugation at 3,000 *xg* for 5 min, then culture supernatants were re-spun to further remove cellular contamination. Supernatants were precipitated in cold ethanol at a final ethanol concentration of 75%. Samples were left at -80°C overnight, then proteins were collected by centrifugation at 21,000 *xg* for 15 min at 4°C. Precipitates were washed once with 75% cold ethanol, then air-dried pellets were dissolved in urea-lysis buffer [50% urea, 150 mM NaCl, 20 mM Tris-HCl (pH 8.0)]. Samples were analyzed by SDS-PAGE on Tris-tricine 7% polyacrylamide gels run at 110 V (constant) for 50 min, then stained with Coomassie brilliant blue dye.

### *Ethidium bromide efflux assay*

*E. coli* strains were cultured in LB-medium supplemented with 0.4% glucose and Tp or Tet to log phase, then collected by centrifugation and resuspended to the same density in pre-warmed LB-medium supplemented with 0.4% L-arabinose and Tp or Tet. Samples were induced at 37°C for 1 h, then collected by centrifugation and washed once in 1x M9 salts. Cells were then resuspended to an OD<sub>600</sub> of 0.2 in 1x M9 salts supplemented with 25 µM ethidium bromide, then incubated at 37°C for 2 min. Samples were washed twice with 1x M9 salts at 37°C, and were then wet-mounted for visualization by fluorescent microscopy.

### *Bioinformatic analyses*

Transmembrane prediction analyses were performed using the TMHMM and TMPred servers, and signal sequence analyses were performed with the SignalP-5.0 and Signal-BLAST servers (134, 135, 136, 137). Protein sequences were aligned using Clustal Omega (149). Protein alignments were rendered with BoxShade ([https://embnet.vital-it.ch/software/BOX\\_form.html](https://embnet.vital-it.ch/software/BOX_form.html)). Pairwise comparison values were calculated using the SIAS pairwise alignment server (<http://imed.med.ucm.es/Tools/sias.html>).

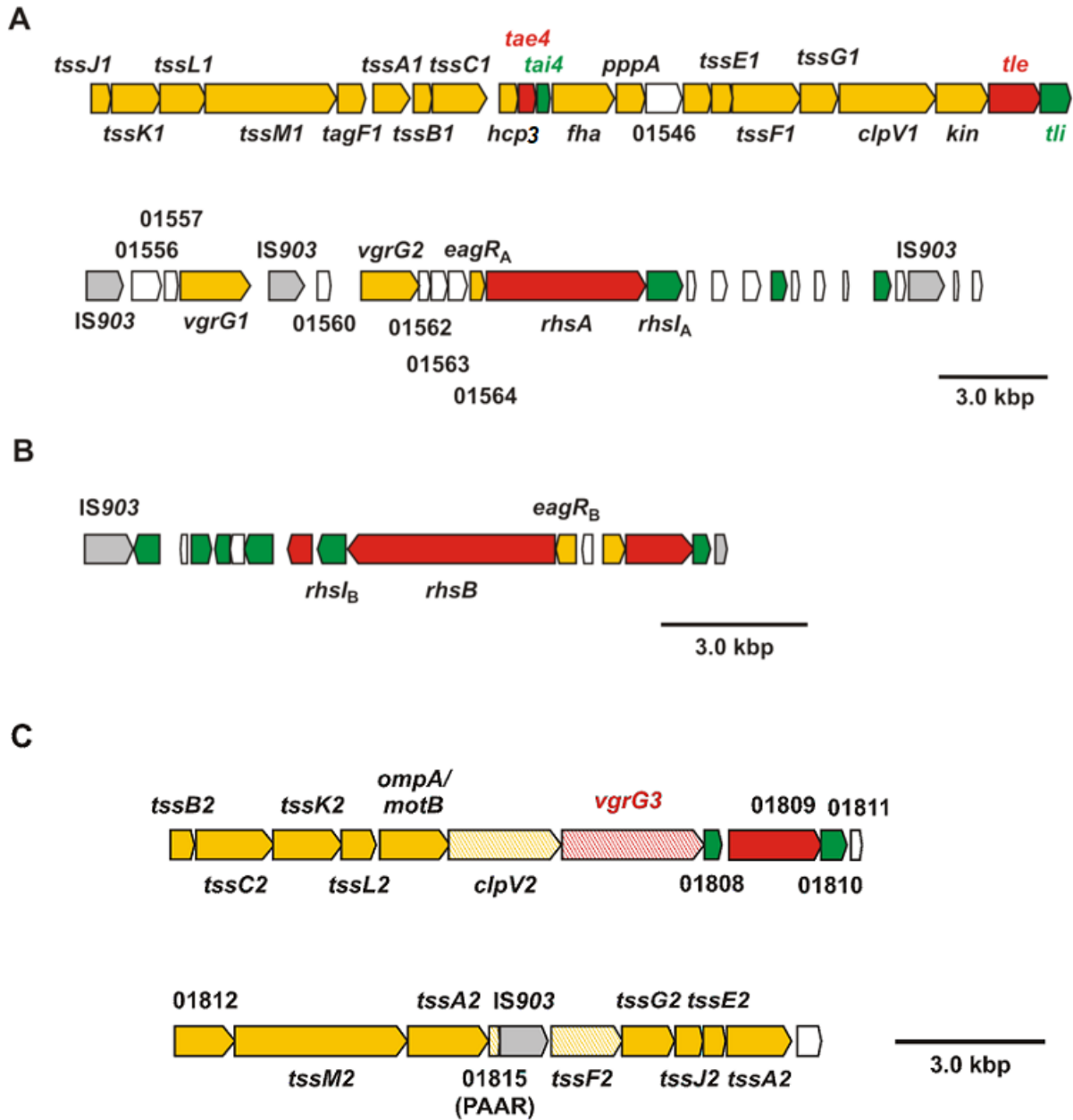


**Figure 2.1. T6SS and Rhs loci in *E. cloacae* ATCC 13047.** T6SS factors are colored yellow, predicted or confirmed effectors are colored red, and predicted or confirmed immunities are colored green. Faded colors indicate genetic lesions in the gene. (A) The T6SS-1 locus. (B) The RhsB locus. (C) The T6SS-2 locus.

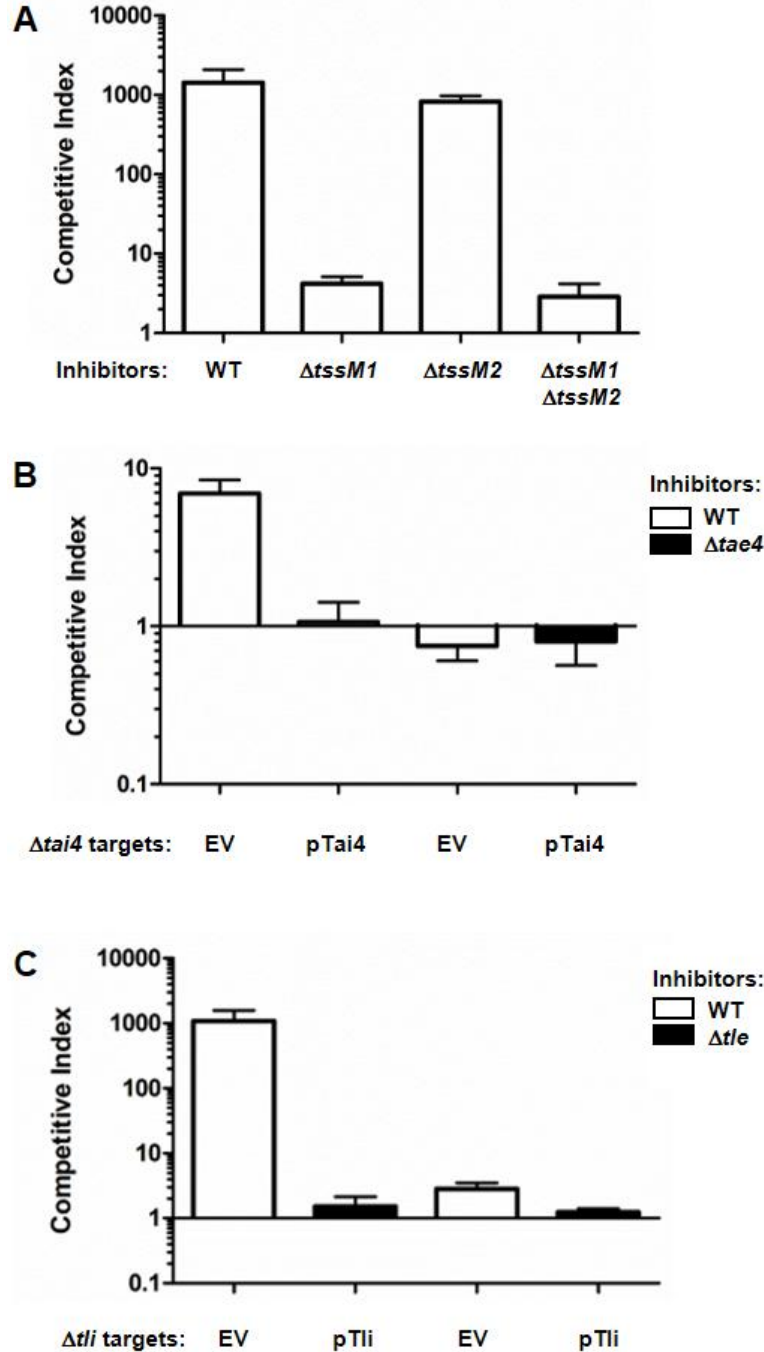


**Figure 2.2. The T6SS-1 locus deploys multiple effectors.** *E. cloacae* inhibitor cells were incubated at a 1:1 ratio with target cells. Cells were quantified as colony-forming units (CFUs) at the beginning of the co-culture and after 4 h. Competitive indices were calculated as the ratio of inhibitor to target CFUs at the end of the competition normalized to the starting ratio. Data represent the average and standard error of the mean for three independent experiments. (A) Indicated *E. cloacae* inhibitors versus *E. coli*. (B) and (C) Indicated *E. cloacae* inhibitors versus indicated *E. cloacae* targets carrying plasmid constructs. WT=wild-type, EV=empty vector.

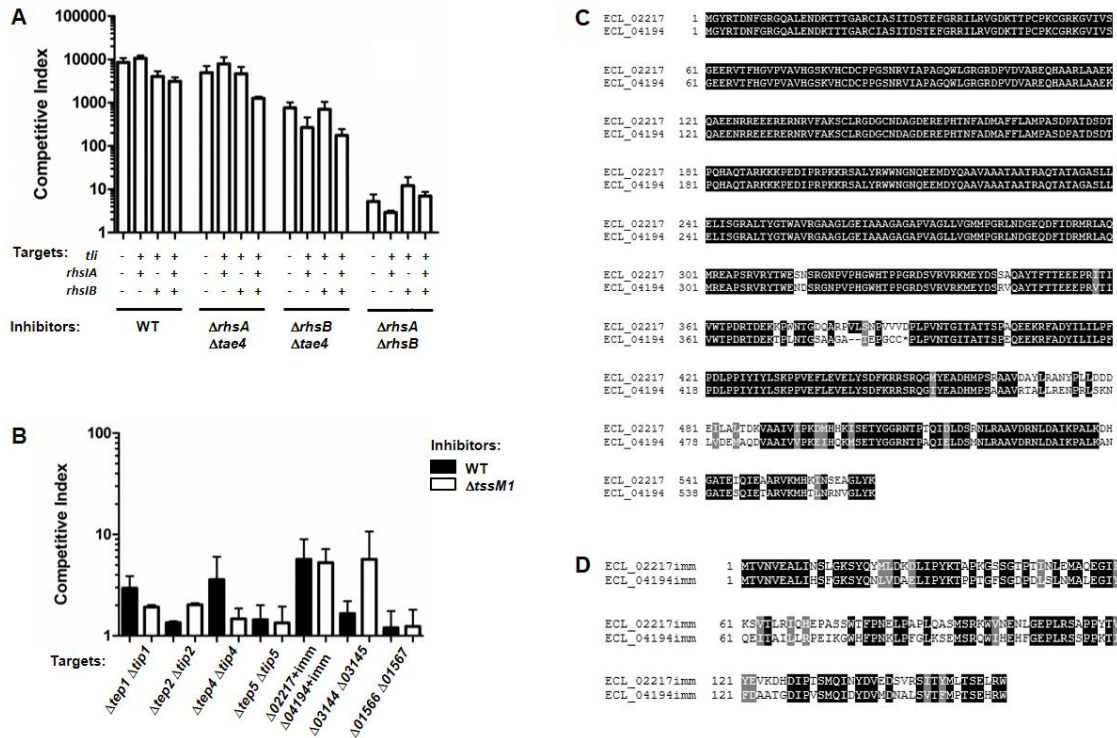


**Figure 2.3. The T6SS-1 competitive advantage extends beyond the 4 effectors identified so far.** (A) *E. cloacae* inhibitors were incubated at a 1:1 ratio against *E. coli* targets carrying the indicated plasmid constructs for 4 hours. Data represent the average and standard error of the mean for three independent experiments. (B) Indicated *E. cloacae* inhibitors were incubated at a 1:1 ratio against indicated *E. cloacae* targets for 4 hours. Data represent the average and standard error of the mean for three independent experiments. (C) Multiple sequence alignment of 2 putative *E. cloacae* effectors, ECL\_04194 and ECL\_02217, and (D) their putative cognate immunities.

**Table 2.1. Summary of effectors tested in this study.**

<b>Gene</b>	<b>Name</b>	<b>Predicted activity</b>	<b>T6SS association</b>
ECL_01567	RhsA <sup>a</sup>	? (cytoplasmic)	Within T6SS-1, contains PAAR
ECL_03140	RhsB <sup>a</sup>	DNase <sup>b</sup>	Contains PAAR
ECL_01553	Tle <sup>a</sup>	Lipase	Within T6SS-1
ECL_01541	Tae4 <sup>a</sup>	Murein amidase	Within T6SS-1, adjacent to <i>hcp3</i>
ECL_00033	Tep1	<i>pmf</i> -dissipating toxin <sup>b</sup>	Adjacent to <i>hcp1</i>
ECL_01377	Tep2	? (periplasmic)	Adjacent to <i>hcp2</i>
ECL_02155	Tep4	?	Adjacent to <i>hcp4</i>
ECL_03984	Tep5	? (periplasmic)	Adjacent to <i>hcp5</i>
ECL_02217	Pyocin S	DNase	Contains PAAR
ECL_04194	Pyocin S	DNase	Contains PAAR
ECL_03144	TcdA/TcdB pore-forming domain	<i>pmf</i> -dissipating toxin	Contains PAAR
ECL_01566	Hypothetical	Nuclease	Within T6SS-1

<sup>a</sup>effector is deployed under laboratory conditions

<sup>b</sup>activity of the toxin has been experimentally confirmed

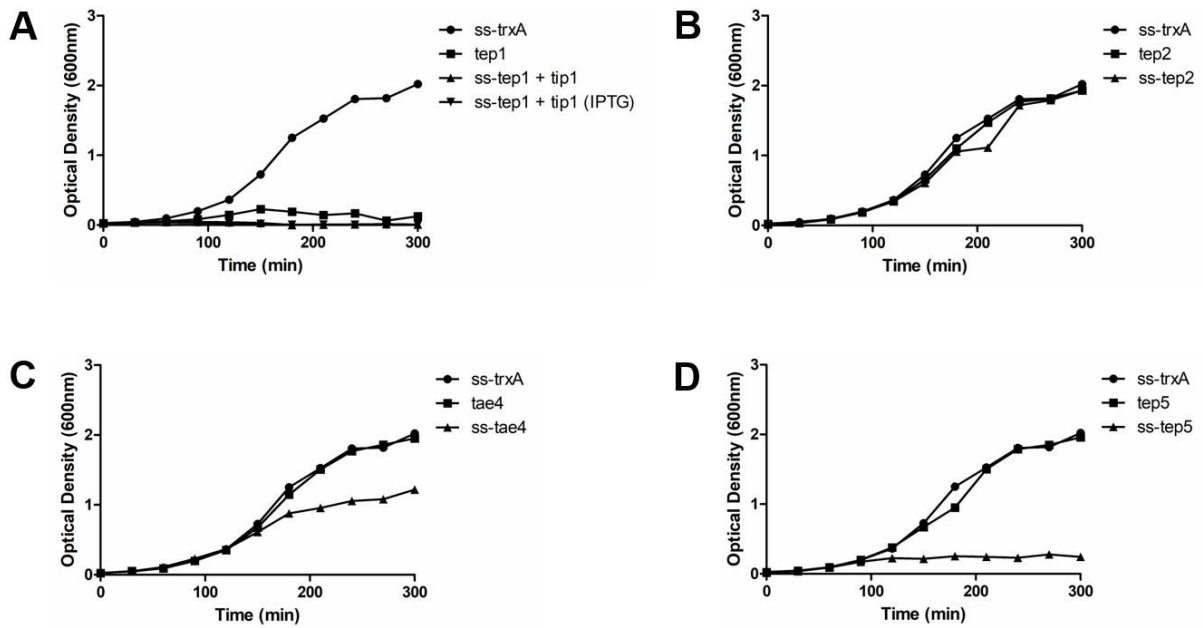


**Figure 2.4. Hcp-linked effectors are toxic to *E. coli*.** Cell densities as measured by OD<sub>600</sub> over time. Intracellular expression of indicated constructs was induced with 0.4% L-arabinose at 0 h in *E. coli*. (A) The *ss-tep1* plasmid could not be separated from the separately-encoded *tip1* plasmid, and as a consequence all *ss-tep1* experiments contain plasmid-expressed Tip1. *tip1* over-expression was induced with .5 mM IPTG at 0 h in the sample indicated (IPTG). Tep1 inhibits *E. coli* from both the cytosol and periplasm. (B) Tep2 does not inhibit *E. coli*. (C) Tae4 inhibits *E. coli* from the periplasm. (D) Tep5 inhibits *E. coli* from the periplasm. ss=signal sequence, *trxA*=thioredoxin A, a non-toxic control.

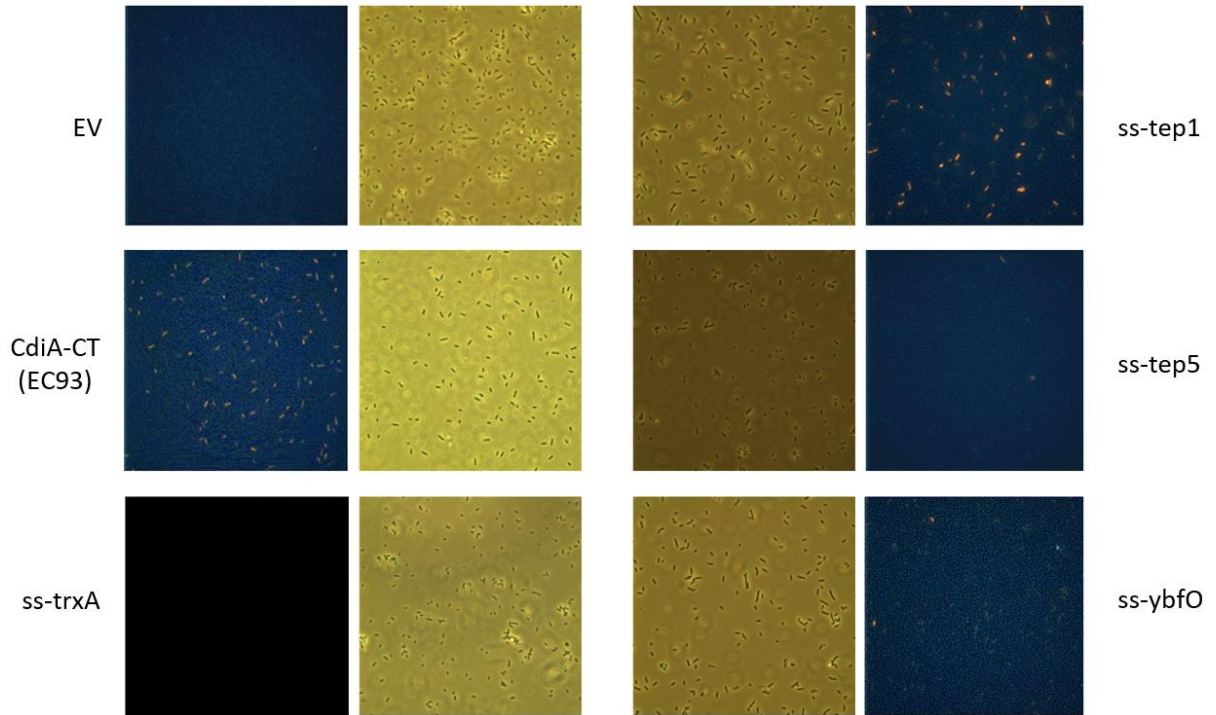


**Figure 2.5. Tep1 prevents ethidium bromide efflux in *E. coli*, suggesting it is a pmf-dissipating toxin.** Wet-mounted fluorescence microscopy of ethidium-bromide-treated *E. coli* expressing the indicated plasmid constructs. Outside panels are fluorescent images indicating ethidium bromide retention. Inside panels are brightfield images indicating cell density. CdiA-CT<sub>EC93</sub> is a known pmf-dissipating toxin. YbfO is a predicted cell-wall-degrading toxin. EV=empty vector, ss=signal sequence.

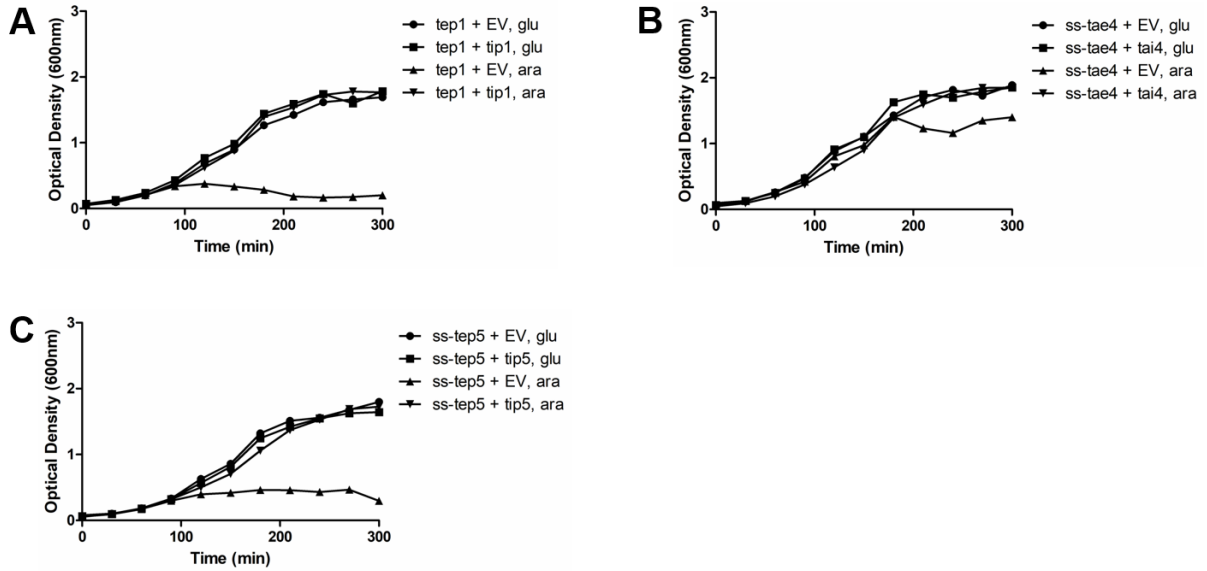


**Figure 2.6. Expression of immunity proteins block the toxicity of the Hcp-linked effectors in *E. coli*.** Cell densities as measured by OD600 over time. Intracellular expression of indicated toxin was induced (ara) or repressed (glu) at 0 h in *E. coli*. Immunities were expressed on a separate plasmid without induction. (A) Tip1 protects against cytoplasmically-expressed Tep1. (B) Tai4 protects against periplasmically-expressed Tae4. (C) Tip5 protects against periplasmically-expressed Tep5. EV=empty vector, ss=signal sequence, glu=0.4% D-glucose, ara=0.4% L-arabinose.

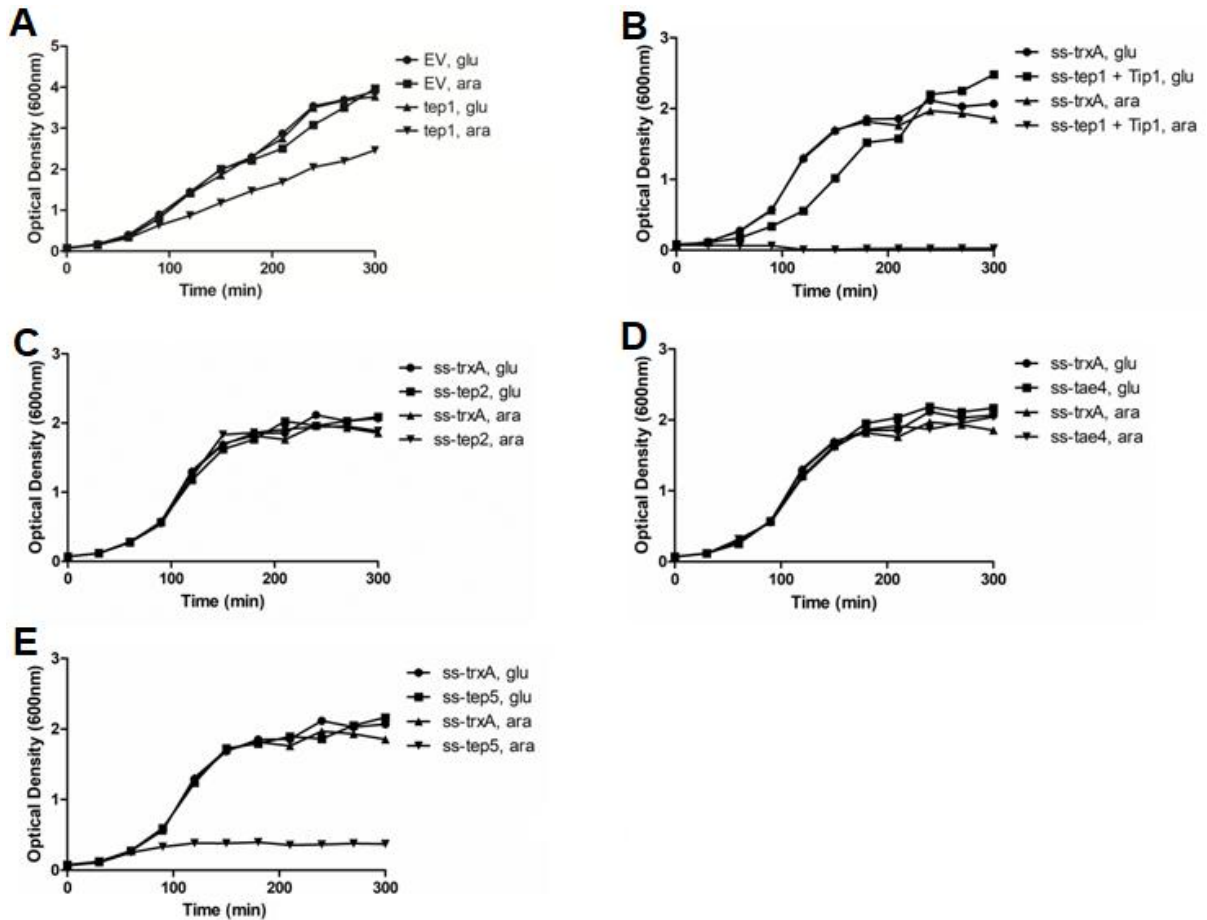


**Figure 2.7. Hcp-linked immunities encoded outside T6SS-1 do not appear to be expressed in *E. cloacae*.** Cell densities as measured by OD600 over time. Intracellular expression of indicated toxin was induced (ara) or repressed (glu) at 0 h in *E. cloacae*. (A) Chromosomal *tip1* does not protect against cytoplasmically-expressed Tep1. (B) Chromosomal *tip1* does not protect against periplasmically-expressed Tep1, even when given an additional plasmid copy of *tip1*. (C) Periplasmically-expressed Tep2 is not toxic to *E. cloacae*. (D) Native expression of chromosomal *tai4* is able to protect against periplasmically-expressed Tae4. (E) Chromosomal *tip5* does not protect against periplasmically-expressed Tep5. WT=wild-type, EV=empty vector, ss=signal sequence, *trxA*=thioredoxin A, a non-toxic control, glu=0.4% D-glucose, ara=0.4% L-arabinose.

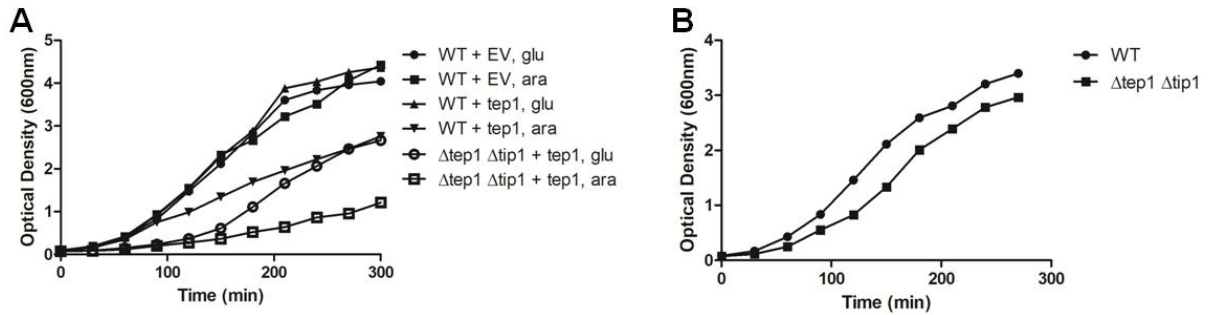


**Figure 2.8. Chromosomal *tip1* does not appear to protect *E. cloacae* from *Tep1* inhibition.** Cell densities as measured by OD600 over time. (A) Chromosomal *tip1* does not appear to provide much, if any, protection against cytoplasmically-expressed *Tep1*. However, the  $\Delta\textit{tep1} \Delta\textit{tip1}$  strain suffers a growth defect, complicating analyses dependent on growth rate. The growth defect is likely further impaired by plasmid burden. Intracellular expression of indicated toxin was induced (ara) or repressed (glu) at 0 h in *E. cloacae*. (B) Parental *E. cloacae* grows faster than the  $\Delta\textit{tep1} \Delta\textit{tip1}$  mutant. Strains were grown in the absence of antibiotic or supplemented sugar. WT=wild-type, EV=empty vector, glu=0.4% D-glucose, ara=0.4% L-arabinose.

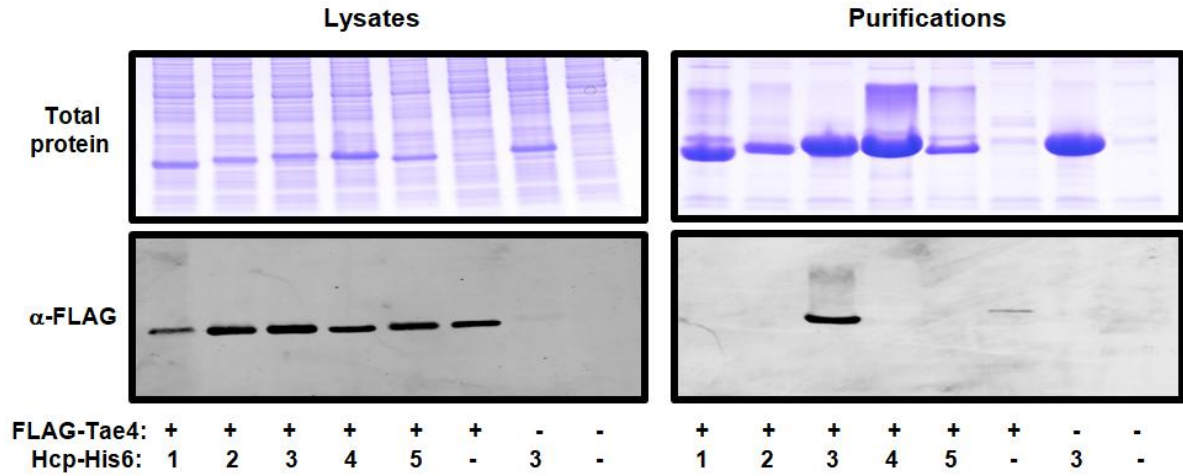


**Figure 2.9. Tae4 interacts with only its cognate Hcp.** Co-expression of the indicated Hcp-His6 construct (or empty vector) and FLAG-Tae4 construct (or empty vector) in *E. coli*. Cells were lysed and subjected to Ni-NTA pulldown. Input (lysate) and bound (purification) fractions were analyzed via SDS-PAGE, Coomassie staining, and α-FLAG immunoblot.

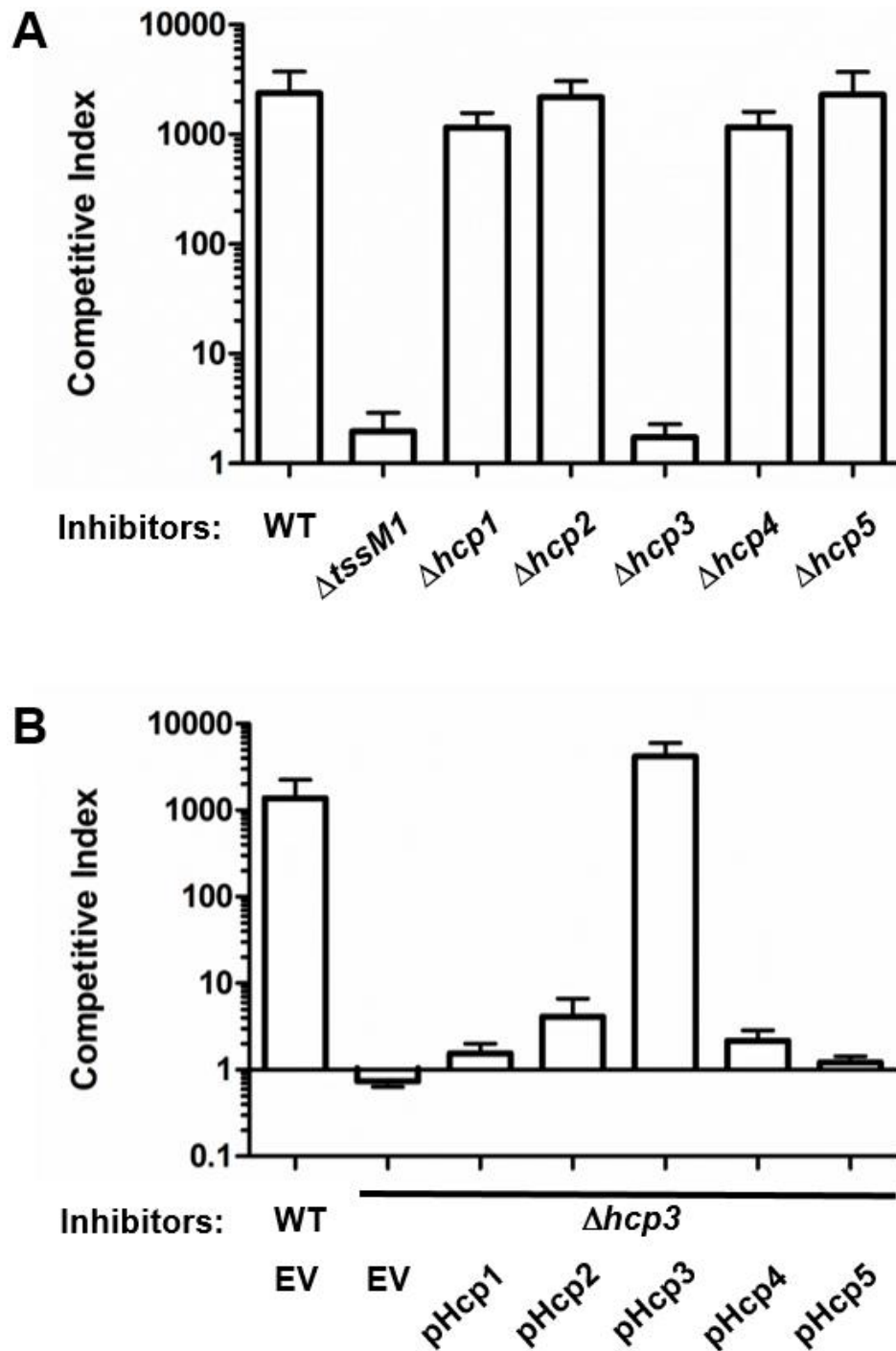


**Figure 2.10. The T6SS-1 apparatus requires Hcp3.** Indicated *E. cloacae* inhibitors were incubated at a 1:1 ratio with *E. coli* target cells for 4 hours. Data represent the average and standard error of the mean for three independent experiments. (A) Hcp3 is the only Hcp required for T6S under laboratory conditions. (B) Indicated *E. cloacae* inhibitors carrying plasmid-expressed Hcp versus *E. coli* targets. Hcp3 is the only Hcp that supports T6S under laboratory conditions. WT=wild-type, EV=empty vector.

**A**

```

ECL_Hcp3_T6SS1      1  MAIDMELKVV--FG---VTCESKDSNHTCWDITTSFHWGASCFGNMSYGGGGGAEKVNFNDA
ECL_Hcp1            1  -SNPBYLELDENCSPLVCPCLVSGREGATEIKSETHNWNIPVWGNTGK--LTGTRHHEE
ECL_Hcp5            1  MAIPVYLWLKDDAGNLIKGSVDWEREGSIELEKLETHNLSIFVWDTGTS--LTGTRHHEE
ECL_Hcp4            1  -AIPVYLELDGDDGAKIDGSDVDHDEREGSIEVTFTHNLRIPVDTALTGR--LTGTRHHEE
ECL_Hcp2            1  -AIPVYLLWPKDDGGANIDGSDVDHDEREGSIEVTFGCHLHLPTDSATGK--LTGTRHHEE
Eh49162_Hcp_T6SS2  1  MAIPVYLLWPKDDGGADIDGSDVDHDEREGSIEVTFQBNHLYIPTDNNITGK--LTGTRHHEE
EhNI1077_Hcp_T6SS2 1  MAIPVYLLWPKDDGGADIDGSDVDHDEREGSIEVTFQBNHLYIPTDNNITGK--LTGTRHHEE

ECL_Hcp3_T6SS1      56  HVNALIDRSSTALDRHCASGKHLIKVLELV--CKAGGQVEYSRITLEDVIVTSWQYTG
ECL_Hcp1            58  VMFCKEEDRWVTPFLFRALSTGRILCSATIRMYCINAGLECEYFNIMENVKITSITEDT
ECL_Hcp5            59  FVFKKEIDSSSPYLKAVATGQILKSAEYKWHINDAGOEVEYFNILLESVKVVSITPDM
ECL_Hcp4            58  IVFKKEIDSSSPYLKAVATGQILKSAEYKWHINDAGOEVEYFNHLNLRVVSVTEPLM
ECL_Hcp2            58  LVFKKEIDSSSPYLKAVATGQILKSAEYKWHINDAGOEVEYFNMLEGVKVVSVCPDM
Eh49162_Hcp_T6SS2  59  FVFKKEIDSSSPYLKAVATGQILKSAEYKWHINDAGOEVEYFNKLENVKLVKVNPRM
EhNI1077_Hcp_T6SS2  59  FVFKKEIDSSSPYLKAVATGQILKSAEYKWHINDAGOEVEYFNKLENVKLVKVNPRM

ECL_Hcp3_T6SS1      114  AINGITVGV---VIYAFQAAIVKQOYWEQITSGGKGAESAGGNIENKEA
ECL_Hcp1            118  YP---GANITGHELETLRYEKITWKHCDG---NIIISDSWNERATY--
ECL_Hcp5            119  HDTRNCP--GTGHEESTLRYEKITWRVWDG---NIIISDSWNERATV--
ECL_Hcp4            118  HDTKDQTEKHNHLEWELRYEKITWVWCDG---NIIISDSWNERATY--
ECL_Hcp2            118  HDVVDPTTEKHNHLEESTLRYEKITWVWCDG---NIIISDSWNERATY--
Eh49162_Hcp_T6SS2  119  HDTKDPAFEKHNHLEESTLRYEKITWVWCDG---NIIISDSWNERATA--
EhNI1077_Hcp_T6SS2  119  HDTKDPAFEKHNHLEESTLRYEKITWVWCDG---NIIISDSWNERATA--

```

**B**

ECL_Hcp3	100%						
ECL_Hcp1	16.45%	100%					
ECL_Hcp5	19.87%	53.16%	100%				
ECL_Hcp4	22.01%	46.83%	59.74%	100%			
ECL_Hcp2	22.01%	47.46%	61%	71.06%	100%		
Eh49162_Hcp_T6SS2	19.87%	51.26%	67.7%	70.44%	71.69%	100%	
EhNI1077_Hcp_T6SS2	19.87%	51.26%	67.7%	70.44%	71.06%	99.38%	100%
	ECL_Hcp3	ECL_Hcp1	ECL_Hcp5	ECL_Hcp4	ECL_Hcp2	Eh49162_Hcp_T6SS2	EhNI1077_Hcp_T6SS2

**Figure 2.11. The Hcp proteins encoded outside T6SS-1 are related to the ancestral T6SS-2 Hcp protein.** (A) Multiple sequence alignment of all 5 Hcp proteins in *E. cloacae* (ECL) and Hcp proteins encoded in T6SS-2 of 2 different strains of *E. hormaechei* (Eh). Protein sequences were aligned using Clustal Omega and rendered in BoxShade. (B) Pairwise comparison values of the sequence identity of the 7 indicated Hcp proteins. Comparisons were calculated using the SIAS pairwise alignment server.



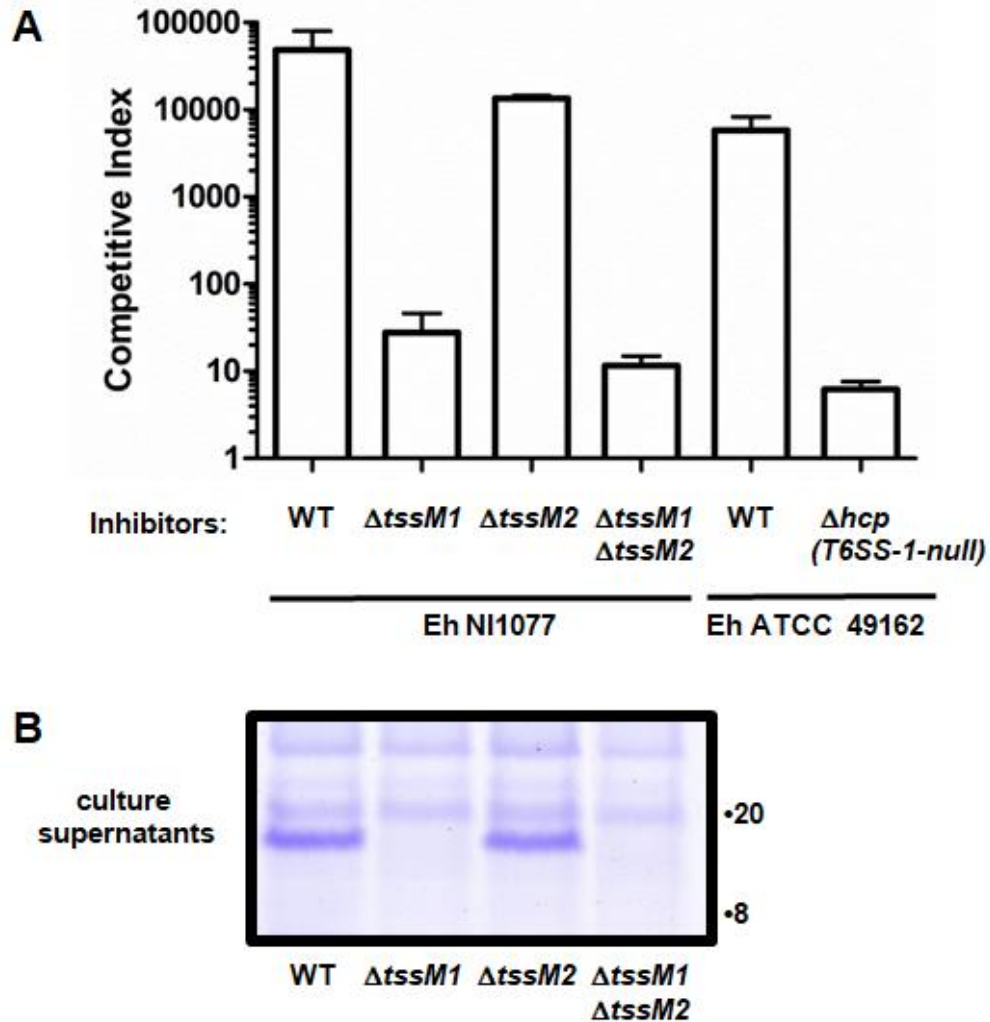


**Figure 2.13. The *E. hormaechei* T6SS-2 apparatus is not active under laboratory conditions.** (A) The T6SS-2 locus in both *E. hormaechei* strains does not contribute to significant inhibition of targets under laboratory conditions. Indicated *E. hormaechei* (Eh) inhibitors were incubated at a 1:1 ratio with *E. coli* target cells for 4 hours. Data represent the average and standard error of the mean for three independent experiments. (B) The T6SS-1 locus from *E. hormaechei* NI1077 contributes to most or all Hcp secretion observed by the strain. Culture supernatants from indicated *E. hormaechei* NI1077 strains were ethanol-precipitated and analyzed via SDS-PAGE and Coomassie staining. Hcp has a predicted molecular weight of ~19 kDa. WT=wild-type.

**Table 2.2. Bacterial strains used in this study.**

Strain	Description <sup>a</sup>	Reference
X90	<i>E. coli</i> F' <i>lacIq lac' pro'/ara</i> $\Delta$ ( <i>lac-pro</i> ) <i>nal1 argE(amb) rif<sup>r</sup> thi-1</i> , Rif <sup>R</sup>	150
<i>E. cloacae</i> ATCC 13047	Type strain (ECL), Amp <sup>R</sup>	American Type Culture Collection
CH8163	ECL <i>rif<sup>r</sup></i> , Amp <sup>R</sup> Rif <sup>R</sup>	132
CH11196	ECL $\Delta$ <i>tssM1::kan</i> , Amp <sup>R</sup> Kan <sup>R</sup>	81
CH12037	ECL $\Delta$ <i>tssM2::kan</i> , Amp <sup>R</sup> Kan <sup>R</sup>	This study
CH12038	ECL $\Delta$ <i>tssM1</i> $\Delta$ <i>tssM2::kan</i> , Amp <sup>R</sup> Kan <sup>R</sup>	This study
CH11202	ECL $\Delta$ <i>tae4::spc</i> , Amp <sup>R</sup> Spec <sup>R</sup>	This study
CH11204	ECL $\Delta$ <i>tae4</i> $\Delta$ <i>tai4::kan</i> , Amp <sup>R</sup> Kan <sup>R</sup>	This study
CH11205	ECL $\Delta$ <i>tae4</i> $\Delta$ <i>tai4</i> , Amp <sup>R</sup>	This study
CH11876	ECL $\Delta$ <i>tle::kan</i> , Amp <sup>R</sup> Kan <sup>R</sup>	This study
CH11895	ECL $\Delta$ <i>tle</i> $\Delta$ <i>tli::spc</i> , Amp <sup>R</sup> Spec <sup>R</sup>	This study
CH11178	ECL $\Delta$ <i>rhsA::kan</i> , Amp <sup>R</sup> Kan <sup>R</sup>	81
CH11179	ECL $\Delta$ <i>rhsA</i> , Amp <sup>R</sup>	81
CH15044	ECL $\Delta$ <i>rhsA</i> $\Delta$ <i>tae4::spc</i> , Amp <sup>R</sup> Spec <sup>R</sup>	This study
CH11186	ECL $\Delta$ <i>rhsB::kan</i> , Amp <sup>R</sup> Kan <sup>R</sup>	81
CH11733	ECL $\Delta$ <i>rhsB</i> , Amp <sup>R</sup>	This study
CH15045	ECL $\Delta$ <i>rhsB</i> $\Delta$ <i>tae4::spc</i> , Amp <sup>R</sup> Spec <sup>R</sup>	This study
CH11748	ECL $\Delta$ <i>rhsB</i> $\Delta$ <i>rhsA::kan</i> , Amp <sup>R</sup> Kan <sup>R</sup>	This study
CH12493	ECL $\Delta$ <i>tep1::kan</i> , Amp <sup>R</sup> Kan <sup>R</sup>	This study
CH12498	ECL $\Delta$ <i>tep1</i> , Amp <sup>R</sup>	This study
CH12500	ECL $\Delta$ <i>tep1</i> $\Delta$ <i>tip1::kan</i> , Amp <sup>R</sup> Kan <sup>R</sup>	This study
CH11665	ECL $\Delta$ <i>tep2::kan</i> , Amp <sup>R</sup> Kan <sup>R</sup>	This study
CH11670	ECL $\Delta$ <i>tep2</i> , Amp <sup>R</sup>	This study
CH11699	ECL $\Delta$ <i>tep2</i> $\Delta$ <i>tip2::kan</i> , Amp <sup>R</sup> Kan <sup>R</sup>	This study
CH11208	ECL $\Delta$ <i>tep4::spc</i> , Amp <sup>R</sup> Spec <sup>R</sup>	This study
CH11212	ECL $\Delta$ <i>tep4</i> $\Delta$ <i>tip4::kan</i> , Amp <sup>R</sup> Kan <sup>R</sup>	This study
CH11644	ECL $\Delta$ <i>tep5::kan</i> , Amp <sup>R</sup> Kan <sup>R</sup>	This study
CH11675	ECL $\Delta$ <i>tep5</i> , Amp <sup>R</sup>	This study
CH11700	ECL $\Delta$ <i>tep5</i> $\Delta$ <i>tip5::kan</i> , Amp <sup>R</sup> Kan <sup>R</sup>	This study
CH11715	ECL $\Delta$ 02217: <i>kan</i> , Amp <sup>R</sup> Kan <sup>R</sup>	This study
CH11731	ECL $\Delta$ 02217 $\Delta$ 02217 <i>imm::spc</i> , Amp <sup>R</sup> Spec <sup>R</sup>	This study
CH11740	ECL $\Delta$ 02217 $\Delta$ 02217 <i>imm</i> , Amp <sup>R</sup>	This study
CH11901	ECL $\Delta$ 02217 $\Delta$ 02217 <i>imm</i> $\Delta$ 04194: <i>kan</i> , Amp <sup>R</sup> Kan <sup>R</sup>	This study
CH11922	ECL $\Delta$ 02217 $\Delta$ 02217 <i>imm</i> $\Delta$ 04194, Amp <sup>R</sup>	This study
CH11943	ECL $\Delta$ 02217 $\Delta$ 02217 <i>imm</i> $\Delta$ 04194 $\Delta$ 04194 <i>imm::kan</i> , Amp <sup>R</sup> Kan <sup>R</sup>	This study
CH11716	ECL $\Delta$ 03144: <i>kan</i> , Amp <sup>R</sup> Kan <sup>R</sup>	This study
CH1347	ECL $\Delta$ 03144, Amp <sup>R</sup>	This study

CH11902	ECL $\Delta 03144 \Delta 03145::kan$ , Amp <sup>R</sup> Kan <sup>R</sup>	This study
CH11714	ECL $\Delta 01556::kan$ , Amp <sup>R</sup> Kan <sup>R</sup>	This study
CH11807	ECL $\Delta 01556$ , Amp <sup>R</sup>	This study
CH11830	ECL $\Delta 01556 \Delta 01557::kan$ , Amp <sup>R</sup> Kan <sup>R</sup>	This study
CH6247	X90 (DE3) $\Delta rna \Delta slyD$ , Rif <sup>R</sup>	Fernando Garza-Sánchez
CH11472	ECL $\Delta hcp1::kan$ , Amp <sup>R</sup> Kan <sup>R</sup>	This study
CH11652	ECL $\Delta hcp2::kan$ , Amp <sup>R</sup> Kan <sup>R</sup>	This study
CH11199	ECL $\Delta hcp3::spc$ , Amp <sup>R</sup> Spec <sup>R</sup>	This study
CH11653	ECL $\Delta hcp4::kan$ , Amp <sup>R</sup> Kan <sup>R</sup>	This study
CH11654	ECL $\Delta hcp5::kan$ , Amp <sup>R</sup> Kan <sup>R</sup>	This study
MFD $_{pir}$	MG1655 RP4-2-Tc::[ $\Delta Mu1::aac(3)IV-\Delta aphA-\Delta nic35-\Delta Mu2::zeo$ ] $dapA::(erm-pir) \Delta recA$ , Apr <sup>R</sup> Zeo <sup>R</sup> Erm <sup>R</sup>	147
NI1077	<i>E. hormaechei</i> NI1077	151
CH13867	<i>E. hormaechei</i> NI1077 $\Delta tssM1$	This study
CH13279	<i>E. hormaechei</i> NI1077 $\Delta tssM2::spc$ , SpecR	This study
CH13868	<i>E. hormaechei</i> NI1077 $\Delta tssM2::spc \Delta tssM1$ , SpecR	This study
<i>E. hormaechei</i> ATCC 49162	Type strain	American Type Culture Collection
CH14728	<i>E. hormaechei</i> ATCC 49162 $\Delta hcp$ (T6SS1)	This study

<sup>a</sup>Abbreviations: Amp<sup>R</sup>, ampicillin-resistant; Kan<sup>R</sup>, kanamycin-resistant; Rif<sup>R</sup>, rifampicin-resistant; Spec<sup>R</sup>, spectinomycin-resistant; Apr<sup>R</sup>, aprimycin-resistant; Erm<sup>R</sup>, erythromycin-resistant; Zeo<sup>R</sup>, zeocin-resistant

**Table 2.3. Plasmids used in this study.**

Number	Description <sup>a</sup>	Reference
	pZS21, Kan <sup>R</sup>	152
	pCH450, Tet <sup>R</sup>	153
	pCH450kpn, Tet <sup>R</sup>	71
	pTrc99aCm, Cm <sup>R</sup>	71
	pKOBEG, Cm <sup>R</sup>	144
	pCP20, Amp <sup>R</sup> , Cm <sup>R</sup>	145
	pET21P (cloning vector), Amp <sup>R</sup>	154
	pBluescript II SK+ (cloning vector), Amp <sup>R</sup>	Stratagene
pCH12220	pET21P-K::wapA(M1-T504) (cloning vector), Amp <sup>R</sup>	Fernando Garza-Sánchez
pCH1272	pET24db:: <i>relE</i> (cloning vector), Kan <sup>R</sup>	Dan Bolon
pCH11207	pZS21:: <i>tai4</i> , Kan <sup>R</sup>	This study
pCH14299	pCH450kpn:: <i>tli</i> , Tet <sup>R</sup>	This study
pCH12799	pZS21:: <i>rhsIA</i> , Kan <sup>R</sup>	81
pCH11138	pTrc99aKX:: <i>rhsIB</i> , Cm <sup>R</sup>	81
pCH10524	pSCbadB2, Tp <sup>R</sup>	155
pCH12550	pSCbadB2:: <i>tep1</i> , Tp <sup>R</sup>	This study
pCH12835	pSCbadB2:: <i>dsbA(ss)-tep1</i> , Tp <sup>R</sup>	This study
pCH11465	pTrc99a:: <i>tip1</i> , Cm <sup>R</sup>	This study
pCH12551	pSCbadB2:: <i>tep2</i> , Tp <sup>R</sup>	This study
pCH12572	pSCbadB2:: <i>dsbA(ss)-tep2</i> , Tp <sup>R</sup>	This study
pCH11466	pTrc99a:: <i>tip2</i> , Cm <sup>R</sup>	This study
pCH12552	pSCbadB2:: <i>tae4</i> , Tp <sup>R</sup>	This study
pCH12573	pSCbadB2:: <i>dsbA(ss)-tae4</i> , Tp <sup>R</sup>	This study
pCH12553	pSCbadB2:: <i>tep5</i> , Tp <sup>R</sup>	This study
pCH12574	pSCbadB2:: <i>dsbA(ss)-tep5</i> , Tp <sup>R</sup>	This study
pCH11467	pTrc99a:: <i>tip5</i> , Cm <sup>R</sup>	This study
pCH10626	pSCbadB2:: <i>dsbA(ss)-trxA</i> , Tp <sup>R</sup>	Fernando Garza-Sánchez
pCH12101	pCH450:: <i>cdiA-CT<sub>EC93</sub></i> , Tet <sup>R</sup>	Zachary Ruhe
pCH10610	pSCbadB2:: <i>dsbA(ss)-ybfO</i> , Tp <sup>R</sup>	Fernando Garza-Sánchez
pCH1280	pFG21b, Amp <sup>R</sup>	156
pCH13253	pFG21b:: <i>FLAG-tep3</i> , Amp <sup>R</sup>	This study
pCH13662	pET24db:: <i>hcp1-His6</i> , Kan <sup>R</sup>	This study
pCH13663	pET24db:: <i>hcp2-His6</i> , Kan <sup>R</sup>	This study
pCH13613	pET24db:: <i>hcp3-His6</i> , Kan <sup>R</sup>	This study
pCH13521	pET24db:: <i>hcp4-His6</i> , Kan <sup>R</sup>	This study
pCH13614	pET24db:: <i>hcp5-His6</i> , Kan <sup>R</sup>	This study

pCH11917	pCH450kpn:: <i>hcp1</i> , Tet <sup>R</sup>	This study
pCH12737	pCH450kpn:: <i>hcp2</i> , Tet <sup>R</sup>	This study
pCH11201	pCH450:: <i>hcp3</i> , Tet <sup>R</sup>	This study
pCH11918	pCH450kpn:: <i>hcp4</i> , Tet <sup>R</sup>	This study
pCH12057	pCH450:: <i>hcp5</i> , Tet <sup>R</sup>	This study
pCH70	pKAN, Kan <sup>R</sup> , Amp <sup>R</sup>	143
pCH9384	pSPM, Spec <sup>R</sup> , Amp <sup>R</sup>	67
pCH11050	pKAN:: $\Delta$ ECL_01536 ( <i>tssM1</i> deletion), Kan <sup>R</sup> , Amp <sup>R</sup>	81
pCH12056	pKAN:: $\Delta$ ECL_01813 ( <i>tssM2</i> deletion), Kan <sup>R</sup> , Amp <sup>R</sup>	This study
pCH11270	pKAN:: $\Delta$ ECL_01543 ( <i>tai4</i> deletion), Kan <sup>R</sup> , Amp <sup>R</sup>	This study
pCH11848	pKAN:: $\Delta$ ECL_01553 ( <i>tle</i> deletion), Kan <sup>R</sup> , Amp <sup>R</sup>	This study
Not saved	pSPM:: $\Delta$ ECL_01554 ( <i>tli</i> deletion), Spec <sup>R</sup> , Amp <sup>R</sup>	This study
pCH10958	pKAN:: $\Delta$ ECL_01567 ( <i>rhsA</i> deletion), Kan <sup>R</sup> , Amp <sup>R</sup>	81
pCH11044	pKAN:: $\Delta$ ECL_03140 ( <i>rhsB</i> deletion), Kan <sup>R</sup> , Amp <sup>R</sup>	81
pCH11462	pKAN:: $\Delta$ ECL_00031 ( <i>tep1</i> deletion), Kan <sup>R</sup> , Amp <sup>R</sup>	This study
pCH11460	pKAN:: $\Delta$ ECL_00032 ( <i>tip1</i> deletion), Kan <sup>R</sup> , Amp <sup>R</sup>	This study
pCH11637	pKAN:: $\Delta$ ECL_00032 ( <i>tip1</i> deletion), Kan <sup>R</sup> , Amp <sup>R</sup>	This study
pCH11490	pKAN:: $\Delta$ ECL_00032 ( <i>tip1</i> deletion), Kan <sup>R</sup> , Amp <sup>R</sup>	This study
pCH11272	pKAN:: $\Delta$ ECL_02156 ( <i>tip4</i> deletion), Kan <sup>R</sup> , Amp <sup>R</sup>	This study
pCH11638	pKAN:: $\Delta$ ECL_00032 ( <i>tip1</i> deletion), Kan <sup>R</sup> , Amp <sup>R</sup>	This study
pCH11461	pKAN:: $\Delta$ ECL_03985 ( <i>tip5</i> deletion), Kan <sup>R</sup> , Amp <sup>R</sup>	This study
pCH11849	pKAN:: $\Delta$ ECL_02217, Kan <sup>R</sup> , Amp <sup>R</sup>	This study
pCH11859	pSpm:: $\Delta$ ECL_02217imm (ORF not annotated), Spec <sup>R</sup> , Amp <sup>R</sup>	This study
pCH11873	pKAN:: $\Delta$ ECL_04194, Kan <sup>R</sup> , Amp <sup>R</sup>	This study
pCH11874	pKAN:: $\Delta$ ECL_04194imm (ORF not annotated), Kan <sup>R</sup> , Amp <sup>R</sup>	This study
pCH11871	pKAN:: $\Delta$ ECL_03144, Kan <sup>R</sup> , Amp <sup>R</sup>	This study
pCH11872	pKAN:: $\Delta$ ECL_03145, Kan <sup>R</sup> , Amp <sup>R</sup>	This study
pCH11869	pKAN:: $\Delta$ ECL_01566, Kan <sup>R</sup> , Amp <sup>R</sup>	This study
pCH11870	pKAN:: $\Delta$ ECL_01567, Kan <sup>R</sup> , Amp <sup>R</sup>	This study
pCH11453	pKAN:: $\Delta$ ECL_00033 ( <i>hcp1</i> deletion), Kan <sup>R</sup> , Amp <sup>R</sup>	This study
pCH11454	pKAN:: $\Delta$ ECL_01377 ( <i>hcp2</i> deletion), Kan <sup>R</sup> , Amp <sup>R</sup>	This study
pCH11455	pKAN:: $\Delta$ ECL_02155 ( <i>hcp4</i> deletion), Kan <sup>R</sup> , Amp <sup>R</sup>	This study
pCH11456	pKAN:: $\Delta$ ECL_03984 ( <i>hcp5</i> deletion), Kan <sup>R</sup> , Amp <sup>R</sup>	This study

pDL6480	pRE118-pheS*, Kan <sup>R</sup>	David Low
pCH13372	pRE118-pheS*:: $\Delta$ tssM1 (NI1077), Kan <sup>R</sup>	This study
pCH13252	pRE118-pheS*:: $\Delta$ tssM2::spc (NI1077), Kan <sup>R</sup> , Spec <sup>R</sup>	This study
pCH14675	pRE118-pheS*:: $\Delta$ hcp(T6SS1) (ATCC 49162), Kan <sup>R</sup>	This study

<sup>a</sup>Abbreviations: Amp<sup>R</sup>, ampicillin-resistant; Cm<sup>R</sup>, chloramphenicol-resistant; Kan<sup>R</sup>, kanamycin-resistance; Tet<sup>R</sup>, tetracycline-resistant; Spec<sup>R</sup>, spectinomycin-resistant; Tp<sup>R</sup>, trimethoprim-resistant

**Table 2.4. Oligonucleotides used in this study.**

<b>Number</b>	<b>Name<sup>a</sup></b>	<b>Sequence<sup>b</sup></b>	<b>Reference</b>
CH2952	pKAN-OE-for	5' - CCG CTC TAG AAC TAG TGG	This study
CH2953	pKAN-OE-rev	5' - GTC GAC GGT ATC GAT AAG C	This study
CH2792	Tai4-Eco-for	5' - TTT <u>GAA TTC</u> TTC TGG AGC CTG AAA TGA AAA AG	This study
CH2793	Tai4-Bam-rev	5' - TTT <u>GGA TCC</u> CTA CTT TGA GGA TTT GAG TGG	This study
CH3418	Tli-Kpn-for	5' - GAG <u>GGT ACC</u> ATG AAA TCG TTC TTA TCA GGC	This study
CH3419	Tli-Xho-rev	5' - ATA <u>CTC GAG</u> CTA TTT AAC CGG AGT TGG TG	This study
CH3776	Tep1-Nco-for	5' - ACG <u>CCA TGG</u> AAG CAT CTG ATT ACT TGA AGA TGA AG	This study
CH3777	Tep1-Hind-rev	5' - AAT <u>AAG CTT</u> CAG ACT CTT AAA CAT GCT ATT TAT CC	This study
CH3123	Tip1-Kpn-for	5' – ATA <u>GGT ACC</u> ATG TTT AAG AGT CTG CTA TCC A	This study
CH3124	Tip1-Xho-rev	5' – TTA <u>CTC GAG</u> TCA ATC GTA CTT ATC AAA GCG	This study
CH3778	Tep2-Nco-for	5' - GAC <u>CCA TGG</u> TCC GTT GCT ATT TTC ATA TGA ATA ATG	This study
CH3779	Tep2-Hind-rev	5' - ACT <u>AAG CTT</u> ACG GGT TTC ATC AGT AGA CC	This study
CH3125	Tip2-Kpn-for	5' – GGT <u>GGT ACC</u> ATG AAA CCC GTT CAC TCA G	This study
CH3126	Tip2-Xho-rev	5' – ATG <u>CTC GAG</u> TCA ATA TCT CTT TGT TCG TAC GAT G	This study
CH3780	Tae4-Nco-for	5' - ACA <u>CCA TGG</u> CTC ATA TGC GTC CTG CTT TTG	This study
CH3781	Tae4-Hind-rev	5' - AGA <u>AAG CTT</u> GCA ATG GCT TTT TCA TTT CAG G	This study

CH3782	Tep5-Nco-for	5' - TGT <u>CCA TGG</u> ATA CCG TCG AGG CGC	This study
CH3783	Tep5-Hind- rev	5' - AGC <u>AAG CTT</u> CTC TTG TTC AGT TAC CAT ATC CG	This study
CH3127	Tip5-Kpn-for	5' - AGA <u>GGT ACC</u> ATG GTA ACT GAA CAA GAG GTT T	This study
CH3128	Tip5-Xho-rev	5' - TCC <u>CTC GAG</u> TTA ATC ATA TAA CCA TCT TCC CGC	This study
CH3995	FLAG-Tep3- Spe-for	5' - AGA <u>ACT AGT</u> ATG TCT CAT ATG CGT CC	This study
CH3544	Hcp1-Kpn-for	5' - TTT <u>GGT ACC</u> ATG TCA AAT CCG GCT TAT TTG	This study
CH3999	Hcp1-H6- Xho-rev	5' - CAC <u>CTC GAG</u> GTA TGT TGC TCG CTC AT	This study
CH3546	Hcp2-Kpn-for	5' - TTT <u>GGT ACC</u> ATG GCT ATA CCC GCA TAT C	This study
CH4000	Hcp2-H6- Xho-rev	5' - AAC <u>CTC GAG</u> TCT GTC TGC CCA AGA ATC	This study
CH3020	Hcp3-Nco-for	5' - ATA <u>CCA TGG</u> CTA TTG ATA TGT TTC	This study
CH3022	Hcp3-H6- Xho-rev	5' - CTA <u>CTC GAG</u> TGC TTC TTT GTT TTC TTT G	This study
CH2962	Hcp4-Kpn-for	5' - GAG <u>GGT ACC</u> ATG GCA ATT CCT GTA TAT CTT TTC	This study
CH4001	Hcp4-H6- Xho-rev	5' - GCA <u>CTC GAG</u> ACG CTCT GCC CAG	This study
CH3651	Hcp5-Nco-for	5' - TTT <u>CCA TGG</u> CTG TAC CGG TCC	This study
CH4002	Hcp5-H6- Xho-rev	5' - TGC <u>CTC GAG</u> AAC CGT AG CTC GCT C	This study
CH3545	Hcp1-Xho-rev	5' - TTT <u>CTC GAG</u> TTT AGT ATG TTG CTC GCT C	This study
CH3547	Hcp2-Xho-rev	5' - TTT <u>CTC GAG</u> ATC ATC TGT CTG CCC AAG	This study

CH3021	Hcp3- Xho-rev	5' - TTT <u>CTC GAG</u> CAC TAC TAT TAT GCT TCT TTG	This study
CH3548	Hcp4- Xho-rev	5' - TTT <u>CTC GAG</u> AAT TAA CGC TCT GCC CAG	This study
CH3652	Hcp5- Xho-rev	5' - TTT <u>CTC GAG</u> GCA CTT CAA ACC GTA GC	This study
CH2897	TssM1-KO-Sac	5' - TTT <u>GAG CTC</u> GAA ATC GAC GCC GGT CTG	81
CH2898	TssM1-KO-Bam	5' - TTT <u>GGA TCC</u> TTT CCT TGC GGC AAT CCG	81
CH2899	TssM1-KO-Eco	5' - TTT <u>GAA TTC</u> CAA GGA CAG CCG TAT GAC	81
CH2900	TssM1-KO-Kpn	5' - TTT <u>GGT ACC</u> GAA TCG ACA TCA GCA TCT C	81
CH2976	TssM2-KO-Sac	5' - TTT <u>GAG CTC</u> GGC AAC CGC CTG ACA C	This study
CH2977	TssM2-KO-OE-rev	5' - CCA CTA GTT CTA GAG CGG CTT CCG TAG TCT TCG GTG C	This study
CH2978	TssM2-KO-OE-for	5' - GCT TAT CGA TAC CGT CGA CGG ACA GTA CGG AAA GCA G	This study
CH2979	TssM2-KO-Kpn	5' - TTT <u>GGT ACC</u> GCC GAG CCA TTC	This study
CH2964	Tae4-KO-Sac	5' - GGG <u>GAG CTC</u> CCC AGC CAG GTA ATA TG	This study
CH2965	Tae4-KO-OE-rev	5' - CCA CTA GTT CTA GAG CGG CTT GTT TCT CCT TGA AAA G	This study
CH2966	Tae4-KO-OE-for	5' - GCT TAT CGA TAC CGT CGA CAC CTT CTG GAG CCT GAA ATG	This study
CH2967	Tae4-KO-OE-rev	5' - TCT GAT AAT GAC CAG GCT CGG TAC C	This study
CH2968	Tai4-KO-OE-for	5' - GCT TAT CGA TAC CGT CGA CTA GTA AAG ATG AAA TCG GC	This study

CH2969	Tai4-KO-Kpn	5' - ATA <u>GGT ACC</u> GTC ACT TCG ATG CGG	This study
CH3373	Tle-KO-Sac	5' - CAA <u>GAG CTC</u> CGG GAT GGT TGC C	This study
CH3374	Tle-KO-Bam	5' - ATT <u>GGA TCC</u> GTC CTG TTA CCA GTC	This study
CH3375	Tle-KO-Xho	5' - AGG <u>CTC GAG</u> ACA TTT CAA TTA TTA GG	This study
CH3376	Tle-KO-Kpn	5' - AAC <u>GGT ACC</u> TGG CGA TAA ACC CGC	This study
CH3377	Tli-KO-Xho	5' - CCA <u>ACT CGA</u> GTT AAA TAG GAA ACG	This study
CH3378	Tli-KO-Kpn	5' - CCA <u>GGT ACC</u> AAA GTG CTG TGT GC	This study
CH2818	RhsA-KO-Sac	5' - TTT <u>GAG CTC</u> ATA CAC CCT CCA GGA AGG	81
CH2819	RhsA-KO- Bam	5' - TTT <u>GGA TCC</u> GCC TTA CAC ATT CCG GTT G	81
CH2820	RhsA-KO-Eco	5' - GAA <u>GAA TTC</u> TGG CAA GAG GAT TAC TTA ATG	81
CH2821	RhsA-KO-Kpn	5' - TTT <u>GGT ACC</u> CAT CAT TAG TAA TGC AAA G	81
CH2905	RhsB-KO-Sac	5' - TTT <u>GAG CTC</u> ACC CGC TCA ATG TCA GAA C	81
CH2906	RhsB-KO-Bam	5' - TTT <u>GGA TCC</u> CCC TGG TGT TAA TGG TGG	81
CH2907	RhsB-KO-Eco	5' - TTT <u>GAA TTC</u> CAA TGA ATA TGC TGA ATG TGA G	81
CH2908	RhsB-KO-Kpn	5' - TTT <u>GGT ACC</u> ACT TCG TCA TTA TCA TCT GC	81
CH3129	Tep1-KO-Sac	5' - GTT <u>GAG CTC</u> CTG ACG GCA CCAC C	This study

CH3130	Tep1-KO-Bam	5' – AGA <u>GGA TCC</u> CAT AAC GTA TCC ATA CTG TTT TTA TGG	This study
CH3131	Tep1-KO-Eco	5' – GAT <u>GAA TTC</u> GCT ATC TAT AAC GAC TTA AAG GAT AAA TAG	This study
CH3132	Tip1-KO-Eco	5' – ATT <u>GAA TTC</u> GCT TTG ATA AGT ACG ATT GAG TTT TA	This study
CH3133	Tip1-KO-Kpn	5' – AAA <u>GGT ACC</u> AGG GAT CAC GTT TTA GTA TGT TG	This study
CH3134	Tep2-KO-Sac	5' – ACA <u>GAG CTC</u> TCA AAC TCA CTG AAA AGG AGC	This study
CH3135	Tep2-KO-Bam	5' – GCA <u>GGA TCC</u> CAT CTG TCT GCC CAA GAA TC	This study
CH3136	Tep2-KO-Eco	5' – GCA <u>GAA TTC</u> AGG TCT ACT GAT GAA ACC C	This study
CH3137	Tip2-KO-Eco	5' – AAC <u>GAA TTC</u> ATA TTG ATT AGC GCA TTG TGA AAG	This study
CH3138	Tip2-KO-Xho	5' – ATC <u>CTC GAG</u> TGC AAA AAA TAA CGT TGA CTC ATC	This study
CH2970	Tep4-KO-Sac	5' - CAC <u>GAG CTC</u> GGT AGA TGT TCA TGA TC	This study
CH2971	Tep4-KO-OE- rev	5' - CCA CTA GTT CTA GAG CGG AAT TAA CGC TCT GCC CAG C	This study
CH2972	Tep4-KO-OE- for	5' - GCT TAT CGA TAC CGT CGA CGG TTT TTA ACT GGC GAG TC	This study
CH2973	Tep4-KO-Kpn	5' - CCC <u>GGT ACC</u> TAG CGT TGA TGA TCA G	This study
CH2974	Tip4-KO-OE- for	5' - GCT TAT CGA TAC CGT CGA CTC ATA AAC GCT ATT TAC CG	This study
CH2975	Tip4-KO-Kpn	5' - CCA <u>CCG GTA</u> CCG ACA GCG CAA GG	This study
CH3139	Tep5-KO-Sac	5' – TTA <u>GAG CTC</u> GTC ATA TGA CAG TTT CCA TTA AGT G	This study
CH3140	Tep5-KO-Bam	5' – GAC <u>GGA TCC</u> CAT ACA CAC CTT CAT AGC CAT T	This study

CH3141	Tep5-KO-Eco	5' – CAT <u>GAA TTC</u> GAC CGG ATA TGG TAA CTG AAC	This study
CH3142	Tip5-KO-Eco	5' – TGG <u>GAA TTC</u> GAT TAA TAA GGA GGA AAA TGA TGG C	This study
CH3143	Tip5-KO-Xho	5' – CAC <u>CTC GAG</u> CCG TAG CTC GCT CAT TC	This study
CH3385	02217-KO-Sac	5' - CAA <u>GAG CTC</u> GCG TGA GCA TGC GAC	This study
CH3386	02217-KO- Bam	5' - TTA <u>GGA TCC</u> GGT AAT TAG TAA ATT G	This study
CH3387	02217-KO- Xho	5' - TAA <u>CTC GAG</u> AAG CGG GGC TGT ACA AAT G	This study
CH3388	02217-KO- Kpn	5' - TTG AGA ATG <u>GTA CCA</u> GAA AAG CCC	This study
CH3389	02217imm- KO-Xho	5' - CTT <u>CTC GAG</u> TAT AAT TCT CAA TTC TC	This study
CH3390	02217imm- KO-Kpn	5' - GGT <u>CGG TAC CGC</u> ACT CTG AAG CGC	This study
CH3432	04194-KO-Sac	5' - GCC <u>GAG CTC</u> CCG CCG CAA CTG C	This study
CH3433	04194-KO- Bam	5' - GTT <u>GGA TCC</u> CAG CGG GTG AAC AAC AAC	This study
CH3434	04194-KO-Eco	5' - TAC <u>GAA TTC</u> TGA CAG TGA ATG TTG AAG CG	This study
CH3435	04194-KO- Kpn	5' - TAT <u>GGT ACC</u> CTG CAA AAA GCC CCT ACC	This study
CH3436	04194imm- KO-Eco	5' - GCA <u>GAA TTC</u> GTA GTG TTC AAT ATA AGC CCC G	This study
CH3437	04194imm- KO-Kpn	5' - TCC <u>GGT ACC</u> CTG GAA CTG AAG CAG GC	This study
CH3391	03144-KO-Sac	5' - GGT <u>GAG CTC</u> CGC ATA TGT GTT TAA GG	This study
CH3392	03144-KO- Bam	5' - CAT <u>GGA TCC</u> CTC TAC TTT ATA TGG	This study

CH3393	03144-KO-Eco	5' - AGA <u>GAA TTC</u> ATG AGG TTG TTA AAT AA	This study
CH3394	03144-KO-Kpn	5' - TCC <u>GGT ACC</u> TTT GCT TAA AGG G	This study
CH3395	03145-KO-Eco	5' - CAA <u>GAA TTC</u> AGG AAA AAA TTG ATT TTA	This study
CH3396	03145-KO-Kpn	5' - TTA <u>GGT ACC</u> TCG ATC CTT GCC G	This study
CH3379	01556-KO-Sac	5' - ACC <u>GAG CTC</u> TGG CTA ATC AGC GAA TG	This study
CH3380	01556-KO-Bam	5' - ACT <u>GGA TCC</u> CTC ATT TAA TCG ATT CG	This study
CH3381	01556-KO-Eco	5' - GAA <u>GAA TTC</u> CCT GAC GAG TTT TGA G	This study
CH3382	01556-KO-Kpn	5' - CAA <u>GGT ACC</u> GTC TGC TTA ATT TCG	This study
CH3383	01557-KO-Eco	5' - ATC <u>GAA TTC</u> AAG CAG ACG GTG AC	This study
CH3384	01557-KO-Kpn	5' - TGC <u>GGT ACC</u> GTC TGC CCC TGG	This study
CH3107	Hcp1-KO-Sac	5' - CAG <u>GAG CTC</u> TAG CGA TAG CAT GGA CG	This study
CH3108	Hcp1-KO-OE-rev	5' - CCA CTA GTT CTA GAG CGG CGGATT TGA CAT ACA AAC TCC	This study
CH3109	Hcp1-KO-Eco	5' - ATG <u>GAA TTC</u> CAA CAT ACT AAA ACG TGA TCC C	This study
CH3110	Hcp1-KO-Kpn	5' - AGC <u>GGT ACC</u> ACC CGC TCC CTG C	This study
CH3111	Hcp2-KO-Sac	5' - CAT <u>GAG CTC</u> CCT CTT CCC TCG CCT C	This study
CH3112	Hcp2-KO-Bam	5' - GGG <u>GGA TCC</u> CAT TCT GAA AGC TCC TTT TCA G	This study
CH3113	Hcp2-KO-Eco	5' - ATT <u>GAA TTC</u> CAG ACA GAT GAT CCG TTG C	This study

CH3114	Hcp2-KO-Kpn	5' – AGA <u>GGT ACC</u> CTG AGT GAA CGG GTT TCA TC	This study
CH2982	Hcp3-KO-Sac	5' - TTT <u>GAG CTC</u> CCA GGT GCA GGA GAT TC	This study
CH2981	Hcp3-KO-OE- rev	5' - CCA CTA GTT CTA GAG CGG CTA CTC TTC GTC GAT GAA C	This study
CH2980	Hcp3-KO-OE- for	5' - GCT TAT CGA TAC CGT CGA CGT AGT GGG TCC GAA AGG G	This study
CH2983	Hcp3-KO-Kpn	5' - AAA <u>GGT ACC</u> TTC CAG AGT GTT ACA TGC	This study
CH3115	Hcp4-KO-Sac	5' – CAC <u>GAG CTC</u> TTC CTG ATT TCC GCT GC	This study
CH3116	Hcp4-KO- Bam	5' – AGG <u>GGA TCC</u> CAT AGT CTA CTC ATC ATC CAT GT	This study
CH3117	Hcp4-KO-Eco	5' – TAG <u>GAA TTC</u> AGA GCG TTA ATT ATG CGT ACT C	This study
CH3118	Hcp4-KO-Kpn	5' - CAT <u>GGT ACC</u> CTG CAG GTT TTC ATA CAC G	This study
CH3119	Hcp5-KO-Sac	5' – CTG <u>GAG CTC</u> GCA TTG CCA CTT TAA AAC CTA AG	This study
CH3120	Hcp5-KO-Bam	5' – CGG <u>GGA TCC</u> CAT CAT TTT CCT CCT TAT TAA TCA TAT AAC	This study
CH3121	Hcp5-KO-Eco	5' – AGC <u>GAA TTC</u> CGG TTT GAA GTG CAA CAA AC	This study
CH3122	Hcp5-KO-Kpn	5' – GCG <u>GGT ACC</u> CGT GAA AAA CAT CAA GGT CAC	This study
CH4114	NI1077-tssM1- KO-Sac	5' - GAA <u>GAG CTC</u> ATT CAG CAG CCC GC	This study
CH4145	NI1077-tssM1- KO-OE-rev	5' - GGC TGT CCT TGC GGC CTT AGT TTC CTT GCG G	This study
CH4146	NI1077-tssM1- KO-OE-for	5' - CCG CAA GGA CAG CCG	This study
CH4115	NI1077-tssM1- KO-Kpn	5' - GTT <u>GGT ACC</u> AGC TTT CG	This study

CH4005	NI1077- tssM2-KO-Sac	5' - TTG <u>GAG CTC</u> ACT CTT CCT GTT GAA TAT GGT G	This study
CH4106	NI1077- tssM2-KO- OE-rev	5' - AAG GTA GCT TCA CGG A	This study
CH4107	NI1077- tssM2-KO- OE-for	5' - TCC GTG AAG CTA CCT TCG AAT AAT GGA CAC TTT ACA G	This study
CH4108	NI1077- tssM2-KO- Kpn	5' - AAA <u>GGT ACC</u> ACC GCA TCC ATG CCA	This study
CH4414	ATCC49162- Hcp-T6SS1- KO-Sac	5' - TGG <u>GAG CTC</u> TGA CCG TTT CCC TGC	This study
CH4415	ATCC49162- Hcp-T6SS1- KO-Bam	5' - CTC TTC GTG <u>GAT CCA</u> CAA TAT TGC TTT CG	This study
CH4416	ATCC49162- Hcp-T6SS1- KO-Eco	5' - AAA <u>GAA TTC</u> TAA CAG AAG TGG GCC CG	This study
CH4417	ATCC49162- Hcp-T6SS1- KO-Kpn	5' - GCC <u>GGT ACC</u> GCT AAA GAT AAT AAT ACC TTG	This study

<sup>a</sup>Abbreviations: OE=overlap-extension, Bam=BamHI, Eco=EcoRI, Hind=HindIII, Kpn=KpnI, Nco=NcoI, Sac=SacI, Spe=SpeI, Xho=XhoI

<sup>b</sup>Restriction endonuclease sites are underlined

### **Chapter 3: The effector Tle requires its cognate immunity for delivery in *E. cloacae***

Note: this project is a collaborative work in progress, and other members of the Hayes lab participated on this project. Fellow graduate student Steven Jensen is responsible for the work presented in Figure 3.3B and 3.3C, and additionally helped with strain and plasmid construction. Former graduate student Christina Beck is responsible for the work presented in Figure 3.4A, and additionally helped with strain and plasmid construction. Research associate Zachary Ruhe started this project, and contributed greatly to project ideas; he also helped with strain and plasmid construction.

## **Abstract**

Here, I investigate a number of molecular and biochemical questions pertaining to the biogenesis and delivery of *Enterobacter cloacae*'s T6SS lipase effector (Tle). I demonstrate that the cognate T6SS lipase immunity (Tli) protein promotes increased abundance of Tle. Moreover, Tli is required for Tle-dependent intoxication of neighboring cells in co-culture assays. Further experiments also demonstrate Tle assembles onto the T6SS apparatus, independent of Tli, via interaction with VgrG; however, subsequent secretion of Tle is Tli-dependent. In-gel mobility-shift assays suggest that Tle undergoes a Tli-dependent biochemical change that persists under denaturing conditions. While the nature of this change is currently unknown, this “converted” Tle protein is more soluble than its “unconverted” form. The converted Tle protein exhibits enzymatic activity, and preliminary data suggest only the converted form of Tle is secreted. Together, the data suggest Tli functions as a Tle-activator. This represents the first report of an immunity gene also functioning as an essential activation element for its cognate effector.

## Introduction

The phospholipid membrane of cells is a conserved hallmark of life on Earth, and represents a key barrier that compartmentalizes the cell away from outside forces. It is also a common target of viruses and antagonistic organisms that seek to enter, or otherwise introduce proteins, into the cell. The Gram-negative bacterial type VI secretion system (T6SS) has been shown to deploy lipases that degrade the membranes of both prokaryotic and eukaryotic organisms (63, 64, 65, 189). These lipases are often encoded adjacent to *vgrG* elements, which may suggest that these lipases are likely to assemble onto the T6SS apparatus via interaction with VgrG (63, 190, 191). Indeed, many lipases have been shown to interact with VgrG either directly or through adaptor proteins (64, 87, 89, 90, 192).

In Chapter 2, I presented data suggesting *Enterobacter cloacae* deploys a putative T6SS lipase effector (Tle), and that Tle-dependent intoxication of target cells can be blocked by expression of the cognate T6SS lipase immunity (Tli) protein (Figure 2.2C). During the investigation of the biogenesis and delivery of this Tle effector, I noticed a remarkable dependency on Tli for Tle-mediated intoxication of target cells. In this chapter, I present key findings that suggest this Tli immunity protein also behaves as an activator of Tle. Tli is required secretion of Tle via the T6SS. Additionally, Tle undergoes a Tli-dependent biochemical change that results in an increase in gel-mobility on SDS-PAGE. I believe this Tli-dependent biochemical change is necessary for the biogenesis of functional Tle.

## Results

### *Tli is an essential collaborator with Tle*

During the validation of a polyclonal *E. cloacae* Tli antibody, I found that this antibody does not detect Tli in  $\Delta tli$  strains, as expected (Figure 3.1A). However, I also noticed the antibody cross-reacts to a protein migrating significantly above Tli during SDS-PAGE. Curiously, this protein disappears when either Tle or Tli is deleted, suggesting it is not simply a  $\beta$ -ME-resistant Tli multimer, but is somehow dependent on Tle as well. This cross-reacting protein migrates around the expected size of Tle, so I reasoned the Tli antibody may be cross-reacting to Tle. To test this, I fused a FLAG epitope onto Tle and heterologously expressed this FLAG-Tle construct in laboratory *Escherichia coli* K-12 in the presence or absence of Tli (Figure 3.1B). I find that the Tle protein appears to co-label with both the FLAG and Tli antibodies, suggesting the Tli antibody does recognize Tle.

Additionally, co-expression of FLAG-Tle with Tli appears to promote increased abundance of Tle, consistent with the disappearance of the putative Tle band in *E. cloacae*  $\Delta tli$  cells observed in Figure 3.1A. Surprisingly, co-expression of FLAG-Tle with Tli promotes the formation of a faster-migrating species of Tle. The formation of this lower band, hereafter referred to as Tle<sup>lower</sup>, is the cause of the observed increase in Tle abundance, especially when Tle is being detected with the Tli antibody. These findings are also observed when FLAG-Tle is expressed in *E. cloacae*.

Next, I investigated whether these Tli-dependent changes to Tle are physiologically relevant. I deleted *tli* in inhibitor cells and asked whether this strain could still inhibit *E. cloacae*  $\Delta tle \Delta tli$  targets. Remarkably, I find that Tli is required for Tle-dependent intoxication of target cells (Figure 3.2). Complementation of *tli* in *trans* is sufficient to rescue this phenotype, indicating I did not simply introduce a polar mutation on the upstream *tle* effector.

### *Tli promotes the formation of a more soluble Tle species*

I next interrogated what biochemical changes are associated with Tle<sup>lower</sup>. Given that I first observed the formation of Tle<sup>lower</sup> using an N-terminal FLAG epitope fusion for detection, I reasoned that a truncation to the C-terminal end of Tle could explain the observed increase in gel mobility. Therefore, I generated a new Tle-FLAG construct with the epitope positioned at the C-terminal end of Tle. Interestingly, in the absence of Tli, this construct is more readily detected via immunoblot than the N-terminal FLAG-Tle construct counterpart (Figure 3.1B and 3.3A). This may suggest that the addition of the FLAG epitope to the C-terminal end of Tle may promote increased stability and/or solubility to the protein. When co-expressed with Tli, I find that Tle-FLAG also forms a doublet that co-labels with both FLAG and Tli antibodies (Figure 3.3A). This suggests both the N- and C-termini are still present on Tle<sup>lower</sup>, and that the increase in gel-mobility is due to a different, currently unexplained, biochemical change. However, the observed stoichiometry between Tle<sup>upper</sup> and Tle<sup>lower</sup> does not appear to be consistent when comparing the results of the FLAG antibody versus Tli antibody. This may suggest that Tle<sup>lower</sup> has

decreased FLAG-reactivity to the C-terminally-positioned FLAG epitope, potentially implicating the C-terminal region of Tle in this Tli-dependent biochemical change.

While I have established that Tli is required for *in vivo* Tle-dependent intoxication of susceptible target cells (Figure 3.2), this does not address whether Tle<sup>lower</sup> is the active form of Tle. Thus, I next set out to purify both forms of Tle in order to assay for *in vitro* catalytic activity. To do so, I co-expressed His6-Tle and Tli in *E. coli*, then Ni-affinity purified Tle under urea-denaturing conditions in order to remove Tli. Purified Tle was then dialyzed in water in order to remove denaturants. Notably, a lot of precipitate formed during dialysis, suggesting I purified insoluble protein. I therefore re-solubilized this post-dialysis precipitate in urea for SDS-PAGE analysis. I find that while both forms of Tle can be successfully purified under denaturing conditions, Tle<sup>lower</sup> is significantly more soluble than the unconverted form (Figure 3.3B). Further attempts to solubilize Tle<sup>upper</sup> have been largely unsuccessful (data not shown). This finding is consistent with Tle<sup>lower</sup> being the active form of Tle.

Next, I tested whether the soluble Tle<sup>lower</sup> species still retains catalytic activity. I find that Tle<sup>lower</sup> can successfully hydrolyze polysorbate 20, indicating this species of Tle retains esterase activity *in vitro* (Figure 3.3C). Furthermore, Tle activity can be blocked by co-incubating with purified Tli-H6, consistent with its role as the cognate immunity to Tle. However, it is still unclear whether Tle<sup>upper</sup> retains catalytic activity given the lack of success at solubilizing it.

### *Tli is required for secretion of Tle*

I next investigated whether Tli is required for assembly of Tle onto the T6SS apparatus. As the T6SS secreted complex consists of 3 structural proteins – Hcp, VgrG, and PAAR – I reasoned that Tle must interact with at least 1 of these 3 proteins. *E. cloacae* utilizes 1 Hcp protein (Hcp3), 2 VgrG proteins (VgrG1 and VgrG2) and 2 PAAR proteins (RhsA and RhsB) (Figure 2.1). Co-culture experiments suggest Tle has no genetic specificity for either VgrG1 or VgrG2, and again no specificity for either PAAR-containing protein RhsA or RhsB. (Figure 3.4A). In Chapter 4, I present data that the 2 VgrG proteins are redundant for each other in supporting T6SS activity, as are the 2 Rhs proteins. While the 2 Rhs proteins are highly divergent in primary sequence (Figure 3.4B), the 2 VgrG proteins are highly conserved and only differ in their C-terminal PAAR-binding domains (Figure 3.4C). Therefore, I reasoned Tle is likely to either interact with the N-terminal VgrG domains, or with Hcp3.

To test this, I heterologously co-expressed Tle-FLAG with either VgrG2-His6 or Hcp3-His6 in *E. coli*, in the presence or absence of Tli. I find that both forms of Tle interact with VgrG2, but neither interact with Hcp3, suggesting that Tle, like other lipases, is assembled onto the T6SS spike complex via interaction with VgrG (Figure 3.5A). Additionally, I find that Tli is not required for Tle assembly onto VgrG, suggesting the interaction between Tle and VgrG2 is direct. Next, I tested whether *E. cloacae* could successfully secrete FLAG-Tle in the absence of Tli: I find that Tli is required for secretion of Tle (Figure 3.5B). Additionally, only the Tle<sup>lower</sup> species appears to be secreted, again suggesting it is the functional form of Tle.

## Discussion

The work presented here demonstrates a novel phenomenon whereby an antibacterial effector is dependent on its cognate immunity for delivery. I find that *E. cloacae* Tli functions as a chaperone to solubilize Tle, and that Tli is required for T6SS-dependent secretion of Tle. Curiously, Tle undergoes a Tli-dependent biochemical change that results in a faster-migrating protein on SDS-PAGE (termed Tle<sup>lower</sup>). This distinct species of Tle is more soluble than its original form, and retains catalytic activity. Moreover, Tle<sup>lower</sup> appears to be the secreted form of Tle. Taken together, this suggests Tli functions as an activator of Tle, in addition to its canonical role as an immunity protein.

These findings represent the first report of an immunity gene also functioning as an essential activation element for its cognate effector. Other known T6SS lipases do not appear to be dependent on their cognate immunities for *in vivo* activity. For example, the *Pseudomonas aeruginosa* Tle<sub>5</sub> effector does not require its cognate Tli<sub>5</sub> for intoxication of neighbors (63). Additionally, a transposon-mutagenesis screen was utilized by Mekalanos and colleagues to identify novel immunity genes, such as the *Vibrio cholerae* T6SS lipase immunity TsiL: they identified new immunities by finding genetic loci that were essential for survival in T6SS+ *V. cholerae* cells but dispensable in T6SS- mutants (64). By using this approach, their data suggest that delivery of the lipase TseL is not dependent on its immunity.

Notably, a number of Tle effectors are encoded next to 2 or more tandem copies of *tli* (63, 65, 87). For example, *Dickeya dadantii* 3937 encodes a predicted Tle effector that is followed by 2 very similar proteins (67). These putative immunity

proteins are 78% identical, and diverge mostly at their N-terminal putative lipoprotein signal sequences (Figure 3.6A). Similarly, *Burkholderia thailandensis* E264 encodes a functional Tle that is preceded by 2 immunity genes (63). These Tli proteins are 56% identical, and also diverge significantly in their putative lipoprotein signal sequences (Figure 3.6B). Across all species, I expect that Tli must be exported to the cell periplasm in order to prevent auto-inhibition, but my findings suggest that a cytoplasmic pool of *E. cloacae* Tli also likely exists that converts Tle into its active form prior to secretion. An enticing model to explain these combined findings is that *D. dadantii* and *B. thailandensis* utilize different *tli* alleles to differentially localize these proteins either cytoplasmically or periplasmically. In contrast, *E. cloacae* only encodes a singular *tli* allele, but it encodes 4 distinct ATG codons in its first 24 codons, suggesting alternate translation start sites might be exploited in order to produce different localization pools of Tli (Figure 3.6C).

Currently, the biochemical nature of the Tli-dependent change to Tle is not understood. Given the increase in mobility on SDS-PAGE, a reasonable conjecture would be that Tle undergoes a truncation event, leading to a smaller species of protein. However, analysis of both N-terminal-FLAG-tagged and C-terminal-FLAG-tagged Tle constructs suggest both termini are present on Tle<sup>lower</sup>. It is possible, though seemingly unlikely, that an internal deletion event could occur in order to produce Tle<sup>lower</sup>. Another explanation may be that Tle<sup>lower</sup> is either folded or circularized, resulting in a smaller Stokes radius and faster mobility. Additionally, it is possible that the addition of a modifying group on Tle, such as phosphates, could sufficiently increase the charge density of the Tle to promote faster migration on SDS-PAGE. It is also unclear why Tle cross-reacts so readily with the anti-Tli

antibody. I will likely not know whether this antibody affinity is biologically relevant or not until the nature of the biochemical change to Tle is elucidated.

## **Materials and Methods**

### *Bacterial growth and conditions*

Bacteria were cultured in shaking lysogeny broth (LB) or on LB-agar at 37°C. Bacteria were supplemented with antibiotics at the following concentrations: 150 µg/mL ampicillin (Amp), 15 µg/mL gentamycin (Gent), 50 µg/mL kanamycin (Kan), 100 µg/mL spectinomycin (Spc), 200 µg/ml rifampicin (Rif), 25 µg/mL tetracycline (Tet), and 100 µg/ml trimethoprim (Tp).

### *Strain construction*

All bacterial strains, plasmids, and oligonucleotides used in this study are listed in Tables 3.1, 3.2, and 3.3. Gene-deletion constructs for *E. cloacae* were generated using overlap-extension PCR (OE-PCR) or via the plasmids pKAN or pSPM as described previously (67, 142, 143). Briefly, OE-PCR constructs were made with upstream and downstream homology PCR fragments overlapped to the CH2952/CH2953 PCR product amplified from either pKAN or pSPM. pKAN or pSPM plasmid constructs were generated by restriction cloning PCR fragments from upstream and downstream of the target gene into pKAN or pSPM to flank the antibiotic-resistance cassette. Restriction enzymes used are specified in the oligonucleotide names listed in Table 3.3.

Resulting constructs were PCR-amplified, DpnI-digested to remove methylated template DNA, then directly electroporated into *E. cloacae* cells expressing phage  $\lambda$ -Red recombinase proteins as described (144). Transformants were selected on LB-agar supplemented with either Kan or Spc. All chromosomal deletions were confirmed by whole-cell PCR analysis. Kan markers were cured as necessary via pCP20 (145).

For construction of *attTn7::tli* and *attTn7::( $\Delta$ ss)tli* mutants, MFD*pir* cells containing either plasmid pCH14683 or pCH14685, and MFD*pir* cells carrying the helper plasmid pTNS2, were bi-parentally mated with the respective recipient strain (194). Integrants were selected on LB-agar supplemented with Gent.

### *Plasmid construction*

All plasmids and oligonucleotides used in this study are listed in supplemental Tables 3.2 and 3.3. All PCR products were purified, digested with the restriction enzymes indicated in the oligonucleotide names (Table 3.3), and ligated to a vector treated with the same enzymes. Plasmids were confirmed by DNA sequencing (University of California, Berkeley). Plasmid transformations were performed by making strains TSS competent (148). Constructs were cloned directly into the final vector, with exceptions or complications described below.

To generate pCH11631 (pTrc99a::*hcp3-His6*), *hcp3* was PCR-amplified off *E. cloacae* using CH3020/CH3022 and restriction cloned with NcoI/XhoI into pCH6478. To generate pCH14981 (pTrc99a::*vgrG2-His6*), the VgrG2-VSV fusion

construct was PCR-amplified off CH12884 (see Chapter 4 methods) using CH4452/CH4453 and restriction cloned using EcoRI/XhoI into pCH3257 to generate pCH14231. Next, the VSV tag was swapped to a His6 tag by moving the EcoRI/SpeI restriction dropout from pCH14231 into pCH6672 to generate pCH2254. Finally, the EcoRI/XhoI restriction dropout from pCH2254 was moved into pTrc99a to generate pCH14981.

### *Competitions*

Indicated *E. cloacae* strains were used as inhibitor cells on LB-agar co-cultures against indicated *E. cloacae* targets. Cells were grown in LB-medium (supplemented with appropriate antibiotics when plasmid-bearing) to log phase, then collected by centrifugation and resuspended in 1x M9 salts. Inhibitors and targets were mixed 1:1 at OD 17 each (200 uL total volume), then 100 uL of the mixture was spread on LB-agar without antibiotics and incubated at 37°C for 3 or 4 h (as indicated). Culture aliquots were taken at the beginning and end of the co-culture to quantify viable inhibitor and target cells as colony forming units. At the end of co-cultures, cells were harvested in 1.5 mL of 1x M9 salts. For competitions with plasmid-induced proteins, inhibitors were grown in LB-medium supplemented with 0.4% L-arabinose and Tet. Co-cultures were then performed as above on LB-agar supplemented with 0.4% L-arabinose.

For all competitions, cell suspensions were serially diluted into 1x M9 salts and plated onto LB-agar supplemented with appropriate antibiotics to separately

enumerate inhibitor and target cells. Competitive indices were calculated as the ratio of inhibitor to target cells at 3 or 4 h divided by the initial inhibitor to target cell ratio.

### *Immunoblots*

Cell cultures were grown to log phase in LB-medium supplemented with appropriate antibiotics, and additionally 0.4% L-arabinose when indicated, then collected by centrifugation at 3,000  $xg$  for 5 min. Cell pellets were then resuspended in urea-lysis buffer [50% urea, 150 mM NaCl, 20 mM Tris-HCl (pH 8.0)] and subjected to a freeze-thaw cycle to extract proteins. Samples were analyzed by SDS-PAGE on Tris-tricine polyacrylamide gels run at 110 V (constant). The polyacrylamide concentration for experiments in Figure 3.5 was 7%; for all other immunoblots, the gels were made at a 10% polyacrylamide concentration. All gels were run for 1 hr 15 min, with the exception of Figure 3.1A, which was run for 1 h 50 min.

Gels were soaked for 10 min in 25 mM Tris, 192 mM glycine (pH 8.6), 20% methanol, then electroblotted to nitrocellulose (Figure 3.1A) or low-fluorescence PVDF (all other immunoblot experiments) membranes using a semi-dry transfer apparatus at 17 V (constant) for 30 min. Membranes were then blocked with 4% non-fat milk in PBS for 30 min at room temperature, and incubated with primary antibodies in 0.1% non-fat milk in PBS overnight at 4°C. Rabbit polyclonal antisera (Cocalico Biologicals, Stevens, PA) to Tli-His6 was used at a 1:5,000 dilution and

mouse anti-FLAG (Sigma) was used at a 25,000 dilution. Blots were incubated with 800CW-conjugated goat anti-rabbit IgG (1:125,000 dilution, LICOR) or 680LT-conjugated goat anti-mouse IgG (1:125,000 dilution, LICOR) in PBS. Immunoblots were visualized with a LI-COR Odyssey infrared imager.

### *Ni<sup>2+</sup>-affinity purifications*

For Tle interaction experiments (Figure 3.5A), *E. coli* K12 strain CH2016 carrying indicated plasmids were grown to log phase in LB-medium supplemented with appropriate antibiotics, then protein expression was induced with 0.4% L-arabinose for 2 h. Cells were collected by centrifugation and resuspended in binding buffer [20 mM sodium phosphate (pH 7.0), 150 mM NaCl, 30 mM imidazole, 0.05% Triton X-100]. Each cell suspension was broken by 2 passages through a French press, then insoluble debris was removed via centrifugation at 23,000 *xg* for 10 min at 4°C. The clarified lysate was added to Ni<sup>2+</sup>-NTA agarose resin (Thermo Fisher Scientific) and incubated on a rotisserie for 1 h at 4°C. Following incubation, the beads were washed extensively in binding buffer, then eluted in binding buffer supplemented with 20 mM EDTA. Samples were analyzed by SDS-PAGE and immunoblot, as described above.

For purification of His6-Tle for *in vitro* esterase analysis, *E. coli* K12 strain CH2016 carrying pET21P::*His6-tle* and pCH450::( $\Delta$ ss)*tli* was grown to log phase in medium supplemented with Amp and Tet, then *tli* expression was induced with 0.4% L-arabinose for 1.5 h and *tle* expression was induced with 1.5 mM Isopropyl-beta-D-

thiogalactoside (IPTG) for 30 min. Cells were collected by centrifugation and resuspended in purification buffer [20 mM sodium phosphate (pH 7.0), 150 mM NaCl, 30 mM imidazole]. Each cell suspension was broken by 2 passages through a French press, then insoluble debris was removed via centrifugation at 23,000  $xg$  for 10 min at 4°C. The clarified lysate was added to Ni<sup>2+</sup>-NTA agarose resin (Thermo Fisher Scientific) and incubated on a rotisserie for 1.5 h at 4°C. Following incubation, the beads were washed extensively in guanidine wash buffer (6M guanidine, 20 mM imidazole), then eluted in urea-lysis buffer supplemented with 25 mM EDTA. Proteins were subsequently dialyzed in water overnight at 4°C. Soluble Tle was subsequently used in the *in vitro* esterase assay described below. Dialysis precipitate was resuspended in urea-lysis buffer. Samples were analyzed by SDS-PAGE on 10% Tris-tricine polyacrylamide gels run at 110 V (constant) for 2 h, then stained with Coomassie brilliant blue dye.

For purification of ( $\Delta$ ss)Tli-His6 for *in vitro* esterase analysis, *E. coli* K12 strain CH2016 carrying pET21P::( $\Delta$ ss)tli-His6 was grown to log phase in medium supplemented with Amp, then expression was induced with 1.5 mM IPTG for 1 h. Cells were collected by centrifugation and resuspended in purification buffer. Each cell suspension was broken by 2 passages through a French press, then insoluble debris was removed via centrifugation at 23,000  $xg$  for 10 min at 4°C. The clarified lysate was added to Ni<sup>2+</sup>-NTA agarose resin (Thermo Fisher Scientific) and incubated on a rotisserie for 1 h at 4°C. Following incubation, the beads were washed extensively in purification buffer, then eluted and dialyzed as described for His6-Tle.

The purification of ( $\Delta$ ss)Tli-His6 was validated by SDS-PAGE and Coomassie brilliant blue dye staining.

#### *Esterase assay*

60 nM His-Tle was incubated in reaction buffer [20 mM Tris-HCl (pH 7.5), 100 mM NaCl, 3 mM CaCl<sub>2</sub>, 2% polysorbate 20] and incubated on a rotisserie at ambient temperature for 2.5 h. 200 nM Tli-His6 was added as indicated. Samples were assayed for optical density (550 nm) at indicated time points.

#### *Tle secretion assay*

*E. cloacae* strains were grown in LB-medium supplemented with Tet and grown to log phase, then Tle and Tli expression was induced with 0.4% L-arabinose for 1.5 h. Cells were collected by centrifugation at 3,000 *xg* for 5 min, then cell pellets were washed once in 1x M9 salts, then resuspended in urea-lysis buffer and subjected to a freeze-thaw cycle to extract proteins for SDS-PAGE and immunoblot analysis (described above). Culture supernatants were re-spun to further remove cellular contamination, then filter-sterilized. Supernatant samples were then incubated with 0.2% sodium deoxycholate for 20 min at ambient temperature, then treated with 4% TCA and incubated at 4°C for 1 h. Protein precipitates were collected by centrifugation and washed twice with -20°C acetone, then resuspended in urea-lysis buffer and analyzed via SDS-PAGE and immunoblot, as described above.

### *Bioinformatic analyses*

Signal sequence analyses were performed with the SignalP-5.0 server (136). Protein sequences were aligned using Clustal Omega (149). Protein alignments were rendered with BoxShade ([https://embnet.vital-it.ch/software/BOX\\_form.html](https://embnet.vital-it.ch/software/BOX_form.html)). Pairwise comparison values were calculated using the SIAS pairwise alignment server (<http://imed.med.ucm.es/Tools/sias.html>).

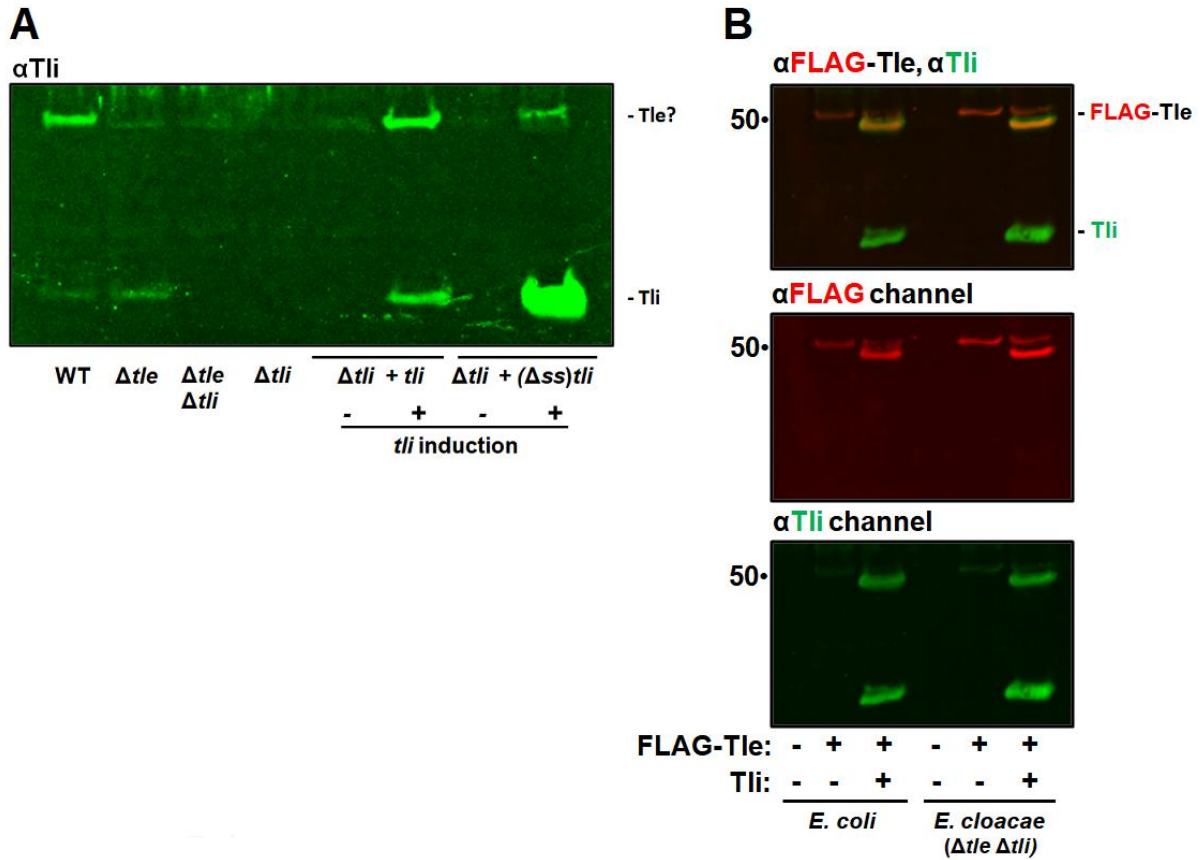


**Figure 3.1. Tli promotes increased abundance of its cognate Tle effector.** (A) Cell lysates of indicated *E. cloacae* mutants were analyzed via SDS-PAGE and  $\alpha$ -Tli immunoblot. L-arabinose-inducible *tli* alleles were complemented via *attTn7* integration. Induced strains were grown in media supplemented with 0.4% L-arabinose. WT=wild-type. (B) Cell lysates carrying the indicated plasmid constructs were analyzed via SDS-PAGE and dual  $\alpha$ -FLAG (red)  $\alpha$ -Tli (green) immunoblot. All strains were induced with 0.4% L-arabinose for 30 min prior to analysis. Tle has a predicted molecular weight of 52 kDa, and Tli (including its signal sequence) has a predicted molecular weight of 28 kDa.

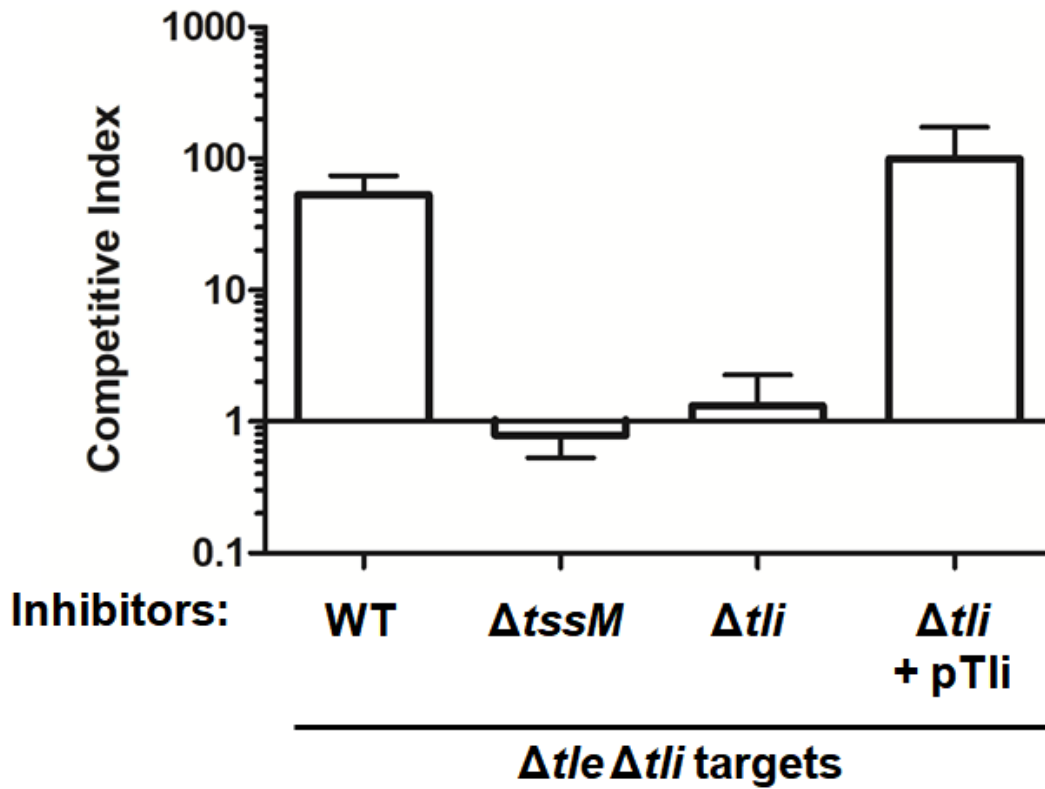


**Figure 3.2. Tli is essential for *in vivo* Tle function.** Indicated *E. cloacae* inhibitors were incubated at a 1:1 ratio with *E. cloacae*  $\Delta tle \Delta tli$  targets for 3 hours. Cells were quantified as colony-forming units (CFUs) at the beginning of the co-culture and after 3 h. Competitive indices were calculated as the ratio of inhibitor to target CFUs at the end of the competition normalized to the starting ratio. Data represent the average and standard error of the mean for three independent experiments. WT=wild-type.

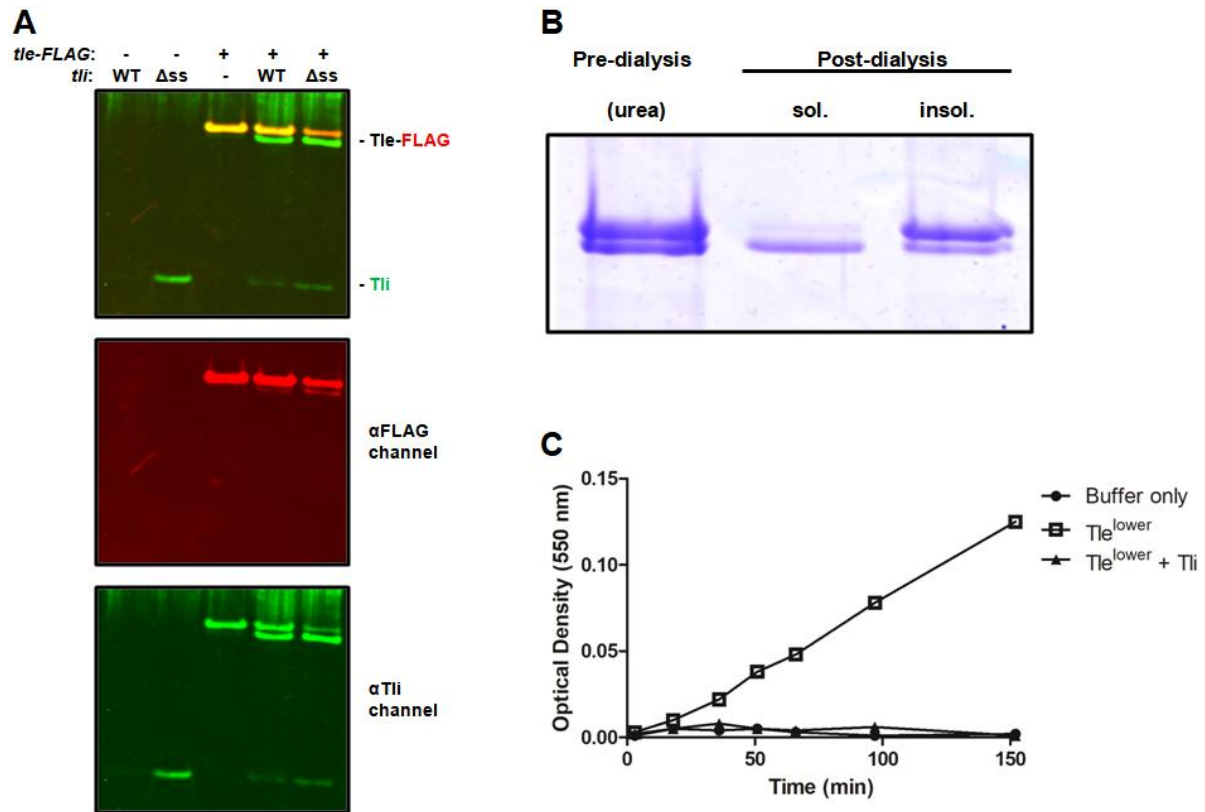


**Figure 3.3. Tli promotes the formation of a distinct T1e species.** (A) Cell lysates of *E. coli* carrying the indicated plasmid constructs were analyzed via SDS-PAGE and dual  $\alpha$ -FLAG (red)  $\alpha$ -Tli (green) immunoblot. T1e has a predicted molecular weight of 52 kDa, and Tli (including its signal sequence) has a predicted molecular weight of 28 kDa. WT=wild-type, ss=signal sequence. (B) *E. coli* expressing plasmid-borne Tli and His6-T1e were lysed and subjected to Ni-NTA purification under urea denaturing conditions. Bound proteins were released off the resin and subsequently dialyzed in water. Indicated protein fractions were analyzed via SDS-PAGE and Coomassie staining. (C) Soluble T1e<sup>lower</sup>, derived from (B), was subjected to an *in vitro* esterase assay in the presence and absence of purified Tli. Optical density<sub>550</sub> measures the hydrolysis of polysorbate 20 substrate.

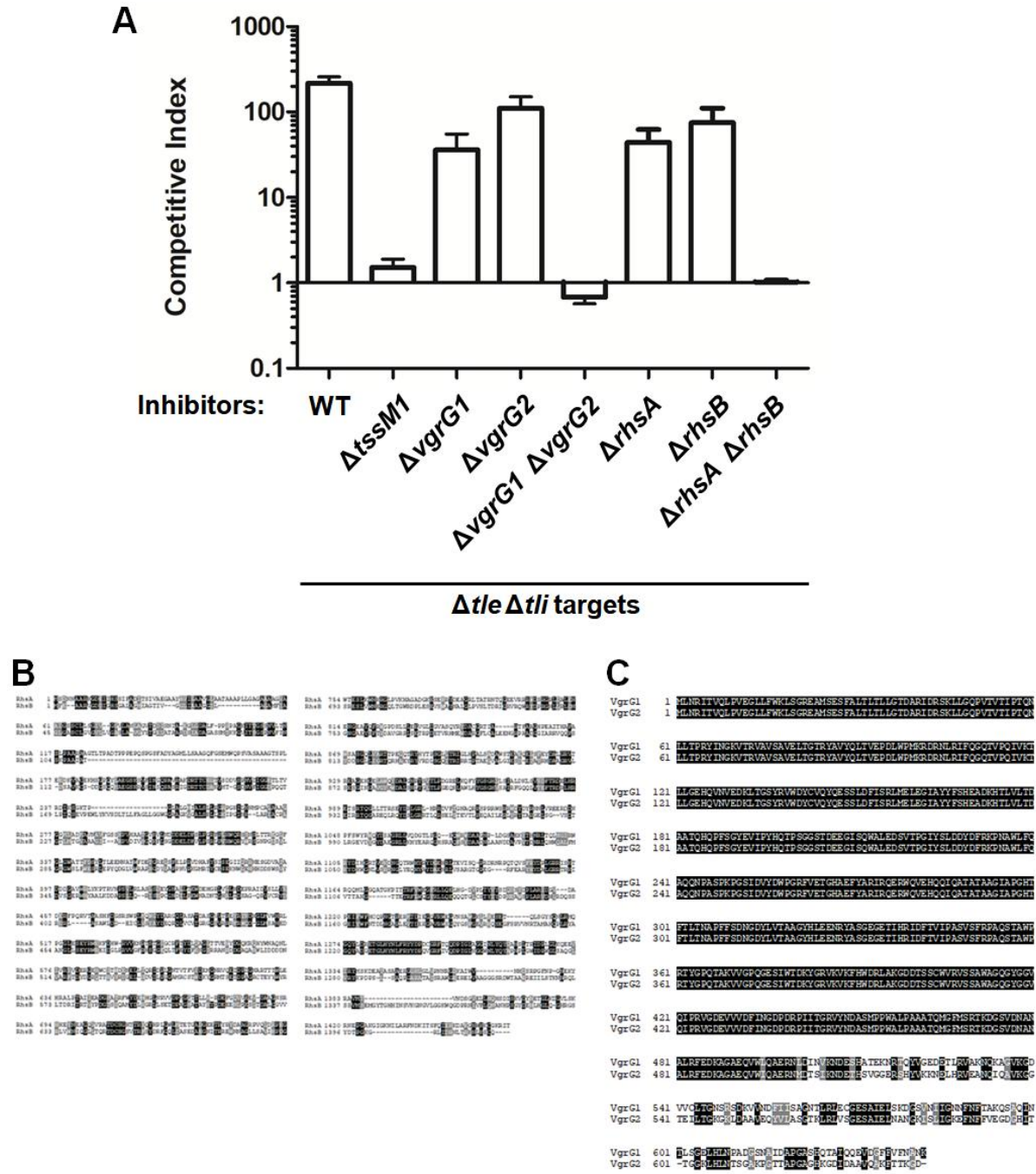


**Figure 3.4. Tle lacks genetic specificity to functionally-redundant T6SS factors.** (A) Indicated *E. cloacae* inhibitors were incubated at a 1:1 ratio with *E. cloacae*  $\Delta tle \Delta tli$  targets for 4 hours. Cells were quantified as colony-forming units (CFUs) at the beginning of the co-culture and after 4 h. Data represent the average and standard error of the mean for three independent experiments. WT=wild-type. (B) Multiple sequence alignment of *E. cloacae* PAAR-containing RhsA and RhsB proteins. (C) Multiple sequence alignment of *E. cloacae* VgrG1 and VgrG2 proteins. Protein sequences were aligned using Clustal Omega and rendered in BoxShade.

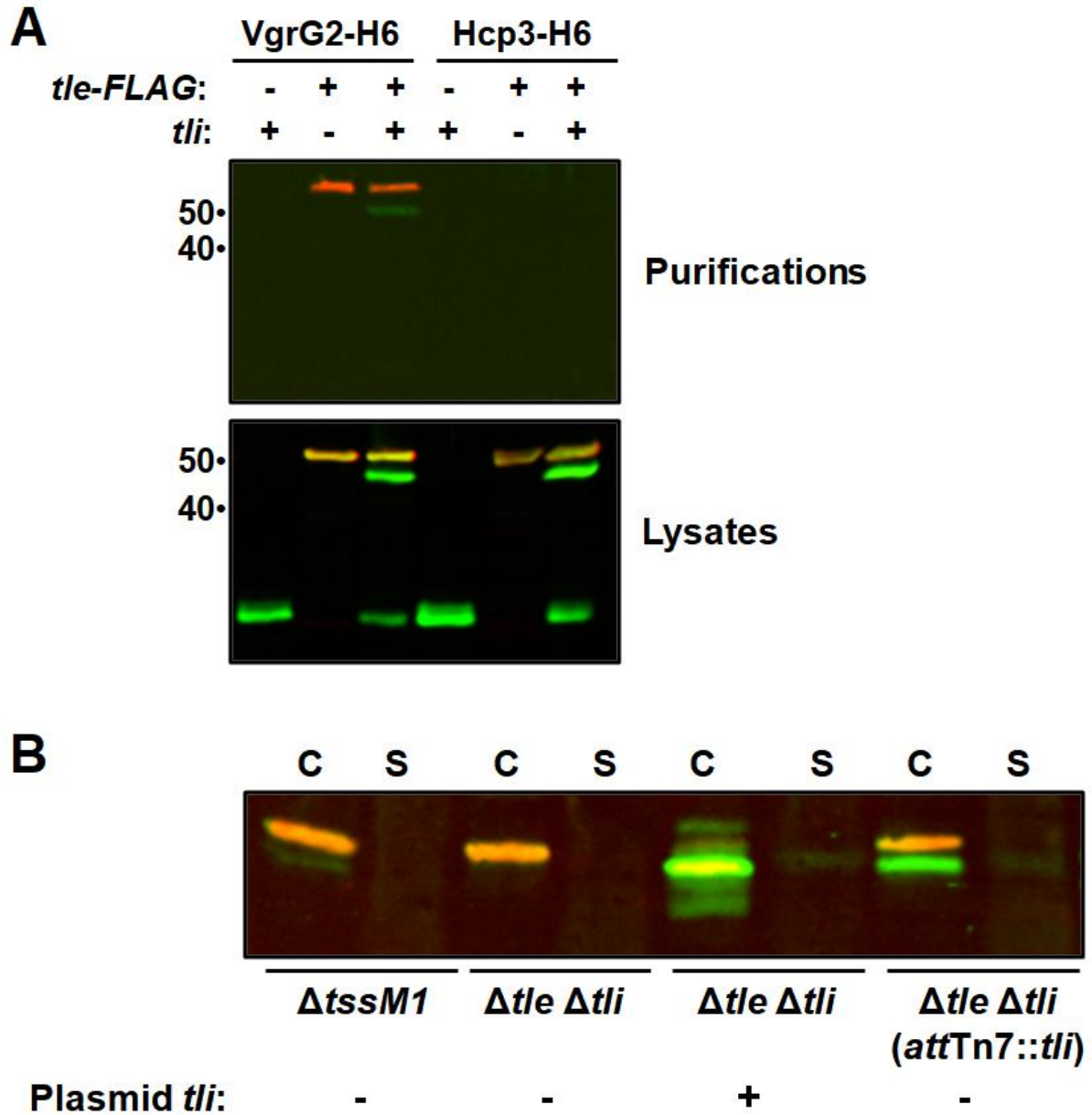


**Figure 3.5. Tli is required for secretion of Tle.** (A) *E. coli* expressing indicated plasmid constructs were lysed and subjected to Ni-NTA purification. Protein fractions were analyzed via SDS-PAGE and dual  $\alpha$ -FLAG (red) and  $\alpha$ -Tli (green) immunoblot. Tle has a predicted molecular weight of 52 kDa, and Tli (including its signal sequence) has a predicted molecular weight of 28 kDa. (B) Indicated *E. cloacae* strains expressing FLAG-Tle were cultured, then cell lysates (C) and TCA-precipitated culture supernatants (S) were analyzed via SDS-PAGE and dual  $\alpha$ -FLAG (red) and  $\alpha$ -Tli (green) immunoblot. Tli was complemented to strains either on a plasmid, or as a chromosomal integration (*attTn7::tli*).

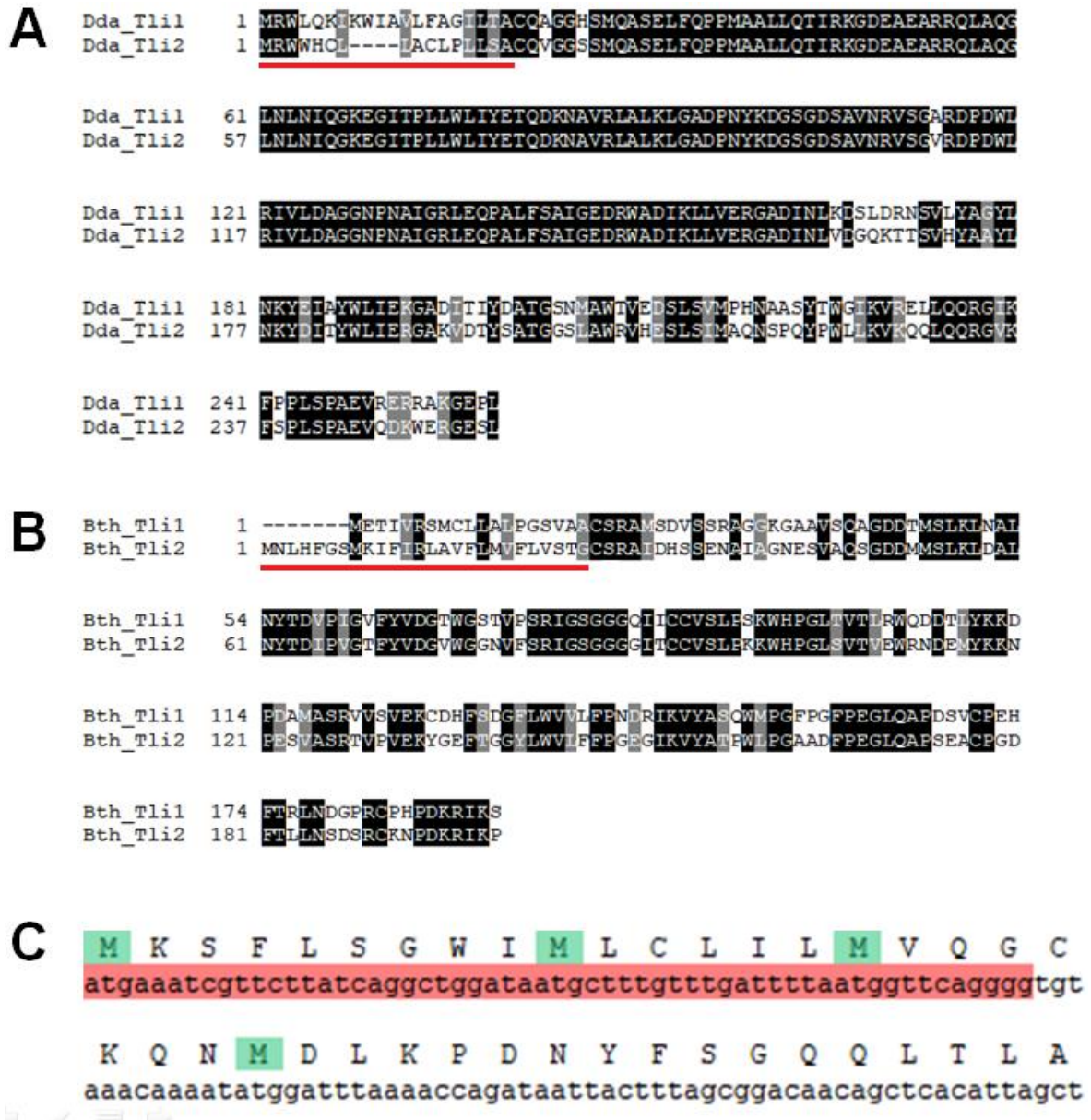


**Figure 3.6. Tli proteins might be expressed both periplasmically and cytoplasmically.** (A) Multiple sequence alignment of *D. dadantii* 3937 (Dda) Tli1 (Dda3937\_00830) and Tli2 (Dda3937\_00829) proteins. The predicted lipoprotein signal sequence is underlined in red. (B) Multiple sequence alignment of *B. thailandensis* E264 (Bth) Tli1 (BTH\_I2700) and Tli2 (BTH\_I2699) proteins. The predicted lipoprotein signal sequence is underlined in red. Protein sequences were aligned using Clustal Omega and rendered in BoxShade. (C) Diagram of the *E. cloacae* tli sequence (5' end). The predicted lipoprotein signal sequence is highlighted in red. Start codons are highlighted in green. Signal sequence analyses were performed with Signal-P.

**Table 3.1. Bacterial strains used in this study.**

<b>Strain</b>	<b>Description<sup>a</sup></b>	<b>Reference</b>
X90	<i>E. coli</i> F' <i>lacIq lac' pro'/ara</i> $\Delta(lac-pro)$ <i>nalI argE(amb) rif<sup>r</sup> thi-1</i> , Rif <sup>R</sup>	150
<i>E. cloacae</i> ATCC 13047	Type strain (ECL), Amp <sup>R</sup>	American Type Culture Collection
MFDpir	MG1655 RP4-2-Tc::[ $\Delta$ Mu1::aac(3)IV- $\Delta$ aphA- $\Delta$ nic35- $\Delta$ Mu2::zeo] <i>dapA::(erm-pir)</i> $\Delta$ recA, Apr <sup>R</sup> Zeo <sup>R</sup> Erm <sup>R</sup>	147
CH2016	X90 (DE3) $\Delta$ rna $\Delta$ slyD::kan, Rif <sup>R</sup> Kan <sup>R</sup>	156
CH11196	ECL $\Delta$ tssM1::kan, Amp <sup>R</sup> Kan <sup>R</sup>	81
CH11876	ECL $\Delta$ tle::kan, Amp <sup>R</sup> Kan <sup>R</sup>	This study
CH14442	ECL $\Delta$ tli, Amp <sup>R</sup>	This study
CH14587	ECL $\Delta$ tli::kan, Amp <sup>R</sup> Kan <sup>R</sup>	This study
CH14588	ECL $\Delta$ tli, Amp <sup>R</sup>	This study
CH14777	ECL $\Delta$ tli attTn7::tli, Amp <sup>R</sup> Gent <sup>R</sup>	This study
CH14779	ECL $\Delta$ tli attTn7::( $\Delta$ ss)tli, Amp <sup>R</sup> Gent <sup>R</sup>	This study
CH11895	ECL $\Delta$ tle $\Delta$ tli::spc, Amp <sup>R</sup> Spec <sup>R</sup>	This study
CH14665	ECL $\Delta$ tle $\Delta$ tli::spc attTn7::tli, Amp <sup>R</sup> Spec <sup>R</sup>	This study
CH12037	ECL $\Delta$ tssM2::kan, Amp <sup>R</sup> Kan <sup>R</sup>	This study
CH12384	ECL $\Delta$ vgrG1::kan, Amp <sup>R</sup> Kan <sup>R</sup>	This study
CH11436	ECL $\Delta$ vgrG2::kan, Amp <sup>R</sup> Kan <sup>R</sup>	This study
CH12582	ECL $\Delta$ vgrG2, Amp <sup>R</sup>	This study
CH12414	ECL $\Delta$ vgrG2 $\Delta$ vgrG1::kan, Amp <sup>R</sup> Kan <sup>R</sup>	This study
CH11178	ECL $\Delta$ rhsA::kan, Amp <sup>R</sup> Kan <sup>R</sup>	81
CH11186	ECL $\Delta$ rhsB::kan, Amp <sup>R</sup> Kan <sup>R</sup>	81
CH11748	ECL $\Delta$ rhsB $\Delta$ rhsA::kan, Amp <sup>R</sup> Kan <sup>R</sup>	This study
CH12884	ECL <i>vgrG2-VSV::kan</i> , Amp <sup>R</sup> Kan <sup>R</sup>	This study

<sup>a</sup>Abbreviations: Amp<sup>R</sup>, ampicillin-resistant; Kan<sup>R</sup>, kanamycin-resistant; Rif<sup>R</sup>, rifampicin-resistant; Spec<sup>R</sup>, spectinomycin-resistant; Gent<sup>R</sup>, gentamycin-resistant; Apr<sup>R</sup>, aprimycin-resistant; Erm<sup>R</sup>, erythromycin-resistant; Zeo<sup>R</sup>, zeocin-resistant

**Table 3.2. Plasmids used in this study.**

<b>Number</b>	<b>Description<sup>a</sup></b>	<b>Reference</b>
	pCH450, Tet <sup>R</sup>	153
	pCH450kpn, Tet <sup>R</sup>	71
	pTrc99a, Amp <sup>R</sup>	GE Healthcare
	pET21P, Amp <sup>R</sup>	Novagen
	pKOBEG, Cm <sup>R</sup>	144
	pCP20, Amp <sup>R</sup> , Cm <sup>R</sup>	145
pCH7204	pSH21:: <i>arfA</i> (cloning vector), Amp <sup>R</sup>	193
pCH6478	pTrc99a:: <i>cdiA</i> (CT3)- <i>cdiI</i> -His6 <sup>EC3937</sup> (cloning vector), Amp <sup>R</sup>	93
pCH6672	pCH450:: <i>cdiI</i> <sub>2</sub> -His6 <sup>EC93</sup> (cloning vector), Tet <sup>R</sup>	Zachary Ruhe
pCH10524	pSCbadB2, Tp <sup>R</sup>	155
pCH70	pKAN, Kan <sup>R</sup> , Amp <sup>R</sup>	143
pCH9384	pSPM, Spec <sup>R</sup> , Amp <sup>R</sup>	67
pCH11050	pKAN:: $\Delta$ ECL_01536 ( <i>tssM1</i> deletion), Kan <sup>R</sup> , Amp <sup>R</sup>	81
pCH10958	pKAN:: $\Delta$ ECL_01567 ( <i>rhsA</i> deletion), Kan <sup>R</sup> , Amp <sup>R</sup>	81
pCH11044	pKAN:: $\Delta$ ECL_03140 ( <i>rhsB</i> deletion), Kan <sup>R</sup> , Amp <sup>R</sup>	81
	pET21P:: <i>tli</i> -His6, Amp <sup>R</sup> (for generation of Tli antiserum)	Zachary Ruhe
pCH14385	pCH450:: <i>FLAG-tle</i> , Tet <sup>R</sup>	This study
pCH2525	pCH450:: <i>FLAG-tle-tli</i> , Tet <sup>R</sup>	This study
pCH14790	pCH450:: <i>tle-FLAG</i> , Tet <sup>R</sup>	This study
pCH11935	pCH450:: <i>tli</i> , Tet <sup>R</sup>	This study
pCH12112	pCH450:: $(\Delta ss)tli$ , Tet <sup>R</sup>	This study
pCH2199	pSH21:: <i>his6-tle</i> , Amp <sup>R</sup>	This study
pCH14623	pET21P:: $(\Delta ss)tli$ -His6, Amp <sup>R</sup>	This study
pCH14231	pCH450:: <i>vgrG2-VSV</i> (cloning vector), Tet <sup>R</sup>	This study
pCH2254	pCH450:: <i>vgrG2-His6</i> (cloning vector), Tet <sup>R</sup>	This study
pCH14981	pTrc99a:: <i>vgrG2-His6</i> , Amp <sup>R</sup>	This study
pCH11631	pTrc99a:: <i>hcp3-His6</i> , Amp <sup>R</sup>	This study
pCH15077	pSCbadB2:: <i>tle-FLAG</i> , Tp <sup>R</sup>	This study
pCH11848	pKAN:: $\Delta$ ECL_01553 ( <i>tle</i> deletion), Kan <sup>R</sup> , Amp <sup>R</sup>	This study
Not saved	pSPM:: $\Delta$ ECL_01553-01554 ( <i>tle-tli</i> deletion), Spec <sup>R</sup> , Amp <sup>R</sup>	This study
	pKAN:: $\Delta$ ECL_01554 ( <i>tli</i> deletion), Kan <sup>R</sup> , Amp <sup>R</sup>	Zachary Ruhe
pCH12056	pKAN:: $\Delta$ ECL_01813 ( <i>tssM2</i> deletion), Kan <sup>R</sup> , Amp <sup>R</sup>	This study
pCH12370	pKAN:: $\Delta$ ECL_01558 ( <i>vgrG1</i> deletion), Kan <sup>R</sup> , Amp <sup>R</sup>	This study
pCH11502	pKAN:: $\Delta$ ECL_01561 ( <i>vgrG2</i> deletion), Kan <sup>R</sup> , Amp <sup>R</sup>	This study

	pTNS2, Amp <sup>R</sup>	194
pCH14683	pUC18R6K::mini-Tn7(Gm):: <i>tli</i> , Gent <sup>R</sup> , Amp <sup>R</sup>	Zachary Ruhe
pCH14685	pUC18R6K::mini-Tn7(Gm)::( $\Delta$ <i>ss</i> ) <i>tli</i> , Gent <sup>R</sup> , Amp <sup>R</sup>	Zachary Ruhe

<sup>a</sup>Abbreviations: Amp<sup>R</sup>, ampicillin-resistant; Cm<sup>R</sup>, chloramphenicol-resistant; Gent<sup>R</sup>, gentamycin-resistant; Kan<sup>R</sup>, kanamycin-resistant; Tet<sup>R</sup>, tetracycline-resistant; Spec<sup>R</sup>, spectinomycin-resistant

**Table 3.3. Oligonucleotides used in this study.**

<b>Number</b>	<b>Name<sup>a</sup></b>	<b>Sequence<sup>b</sup></b>	<b>Reference</b>
CH4469	Tle-Eco-for	5' - AGG <u>GAA TTC</u> CGA ATG TAC AAC ATA AAA TTT GTC	This study
ZR248	Tle-Xho-rev	5' - TTT <u>CTC GAG</u> CTG ATA AGA ACG ATT TCA TGC ACG	This study
CH4537	FLAG-Tle-Eco-for	5'- TTT <u>GAA TTC</u> CGA ATG GAT TAT AAA GAT GAT GAT GAC AAA ATG TAC AAC ATA AAA TTT GTC	This study
CH4538	Tle-FLAG-Xho-rev	5'- TTT <u>CTC GAG</u> CTA CTT GTC ATC ATC ATC TTT ATA ATC TGC ACG ACT CCT AAT AAT TGA AAT	This study
CH3418	Tli-Kpn-for	5' - GAG <u>GGT ACC</u> ATG AAA TCG TTC TTA TCA GGC	This study
CH3719	Tli(M24)-Kpn-for	5' - AAA <u>GGT ACC</u> ATG GAT TTA AAA CCA G	This study
CH3419	Tli-Xho-rev	5' - ATA <u>CTC GAG</u> CTA TTT AAC CGG AGT TGG TG	This study
CH4703	Tle-Spe-for	5'- TTT <u>ACT AGT</u> ATG TAC AAC ATA AAA TTT GTC TAT CTT TTC AG	This study
ZR246	Tli-H6-Xho-rev	5' - TTT <u>CTC GAG</u> CTA GTG GTG GTG GTG GTG GTG TTT AAC CGG AGT TGG TGG C	This study
CH3020	Hcp3-Nco-for	5' - ATA <u>CCA TGG</u> CTA TTG ATA TGT TTC	This study
CH3022	Hcp3-His6-Xho-rev	5' - CTA <u>CTC GAG</u> TGC TTC TTT GTT TTC TTT G	This study
CH2897	TssM1-KO-Sac	5'- TTT <u>GAG CTC</u> GAA ATC GAC GCC GGT CTG	81
CH2898	TssM1-KO-Bam	5'- TTT <u>GGA TCC</u> TTT CCT TGC GGC AAT CCG	81

CH2899	TssM1-KO-Eco	5' - TTT <u>GAA TTC</u> CAA GGA CAG CCG TAT GAC	81
CH2900	TssM1-KO-Kpn	5' - TTT <u>GGT ACC</u> GAA TCG ACA TCA GCA TCT C	81
CH2976	TssM2-KO-Sac	5' - TTT <u>GAG CTC</u> GGC AAC CGC CTG ACA C	This study
CH2977	TssM2-KO-OE-rev	5' - CCA CTA GTT CTA GAG CGG CTT CCG TAG TCT TCG GTG C	This study
CH2978	TssM2-KO-OE-for	5' - GCT TAT CGA TAC CGT CGA CGG ACA GTA CGG AAA GCA G	This study
CH2979	TssM2-KO-Kpn	5' - TTT <u>GGT ACC</u> GCC GAG CCA TTC	This study
CH2952	pKAN-OE-for	5' - CCG CTC TAG AAC TAG TGG	This study
CH2953	pKAN-OE-rev	5' - GTC GAC GGT ATC GAT AAG C	This study
CH2818	RhsA-KO-Sac	5' - TTT <u>GAG CTC</u> ATA CAC CCT CCA GGA AGG	81
CH2819	RhsA-KO-Bam	5' - TTT <u>GGA TCC</u> GCC TTA CAC ATT CCG GTT G	81
CH2820	RhsA-KO-Eco	5' - GAA <u>GAA TTC</u> TGG CAA GAG GAT TAC TTA ATG	81
CH2821	RhsA-KO-Kpn	5' - TTT <u>GGT ACC</u> CAT CAT TAG TAA TGC AAA G	81
CH2905	RhsB-KO-Sac	5' - TTT <u>GAG CTC</u> ACC CGC TCA ATG TCA GAA C	81
CH2906	RhsB-KO-Bam	5' - TTT <u>GGA TCC</u> CCC TGG TGT TAA TGG TGG	81
CH2907	RhsB-KO-Eco	5' - TTT <u>GAA TTC</u> CAA TGA ATA TGC TGA ATG TGA G	81
CH2908	RhsB-KO-Kpn	5' - TTT <u>GGT ACC</u> ACT TCG TCA TTA TCA TCT GC	81

CH3040	VgrG1-KO-Sac	5' – GTT <u>GAG CTC</u> GTT ATG GAT GTC ATT TTG TCA ATC	81
CH3041	VgrG1-KO-Bam	5' – AAT <u>GGA TCC</u> GAG CAT AAT CGT TAT TCC GTA ATG	81
CH3042	VgrG1-KO-Eco	5' – AAG <u>GAA TTC</u> AAT AAG TAA ACG TAA TTA GAA AC	81
CH3043	VgrG1-KO-Kpn	5' – CTT <u>GGT ACC</u> AGC AAA AGT TCG ATT TAT TCA AC	81
CH3195	Vgrg2-KO-Sac	5' - TTT <u>GAG CTC</u> CCC TTG CTA CGG CCA AAC	81
CH3196	Vgrg2-KO-Bam	5' - TTT <u>GGA TCC</u> TCG TTA TTC CAC TAT GGG C	81
CH3197	Vgrg2-KO-Xho	5' - TTT <u>CTC GAG</u> GCT GGA GCG GTG CTT G	81
CH3198	Vgrg2-KO-Kpn	5' - TTT <u>GGT ACC</u> CGA GTC CAG ACA ATC AGG	81
CH3937	Vgrg2(T401)-Sac	5' - ACA <u>CGA GCT CCT</u> GCT GGG TG - 3'	This study
CH3945	VgrG2-VSV-rev	5' - CAA GAC GAT TCA TTT CAA TAT CAG TAT AAC TAG TAT CAC CCT TGG TCG TGA ATT TCG C	This study
CH3946	VSV-Not-rev	5' - TTT <u>GCG GCC GCA</u> TCC TTA TTT GCC AAG ACG ATT CAT TTC AAT ATC AGT AT	This study
CH3373	Tle-KO-Sac	5' - CAA <u>GAG CTC</u> CGG GAT GGT TGC C	This study
CH3374	Tle-KO-Bam	5' - ATT <u>GGA TCC</u> GTC CTG TTA CCA GTC	This study
CH3375	Tle-KO-Xho	5' - AGG <u>CTC GAG</u> ACA TTT CAA TTA TTA GG	This study
CH3376	Tle-KO-Kpn	5' - AAC <u>GGT ACC</u> TGG CGA TAA ACC CGC	This study

CH3377	Tli-KO-Xho	5' - CCA <u>ACT CGA GTT</u> AAA TAG GAA ACG	This study
CH3378	Tli-KO-Kpn	5' - CCA <u>GGT ACC</u> AAA GTG CTG TGT GC	This study
CH3020	Hcp3-Nco-for	5' - ATA <u>CCA TGG</u> CTA TTG ATA TGT TTC	This study
CH3022	Hcp3-Xho-rev	5' - CTA <u>CTC GAG</u> TGC TTC TTT GTT TTC TTT G	This study
CH4452	VgrG2-Eco-for	5' - ATA <u>GAA TTC</u> ATG CTC AAC CGA ATT ACC	This study
CH4453	VSV-Xho-rev	5' - TGC <u>CTC GAG</u> ATC CTT ATT TGC CAA GAC G	This study

<sup>a</sup>Abbreviations: OE=overlap-extension, Bam=BamHI, Eco=EcoRI, Kpn=KpnI, Nco=NcoI, Not=NotI, Sac=SacI, Spe=SpeI, Xho=XhoI

<sup>b</sup>Restriction endonuclease sites are underlined.

## **Chapter 4: Formation of the VgrG $\beta$ -spike is dependent on Rhs in *E. cloacae***

Note: other members of the Hayes lab participated on this project. Former graduate student Christina Beck and former undergraduate Ian Singleton contributed to the work presented in Figure 4.1. Christina also contributed to the work presented in Figure 4.3, and additionally helped with plasmid and strain construction for this work. Research associate Zachary Ruhe helped with strain construction and methods for Figure 4.7.

## Abstract

Here, I examine the roles of two effector proteins, RhsA and RhsB, in *Enterobacter cloacae* ATCC 13047 T6SS activity. The Hayes lab has previously shown that these proteins carry toxic C-terminal domains, which are delivered via the T6SS into target cells, where they function as toxic effector molecules. RhsA and RhsB also contain N-terminal PAAR domains, which have been shown to play an essential structural role in the T6SS apparatus. I find that at least one Rhs protein is required to support T6SS activity in *E. cloacae*. However, truncated Rhs proteins containing PAAR domains are not sufficient to restore T6SS activity to  $\Delta rhsA \Delta rhsB$  mutants. By contrast, truncated Rhs proteins that lack only the C-terminal toxin domain are sufficient to restore T6SS activity. Additionally, I demonstrate that Rhs is required to stabilize the  $\beta$ -spike of trimeric VgrG. Rhs-VgrG<sub>3</sub> complexes are resistant to boiling in SDS, and are readily detected as high-mass complexes by immunoblotting. Rhs-VgrG<sub>3</sub> complexes form in *E. cloacae* mutants carrying deletions of essential T6SS structural genes ( $\Delta tssM$ ,  $\Delta tssF$  and  $\Delta hcp$ ), as well as in T6SS-negative *Escherichia coli* K-12 strains. These latter observations suggest that Rhs promotes VgrG trimerization prior to docking with the T6SS baseplate at the cytoplasmic membrane. I propose that full-length Rhs proteins provide a chaperone function that is distinct from that previously described for small PAAR domain proteins.

## Introduction

Rearrangement hotspot (Rhs) and Rhs-like proteins are a group of widespread polymorphic toxins in bacteria (see Chapter 1). Beyond the Gram-negative type VI secretion system (T6SS), these proteins have also been associated with other toxin export systems such as the Gram-negative *Photorhabdus* virulence cassette pathway, the Gram-negative *Photorhabdus/Yersinia* insecticidal ABC toxin complex, the Gram-positive type VII secretion system, and the widespread PrsW-peptidase-dependent export system (96). Additionally, some Rhs toxins are either self-sufficient for export, or are not currently associated with known export pathways. For example, the rice pathogen *Xanthomonas oryzae* Rhs protein XadM has been shown to be a surface-associated adhesin that is important for plant attachment, biofilm formation, and ultimately plant virulence (160). Furthermore, the Rhs-like WapA protein in *Bacillus subtilis* is a cell-wall associated protein that is used to inhibit neighboring susceptible cells (67).

Rhs elements were first described in 1979 as large DNA sequence repeats that were originally thought to promote chromosomal duplication in *Escherichia coli* K-12 (161, 162). *E. coli* K-12 encodes 4 full-length Rhs proteins, all of which have conserved sequence up to the polymorphic C-terminal region, and which therefore contribute to genetic recombination events (163, 164). In 1995, Hill and colleagues demonstrated that the C-terminal region of *E. coli* RhsA had toxic activity; this was the first hint that Rhs proteins are polymorphic toxin delivery systems (165). After the discovery of the T6SS, it was later recognized that Rhs proteins are often genetically linked to T6SSs, and in 2011 it was finally proposed that the function of

Rhs proteins is to encode toxins that mediate in inter-bacterial growth inhibition (93). However, *E. coli* K-12 does not encode a T6SS; therefore, the role of Rhs in this strain remains unclear.

The T6SS PAAR domain has been described as a critical component of the T6SS apparatus, as it interacts with the VgrG trimer to help form the membrane-puncturing “spike” of the secreted complex (28). Many Rhs proteins encode a PAAR-repeat domain in the N-terminal region of the protein, and it has been estimated that around 10-15% of all PAAR-encoding proteins are Rhs proteins (28). This supports a model where not only can the Rhs toxin be deployed via the T6SS, but that Rhs also contributes to the overall structure of the T6SS apparatus.

In Chapter 2 I established that the T6SS-1 locus of *Enterobacter cloacae* ATCC 13047 mediates all inter-bacterial inhibition (Figure 2.2A), and identified 4 effectors deployed as cargo of this locus (Table 2.1). However, deletion of the 2 *rhs* effectors abrogated inter-bacterial inhibition, even though 2 other effectors remained intact in the strain (Figure 2.3A). This suggests Rhs is a required component of the *E. cloacae* T6SS, and given that no other PAAR domain is encoded within the T6SS-1 locus, it is likely that T6SS-1 requires Rhs for its PAAR domain. Here, I find that the Rhs PAAR domain is insufficient to support T6SS activity in this organism, suggesting Rhs plays an additional role in the structure or assembly of the T6SS apparatus. I then demonstrate that Rhs functions as a chaperone for VgrG, and is therefore critical to both the assembly and the structure of the spike complex.

## Results

### *Rhs is required for T6SS in E. cloacae*

Initial data suggested that *rhs* is required for T6SS activity in *E. cloacae* (Figure 2.3A). I further explored this finding by testing the effects of individual *rhs* deletions, as well as deletion combinations of *vgrG* and *rhs*. I find that while individual deletions of *rhs* leave *E. cloacae* competent for inter-bacterial inhibition, the co-deletion of both *rhs* genes phenocopies known T6SS<sup>-</sup> mutations (*tssM*<sup>-</sup> and *vgrG*<sup>-</sup>) (Figure 4.1A). This suggests *rhs* is not only used as an effector for inhibition, but is also required for T6SS activity overall. To confirm that this was indeed the case, I analyzed culture supernatants and found the  $\Delta rhsA \Delta rhsB$  mutant fails to secrete Hcp, indicating a defect in secretion itself (Figure 4.1B).

Both RhsA and RhsB encode PAAR domains near the N-terminus of each protein, and PAAR domains have previously been shown to interact with the C-terminus of VgrG (28). Moreover, PAAR domains have been demonstrated as a required component of the T6SS in *Vibrio cholerae*, *Acinetobacter baylyi*, and *Serratia marcescens* (28, 29). In both competition and secretion assays, I find a genetic interaction exists between *E. cloacae*'s RhsA and VgrG2, and between RhsB and VgrG1. The  $\Delta rhsA \Delta vgrG1$  mutant has abrogated T6SS activity, as does the  $\Delta rhsB \Delta vgrG2$  mutant: this suggests RhsA and VgrG2 work together to create one functional T6SS apparatus, while RhsB and VgrG1 work together to create a different, functional apparatus. Co-deletion of *rhsA* with its non-cognate *vgrG1* therefore breaks both assembly pathways, and similarly does the co-deletion of *rhsB* with its non-cognate *vgrG2* (Figure 4.1).

### *The Rhs $\beta$ -encapsulation structure and core domains promote T6SS activity*

I then tested whether Rhs proteins are required for T6SS activity simply because they provide the PAAR domain for the apparatus. I find that over-expressing the PAAR domain of RhsA is insufficient for rescuing inter-bacterial inhibition activity in the  $\Delta rhsA \Delta rhsB$  mutant, whereas over-expressing the full RhsA protein is successful in restoring inhibition activity (Figure 4.2A and 4.2B). This suggests Rhs is providing more than just the PAAR domain in order to support T6SS activity. It is also worth noting that co-induction of the upstream accessory protein effector-associated gene with Rhs (EagR) is required for the successful RhsA complementation phenotype, even though the native chromosomal *eagR<sub>A</sub>* is unaltered in the  $\Delta rhsA \Delta rhsB$  mutant (Figure 4.2B). In other words, over-expression of RhsA compared to *EagR<sub>A</sub>* acted as a dominant-negative on the system. I then determined that the relative stoichiometry of *EagR<sub>A</sub>* to RhsA is important, as the same strain can successfully inhibit *E. coli* when plasmid-encoded RhsA is not induced (Figure 4.2C). Together, this suggests *EagR* and Rhs work together to support T6SS activity, but that *EagR* cannot be under-expressed relative to Rhs expression levels. The role of *EagR* will be further explored in Chapter 5.

Next, I investigated what domains of Rhs are required for T6SS activity, given the N-terminal PAAR-containing domain was insufficient at promoting T6SS activity. Rhs proteins contain Rhs-repeat motifs that are predicted to form a hollow shell-like structure that encapsulates the C-terminal toxin domain; moreover, this shell-like structure is plugged on one end by the Rhs “core” domain, which is responsible for catalytically cleaving the C-terminal toxin domain off of the protein

(72). I introduced stop-codons at multiple positions in both *rhsA* and *rhsB* to test whether the  $\beta$ -encapsulation shell and core domains promote T6SS activity.

I find that for both RhsA and RhsB, the PAAR domain is again insufficient at promoting T6SS activity: neither the RhsA<sub>1-250</sub> nor the RhsB<sub>1-206</sub> constructs, both of which end after the PAAR domain, support inter-bacterial inhibition or Hcp secretion (Figure 3.3A, 3.3B, and 3.3C). Truncating Rhs within the  $\beta$ -encapsulation structure of both RhsA (RhsA<sub>1-966</sub>) and RhsB (RhsB<sub>1-857</sub>) also failed to promote T6SS activity. Truncating RhsB just before the Rhs core domain (RhsB<sub>1-1161</sub>) provided a very limited amount of T6SS activity (most observable in Figure 3.3B), whereas keeping the RhsB core domain intact and deleting only the toxin domain (RhsB<sub>1-1277</sub>) retained T6SS activity comparable to that of full-length RhsB. This suggests that the Rhs  $\beta$ -encapsulation domain and core domain are important for promoting T6SS activity.

Rather than truncating the entire core domain of RhsA, I engineered a more narrowly truncated RhsA ending before the very C-terminus of the core domain (RhsA<sub>1-1323</sub>), removing residues of the core domain required for proteolytic cleavage of the toxin domain (72, Chapter 5). This mutant demonstrated a significant amount of T6SS activity, again suggesting the Rhs core domain is important for promoting T6SS activity. Furthermore, truncating only the toxin domain of RhsA (RhsA<sub>1-1330</sub>) provided more inhibition and Hcp secretion than the RhsA<sub>1-1323</sub> mutant (Figure 3.3B and 3.3C). Taken together, these data suggest the Rhs  $\beta$ -encapsulation domain and the Rhs core domain are involved in promoting T6SS activity. Given that the core domain helps plug one end of the  $\beta$ -encapsulation domain, both domains may be

considered part of the same structural domain of Rhs and act together to facilitate T6SS activity.

While all of the 8 tested truncation mutants were designed to still express the PAAR domain, it is a formal possibility that not all of the Rhs mutant proteins are stable, and therefore fail to support T6SS activity simply because insufficient Rhs protein is available to the cell. To test this hypothesis, I developed an antibody against RhsA<sub>82-467</sub> to visualize protein expression. This antibody does not cross-react against RhsB, but unfortunately does not detect endogenous levels of RhsA with ease (data not shown), suggesting RhsA is expressed in the cell at low levels. Therefore, I assayed RhsA levels via a purification strategy: EagR<sub>A</sub>-His6 was expressed in the RhsA-truncation-mutant strains to assess these RhsA mutants for both stability and successful interaction with a known binding partner (the binding site for EagR is located at the Rhs N-terminus and is further explored in Chapter 5). I find that only the RhsA<sub>1-966</sub> mutant fails to make a stable protein capable of pulldown via EagR<sub>A</sub> (Figure 4.3D). Given the RhsA<sub>1-966</sub> mutation disrupts the  $\beta$ -encapsulation domain, it is not surprising this construct does not make a stable protein. However, the other 3 RhsA truncations are stable and associate with EagR<sub>A</sub>, and therefore lend confidence to the interpretation that the PAAR domain is insufficient in supporting T6SS activity.

### *Rhs promotes VgrG spike formation*

RhsA is believed to interact with VgrG2 via its PAAR domain. Therefore, I next tested whether the 4 RhsA truncation constructs do indeed interact with VgrG2. I fused a vesicular stomatitis virus glycoprotein-G (VSV-G) epitope to the C-terminus of the native *vgrG2* locus in *E. cloacae* and assayed for RhsA interaction via  $\alpha$ -VSV immuno-precipitation. Addition of the VSV epitope does not reduce functionality of VgrG2 (Figure 4.4A). To my surprise, the PAAR-domain-alone truncation construct RhsA<sub>1-250</sub> does not co-purify with VgrG2-VSV, although wild-type RhsA, RhsA<sub>1-1323</sub>, and RhsA<sub>1-1330</sub> all successfully co-purifies (Figure 4.4B). RhsA<sub>1-1323</sub> appears to co-purify less readily than RhsA<sub>1-1330</sub> and wild-type RhsA, which is consistent with the diminished T6SS activity observed with this mutant (Figure 4.3B and 4.3C).

Moreover, I noticed the presence of high-mass complexes purified from the wild-type, RhsA<sub>1-1323</sub>, and RhsA<sub>1-1330</sub> mutant strains, but not the RhsA<sub>1-250</sub> strain. These complexes resist dissociation even when boiled in SDS load dye, and co-label with both  $\alpha$ -VgrG2-VSV and  $\alpha$ -RhsA antibodies (Figure 4.4B). It has previously been reported that the T4 bacteriophage protein gp5, which is homologous to the VgrG C-terminal  $\beta$ -spike structure, is resistant to both thermal and chemical denaturation (166). My data therefore suggest Rhs is required for T6SS activity because it helps form this SDS- and boiling-resistant trimeric VgrG spike complex. However, these stable VgrG-complexes all co-label with  $\alpha$ -RhsA antibody, suggesting the stable complex also contains Rhs. Moreover, the slowest-migrating band in my immuno-precipitation runs above the 245 kDa molecular weight marker: the size of this complex is consistent with the mass of 3 VgrG monomers (each 73 kDa) associated

with 1 Rhs protein (148 kDa without the toxin domain). The known VgrG-PAAR structure contains VgrG<sub>3</sub>:PAAR<sub>1</sub> stoichiometry (28), thus, it is probable that the RhsA<sub>1-250</sub> mutant is insufficient for promoting proper VgrG-trimerization and therefore fails to form stable interaction with VgrG monomer, leading to a lack of co-purification in this assay. Additionally, plasmid-expressed EagR<sub>A</sub>-RhsA successfully complements the  $\Delta r$ hsA mutation in this assay, while constructs that do not contain the  $\beta$ -encapsulation domain nor core domain do not complement  $\Delta r$ hsA (Figure 4.4C). Together, these data suggest that Rhs functions to promote the formation of a highly-stable VgrG-Rhs complex, and that this stable form is likely the functional form of the membrane-puncturing T6SS spike complex.

I next investigated if other T6SS factors, especially those reported to interact directly with VgrG, namely *tssF* and *hcp* (36, 167), are necessary for the formation of this stable VgrG complex. Deletion of *tssM*, *tssF*, and *hcp* all phenocopy wild-type for stable VgrG-complex formation, whereas deletion of *eagR<sub>A</sub>* and *r*hsA phenocopy each other and impair VgrG-complex formation (Figure 4.5A). TssF and Hcp are believed to interact with the N-terminus of VgrG (36, 167), whereas PAAR interacts with the C-terminus of VgrG: my data therefore suggests RhsA (and its partner EagR<sub>A</sub>) facilitate specifically the C-terminal trimerization of VgrG<sub>2</sub>, and that the VgrG C-terminal  $\beta$ -spike structure is what is resistant to heat and chemical perturbation. Additionally, the wild-type levels of VgrG trimerization observed in the  $\Delta t$ ssF mutant suggest VgrG trimerization occurs prior to association with the baseplate complex.

There is some discrepancy in the amount of VgrG2 spike complex observed in  $\Delta rhsA$  strains. In Figure 4.4B, all strains used are in a  $\Delta rhsB$  background, and no spike complex is detected in the *rhs<sup>-</sup>* strain. In contrast, the strains used in Figure 4.5A all express RhsB, and have detectable, if low, levels of the VgrG2 spike complex, even in a  $\Delta rhsA$  background. This suggests RhsB may facilitate low levels of non-cognate VgrG2 trimerization. It has previously been shown that RhsB and VgrG1 work together to form 1 spike complex assembly, while RhsA and VgrG2 work together to form a different complex (81, Figure 4.1). It is possible RhsB may support low levels of VgrG2 trimerization, but at an insufficient level to support T6SS activity (as detected via growth inhibition or secretion assays).

Another explanation may be that VgrG is forming hetero-trimers, which is believed to occur in *V. cholerae* and *Pseudomonas aeruginosa* (4, 188). The hetero-trimer would have a very similar mass to the VgrG2 homo-trimer; therefore, VgrG hetero-trimers would have the same appearance as homo-trimers in this assay. RhsB may therefore be interacting with VgrG1 to support VgrG hetero-trimerization, as opposed to interacting directly with VgrG2. To test this hypothesis, I performed the same pulldown assay with a  $\Delta vgrG1 \Delta rhsA$  strain: I find that RhsB still supports non-cognate VgrG2 trimerization, even in the absence of VgrG1 (Figure 4.5B). While this does not rule out the possibility of VgrG hetero-trimers forming in *E. cloacae*, these data suggest RhsB is capable of promoting non-cognate VgrG2 trimerization, though at levels apparently below physiological significance.

Next, I tested whether RhsA is capable of promoting VgrG trimerization in a T6SS-negative *Escherichia coli* K-12 strain. VgrG2-VSV does not form significant

amounts of the SDS- and boiling-resistant high-mass complex in *E. coli* until both RhsA and EagR<sub>A</sub> are also co-expressed (Figure 4.6). It is worth noting that there does appear to be a slight amount of stable VgrG-Rhs complex when RhsA and VgrG2-VSV were expressed without EagR<sub>A</sub>, but more of this complex is observed when EagR<sub>A</sub> is also added. Moreover, low levels of an additional high-mass complex can be observed above the major high-mass band; this is more evident when the samples are not boiled prior to SDS-PAGE analysis. In the absence of boiling, a high-mass VgrG-containing complex, migrating above the major band, can be observed even when VgrG2 is expressed without either RhsA or EagR<sub>A</sub>; however, the appearance of this band is significantly reduced when samples are boiled. This suggests that VgrG is capable of mis-oligomerization, perhaps as a hexamer rather than a trimer, but that this complex is boiling-sensitive, unlike the major high-mass complex.

#### *Rhs is important, but not essential, for T6SS sheath assembly*

I then investigated T6SS assembly dynamics using a TssB-GFP fusion construct to test whether deletion of *rhs* affects sheath assembly. TssB-GFP polymers can be readily seen via fluorescent microscopy, and time-lapse imaging allows us to visualize sheath assembly, contraction, and disassembly duty cycles. I find that co-deletion of *rhsA* and *rhsB* drastically reduces the overall number of TssB-GFP foci and firing events, but that there are still rare firing events observed (Figure 4.7). In contrast, the co-deletion of *vgrG1* and *vgrG2* does not support detectable sheath assembly: no TssB-GFP foci were ever observed. This is also true of the *tssM* deletion, suggesting both TssM and VgrG are absolutely required for sheath

assembly, whereas Rhs strongly promotes sheath assembly but is not fully essential for the process.

This exposes a seeming contradiction in the data, where *rhs*<sup>-</sup> cells are neither able to inhibit neighboring target cells nor able to secrete Hcp (Figure 4.1), but do appear to undergo occasional firing of the apparatus. It is currently unclear whether the firing cycles observed in *rhs*<sup>-</sup> cells are productive, functional secretion events and are simply too rare to promote observable levels of inhibition or secretion, or if the resulting apparatus of *rhs*<sup>-</sup> cells is somehow structurally defective. As discussed previously, VgrG appears to be capable of mis-oligomerization; it is possible a mis-formed VgrG complex may form in the absence of *rhs*, and allows for subsequent assembly of the apparatus but does not successfully allow full T6SS activity.

Together, my data suggests both the Rhs  $\beta$ -encapsulation domain and core domain promote the VgrG C-terminal-trimerization event, but live-imaging microscopy reveals Rhs is not essential for T6SS sheath assembly. It is possible that the VgrG C-terminal-trimerization event is a difficult folding event that must nevertheless occur for T6SS apparatus assembly and subsequent secretion and inhibition phenomena, and that Rhs serves as a chaperone to increase the rate of successful VgrG trimerization. It is worth noting that I have never successfully detected endogenously expressed VgrG-VSV in cell lysates; this suggests VgrG is expressed at low levels in *E. cloacae*, and may even be the rate-limiting step of T6SS assembly in this organism. I therefore investigated whether over-expression of VgrG2-VSV could bypass the need for the RhsA chaperone entirely. Unfortunately, VgrG2-VSV over-expression resulted in growth-defective cells, and morphological

defects can be observed via light microscopy (Figure 4.8A). Nevertheless, attempts to rescue the  $\Delta rhsA \Delta rhsB$  mutant's T6SS-null phenotype were somewhat successful: over-expression of VgrG2-VSV in these cells leads to mildly elevated levels of Hcp secretion compared to over-expression of the same construct in  $\Delta tssF$  cells (Figure 4.8B). This is consistent with the hypothesis that proper VgrG-trimerization is kinetically limiting and that Rhs increases the rate of successful trimerization.

## Discussion

The work presented here demonstrates Rhs is required for the T6SS in *E. cloacae*, and that it functions as a chaperone for VgrG. I find that the Rhs PAAR domain is insufficient to support T6SS activity; instead, the Rhs  $\beta$ -encapsulation structure and core domains are required to promote T6SS activity. My findings suggest Rhs stabilizes the C-terminal  $\beta$ -spike of trimeric VgrG, and that VgrG trimerization occurs prior to docking with the T6SS baseplate. Together, this presents a new model for T6SS assembly, and describes a novel function for Rhs proteins.

There is some controversy in the field about the function of the PAAR domain. It was originally described as an essential component of the T6SS in *V. cholerae* and *Acinetobacter baylyi*, but those data demonstrate only an attenuation of T6SS activity in *V. cholerae* PAAR mutants (28). The authors additionally describe that the function of the PAAR domain is to sharpen the tip of the spike complex, presumably to promote membrane-puncturing activity. However, more recent crystal structures

and electron micrographs of the *P. aeruginosa* spike complex reveal that the PAAR-containing Tse6 effector hangs off this sharp tip such that the effector cargo may in fact occlude the tip of the spike complex (73, 176). Moreover, some T6SSs do not appear to require a PAAR protein at all (19, 167). Additionally, Leiman and colleagues have revealed to us in private communications that T4 phage has reduced, but not fully abolished, virulence when the PAAR homolog gp5.4 is deleted.

My work proposes a novel function of full-length Rhs proteins that is distinct from that previously described for small PAAR domain proteins: I find that Rhs functions as a chaperone for VgrG trimerization. It is unlikely that the PAAR domain is sufficient for chaperoning VgrG, as the data presented in this chapter support a model where the Rhs  $\beta$ -encapsulation structure is necessary for this chaperone activity. Additionally, the published *V. cholerae* PAAR-VgrG2 complex crystal structure was generated by creating a hybrid T4 phage gp5-VgrG2 protein and co-expressing this with *V. cholerae* PAAR (28). Given this strategy for purification, it is highly likely the group initially tried co-expressing the *V. cholerae* PAAR and full-length VgrG2, but were unsuccessful at purifying full-length VgrG trimers. This would suggest *V. cholerae* VgrG2 also requires a chaperone, and that PAAR does not fulfill this responsibility.

While I find that the *E. cloacae* T6SS requires Rhs to chaperone VgrG, it is worth noting that not all organisms with functional T6SSs encode Rhs proteins, including the above mentioned *V. cholerae*. This raises the question of whether this requirement for a VgrG chaperone is universal or not. There is only 1 published structure of a full-length VgrG trimer, and that is the *P. aeruginosa* VgrG1 structure

(92). In this publication, Spínola-Amilibia *et. al.* successfully purified the VgrG trimer when it was heterologously expressed in *E. coli*, suggesting that *P. aeruginosa* VgrG1 does not require a chaperone. In contrast, the *V. cholerae* VgrG2 trimer mentioned above appears to require a chaperone (28). In this publication, Leiman and colleagues noted “solubility” issues with the majority of tested VgrGs, and instead utilized their chimeric approach to generate “VgrG” trimers by grafting the *V. cholerae* VgrG2 C-terminus to the T4 phage homolog gp5, which does readily trimerize without a chaperone (28, 166, 168). This suggests that *V. cholerae* VgrG2, and likely other VgrGs tested but not described in their publication, do require a chaperone for trimerization, and that what was described as a “solubility” defect was actually a stability defect. Given that *V. cholerae* does not encode *rhs*, if this organism does require a VgrG chaperone, then that function must be carried out by either a novel protein or via a known protein with undiscovered additional function.

It is currently unclear why *P. aeruginosa* VgrG1 and T4 gp5 will successfully trimerize on their own, whereas *E. cloacae* and *V. cholerae* VgrGs will not. It has been previously noted that while a number of viral proteins have been found to contain triple-stranded  $\beta$ -helical regions, the T4 gp5 helix (homologous to the VgrG C-terminus) is distinct in that it is capable of readily self-folding, and is also noted to be both the longest and most regular of these viral structures (166). The gp5 trimer is composed of helical strands interdigitated in a highly consistent ABC-ABC-ABC... pattern (169). In contrast, the *P. aeruginosa* VgrG1  $\beta$ -helix is significantly shorter, and has a less regular strand pattern of AB-CCC-ABC-ABC-AB-CCC (92). Now that a stable *E. cloacae* spike complex can be readily formed in *E. coli*, an important future

experiment would be to purify this complex and solve its structure in order to determine how similar the *E. cloacae* VgrG trimer is to that of *P. aeruginosa*'s.

It possible that these less stable VgrG trimers take on more complicated folds, and that these complexes only become stable upon complete and successful folding. For example, the *Salmonella typhimurium* phage P22 has a triple-stranded  $\beta$ -helical spike complex that undergoes a multi-step folding pathway, and while native complexes are found to be both thermostable and resistant to detergent, intermediate or off-pathway complexes possess reduced stability profiles (170-173). In dramatic contrast to these previously described  $\beta$ -helical structures, the spike complex of the broad-range  $\phi 92$  phage and the partial *E. coli* O157 VgrG1 C-terminal complex both form a  $\beta$ -prism structure composed of anti-parallel  $\beta$ -sheets, with each monomer contributing one face of the triangular prism (174, 175). This suggests significant variation exists in the structure of these membrane-puncturing spike complexes in nature, and leads to potential variation in the folding efficiency of these structures.

Another explanation for the necessity of a VgrG chaperone in *E. cloacae* is that *E. cloacae* appears to express VgrG at very low levels. This is supported by the fact that I have not been successful at detecting endogenously expressed VgrG in this organism. While not conclusive, the experiments performed in Figure 4.8 suggest that increasing the concentration of VgrG monomer in the cell facilitates VgrG trimerization and bypasses the need for a VgrG chaperone. Taken together, both VgrG expression levels and structure may contribute to the need for a chaperone.

## Materials and Methods

### *Bacterial growth and conditions*

Bacteria were cultured in shaking lysogeny broth (LB) or on LB-agar at 37°C. Bacteria were supplemented with antibiotics at the following concentrations: 150 µg/mL ampicillin (Amp), 66 µg/mL chloramphenicol (Cm), 50 µg/mL kanamycin (Kan), 100 µg/mL spectinomycin (Spc), 200 µg/ml rifampicin (Rif), and 25 µg/mL tetracycline (Tet).

### *Strain construction*

All bacterial strains, plasmids, and oligonucleotides used in this study are listed in Tables 4.1, 4.2, and 4.3. Gene-deletion constructs for *E. cloacae* were generated using overlap-extension PCR (OE-PCR) or via the plasmids pKAN or pSPM as described previously (67, 142, 143). Briefly, OE-PCR constructs were made with upstream and downstream homology PCR fragments overlapped to the CH2952/CH2953 PCR product amplified from either pKAN or pSPM. pKAN or pSPM plasmid constructs were generated by restriction cloning PCR fragments from upstream and downstream of the target gene into pKAN or pSPM to flank the antibiotic-resistance cassette. Restriction enzymes used are specified in the oligonucleotide names listed in Table 4.3.

Resulting constructs were PCR-amplified, DpnI-digested to remove methylated template DNA, then directly electroporated into *E. cloacae* cells

expressing phage  $\lambda$ -Red recombinase proteins as described (144). Transformants were selected on LB-agar supplemented with either Kan or Spc. All chromosomal deletions were confirmed by whole-cell PCR analysis. Kan or Spc markers were cured as necessary via pCP20 (145).

The gene deletion for *eagR<sub>A</sub>* (ECL\_01566) was introduced via the allele-exchange plasmid pRE118 (146). Briefly, the deletion construct was generated with pKAN, then the Kan marker was deleted via SpeI/EcoRI restriction digest and subsequently endfilled with T4 polymerase. This markerless deletion construct was then restriction cloned into pRE118 using SacI/KpnI. The resulting plasmid was then transformed into the MFD*pir* strain and mated into CH14452 recipients (147). Integrants were selected on LB-agar supplemented with Kan, then 3 rounds of chloro-phenylalanine counter-selection was performed on 1x M9 minimal media supplemented with 0.5% glucose and 10 mM d/l-*p*-chlorophenylalanine. Clones were screened for Kan-sensitivity, and Kan-sensitive clones were screened via whole-cell PCR analysis.

### *Plasmid construction*

All plasmids and oligonucleotides used in this study are listed in Tables 4.2 and 4.3. All PCR products were purified, digested with the restriction enzymes indicated in the oligonucleotide names (Table 4.3), and ligated to a vector treated with the same enzymes. Plasmids were confirmed by DNA sequencing (University of California, Berkeley). Plasmid transformations were performed by

making strains TSS competent (148). Constructs were cloned directly into the final vector, with exceptions or complications described below.

For generation of most *rhsA* and *rhsB* chromosomal truncation constructs, the upstream region of homology was cloned using SacI/BamI into pCH10958 for *rhsA* constructs and pCH11044 for *rhsB* constructs. For the *rhsB(E1161stop)* and *rhsB(Q1277stop)* truncations, the downstream region of homology was PCR-amplified with CH2907/CH2834 and cloned into pKAN using EcoRI/XhoI. The *rhsB(E1161stop)* upstream region of homology was PCR-amplified with CH3234/CH3235 and cloned into the previous plasmid using SacI/BamI. The *rhsB(Q1277stop)* upstream region of homology was PCR-amplified with CH3234/CH3831 and cloned into the earlier plasmid using SacI/NotI.

For generation of chromosomal *vgrG2-VSV*, the upstream region of homology was PCR-amplified with CH3937/CH3945, then this piece was re-amplified using CH3937/CH3946 to complete the VSV tag. This PCR was then cloned into pCH11502 using SacI/NotI. To make the pSPM version of this construct, the NotI/EcoRI dropout from pSPM was cloned into pCH11502. Plasmid-expressed VgrG2-VSV was PCR-amplified off of the resulting chromosomal *vgrG2-VSV* strain using CH4452/CH4453.

For generation of *rhA* and *eagR<sub>A</sub>-rhsA* constructs, constructs were piecewise assembled with either the CH3914/CH4325 PCR or CH4400/CH4325 PCR cloned into pCH450 using EcoRI/NcoI, then the CH4326/CH4327 PCR was added using NcoI/KpnI, and finally the CH4328/CH4329 PCR was added using KpnI/SbfI.

## *Competitions*

*E. cloacae* strains were used as inhibitor cells on LB-agar co-cultures against X90 *E. coli* targets. Cells were grown in LB-medium (supplemented with appropriate antibiotics when plasmid-bearing) to log phase, then collected by centrifugation and resuspended in 1x M9 salts. Inhibitors and targets were mixed 1:1 at OD 17 each (200 uL total volume), then 100 uL of the mixture was spread on LB-agar without antibiotics and incubated at 37°C for 3 or 4 h (as indicated). Culture aliquots were taken at the beginning and end of the co-culture to quantify viable inhibitor and target cells as colony forming units. At the end of the co-culture, cells were harvested in 1.5 mL of 1x M9 salts. For competitions with plasmid-induced proteins, inhibitors were grown in LB-medium supplemented with 0.4% L-arabinose and Tet unless indicated otherwise. Co-cultures were then performed as above on LB-agar supplemented with 0.4% L-arabinose.

For all competitions, cell suspensions were serially diluted into 1x M9 salts and plated onto LB-agar supplemented with appropriate antibiotics to separately enumerate inhibitor and target cells. Competitive indices were calculated as the ratio of inhibitor to target cells at 3 or 4 h divided by the initial inhibitor to target cell ratio.

## *Hcp secretion assay*

*E. cloacae* strains were cultured to log phase, then collected by centrifugation at 3,000 *xg* for 5 min. Cell pellets were washed once in 1x M9 salts, then

resuspended in urea-lysis buffer [50% urea, 150 mM NaCl, 20 mM Tris-HCl (pH 8.0)] and subjected to a freeze-thaw cycle to extract proteins for SDS-PAGE and immunoblotting. Culture supernatants were re-spun to further remove cellular contamination. Supernatants were precipitated in cold ethanol at a final ethanol concentration of 75%. Samples were left at -80 °C overnight, then proteins were collected by centrifugation at 21,000  $xg$  for 15 min at 4°C. Precipitates were washed once with 75% cold ethanol, then air-dried pellets were dissolved in urea-lysis buffer. Samples were analyzed by SDS-PAGE on Tris-tricine 10% polyacrylamide gels run at 110 V (constant) for 1 h, then gels were soaked for 10 min in 25 mM Tris, 192 mM glycine (pH 8.6), 20% methanol. Gels were then electroblotted to nitrocellulose membranes using a semi-dry transfer apparatus at 17 V (constant) for 30 min. Membranes were subsequently blocked and imaged as described below.

### *Ni<sup>2+</sup>-affinity pulldown*

*E. cloacae* strains carrying pTrc(CmR)::*eagR<sub>A</sub>-His6* were grown to log phase in LB-medium supplemented with Cm and protein expression was induced with 1 mM isopropyl-beta-D-thiogalactoside (IPTG) for 30 min. Cells were then collected by centrifugation and resuspended in binding buffer [20 mM Tris-HCl (pH 7.5), 500 mM NaCl, 40 mM imidazole, 2% glycerol, 1% Triton X-100]. Each cell suspension was broken by 2 passages through a French press, then insoluble debris was removed via centrifugation at 23,000 $xg$  for 10 min at 4°C. The clarified lysate was added to Ni<sup>2+</sup>-NTA agarose resin (Thermo Fisher Scientific) and incubated on a

rotisserie for 1 h at 4°C. Following incubation, the beads were washed extensively in binding buffer, then eluted in binding buffer supplemented with 250 mM imidazole.

Samples were analyzed by SDS-PAGE on Tris-tricine 7% polyacrylamide gels run at 110 V (constant) for 1 h. Gels were soaked for 10 min in 25 mM Tris, 192 mM glycine (pH 8.6), 20% methanol, then electroblotted to low-fluorescence PVDF membranes using a semi-dry transfer apparatus at 17 V (constant) for 30 min. Membranes were subsequently blocked and imaged as described below.

#### *Co-immunoprecipitation pulldown*

*E. cloacae* strains were grown to log phase in LB-medium supplemented with .4% L-arabinose. Cells were then collected by centrifugation and resuspended in co-immunoprecipitation buffer [20 mM Tris-HCl (pH 7.5), 2% glycerol, 150 mM NaCl, 1% Triton X-100]. Each cell suspension was broken by 2 passages through a French press, then insoluble debris was removed via centrifugation at 23,000 $g$  for 10 min at 4°C. The clarified lysate was added to anti-VSV-G agarose beads (Sigma) and incubated on a rotisserie for 1 h at 4°C. Following incubation, the beads were washed extensively in co-immunoprecipitation buffer, then eluted by boiling the beads in SDS-PAGE sample-loading buffer for 5 min.

Samples were analyzed by SDS-PAGE on Tris-tricine 7% polyacrylamide gels run at 110 V (constant) for either 1 h (Figure 4.4B) or 2.5 h (Figure 4.4C and 4.5). Gels were soaked for 10 min in 25 mM Tris, 192 mM glycine (pH 8.6), 10% methanol, then electroblotted to low-fluorescence PVDF membranes using a semi-

dry transfer apparatus at 17 V (constant) for 1 h. Membranes were subsequently blocked and imaged as described below.

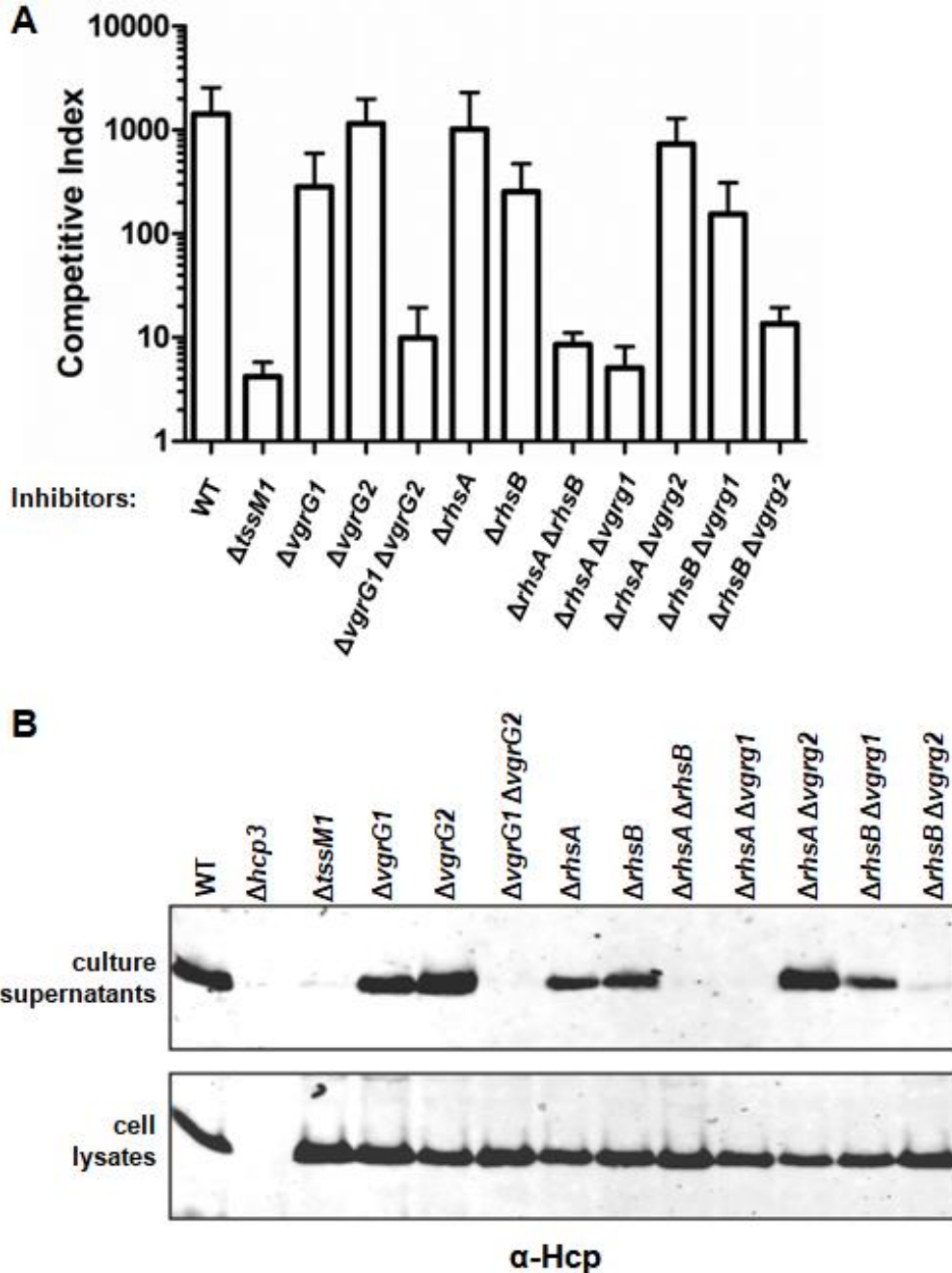
### *Immunoblots*

For immunoblotting of *E. coli* lysates, cultures were initially grown in LB-medium supplemented with 0.04% L-arabinose, then cultured to log phase and collected by centrifugation at 3,000  $xg$  for 5 min. Cell pellets were then resuspended in urea-lysis buffer and subjected to a freeze-thaw cycle to extract proteins. Samples were analyzed by SDS-PAGE on Tris-tricine 7% polyacrylamide gels run at 110 V (constant) for 2.5 h. Gels were soaked for 10 min in 25 mM Tris, 192 mM glycine (pH 8.6), 10% methanol, then electroblotted to low-fluorescence PVDF membranes using a semi-dry transfer apparatus at 17 V (constant) for 1 h.

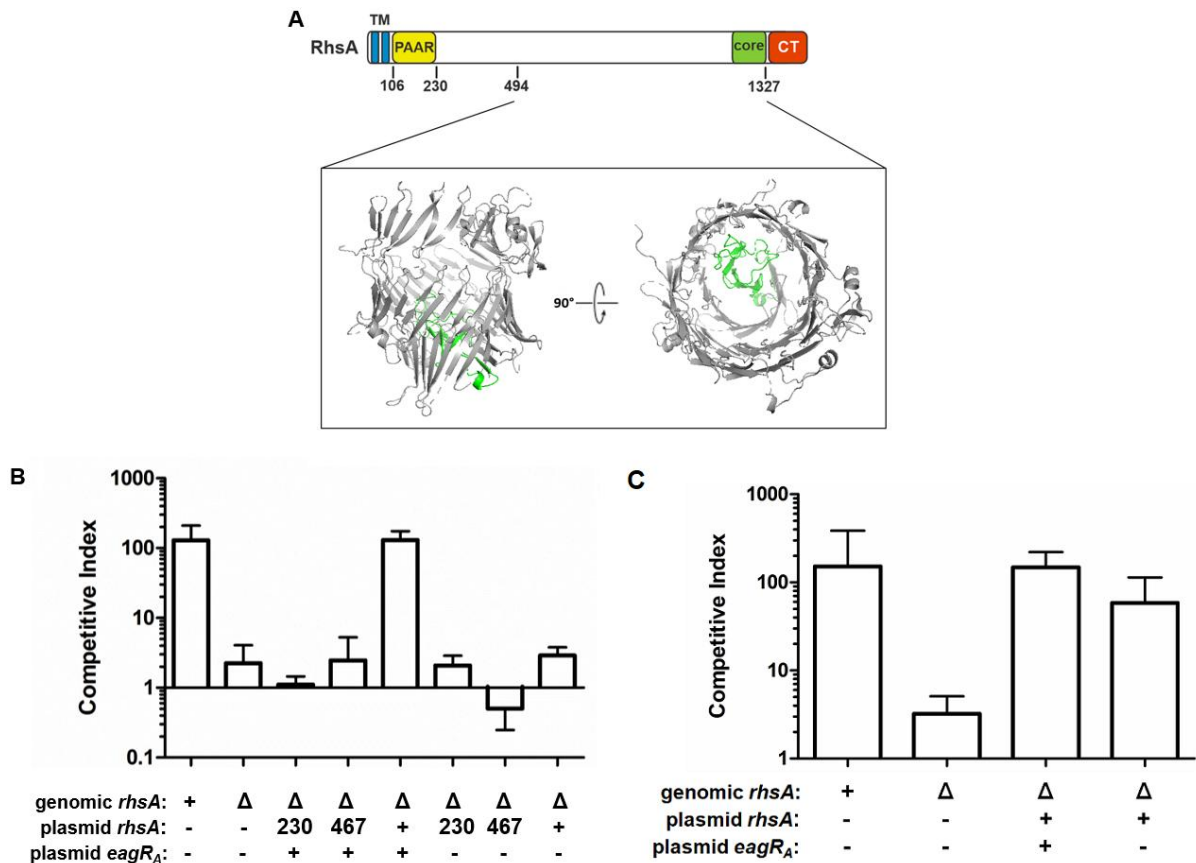
For all immunoblots, membranes were blocked with 4% non-fat milk in PBS for 30 min at ambient temperature, and incubated with primary antibodies in 0.1% non-fat milk in PBS overnight at 4°C. Rabbit polyclonal antisera (Cocalico Biologicals, Stevens, PA) to Hcp3-His6 was used at a 1:10,000 dilution and antisera to RhsA<sub>82-467</sub>-H6 was used at a 1:5,000 dilution. Mouse anti-VSV-G (Sigma) was used at a 150,000 dilution. Blots were incubated with 800CW-conjugated goat anti-rabbit IgG (1:125,000 dilution, LICOR) or 680LT-conjugated goat anti-mouse IgG (1:125,000 dilution, LICOR) in PBS. Immunoblots were visualized with a LI-COR Odyssey infrared imager.

## *Microscopy*

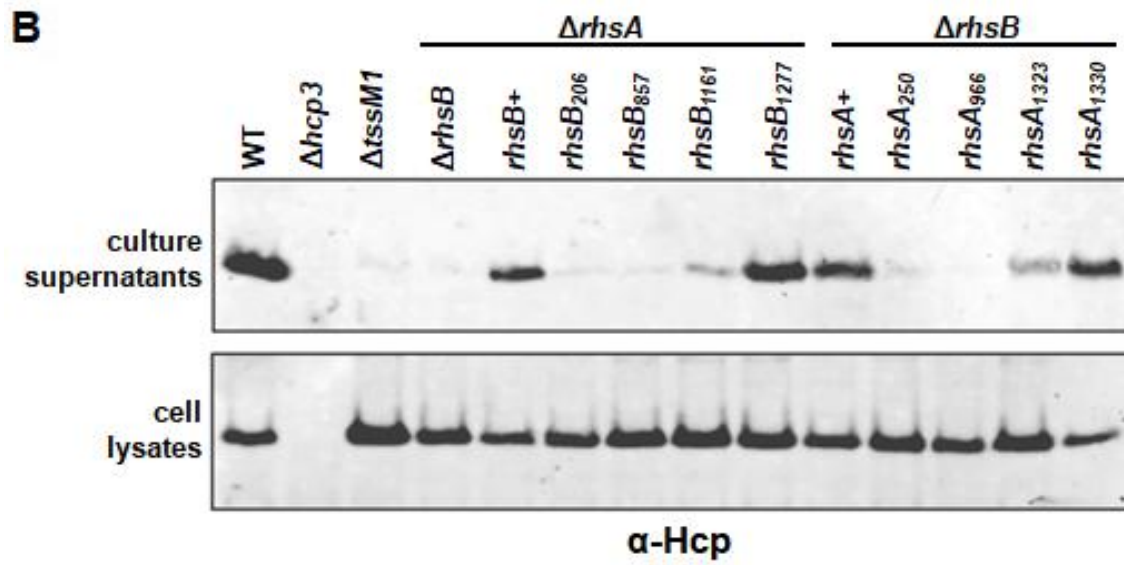
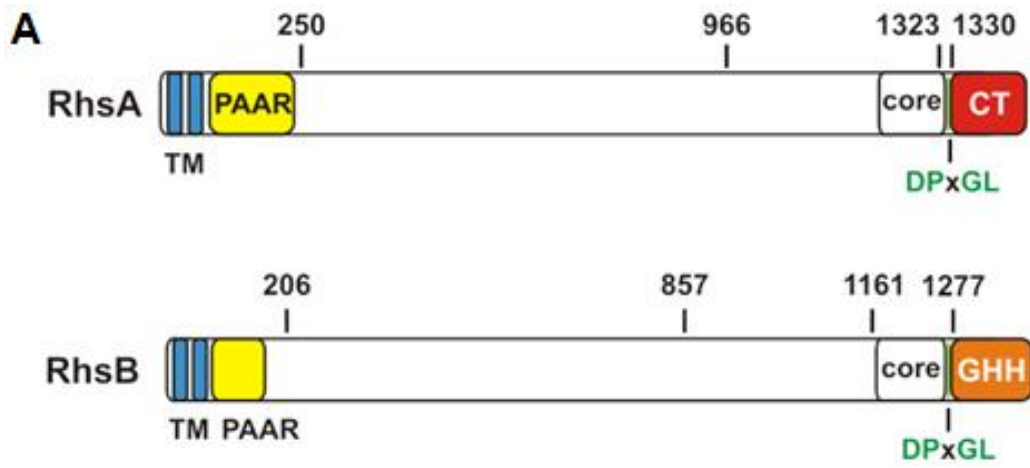
*E. cloacae* strains were cultured from a colony into 0.5x LB-medium to log phase. Cells were then concentrated by centrifugation and spotted onto a thin pad of 1% agarose in 1x M9 minimal media and covered with a glass coverslip. Timelapse GFP-fluorescence microscopy was performed with frames taken every 5 seconds for 2.5 min per field of view, followed by a brightfield image once the timelapse was completed. ImageJ was used for all image analysis and manipulations.



**Figure 4.1. Rhs is required for T6SS activity.** Rhs is required for T6SS activity, and there is a genetic interaction between RhsA and VgrG2, and between RhsB and VgrG1. (A) Indicated *E. cloacae* inhibitors were incubated at a 1:1 ratio with *E. coli* targets for 4 hours. Cells were quantified as colony-forming units (CFUs) at the beginning of the co-culture and after 4 h. Competitive indices were calculated as the ratio of inhibitor to target CFUs at the end of the competition normalized to the starting ratio. Data represent the average and standard error of the mean for three independent experiments. (B) Cell lysates and supernatants of indicated strains were analyzed via SDS-PAGE and  $\alpha$ -Hcp3 immunoblot.



**Figure 4.2. PAAR is insufficient to complement the Rhs deletion.** (A) Schematic of RhsA with the predicted protein structure of the indicated region. Structure prediction was performed with the Phyre2 server (182). (B) *E. cloacae*  $\Delta rhsB$  (first column) or  $\Delta rhsA \Delta rhsB$  (all other columns) inhibitors carrying the indicated plasmid constructs were induced and incubated at a 1:1 ratio with *E. coli* targets for 3 hours on inducing media. Data represent the average and standard error of the mean for three independent experiments. (C) Indicated *E. cloacae* inhibitors were incubated at a 1:1 ratio with *E. coli* targets for 3 hours without induction of the plasmid at any point. Data represent the average and standard error of the mean for three independent experiments. Construct 230 contains RhsA residues 1-230, and construct 467 contains RhsA residues 1-467. A + indicates the full-length gene is present. When present, *eagR<sub>A</sub>* is encoded in *cis* upstream of *rhsA*.



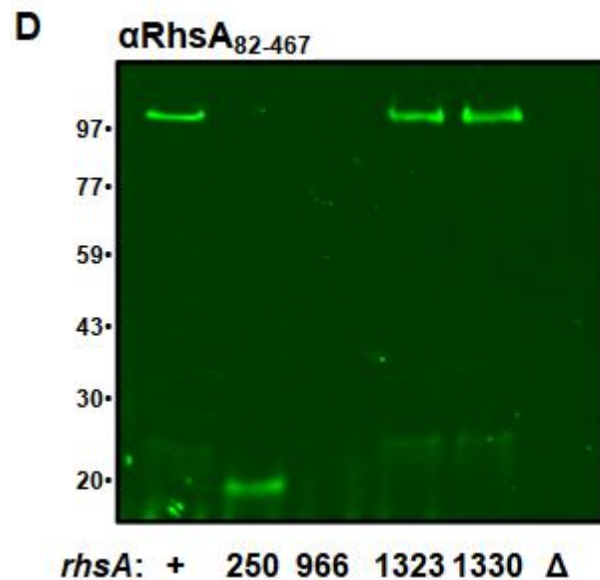
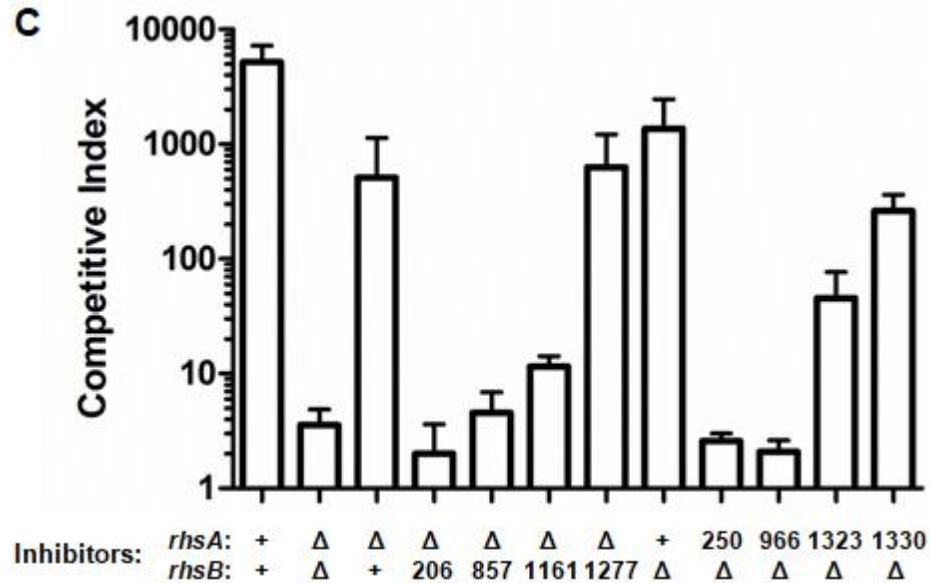


**Figure 4.3. The Rhs  $\beta$ -encapsulation structure promotes T6SS activity.**

(A) Schematic of RhsA and RhsB. The labeled numbers indicate the location of introduced truncation mutants in the subsequent experiments. (B) Cell lysates and supernatants of indicated strains were analyzed via SDS-PAGE and  $\alpha$ -Hcp3 immunoblot. (C) Indicated *E. cloacae* inhibitors were incubated at a 1:1 ratio with *E. coli* targets for 4 hours. Data represent the average and standard error of the mean for three independent experiments. (D) EagR<sub>A</sub>-His6 was induced off a plasmid in the indicated *E. cloacae* strains (all in a  $\Delta$ *rgsB* background), then cells were lysed and subjected to Ni-NTA pulldown. The bound fractions were analyzed via SDS-PAGE and  $\alpha$ -RhsA immunoblot.

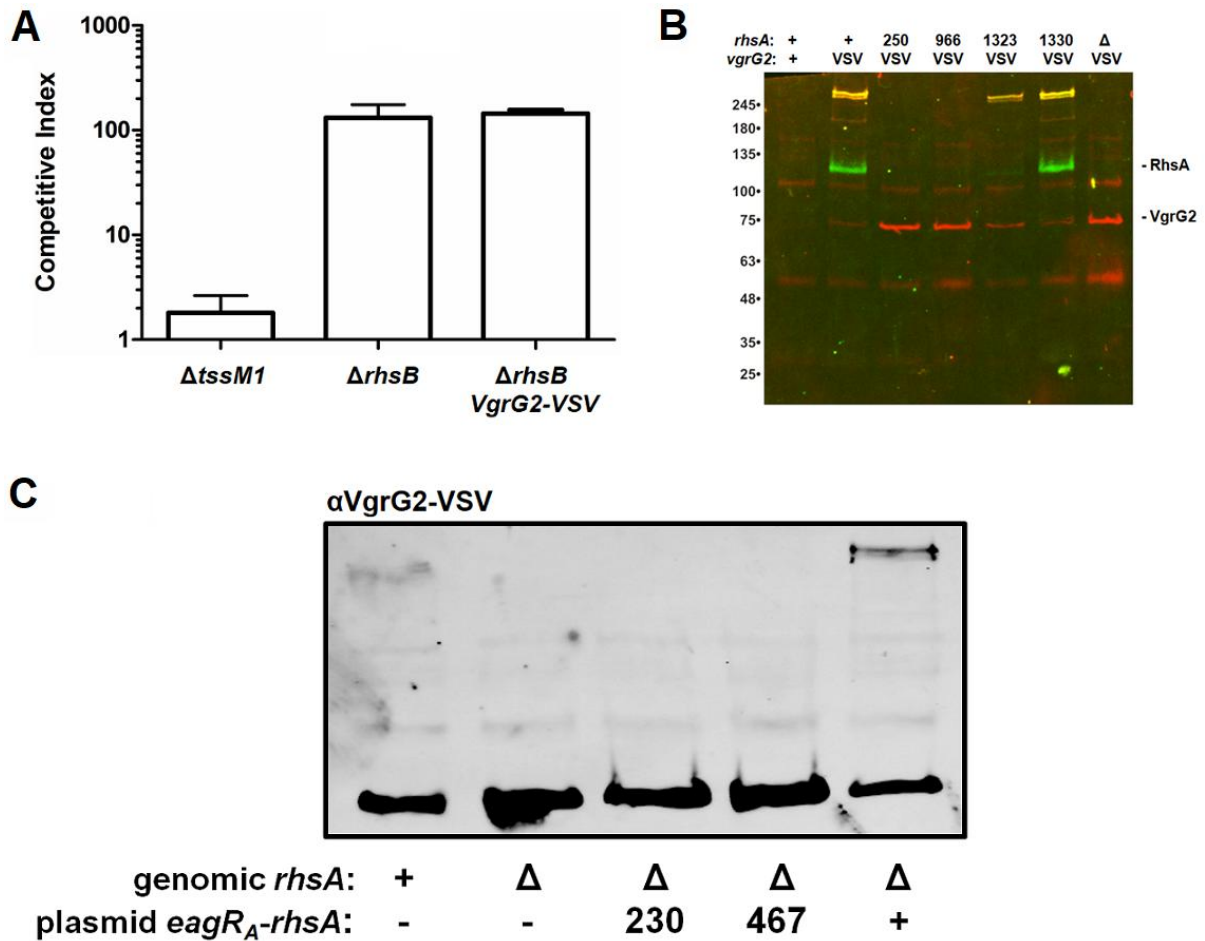


**Figure 4.4. Rhs promotes VgrG spike formation in *E. cloacae*.** (A) Indicated *E. cloacae* inhibitors were incubated at a 1:1 ratio with *E. coli* targets for 3 hours. Data represent the average and standard error of the mean for three independent experiments. (B) Lysates of the indicated *E. cloacae* strains (all in a  $\Delta rhsB$  background) were subjected to  $\alpha$ -VSV immunoprecipitation. The bound fractions were subsequently analyzed via SDS-PAGE and dual  $\alpha$ -VSV (red)  $\alpha$ -RhsA (green) immunoblot. Labeled Rhs numbers indicate the position of truncation. VgrG2-VSV has a predicted molecular weight of 73 kDa, and RhsA $_{\Delta CT}$  has a predicted molecular weight of 148 kDa. (C) Indicated *E. cloacae*  $\Delta rhsB$  strains were grown in plasmid-inducing media, then subjected to  $\alpha$ -VSV immunoprecipitation. The bound fractions were subsequently analyzed via SDS-PAGE and  $\alpha$ -VSV immunoblot. Construct 230 contains RhsA residues 1-230, and construct 467 contains RhsA residues 1-467; both contain full-length *eagR<sub>A</sub>* encoded in *cis*. A + indicates full-length *rhsA* is present.

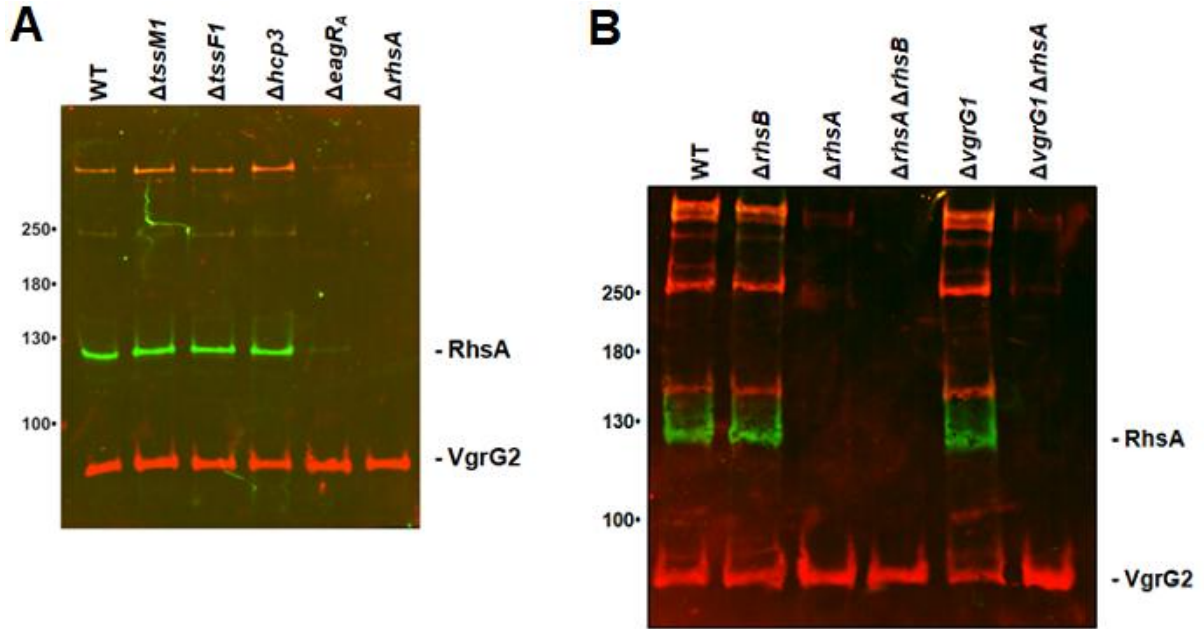


**Figure 4.5. VgrG spike formation is not dependent on other T6SS apparatus sub-complexes, but does require Rhs.** (A) and (B) Lysates of the indicated *E. cloacae* strains were subjected to  $\alpha$ -VSV immunoprecipitation. The bound fractions were subsequently analyzed via SDS-PAGE and dual  $\alpha$ -VSV (red)  $\alpha$ -RhsA (green) immunoblot.

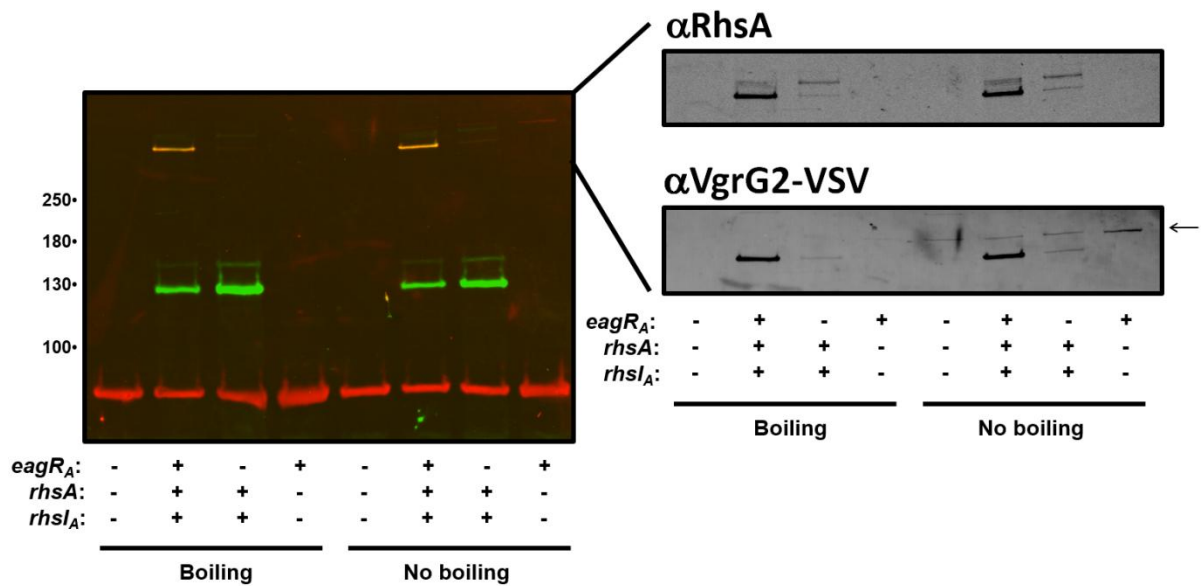


**Figure 4.6. EagR and Rhs are sufficient to support VgrG spike formation when heterologously expressed in *E. coli*.** *E. coli* expressing the indicated plasmid constructs were lysed and analyzed via SDS-PAGE and dual  $\alpha$ -VSV (red)  $\alpha$ -RhsA (green) immunoblot. Samples were differentially heat-treated with boiling or kept at ambient temperature as indicated. The right greyscale images show the top of the immunoblot for each indicated antibody channel in isolation. The arrow indicates a

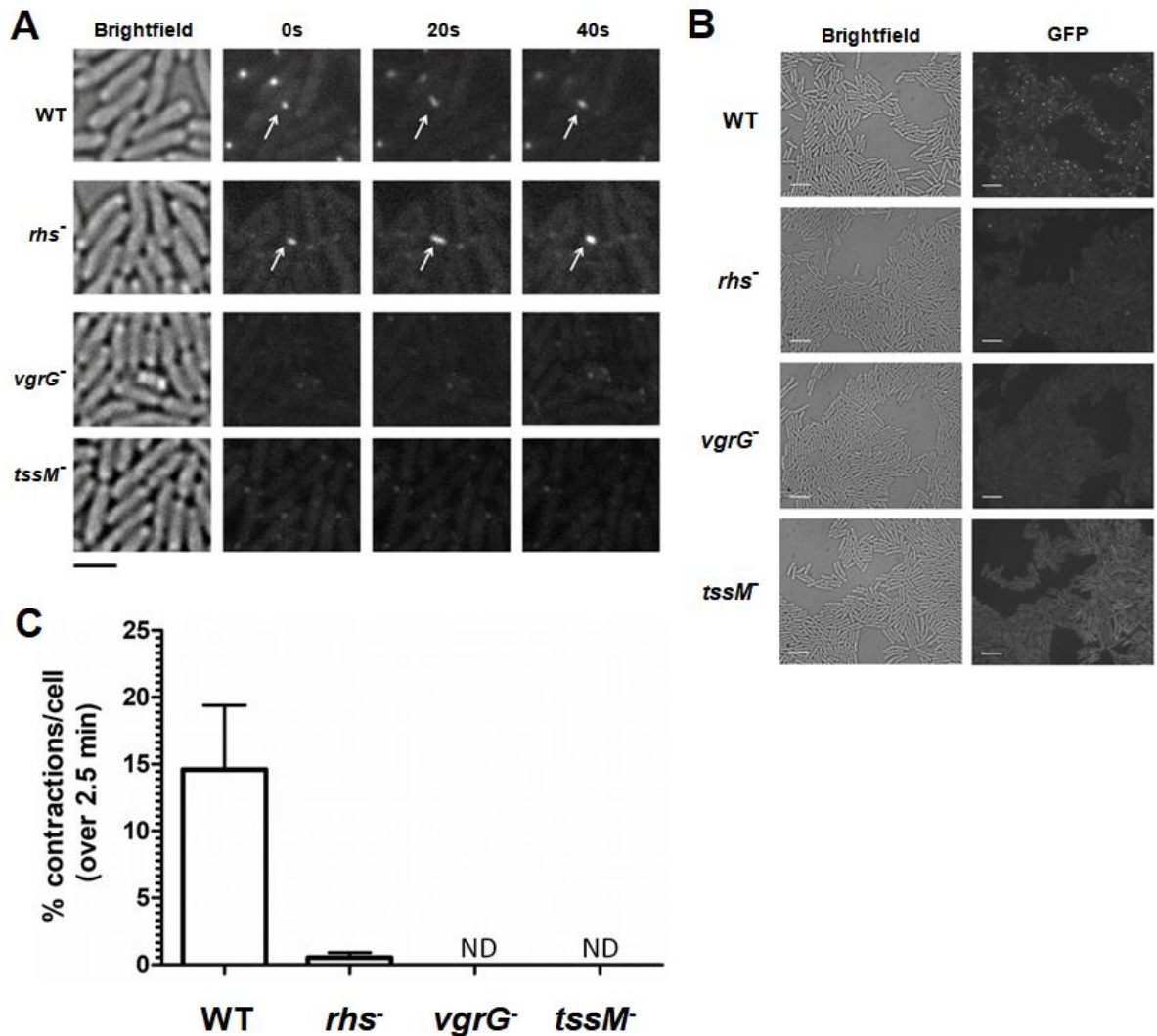


**Figure 4.7. Rhs promotes TssBC sheath assembly.** Indicated *E. cloacae* TssB-GFP fusion strains were analyzed via timelapse GFP-fluorescence microscopy. (A) Timelapse depiction of elongation-contraction-dissassembly cycles in indicated strains. Time-lapses are representative for observed firing cycles in each strain. Scale-bar is 2  $\mu$ m and applies to all images in the panel. (B) Single frame images depicting the representative amount of TssB-GFP foci formed in the indicated strains. Scale-bar is 5  $\mu$ m. (C) Quantification of observed firing cycles in the indicated strains. Data from >900 cells per strain represent the average and standard error of the mean for three independent experiments. WT=wild-type, ND=none detected.

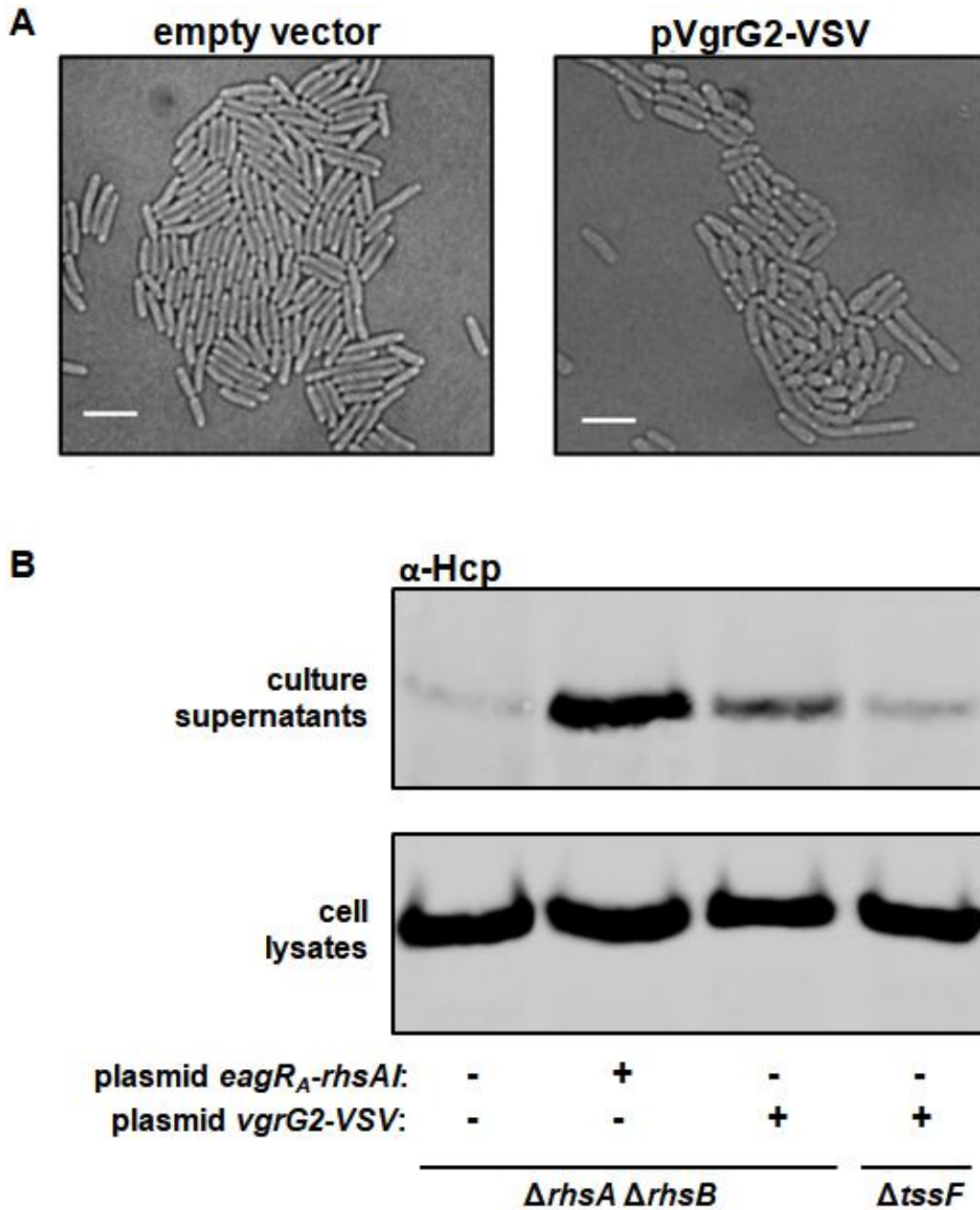


**Figure 4.8. VgrG over-expression may bypass the need for Rhs.** (A) *tssB-GFP E. cloacae* strains carrying the indicated plasmids were grown in inducing media, then subsequently imaged via light microscopy. VgrG2-overexpressing cells have morphological defects and inclusion bodies. Scale-bar is 2  $\mu$ m. (B) Indicated *E. cloacae* strains were grown in inducing media, then cell lysates and supernatants were analyzed via SDS-PAGE and  $\alpha$ -Hcp3 immunoblot.

**Table 4.1. Bacterial strains used in this study.**

Strain	Description <sup>a</sup>	Reference
X90	<i>E. coli</i> F' <i>lacIq lac' pro' /ara Δ(lac-pro) nal1 argE(amb) rif<sup>r</sup> thi-1</i> , Rif <sup>R</sup>	150
<i>E. cloacae</i> ATCC 13047	Type strain (ECL), Amp <sup>R</sup>	American Type Culture Collection
MFDpir	MG1655 RP4-2-Tc::[ΔMu1::aac(3)IV-ΔaphA-Δnic35-ΔMu2::zeo] dapA::(erm-pir) ΔrecA, Apr <sup>R</sup> Zeo <sup>R</sup> Erm <sup>R</sup>	147
CH2016	X90 (DE3) Δ <i>rna</i> Δ <i>slyD</i> :: <i>kan</i> , Rif <sup>R</sup> Kan <sup>R</sup>	156
CH11196	ECL Δ <i>tssM1</i> :: <i>kan</i> , Amp <sup>R</sup> Kan <sup>R</sup>	81
CH11178	ECL Δ <i>rhsA</i> :: <i>kan</i> , Amp <sup>R</sup> Kan <sup>R</sup>	81
CH11179	ECL Δ <i>rhsA</i> , Amp <sup>R</sup>	81
CH11186	ECL Δ <i>rhsB</i> :: <i>kan</i> , Amp <sup>R</sup> Kan <sup>R</sup>	81
CH11733	ECL Δ <i>rhsB</i> , Amp <sup>R</sup>	This study
CH11199	ECL Δ <i>hcp3</i> :: <i>spc</i> , Amp <sup>R</sup> Spec <sup>R</sup>	This study
CH11748	ECL Δ <i>rhsB</i> Δ <i>rhsA</i> :: <i>kan</i> , Amp <sup>R</sup> Kan <sup>R</sup>	This study
CH11903	ECL Δ <i>rhsB</i> Δ <i>rhsA</i> , Amp <sup>R</sup>	This study
CH11436	ECL Δ <i>vgrG2</i> :: <i>kan</i> , Amp <sup>R</sup> Kan <sup>R</sup>	This study
CH12582	ECL Δ <i>vgrG2</i> , Amp <sup>R</sup>	This study
CH12414	ECL Δ <i>vgrG2</i> Δ <i>vgrG1</i> :: <i>kan</i> , Amp <sup>R</sup> Kan <sup>R</sup>	This study
CH12415	ECL Δ <i>rhsA</i> Δ <i>vgrG1</i> :: <i>kan</i> , Amp <sup>R</sup> Kan <sup>R</sup>	This study
CH12416	ECL Δ <i>rhsA</i> Δ <i>vgrG2</i> :: <i>kan</i> , Amp <sup>R</sup> Kan <sup>R</sup>	This study
CH12384	ECL Δ <i>vgrG1</i> :: <i>kan</i> , Amp <sup>R</sup> Kan <sup>R</sup>	This study
CH12385	ECL Δ <i>rhsB</i> Δ <i>vgrG1</i> :: <i>kan</i> , Amp <sup>R</sup> Kan <sup>R</sup>	This study
CH12386	ECL Δ <i>rhsB</i> Δ <i>vgrG2</i> :: <i>kan</i> , Amp <sup>R</sup> Kan <sup>R</sup>	This study
CH11530	ECL Δ <i>rhsA</i> <i>rhsB</i> (L206stop):: <i>kan</i> , Amp <sup>R</sup> Kan <sup>R</sup>	This study
CH11642	ECL Δ <i>rhsA</i> <i>rhsB</i> (S857stop):: <i>kan</i> , Amp <sup>R</sup> Kan <sup>R</sup>	This study
CH11531	ECL Δ <i>rhsA</i> <i>rhsB</i> (E1161stop):: <i>kan</i> , Amp <sup>R</sup> Kan <sup>R</sup>	This study
CH12486	ECL Δ <i>rhsA</i> <i>rhsB</i> (Q1277stop):: <i>kan</i> , Amp <sup>R</sup> Kan <sup>R</sup>	This study
CH12497	ECL Δ <i>rhsB</i> <i>rhsA</i> (G250stop):: <i>kan</i> , Amp <sup>R</sup> Kan <sup>R</sup>	This study
CH12226	ECL Δ <i>rhsB</i> <i>rhsA</i> (G966stop):: <i>kan</i> , Amp <sup>R</sup> Kan <sup>R</sup>	This study
CH11749	ECL Δ <i>rhsB</i> <i>rhsA</i> (I1323stop):: <i>kan</i> , Amp <sup>R</sup> Kan <sup>R</sup>	This study
CH12492	ECL Δ <i>rhsB</i> <i>rhsA</i> (Q1330stop):: <i>kan</i> , Amp <sup>R</sup> Kan <sup>R</sup>	This study
CH12482	ECL <i>tssB1-sfGFP</i> :: <i>kan</i> , Amp <sup>R</sup> Kan <sup>R</sup>	This study
CH12483	ECL <i>tssB1-sfGFP</i> , Amp <sup>R</sup>	This study
CH12485	ECL <i>tssB1-sfGFP</i> Δ <i>rhsA</i> :: <i>kan</i> , Amp <sup>R</sup> Kan <sup>R</sup>	This study
CH12555	ECL <i>tssB1-sfGFP</i> Δ <i>rhsA</i> , Amp <sup>R</sup>	This study
CH12594	ECL <i>tssB1-sfGFP</i> Δ <i>rhsA</i> Δ <i>rhsB</i> :: <i>kan</i> , Amp <sup>R</sup> Kan <sup>R</sup>	This study
CH12561	ECL <i>tssB1-sfGFP</i> Δ <i>tssM1</i> :: <i>kan</i> , Amp <sup>R</sup> Kan <sup>R</sup>	This study
CH12562	ECL <i>tssB1-sfGFP</i> Δ <i>vgrG1</i> :: <i>spc</i> , Amp <sup>R</sup> Spec <sup>R</sup>	This study
CH12564	ECL <i>tssB1-sfGFP</i> Δ <i>vgrG1</i> :: <i>spc</i> Δ <i>vgrG2</i> :: <i>kan</i> , Amp <sup>R</sup> Kan <sup>R</sup> Spec <sup>R</sup>	This study

CH13104	ECL $\Delta rhsB::kan vgrG2-VSV::spc$ , Amp <sup>R</sup> Kan <sup>R</sup> Spec <sup>R</sup>	This study
CH13105	ECL $\Delta rhsB rhsA(G250stop)::kan vgrG2-VSV::spc$ , Amp <sup>R</sup> Kan <sup>R</sup> Spec <sup>R</sup>	This study
CH13106	ECL $\Delta rhsB rhsA(G966stop)::kan vgrG2-VSV::spc$ , Amp <sup>R</sup> Kan <sup>R</sup> Spec <sup>R</sup>	This study
CH13107	ECL $\Delta rhsB rhsA(I1323stop)::kan vgrG2-VSV::spc$ , Amp <sup>R</sup> Kan <sup>R</sup> Spec <sup>R</sup>	This study
CH13108	ECL $\Delta rhsB rhsA(Q1330stop)::kan vgrG2-VSV::spc$ , Amp <sup>R</sup> Kan <sup>R</sup> Spec <sup>R</sup>	This study
CH13109	ECL $\Delta rhsB \Delta rhsA::kan vgrG2-VSV::spc$ , Amp <sup>R</sup> Kan <sup>R</sup> Spec <sup>R</sup>	This study
CH12884	ECL $vgrG2-VSV::kan$ , Amp <sup>R</sup> Kan <sup>R</sup>	This study
CH14452	ECL $vgrG2-VSV$ , Amp <sup>R</sup>	This study
CH13230	ECL $\Delta tssM1::kan vgrG2-VSV::spc$ , Amp <sup>R</sup> Kan <sup>R</sup> Spec <sup>R</sup>	This study
ZR274	ECL $\Delta tssF1::kan$ , Amp <sup>R</sup> Kan <sup>R</sup>	Zachary Ruhe
CH13754	ECL $\Delta tssF1::kan vgrG2-VSV::spc$ , Amp <sup>R</sup> Kan <sup>R</sup> Spec <sup>R</sup>	This study
CH14730	ECL $vgrG2-VSV \Delta hcp3::spc$ , Amp <sup>R</sup> Spec <sup>R</sup>	This study
CH14738	ECL $vgrG2-VSV \Delta eagR_A$ , Amp <sup>R</sup>	This study
CH13286	ECL $\Delta rhsA::kan vgrG2-VSV::spc$ , Amp <sup>R</sup> Kan <sup>R</sup> Spec <sup>R</sup>	This study
CH4875	ECL $\Delta vgrG1$ , Amp <sup>R</sup>	This study
CH4927	ECL $\Delta vgrG1 vgrG2-VSV::spc$ , Amp <sup>R</sup> Spec <sup>R</sup>	This study
CH4924	ECL $\Delta rhsA \Delta vgrG1$ , Amp <sup>R</sup>	This study
CH4934	ECL $\Delta rhsA \Delta vgrG1 vgrG2-VSV::spc$ , Amp <sup>R</sup> Spec <sup>R</sup>	This study

<sup>a</sup>Abbreviations: Amp<sup>R</sup>, ampicillin-resistant; Kan<sup>R</sup>, kanamycin-resistant; Rif<sup>R</sup>, rifampicin-resistant; Spec<sup>R</sup>, spectinomycin-resistant; Apr<sup>R</sup>, aprimycin-resistant; Erm<sup>R</sup>, erythromycin-resistant; Zeo<sup>R</sup>, zeocin-resistant

**Table 4.2. Plasmids used in this study.**

<b>Number</b>	<b>Description<sup>a</sup></b>	<b>Reference</b>
	pCH450, Tet <sup>R</sup>	153
	pCH450kpn, Tet <sup>R</sup>	71
	pTrc99aCm, Cm <sup>R</sup>	71
	pBAD24, Amp <sup>R</sup>	157
	pKOBEG, Cm <sup>R</sup>	144
	pCP20, Amp <sup>R</sup> , Cm <sup>R</sup>	145
	pET21P, Amp <sup>R</sup>	Novagen
pCH11163	pET21P:: <i>hcp3-his6</i> , Amp <sup>R</sup> (for generation of Hcp3 antiserum)	This study
pCH11463	pET21P:: <i>rhsA(82-467)-his6</i> , Amp <sup>R</sup> (for generation of RhsA antiserum)	This study
pCH13524	pCH450kpn:: <i>eagR<sub>A</sub>-rhsA(G230stop)</i> , Tet <sup>R</sup>	This study
pCH13631	pCH450kpn:: <i>eagR<sub>A</sub>-rhsA(A467stop)</i> , Tet <sup>R</sup>	This study
pCH12766	pCH450kpn:: <i>rhsA(G230stop)</i> , Tet <sup>R</sup>	This study
pCH12767	pCH450kpn:: <i>rhsA(A467stop)</i> , Tet <sup>R</sup>	This study
pCH13938	pTrc99a:: <i>eagR<sub>A</sub>-His6</i> , Cm <sup>R</sup>	This study
pCH14397	pBAD24:: <i>vgrG2-VSV</i> , Amp <sup>R</sup>	This study
pCH13568	pCH450kpn:: <i>eagR<sub>A</sub></i> , Tet <sup>R</sup>	This study
pCH14190	pCH450:: <i>rhsA-rhsI<sub>A</sub></i> , Tet <sup>R</sup>	This study
pCH14152	pCH450:: <i>eagR<sub>A</sub>-rhsA-rhsI<sub>A</sub></i> , Tet <sup>R</sup>	This study
pCH14231	pCH450:: <i>vgrG2-VSV</i> , Tet <sup>R</sup>	This study
pCH70	pKAN, Kan <sup>R</sup> , Amp <sup>R</sup>	143
pCH9384	pSPM, Spec <sup>R</sup> , Amp <sup>R</sup>	67
pCH11050	pKAN:: $\Delta$ ECL_01536 ( <i>tssM1</i> deletion), Kan <sup>R</sup> , Amp <sup>R</sup>	81
pCH10958	pKAN:: $\Delta$ ECL_01567 ( <i>rhsA</i> deletion), Kan <sup>R</sup> , Amp <sup>R</sup>	81
pCH11044	pKAN:: $\Delta$ ECL_03140 ( <i>rhsB</i> deletion), Kan <sup>R</sup> , Amp <sup>R</sup>	81
pCH11502	pKAN:: $\Delta$ ECL_01561 ( <i>vgrG2</i> deletion), Kan <sup>R</sup> , Amp <sup>R</sup>	This study
pCH12370	pKAN:: $\Delta$ ECL_01558 ( <i>vgrG1</i> deletion), Kan <sup>R</sup> , Amp <sup>R</sup>	This study
pCH11459	pSPM:: $\Delta$ ECL_01558 ( <i>vgrG1</i> deletion), Spec <sup>R</sup> , Amp <sup>R</sup>	This study
pCH11632	pKAN:: $\Delta$ ECL_03140(L206stop) [ <i>rhsB</i> truncation], Kan <sup>R</sup> , Amp <sup>R</sup>	This study
pCH11635	pKAN:: $\Delta$ ECL_03140(S957stop) [ <i>rhsB</i> truncation], Kan <sup>R</sup> , Amp <sup>R</sup>	This study
pCH11633	pKAN:: $\Delta$ ECL_03140(E1161stop) [ <i>rhsB</i> truncation], Kan <sup>R</sup> , Amp <sup>R</sup>	This study
pCH12437	pKAN:: $\Delta$ ECL_03140(Q1277stop) [ <i>rhsB</i> truncation], Kan <sup>R</sup> , Amp <sup>R</sup>	This study
pCH11981	pKAN:: $\Delta$ ECL_01567(G250stop) [ <i>rhsA</i> truncation], Kan <sup>R</sup> , Amp <sup>R</sup>	This study
pCH12003	pKAN:: $\Delta$ ECL_01567(G966stop) [ <i>rhsA</i> truncation], Kan <sup>R</sup> , Amp <sup>R</sup>	This study

	Kan <sup>R</sup> , Amp <sup>R</sup>	
pCH11635	pKAN:: <i>ECL_01567(I1323stop)</i> [ <i>rhsA</i> truncation], Kan <sup>R</sup> , Amp <sup>R</sup>	This study
pCH12291	pKAN:: <i>ECL_01567(Q1330stop)</i> [ <i>rhsA</i> truncation], Kan <sup>R</sup> , Amp <sup>R</sup>	This study
pCH12509	pKAN:: <i>ECL_01539-sfGFP</i> ( <i>tssB1-GFP</i> fusion), Kan <sup>R</sup> , Amp <sup>R</sup>	Zachary Ruhe
pCH13002	pSPM:: <i>ECL_01561-VSV</i> ( <i>vgrG2-VSV</i> fusion), Spec <sup>R</sup> , Amp <sup>R</sup>	This study
pCH12883	pKAN:: <i>ECL_01561-VSV</i> ( <i>vgrG2-VSV</i> fusion), Kan <sup>R</sup> , Amp <sup>R</sup>	This study
pCH12318	pKAN:: <i>ΔECL_01566</i> ( <i>eagR<sub>A</sub></i> deletion), Kan <sup>R</sup> , Amp <sup>R</sup>	This study
pDL6480	pRE118- <i>pheS*</i> , Kan <sup>R</sup>	David Low
pCH14625	pRE118- <i>pheS*::ΔeagR<sub>A</sub></i> , Kan <sup>R</sup>	This study

<sup>a</sup>Abbreviations: Amp<sup>R</sup>, ampicillin-resistant; Cm<sup>R</sup>, chloramphenicol-resistant; Kan<sup>R</sup>, kanamycin-resistant; Tet<sup>R</sup>, tetracycline-resistant; Spec<sup>R</sup>, spectinomycin-resistant

**Table 4.3. Oligonucleotides used in this study.**

<b>Number</b>	<b>Name<sup>a</sup></b>	<b>Sequence<sup>b</sup></b>	<b>Reference</b>
CH3020	Hcp3-Nco-for	5' - ATA <u>CCA TGG</u> CTA TTG ATA TGT TTC	This study
CH3022	Hcp3-Xho-rev	5' - CTA <u>CTC GAG</u> TGC TTC TTT GTT TTC TTT G	This study
CH2960	RhsA(V82)- Nco-for	5' - TGG <u>CCA TGG</u> TTA CTG ACG ATA TCA G	This study
CH2879	RhsA(A467)- Spe-rev	5' - AAA <u>ACT AGT</u> GGC AGC GGT TAC GCG CTG TGG	This study
CH4190	EagR <sub>A</sub> -Kpn- for	5' - AGT <u>GGT ACC</u> ATG AAA TAC ACC CTC CAG G	This study
CH2911	EagR <sub>A</sub> -Xho- rev	5' - TCA <u>CTC GAG</u> CCT TAC ACA TTC CGG	This study
CH2877	EagR <sub>A</sub> -H6- Spe-rev	5' - CAT <u>ACT AGT</u> CAC ATT CCG GTT GTC GTT AAG C	This study
CH2878	RhsA-Kpn-for	5' - GTG <u>GGT ACC</u> ATG AGC GAT AAC AAC GCG GCC	This study
CH3555	RhsA(G23ostop)-Xho-rev	5' - CAG <u>CTC GAG</u> TTA GCC GAT GAT CAC ATT CG	This study
CH3687	RhsA(A467stop)-Xho-rev	5' - AAA <u>CTC GAG</u> TTA GGC AGC GGT TAC GCG	This study
CH4452	VgrG2-Eco-for	5' - ATA <u>GAA TTC</u> ATG CTC AAC CGA ATT ACC	This study
CH4453	VSV-Xho-rev	5' - TGC <u>CTC GAG</u> ATC CTT ATT TGC CAA GAC G	This study
CH3914	RhsA-Eco-for	5' - TTT <u>GAA TTC</u> GGC ATG AGC GAT AAC AAC	This study
CH4325	RhsA- Nco(int)-rev	5' - AGG <u>CCA TGG</u> TCG TTA TAG	This study

CH4326	RhsA- Nco(int)-for	5' - CGA <u>CCA TGG</u> CCT GAT GG	This study
CH4327	RhsA- Kpn(int)-rev	5' - CAG <u>CGG TAC CAG</u> CTG AAC	This study
CH4328	RhsA- Kpn(int)-for	5' - TTC AGC <u>TGG TAC CGC</u> TGG	This study
CH4329	RhsIA-Sbf-rev	5' - ACC CTC GAG <u>CCT GCA GGT</u> GTG GTC GAA CAT TAA CAT ATT AAA TCG	This study
CH4400	EagRA-Eco- for	5' - AGT <u>GAA TTC</u> ATG AAA TAC ACC CTC CAG G	This study
CH2818	RhsA-KO-Sac	5' - TTT <u>GAG CTC</u> ATA CAC CCT CCA GGA AGG	81
CH2819	RhsA-KO- Bam	5' - TTT <u>GGA TCC</u> GCC TTA CAC ATT CCG GTT G	81
CH2820	RhsA-KO-Eco	5' - GAA <u>GAA TTC</u> TGG CAA GAG GAT TAC TTA ATG	81
CH2821	RhsA-KO-Kpn	5' - TTT <u>GGT ACC</u> CAT CAT TAG TAA TGC AAA G	81
CH2905	RhsB-KO-Sac	5'- TTT <u>GAG CTC</u> ACC CGC TCA ATG TCA GAA C	81
CH2906	RhsB-KO-Bam	5'- TTT <u>GGA TCC</u> CCC TGG TGT TAA TGG TGG	81
CH2907	RhsB-KO-Eco	5'- TTT <u>GAA TTC</u> CAA TGA ATA TGC TGA ATG TGA G	81
CH2908	RhsB-KO-Kpn	5'- TTT <u>GGT ACC</u> ACT TCG TCA TTA TCA TCT GC	81
CH2897	TssM1-KO-Sac	5'- TTT <u>GAG CTC</u> GAA ATC GAC GCC GGT CTG	81
CH2898	TssM1-KO- Bam	5'- TTT <u>GGA TCC</u> TTT CCT TGC GGC AAT CCG	81

CH2899	TssM1-KO-Eco	5' - TTT <u>GAA TTC</u> CAA GGA CAG CCG TAT GAC	81
CH2900	TssM1-KO-Kpn	5' - TTT <u>GGT ACC</u> GAA TCG ACA TCA GCA TCT C	81
CH2982	Hcp3-KO-Sac	5' - TTT <u>GAG CTC</u> CCA GGT GCA GGA GAT TC	This study
CH2981	Hcp3-KO-OE-rev	5' - CCA CTA GTT CTA GAG CGG CTA CTC TTC GTC GAT GAA C	This study
CH2980	Hcp3-KO-OE-for	5' - GCT TAT CGA TAC CGT CGA CGT AGT GGG TCC GAA AGG G	This study
CH2983	Hcp3-KO-Kpn	5' - AAA <u>GGT ACC</u> TTC CAG AGT GTT ACA TGC	This study
CH2952	pKAN-OE-for	5' - CCG CTC TAG AAC TAG TGG	This study
CH2953	pKAN-OE-rev	5' - GTC GAC GGT ATC GAT AAG C	This study
CH3040	VgrG1-KO-Sac	5' - GTT <u>GAG CTC</u> GTT ATG GAT GTC ATT TTG TCA ATC	81
CH3041	VgrG1-KO-Bam	5' - AAT <u>GGA TCC</u> GAG CAT AAT CGT TAT TCC GTA ATG	81
CH3042	VgrG1-KO-Eco	5' - AAG <u>GAA TTC</u> AAT AAG TAA ACG TAA TTA GAA AC	81
CH3043	VgrG1-KO-Kpn	5' - CTT <u>GGT ACC</u> AGC AAA AGT TCG ATT TAT TCA AC	81
CH3195	Vgrg2-KO-Sac	5' - TTT <u>GAG CTC</u> CCC TTG CTA CGG CCA AAC	81
CH3196	Vgrg2-KO-Bam	5' - TTT <u>GGA TCC</u> TCG TTA TTC CAC TAT GGG C	81
CH3197	Vgrg2-KO-Xho	5' - TTT <u>CTC GAG</u> GCT GGA GCG GTG CTT G	81
CH3198	Vgrg2-KO-	5' - TTT <u>GGT ACC</u> CGA GTC CAG	81

	Kpn	ACA ATC AGG	
CH3232	RhsB(L206stop)-Sac	5' - GCC <u>GAG CTC</u> GGC GCA TCC TGC CTT GGC	This study
CH3233	RhsB(L206stop)-Bam	5' - CAG <u>GGA TCC</u> TGC CCA GCT ACT TAG AGA GCG C	This study
CH3318	RhsB(S957stop)-Sac	5' - TTT <u>GAG CTC</u> TGC TGA GTG CCG TGA TC	This study
CH3319	RhsB(S957stop)-Bam	5' - TTT <u>GGA TCC</u> ACT AGC TTT CGA TAC CCA GCG C	This study
CH3234	RhsB(E1161stop)-Sac	5' - TAC <u>GAG CTC</u> GAA GGG CGT CTG CTG AAG C	This study
CH3235	RhsB(E1161stop)-Bam	5' - TGT <u>GGA TCC</u> AGT AAA TCT AAC CGC TGC TCT GG	This study
CH3831	RhsB(Q1277stop)-Not	5' - AAC <u>GCG GCC GCT</u> TAC GCG GAG AGT CCC CAC	This study
CH2834	RhsI <sub>B</sub> -Xho-rev	TTT <u>CTC GAG</u> GTA TCC TAG CCA TAA AAA TAA TC	81
CH3558	RhsA(G250stop)-Sac	5' - GCG <u>GAG CTC</u> CTA ACC TGG CGG GTG	This study
CH3559	RhsA(G250stop)-Bam	5' - GAG <u>GGA TCC</u> TTA CCC CAG TGC CAG C	This study
CH3560	RhsA(G966stop)-Sac	5' - GGT <u>GAG CTC</u> CCG CTG GGA CAG C	This study
CH3561	RhsA(G966stop)-Bam	5' - GCT <u>GGA TCC</u> TTA CCC GCT GCC GTA G	This study
CH3316	RhsA(I1323stop)-Sac	5' - TTT <u>GAG CTC</u> ACA GAA GTG ATC AGC CAG	This study
CH3317	RhsA(I1323stop)-Bam	5' - TTT <u>GGA TCC</u> CTA TAT TCG GGT TAG ACT ATT AGC	This study
CH3699	RhsA(Q1330stop)	5' - TAA <u>GAG CTC</u> GCG GGA AGA	This study

	op)-Sac	ACG GG	
CH3698	RhsA(Q133ost op)-Bam	5' - AAC <u>GGA TCC</u> TTA TTT TAA TCC CAG AGG GTC	This study
CH3937	Vgrg2(T401)- Sac	5' - ACA <u>CGA GCT CCT</u> GCT GGG TG - 3'	This study
CH3945	VgrG2-VSV- rev	5' - CAA GAC GAT TCA TTT CAA TAT CAG TAT AAC TAG TAT CAC CCT TGG TCG TGA ATT TCG C	This study
CH3946	VSV-Not-rev	5' - TTT <u>GCG GCC GCA</u> TCC TTA TTT GCC AAG ACG ATT CAT TTC AAT ATC AGT AT	This study
CH2901	EagRA-KO- Sac	5'- TTT <u>GAG CTC</u> ATG CTC CGC TGC GTT ATA	This study
CH2902	EagRA-KO- Spe	5'- TTT <u>ACT AGT</u> CGT GTT ATC CTG CCA GGC	This study
CH3775	EagRA-KO- Eco	5' - GAT <u>GAA TTC</u> TAC TCT CTC GGC ACT CAG	This study
CH2904	EagRA-KO- Kpn	5'- TTT <u>GGT ACC</u> CAG AGA GCA ACA TGC CGG	This study

<sup>a</sup>Abbreviations: OE=overlap-extension, Bam=BamHI, Eco=EcoRI, Hind=HindIII, Kpn=KpnI, Nco=NcoI, Not=NotI, Sac=SacI, Sbf=SbfI, Spe=SpeI, Xho=XhoI

<sup>b</sup>Restriction endonuclease sites are underlined.

## **Chapter 5: EagR is required for Rhs-dependent T6SS activity but not for Rhs-CT processing.**

Note: former graduate student in the Hayes lab, Christina Beck, helped with strain construction for this work.

### **Abstract**

Here, I examine the roles of two chaperone proteins, EagR<sub>A</sub> and EagR<sub>B</sub>, in *Enterobacter cloacae* ATCC 13047 T6SS activity. Effector-associated gene with Rhs, EagR, is encoded upstream of its cognate *rhs* gene. In the previous chapter, I showed that at least one Rhs protein is required to support T6SS activity in *E. cloacae*. Here, I show that EagR is required for activity of its cognate Rhs protein, and therefore at least one EagR protein is also required to support T6SS activity. Additionally, I show that a mutant Rhs that no longer binds to EagR can no longer support T6SS activity. However, cleavage of the Rhs C-terminal toxin (CT) domain occurs independently of EagR or any other T6SS factors. This cleavage event is required for CT delivery, but not for overall Rhs-mediated T6SS activity. I additionally show the processed CT polypeptide remains associated with the remaining EagR-Rhs complex, suggesting this CT-domain is sequestered within the Rhs  $\beta$ -encapsulation structure.

## Introduction

A number of type VI secretion system (T6SS) effectors have been reported to require other T6SS-associated proteins for proper assembly onto the T6SS apparatus. Moreover, many of these effectors are stabilized by the interaction with these T6SS factors. I have previously discussed how some small effectors are known to interact directly with the T6SS structural component Hcp, and have also been shown to be stabilized via this interaction (see Chapter 1; 81, 88). In this manner, Hcp can serve as both a structural component of the T6SS apparatus, as well as an effector chaperone. However, in many cases, stabilization or assembly of T6SS effectors is dependent on accessory proteins. Three such families of effector accessory proteins are described in the literature: the DUF4123 family, the DUF2169 family, and the DUF1795 family. It is likely other such families exist but have yet to be identified.

The DUF4123 family of effector accessory proteins was first discovered in *Vibrio cholerae*, and has been found to serve as VgrG-adaptors (89, 90, 97). This family of proteins, named T6SS adaptor proteins (Tap), has been shown to be required for the interaction between the effector TseL and VgrG-1 in *V. cholerae* (90). Moreover, Tap-1 is required specifically for TseL delivery, but not overall T6SS activity (89, 90). Tap-encoding genes have been identified across Proteobacteria, and have even been used as a predictor to find new T6SS effectors (89, 90). Recently, a DUF4123 family of chaperone protein has been shown to facilitate the delivery of the *Pseudomonas aeruginosa* effector TseT; interestingly, this chaperone recruits TseT to PAAR, not VgrG, but is not required for the TseT-PAAR interaction (188).

Additionally, a Tap adaptor is also found in *Agrobacterium tumefaciens*, and has been shown to be essential for the loading of the *A. tumefaciens* effector Tde1 onto the C-terminal extension of *A. tumefaciens* VgrG1 (97).

*A. tumefaciens* also utilizes a second family of effector accessory proteins, known as the DUF2169 family. These proteins were shown to serve as both a chaperone and as a predicted VgrG-adaptor for the *A. tumefaciens* Tde2 effector (68, 97). This accessory protein has genetic specificity to the C-terminal extension of *A. tumefaciens* VgrG2, and is both essential and specific for Tde2 delivery (97). DUF2169 genes are associated with *vgrG* and *tde* alleles across Proteobacteria, including in *Burkholderia* and *Vibrio* species, indicating this is likely a conserved pathway of effector delivery (97). Interestingly, this Tde2 effector has a putative PAAR domain, so the observed “adaptor” function of DUF2169 is curious since PAAR is expected to be the VgrG-interaction domain of Tde2. Instead, DUF2169 may serve as a chaperone for the PAAR domain of its effector, and may therefore be required to promote the direct interaction between VgrG and effector.

Finally, the DUF1795 accessory family, now named effector-associated gene (*eag*), has been shown to have chaperone activity for its cognate effectors (69, 73). Eag proteins are frequently encoded upstream of *rhs* alleles across a variety of Proteobacteria, and were in fact originally named effector-associated gene with Rhs (EagR). EagR was originally demonstrated to help stabilize Rhs in *Serratia marcescens*, and was also shown to be essential for the delivery of its cognate Rhs effector (69). Similarly, the *P. aeruginosa* effector Tse6 also requires its upstream EagT6 for stability (73). Moreover, Mougous and colleagues have recently

demonstrated that EagT6 is required for loading Tse6 onto VgrG1 in *P. aeruginosa* (176). They also show that EagT6 interacts with the hydrophobic N-terminus of Tse6, which is predicted to form transmembrane domains, and that the presence of these transmembrane domains destabilizes Tse6 in the absence of EagT6 (176). Currently, all described Eag-dependent effectors encode PAAR domains; however, it is currently unclear whether this correlation is functionally significant. In this chapter, I postulate that Eag accessory proteins may serve as PAAR-folding chaperones, and that the correlation between Eag and PAAR-encoding effectors would therefore be functionally relevant.

As discussed in Chapter 4, Rhs proteins are predicted to form a shell-like  $\beta$ -encapsulation structure that surrounds the polymorphic C-terminally-encoded toxin. In this manner, Rhs proteins themselves may serve as a chaperone or translocation system for their C-terminal toxins. In this chapter, I explore the role of EagR proteins in *Enterobacter cloacae*, and also address questions pertaining to the Rhs toxin domain. I demonstrate that EagR is required for Rhs activity in *E. cloacae*. I also show that Rhs undergoes auto-proteolytic C-terminal processing of its toxin domain, but that this cleavage event is not dependent on EagR.

## **Results**

### *EagR is required for Rhs activity*

Chapter 4 presented data suggesting EagR interacts directly with Rhs in order to promote Rhs activity (Figure 4.3D). To test if EagR is required for Rhs activity, I

deleted *eagR<sub>A</sub>* and *eagR<sub>B</sub>* and analyzed the resulting phenotypes of those deletions. I find that deletion of *eagR<sub>A</sub>* abrogates *rhsA*-mediated inter-bacterial inhibition, and that this phenotype can be rescued with *eagR<sub>A</sub>* complemented in *trans* (Figure 5.1A). However, *eagR<sub>B</sub>* is not successful at complementing the *eagR<sub>A</sub>* deletion, suggesting *eagR* only works with its cognate downstream *rhs* allele. Moreover, the deletion of *eagR<sub>B</sub>* does not impair *rhsA*-mediated inhibition, again suggesting *eagR* supports activity of its cognate *rhs*. The same experiments were done to analyze *rhsB*-mediated inhibition, and similarly, I find that *EagR<sub>B</sub>* supports *RhsB* activity but not *RhsA* activity (Figure 5.1B).

Next, I asked whether *EagR* is required to support the overall T6SS-promoting activity of *Rhs* rather than specific *Rhs*-mediated toxicity via the *Rhs* C-terminal toxin domain. I find that co-deletion of *eagR<sub>A</sub>* and *eagR<sub>B</sub>* phenocopies known T6SS- mutants, suggesting *EagR* is required for T6SS activity in *E. cloacae* (Figure 5.2). *Eag* proteins are predicted to bind to the N-terminus of their downstream effectors (73, 176); therefore, I next investigated whether deletion of *RhsA*'s putative *EagR<sub>A</sub>*-binding-site would abrogate *EagR<sub>A</sub>* binding and overall *RhsA* activity. I find that deletion of *RhsA* residues 1-82 leads to a protein that no longer stably interacts with *EagR<sub>A</sub>* (Figure 5.3A). I also observe that the *rhsA<sub>Δ1-82</sub>* mutation abrogates *RhsA*-mediated T6SS activity in growth inhibition assays, and additionally does not promote the formation of the stable *VgrG2* trimer (Figure 5.3B and 5.3C). Curiously, the migration rate of the *RhsA<sub>Δ1-82</sub>* protein mimics that of the wild-type *RhsA* protein (Figure 5.3A and 5.3C). It has been reported that hydrophobic proteins tend to migrate faster in SDS-PAGE assays than their mass predicts; this is likely

because hydrophobic proteins have greater affinity for SDS. Thus, the hydrophobic RhsA<sub>1-82</sub> region (Figure 5.4A) may cause the full-length RhsA protein to run faster than its mass predicts, and may match the migration rate of the RhsA<sub>Δ1-82</sub> protein due to this biochemical difference.

While it is clear that EagR is required for Rhs activity, the actual mechanism of EagR function is unknown. EagR<sub>A</sub> binds the N-terminus of RhsA, and this binding site is hydrophobic and is predicted to form 2 transmembrane domains (Figure 5.4A and 5.4B). One possible model for EagR function is to sequester these putative transmembrane domains of Rhs during T6SS apparatus assembly, which occurs in the cytoplasm of inhibitor cells. This keeps Rhs stable and soluble, and allows Rhs to be loaded onto the apparatus, after which EagR may dissociate from the complex. After the T6SS apparatus fires, the Rhs effector is delivered into the target cell periplasm, and the putative transmembrane domains are now accessible and free to associate with the target cell inner-membrane. Finally, the association with the Rhs N-terminus to the inner-membrane may allow for Rhs translocation across the target cell inner-membrane, via some unknown mechanism, in order to deliver its toxic C-terminal domain into the target cell cytoplasm.

If this model is correct, I would predict that periplasmically-expressed EagR in target cells could block Rhs toxin translocation into the cytoplasm and thereby protect target cells from inhibition. I tested this by fusing either a Sec-dependent *dsbA* signal-sequence (data not shown) or a Tat-dependent *sufI* signal-sequence (Figure 5.4C) to *eagR<sub>A</sub>* and *eagR<sub>B</sub>* and asked whether these constructs would protect *E. cloacae* targets susceptible to either the RhsA or RhsB toxin. Unfortunately,

neither *eagR<sub>A</sub>* nor *eagR<sub>B</sub>* successfully protected susceptible cells from Rhs intoxication (Figure 5.4C). It is currently unclear whether the model is simply incorrect, or if limitations in this assay, such as EagR stability and/or folding in the periplasm, lead to this failure to block periplasmic Rhs before it translocated into the cytoplasm.

*Rhs undergoes auto-proteolytic C-terminal processing of its toxin domain*

The Rhs  $\beta$ -encapsulation structure is believed to encapsulate the C-terminal toxin domain of Rhs, and this toxin domain is predicted to be proteolytically cleaved off the rest of the protein by the upstream Rhs core domain (72). To test this hypothesis, I fused a FLAG epitope to the very C-terminus of RhsA and asked whether C-terminal processing occurs. I find that the C-terminus of RhsA does indeed get cleaved, as evidenced by the presence of a smaller, FLAG-labeled, polypeptide in RhsA-FLAG-expressing cell lysates (Figure 5.5A). Moreover, this processing event occurs in a T6SS-negative *Escherichia coli* K-12 strain and is not dependent on *eagR<sub>A</sub>*, suggesting either RhsA is auto-proteolytic, or utilizes conserved, non-T6SS-related, proteases.

Next, I investigated whether the RhsA core domain is involved in the catalysis of the RhsA C-terminal cleavage event. Three putative active site residues in the *yenC* Rhs protein from *Yersinia entomophaga* have been tested and confirmed as critical for C-terminal cleavage in that system (72). Therefore, I introduced a homologous active site mutation, D1323A, into RhsA and found that this mutation

no longer supports C-terminal processing (Figure 5.5B). This is consistent with the model that RhsA is auto-proteolytic. Additionally, I find that EagR<sub>A</sub>-mediated purification of RhsA successfully pulls down both the major Rhs protein as well as the cleaved C-terminal domain; this suggests this C-terminal domain is still associated with the rest of the EagR<sub>A</sub>-RhsA complex even though it exists as a separate polypeptide. This observation is consistent with the model that the C-terminal toxin domain resides within the Rhs  $\beta$ -encapsulation structure.

I next investigated the significance of the RhsA C-terminal processing event to RhsA function. Unfortunately, the addition of the FLAG epitope to the RhsA C-terminus severely attenuates RhsA activity and additionally leads to growth-defective cells (Figure 5.3B and 5.6). Therefore, I introduced the D1323A mutation to a different RhsA construct that does not contain the FLAG epitope. I find that RhsA<sub>D1323A</sub> migrates slower than the wild-type construct, consistent with the conclusion that D1323 is critical for the RhsA C-terminal cleavage event (Figure 5.7A). Next, I tested culture supernatants to assess if RhsA<sub>D1323A</sub> still supports T6SS activity: I find that the RhsA<sub>D1323A</sub> mutant still secretes Hcp at levels comparable to wild-type RhsA, suggesting Rhs toxin cleavage is not required for overall T6SS activity (Figure 5.7B). Additionally, inter-bacterial competition experiments demonstrate that while cleavage of the RhsA toxin does not affect overall T6SS activity, as assayed by growth inhibition of *E. coli* targets, it is however required for inhibition mediated specifically by the RhsA toxin, as assayed by growth inhibition of *E. cloacae*  $\Delta$ *rhsA*  $\Delta$ *rhsI<sub>A</sub>* target cells (Figure 5.7C).

### *Chimeric Rhs supports inhibition of parental E. cloacae*

Given that the Rhs C-terminus undergoes proteolysis such that the toxin domain exists as a separate polypeptide from the rest of the protein, I decided to investigate whether Rhs toxin domains are modular and can be swapped between *rhs* alleles. I find that fusion of the *E. coli* KTE20 Rhs C-terminal domain onto *E. cloacae* RhsA creates a viable chimeric effector that can inhibit parental *E. cloacae*; these susceptible *E. cloacae* targets can be protected by expressing the cognate KTE20 *rhsI* (Figure 5.8A). This suggests a lack of specificity between the Rhs toxin domain and the  $\beta$ -encapsulation structure. The KTE20 Rhs toxin-immunity pair is homologous to a known CDI tRNase toxin-immunity pair from *E. coli* EC869 (Figure 5.8B and 5.8C), whereas the *E. cloacae* RhsA toxin has unknown function but is also cytoplasmically toxic (71, 178). While many Rhs toxins are cytoplasmically active, there are a few that are predicted to be periplasmically-active instead (211). This may suggest that different Rhs proteins utilize different translocation mechanisms to deliver their toxic payload to different compartments of target cells.

Therefore, I next investigated whether the periplasmically-active *ybfO* orphan Rhs toxin from *E. coli* K-12 could be deployed by *E. cloacae* RhsA. I find that while the chimeric RhsA-ybfOC (*ybfC* is the cognate immunity gene) construct supports inhibition of *E. coli*, it does not support inhibition of parental *E. cloacae* (Figure 5.9A). This suggests the chimera creates a viable Rhs protein capable of supporting overall T6SS activity, but that the chimera does not successfully deliver the YbfO toxin. *ybfO* is confirmed to encode a toxic product that is active in the periplasm of both *E. coli* and *E. cloacae* (Figure 5.9B); however, the chimeric RhsA-ybfO

construct does not support auto-proteolytic cleavage of its toxin domain (Figure 5.9C). Analysis of the native *ybfO* proteolytic motif implicates the natural P1324S mutation as a possible source of this lack of cleavage (Figure 5.9D). It is currently unclear whether periplasmic-acting Rhs toxins also require cleavage of the toxin domain for inhibition, or if this cleavage event is required only for toxin translocation into the cytoplasm of target cells.

## Discussion

The work presented here demonstrates EagR is required for Rhs activity in *E. cloacae*. I find that EagR is both essential and specific for delivery of its cognate Rhs effector. Co-deletion of *rhs* abolishes T6SS activity in *E. cloacae*, as does the similar co-deletion of *eagR*. Moreover, I find that EagR<sub>A</sub> interacts with the hydrophobic N-terminus of RhsA, and that this interaction is required for RhsA-dependent VgrG2 trimerization. I also show that the RhsA C-terminal toxin domain is auto-proteolytically cleaved off the rest of the RhsA protein independent of EagR. This processing event is required for successful delivery of the RhsA toxin in target cells, but is not required for overall RhsA-dependent T6SS activity. Finally, I demonstrate that chimeric Rhs effectors can be generated that are capable of inhibiting the parental strain, suggesting a lack of specificity between the Rhs  $\beta$ -encapsulation structure and its toxic cargo. Taken together, this work sheds light into the mechanisms of EagR and Rhs activity.

A number of questions still remain regarding the function and physiology of both EagR and Rhs proteins. It is clear that EagR is required for Rhs activity, yet it is not understood what function EagR truly serves. Mougous and colleagues have recently demonstrated that the Eag-dependent *P. aeruginosa* Tse6 effector interacts directly with *P. aeruginosa* VgrG1, and that this VgrG1-Tse6 complex spontaneously translocates across liposome membranes (176). Unfortunately, it could not be determined whether the putative transmembrane domains (TMDs) of Tse6 are required for this translocation event because deletion of the TMDs abrogated its ability to stably interact with VgrG, even though this  $\Delta$ TMD mutant is more stable than the wild-type Tse6 protein (176.)

If the sole function of Eag is to stabilize the hydrophobic putative TMDs of cargo effectors, then it is unclear why the stable Tse6 $\Delta$ TMD protein is not sufficient for stable interaction with VgrG. *E. cloacae* RhsA is unfortunately naturally expressed at low levels in the cell and cannot be readily detected unless purified or over-expressed (Chapter 4). However, the plasmid-expressed wild-type RhsA construct does not stably interact with VgrG2 unless EagR<sub>A</sub> is co-expressed, even though this over-expressed RhsA is readily detected in cell lysates (Figure 4.6). Additionally, over-expression of the RhsA $\Delta$ 1-82 mutant also fails to stably interact with VgrG, even in the presence of EagR<sub>A</sub> (Figure 5.3C); this again suggests that stabilization of the effector's hydrophobic N-terminus is not the sole function of EagR<sub>A</sub>.

It is possible that Eag proteins also help fold the PAAR domain of their respective effectors in order to facilitate the interaction between effector and VgrG. In support of this hypothesis, I have noticed that the RhsA PAAR domain encodes a

hydrophobic predicted  $\alpha$ -helix not found in other solved PAAR structures (data not shown). Further bioinformatic analysis suggests the overall hydrophobicity profiles of PAAR domains in Eag-dependent effectors may be distinct from those of Eag-independent effectors. For example, the PAAR domains of known Eag-dependent effectors appear to have hydrophilic character that is interspersed with spikes of hydrophobicity (Figure 5.10A). In contrast, the PAAR domain of the Eag-independent *P. aeruginosa* Rhs effector Tse5, as well as that of the Eag-independent *E. coli* EDL933 RhsA effector, has little-to-no hydrophilic character (Figure 5.10B). Taken together, these data suggest that Eag may be also be involved in the folding of these uniquely irregular PAAR domains, consistent with the observation that Eag is required for the interaction between its cargo and VgrG.

An outstanding question in the field is the overall purpose and significance of encapsulating toxins in the Rhs  $\beta$ -shell structure. Busby *et. al.* were the first to propose that these toxins are enclosed within the Rhs shell-like structure (72). Their report describes the *Yersinia entomophaga* insecticidal ABC toxin complex, where only the C protein is Rhs-like. Interestingly, in this system the B and C proteins assemble into a heterodimer in order to form the hollow  $\beta$ -encapsulation structure. Their small-angle X-ray scattering data suggests the B-C complex forms a solid spheroid structure, whereas the structure is hollow when the C-terminal domain of the C protein is deleted.

I have demonstrated that the cleaved RhsA C-terminal toxin domain stays associated with the remaining Eag<sub>R</sub>A-RhsA complex (Figure 5.5B), corroborating their model of the toxin domain residing within the shell. I have additionally found

that the RhsA-KTE20 chimera is a functional effector (Figure 5.8A), suggesting little specificity exists between the RhsA shell and toxin domain. Indeed, the *E. cloacae* RhsA primary sequence can be largely conserved in other organisms; however, these other *rhs* alleles possess differing C-terminal toxin domains (Figure 1.2). This suggests the Rhs shell structure is a general encapsulation device for a variety of toxins. While the RhsA-YbfO chimera failed to deliver its toxic YbfO payload to target cells (Figure 5.9A), this toxin is periplasmic-acting while both the RhsA and KTE20 toxins are cytoplasmic-acting. However, the RhsA-YbfO chimera also fails to cleave its toxin domain (Figure 5.9C), and sequence analysis reveals the catalytic DPxGL motif is mutated in the *ybfO* gene to DSxGL (Figure 5.9D). While I have demonstrated that cleavage of the *E. cloacae* RhsA toxin is required for inhibition of targets via this toxin (Figure 5.7C), it is possible that periplasmically-acting Rhs toxins do not require cleavage of the toxin domain for inhibition. Given that it is not yet understood why the RhsA toxin cleavage event is necessary for inhibition, it remains to be seen whether the lack of a proper cleavage motif in *ybfO* is physiologically relevant, or if this simply represents a loss-of-function mutation in the gene.

It is currently unclear whether the Rhs encapsulation device serves simply as a protective barrier for the toxin, or if there are other physiological considerations driving the evolution of this structure. One explanation for the significance of the Rhs encapsulation structure is that it may serve as a chaperone to help fold the toxin domain. It has been noted that the *P. aeruginosa* Tse6 effector, which is Eag-dependent but does not form any encapsulation domain, can readily refold *in vitro*

(73). In contrast, attempts to refold and elicit *in vitro* activity of the DNase toxin domain of *E. cloacae* RhsB were unsuccessful (data not shown). This is an indication that perhaps Rhs-encoded toxins do not readily unfold and refold.

The translocation mechanism of Rhs proteins and Tse6 across the inner-membrane is currently unclear, but Mougous and colleagues suggest Tse6 is delivered into the periplasm via the T6SS system, and then is somehow subsequently threaded through the inner-membrane in an unfolded state (176). Additionally, ongoing research into the translocation of CDI toxins suggests CDI toxins also translocate across the inner-membrane in an unfolded state (Gregory Ekberg, Hayes lab, unpublished). Therefore, both the Rhs encapsulation device and the toxin domain may be translocated across the target cell inner-membrane in an unfolded state, after which the shell structure spontaneously refolds and facilitates toxin folding post-translocation.

It is also possible that the Rhs  $\beta$ -encapsulation structure is capable of translocating across or inserting into the target cell inner-membrane in a folded state. The spheroid Rhs  $\beta$ -structure is somewhat reminiscent of outer-membrane  $\beta$ -barrel proteins, and spontaneous insertion of the N-terminal putative transmembrane domain into the inner-membrane may facilitate subsequent insertion of the  $\beta$ -shell structure into the membrane. In this scenario, Rhs proteins could potentially deliver a pre-folded toxic payload into the cytosol, bypassing the need to unfold and refold the toxin domain entirely. In conjunction with the observation that the toxin domains of Rhs proteins are rarely found to be

periplasmic-acting, Rhs proteins may therefore have evolved as a method of translocating folded proteins across membranes.

## **Materials and Methods**

### *Bacterial growth and conditions*

Bacteria were cultured in shaking lysogeny broth (LB) or on LB-agar at 37°C. Bacteria were supplemented with antibiotics at the following concentrations: 150 µg/mL ampicillin (Amp), 66 µg/mL chloramphenicol (Cm), 50 µg/mL kanamycin (Kan), 100 µg/mL spectinomycin (Spc), 200 µg/ml rifampicin (Rif), 25 µg/mL tetracycline (Tet), and 100 µg/ml trimethoprim (Tp).

### *Strain construction*

All bacterial strains, plasmids, and oligonucleotides used in this study are listed in Tables 5.1, 5.2, and 5.3. Gene-deletion constructs for *E. cloacae* were generated using overlap-extension PCR (OE-PCR) or via the plasmids pKAN or pSPM as described previously (67, 142, 143). Briefly, OE-PCR constructs were made with upstream and downstream homology PCR fragments overlapped to the CH2952/CH2953 PCR product amplified from either pKAN or pSPM. pKAN or pSPM plasmid constructs were generated by restriction cloning PCR fragments from upstream and downstream of the target gene into pKAN or pSPM to flank the

antibiotic-resistance cassette. Restriction enzymes used are specified in the oligonucleotide names listed in Table 5.3.

Resulting constructs were PCR-amplified, DpnI-digested to remove methylated template DNA, then directly electroporated into *E. cloacae* cells expressing phage  $\lambda$ -Red recombinase proteins as described (144). Transformants were selected on LB-agar supplemented with either Kan or Spc. All chromosomal deletions were confirmed by whole-cell PCR analysis. Kan markers were cured as necessary via pCP20 (145).

#### *Plasmid construction*

All plasmids and oligonucleotides used in this study are listed in Tables 5.2 and 5.3. All PCR products were purified, digested with the restriction enzymes indicated in the oligonucleotide names (Table 5.3), and ligated to a vector treated with the same enzymes. Plasmids were confirmed by DNA sequencing (University of California, Berkeley). Plasmid transformations were performed by making strains TSS competent (148). Constructs were cloned directly into the final vector, with exceptions or complications described below.

Generation of pBAD24::*ugrG2-VSV*, pCH450::*rhsA-rhsIA*, and pCH450::*eagRA-rhsA-rhsIA* is described in Chapter 4. For generation of pCH450::*rhsA-FLAG* and pCH450::*eagRA-rhsA-FLAG*, PCR CH4328/CH4629 was cloned with KpnI/SbfI into pCH450::*rhsA-rhsIA* and pCH450::*eagRA-rhsA-rhsIA*.

For generation of pCH450::*rhsA*<sub>83-1462</sub>-*FLAG*, PCR CH4719/CH4325 was cloned with EcoRI/NcoI into pCH450::*rhsA-FLAG*.

For generation of pCH450::*rhsA*<sub>R1321S</sub>-*FLAG* and pCH450::*eagR*<sub>A</sub>-*rhsA*<sub>R1321S</sub>-*FLAG*, PCR CH4328/CH4631 was cloned with KpnI/SbfI into pCH450::*rhsA-rhsI*<sub>A</sub> and pCH450::*eagR*<sub>A</sub>-*rhsA-rhsI*<sub>A</sub>, then PCR CH4632/CH4629 was cloned into these intermediate plasmids with SpeI/SbfI. For generation of pCH450::*eagR*<sub>A</sub>-*rhsA*<sub>R1321S</sub>-*rhsI*<sub>A</sub>, PCR CH4632/CH3636 was cloned into pCH450::*eagR*<sub>A</sub>-*rhsA*<sub>R1321S</sub>-*FLAG* using SpeI/XhoI.

For generation of pCH450::*rhsA*<sub>R1321S,D1323A</sub>-*FLAG* and pCH450::*eagR*<sub>A</sub>-*rhsA*<sub>R1321S,D1323A</sub>-*FLAG*, PCR CH4898/CH4629 was cloned with SpeI/SbfI into pCH450::*rhsA*<sub>R1321S</sub>-*FLAG* and pCH450::*eagR*<sub>A</sub>-*rhsA*<sub>R1321S</sub>-*FLAG*. For generation of pCH450::*eagR*<sub>A</sub>-*rhsA*<sub>R1321S,D1323A</sub>-*rhsI*<sub>A</sub>, pCH450::*eagR*<sub>A</sub>-*rhsA*<sub>R1321S</sub>-*KTE20*, and pCH450::*eagR*<sub>A</sub>-*rhsA*<sub>R1321S</sub>-*ybfOC*, PCRs CH4898/CH3636, CH4880/CH4881, and CH4878/CH4879, respectively, were cloned with SpeI/XhoI into pCH450::*eagR*<sub>A</sub>-*rhsA*<sub>R1321S</sub>-*FLAG*. The *ybfOC* PCR was amplified from X90 template. The DNA template for the KTE20 Rhs-CT and RhsI alleles was custom synthesized by Integrated DNA Technologies.

For generation of pSCbadB2 constructs, PCR CH4756/CH4757 was cloned with NcoI/HindIII into pCH10524 to create pSCbadB2::*eagR*<sub>A</sub>, and into pCH10626 to create pSCbadB2::*(dsbA)ss-eagR*<sub>A</sub>. PCR CH4758/CH4759 was cloned with NcoI/HindIII into pCH10626 to create pSCbadB2::*(dsbA)ss-eagR*<sub>B</sub>. For generation of pSCbadB2::*(sufI)ss-eagR*<sub>A</sub> and pSCbadB2::*(sufI)ss-eagR*<sub>B</sub>, PCR CH4900/CH4901 was cloned into the earlier *(dsbA)ss-eagR* constructs using BamHI/NcoI.

### *Competitions*

*E. cloacae* strains were used as inhibitor cells on LB-agar co-cultures against either *E. cloacae* derivatives or X90 *E. coli* targets. Cells were grown in LB-medium (supplemented with appropriate antibiotics when plasmid-bearing) to log phase, then collected by centrifugation and resuspended in 1x M9 salts. Inhibitors and targets were mixed 1:1 at OD 17 each (200 uL total volume), then 100 ul of the mixture was spread on LB-agar without antibiotics and incubated at 37°C for 3 or 4 h (as indicated). Culture aliquots were taken at the beginning and end of the co-culture to quantify viable inhibitor and target cells as colony forming units. After co-culture, cells were harvested in 1.5 mL of 1x M9 salts. For competitions with plasmid-induced proteins, inhibitors were grown in LB-medium supplemented with 0.4% L-arabinose and Tet. Co-cultures were then performed as above on LB-agar supplemented with 0.4% L-arabinose.

For all competitions, cell suspensions were serially diluted into 1x M9 salts and plated onto LB-agar supplemented with appropriate antibiotics to separately enumerate inhibitor and target cells. Competitive indices were calculated as the ratio of inhibitor to target cells at 3 or 4 h divided by the initial inhibitor to target cell ratio.

### *Hcp secretion assays*

*E. cloacae* strains were cultured in LB-medium (supplemented with antibiotics and 0.4% L-arabinose when appropriate) to log phase, then collected by

centrifugation at 3,000  $xg$  for 5 min. Cell pellets were washed once in 1x M9 salts, then resuspended in urea-lysis buffer [50% urea, 150 mM NaCl, 20 mM Tris-HCl (pH 8.0)] and subjected to a freeze-thaw cycle to extract proteins for SDS-PAGE and immunoblotting. Culture supernatants were re-spun to further remove cellular contamination. Supernatants were precipitated in cold ethanol at a final ethanol concentration of 75%. Samples were left at -80 °C overnight, then proteins were collected by centrifugation at 21,000  $xg$  for 15 min at 4°C. Precipitates were washed once with 75% cold ethanol, then air-dried pellets were dissolved in urea-lysis buffer. Samples were analyzed by SDS-PAGE on Tris-tricine 10% polyacrylamide gels run at 110 V (constant) for 1 h, then gels were soaked for 10 min in 25 mM Tris, 192 mM glycine (pH 8.6), 20% methanol. Gels were then electroblotted to nitrocellulose membranes using a semi-dry transfer apparatus at 17 V (constant) for 30 min. Membranes were subsequently blocked and imaged as described below.

### *Ni<sup>2+</sup>-affinity pulldowns*

*E. coli* strains were grown in LB-medium supplemented with Amp and Tet to log phase and protein expression was induced with 0.4% L-arabinose and 0.5 mM Isopropyl-beta-D-thiogalactoside (IPTG) for 1 h. Cells were then collected by centrifugation and resuspended in binding buffer [20 mM sodium phosphate (pH 7.0), 150 mM NaCl, 30 mM imidazole, 0.05% Triton X-100]. Each cell suspension was broken by 2 passages through a French press, then insoluble debris was removed via centrifugation at 23,000  $xg$  for 10 min at 4°C. The clarified lysate was added to Ni<sup>2+</sup>-NTA agarose resin and incubated on a rotisserie for 1 h at 4°C.

Following incubation, the beads were washed extensively in binding buffer, then RhsA was eluted off the beads in urea-lysis buffer.

For Figure 5.3A, samples were analyzed by SDS-PAGE on Tris-tricine 7% polyacrylamide gels run at 110 V (constant) for 1 h. Gels were soaked for 10 min in 25 mM Tris, 192 mM glycine (pH 8.6), 20% methanol, then electroblotted to nitrocellulose membranes. For Figure 5.5B, samples were analyzed by SDS-PAGE on Tris-tricine 10% polyacrylamide gels run at 100 V (constant) for 80 min. Gels were soaked for 10 min in 25 mM Tris, 192 mM glycine (pH 8.6), 20% methanol, then electroblotted to low-fluorescence PVDF membranes. Transfers were performed using a semi-dry transfer apparatus at 17 V (constant) for 30 min. Membranes were subsequently blocked and imaged as described below.

### *Immunoblots*

For immunoblotting of *E. cloacae* or *E. coli* lysates, cultures were initially grown in media supplemented with appropriate antibiotics and .04% L-arabinose, then cultured to log phase and collected by centrifugation at 3,000 *xg* for 5 min. Cell pellets were then resuspended in urea-lysis buffer and subjected to a freeze-thaw cycle to extract proteins. For Figure 5.3C, samples were analyzed by SDS-PAGE on Tris-tricine 7% polyacrylamide gels run at 110 V (constant) for 2.5 h. Gels were soaked for 10 min in 25 mM Tris, 192 mM glycine (pH 8.6), 10% methanol, then electroblotted to low-fluorescence PVDF membranes using a semi-dry transfer apparatus at 17 V (constant) for 1 h. For Figure 5.5A, samples were analyzed by SDS-

PAGE on Tris-tricine 10% polyacrylamide gels run at 110 V (constant) for 1 h. Gels were soaked for 10 min in 25 mM Tris, 192 mM glycine (pH 8.6), 20% methanol, then electroblotted to low-fluorescence PVDF membranes using a semi-dry transfer apparatus at 17 V (constant) for 30 min.

For all immunoblots, membranes were blocked with 4% non-fat milk in PBS for 30 min at room temperature, and incubated with primary antibodies in 0.1% non-fat milk in PBS overnight at 4°C. Rabbit polyclonal antisera (Cocalico Biologicals, Stevens, PA) to Hcp3-His6 was used at a 1:10,000 dilution and antisera to RhsA<sub>82-467</sub>-H6 was used at a 1:5,000 dilution. Mouse anti-VSV-G (Sigma) was used at a 150,000 dilution, and mouse anti-FLAG (Sigma) was used at a 25,000 dilution. Blots were incubated with 800CW-conjugated goat anti-rabbit IgG (1:125,000 dilution, LICOR) or 680LT-conjugated goat anti-mouse IgG (1:125,000 dilution, LICOR) in PBS. Immunoblots were visualized with a LI-COR Odyssey infrared imager.

### *Transformation assays*

Plasmids were transformed into TSS-competent *E. cloacae*  $\Delta$ tssM1 and recovered in LB-medium for 75 min, then collected by centrifugation at 3,000  $\times$ g for 5 min. Cell pellets were subsequently resuspended in 120  $\mu$ l of LB-medium, and 50  $\mu$ l of each sample was plated to LB-agar supplemented with Tet and either 0.4% glucose or 0.4% L-arabinose.

### *Growth curves*

Plasmid-bearing strains were plated on LB-agar supplemented with 0.4% glucose and appropriate antibiotics. The following day, strains were inoculated off plates into LB-medium supplemented with 0.4% glucose and appropriate antibiotics and grown to log phase, then collected by centrifugation and resuspended in 1x Mg salts. Cells were then diluted to an OD<sub>600</sub> of .05 in fresh LB-medium supplemented with appropriate antibiotics and 0.4% L-arabinose. Cell growth was monitored by measuring the OD<sub>600</sub> every 30 min for 5 h.

### *Bioinformatic analyses*

Transmembrane prediction analyses were performed using the TMHMM server, and hydrophobicity analyses were performed with the ExPASy ProtScale server (134, 158). Protein sequences were aligned using Clustal Omega (149). Protein alignments were rendered with BoxShade ([https://embnet.vital-it.ch/software/BOX\\_form.html](https://embnet.vital-it.ch/software/BOX_form.html)).

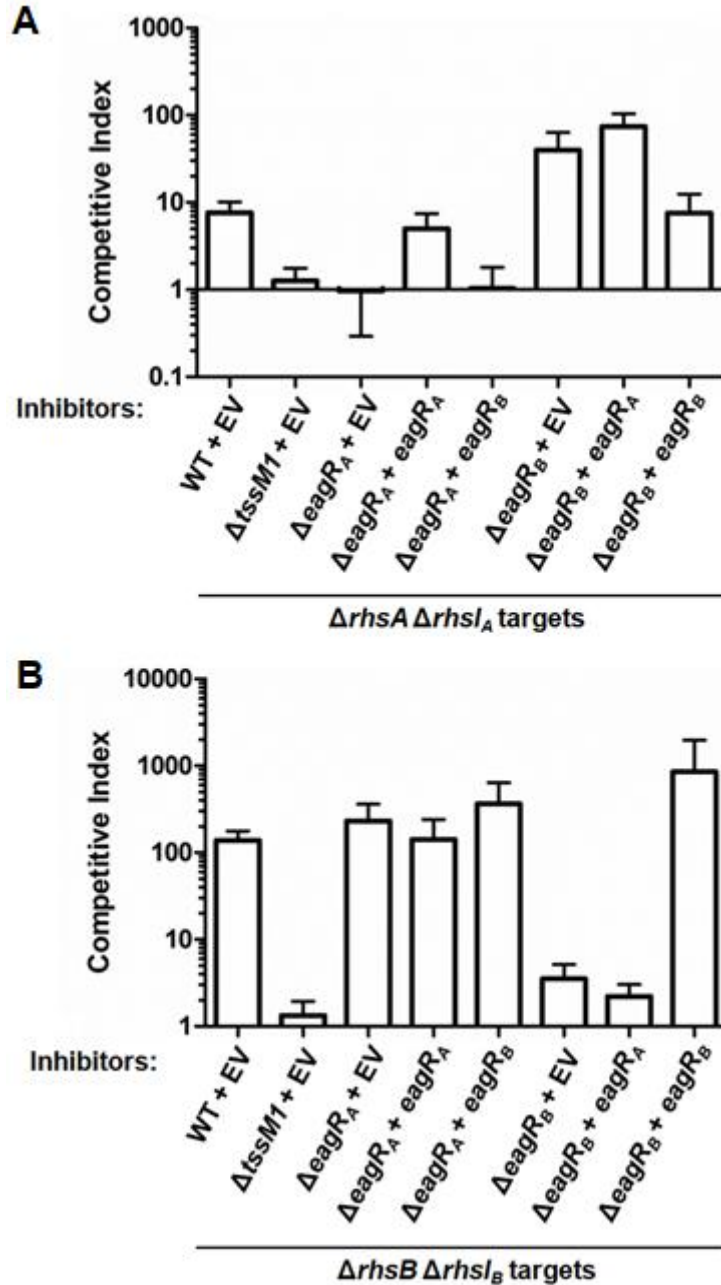


**Figure 5.1. Rhs requires its upstream EagR for toxin delivery.** Indicated *E. cloacae* inhibitors were incubated at a 1:1 ratio with indicated *E. cloacae* targets for 3 hours. Cells were quantified as colony-forming units (CFUs) at the beginning of the co-culture and after 3 h. Competitive indices were calculated as the ratio of inhibitor to target CFUs at the end of the competition normalized to the starting ratio. Data represent the average and standard error of the mean for three independent experiments. (A) EagR<sub>A</sub>, but not EagR<sub>B</sub>, is required for delivery of the RhsA toxin. (B) EagR<sub>B</sub>, but not EagR<sub>A</sub>, is required for delivery of the RhsB toxin. WT=wild-type, EV=empty vector.

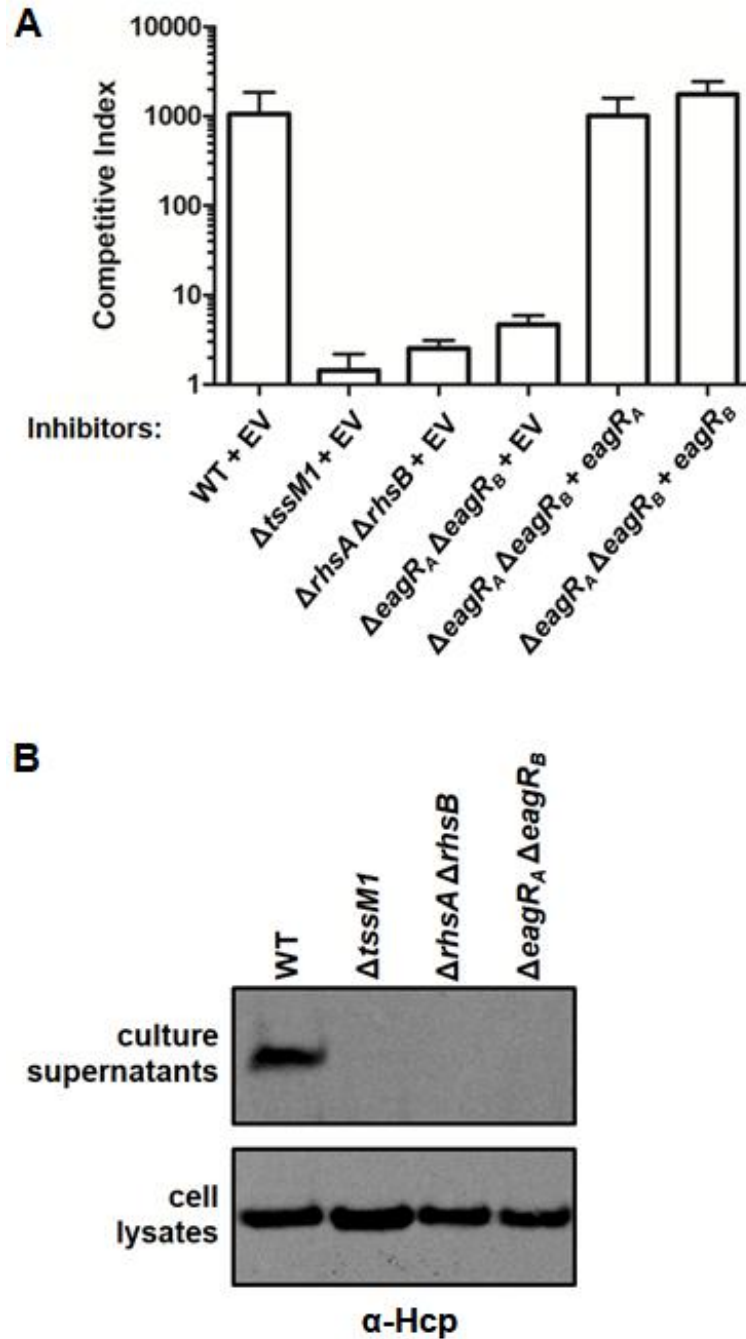


**Figure 5.2. The EagR- mutant phenocopies known T6SS-null mutations.** (A) Indicated *E. cloacae* inhibitors were incubated at a 1:1 ratio with *E. coli* targets for 3 hours. Data represent the average and standard error of the mean for three independent experiments. (B) Cell lysates and supernatants of indicated strains were analyzed via SDS-PAGE and  $\alpha$ -Hcp3 immunoblot. WT=wild-type, EV=empty vector.

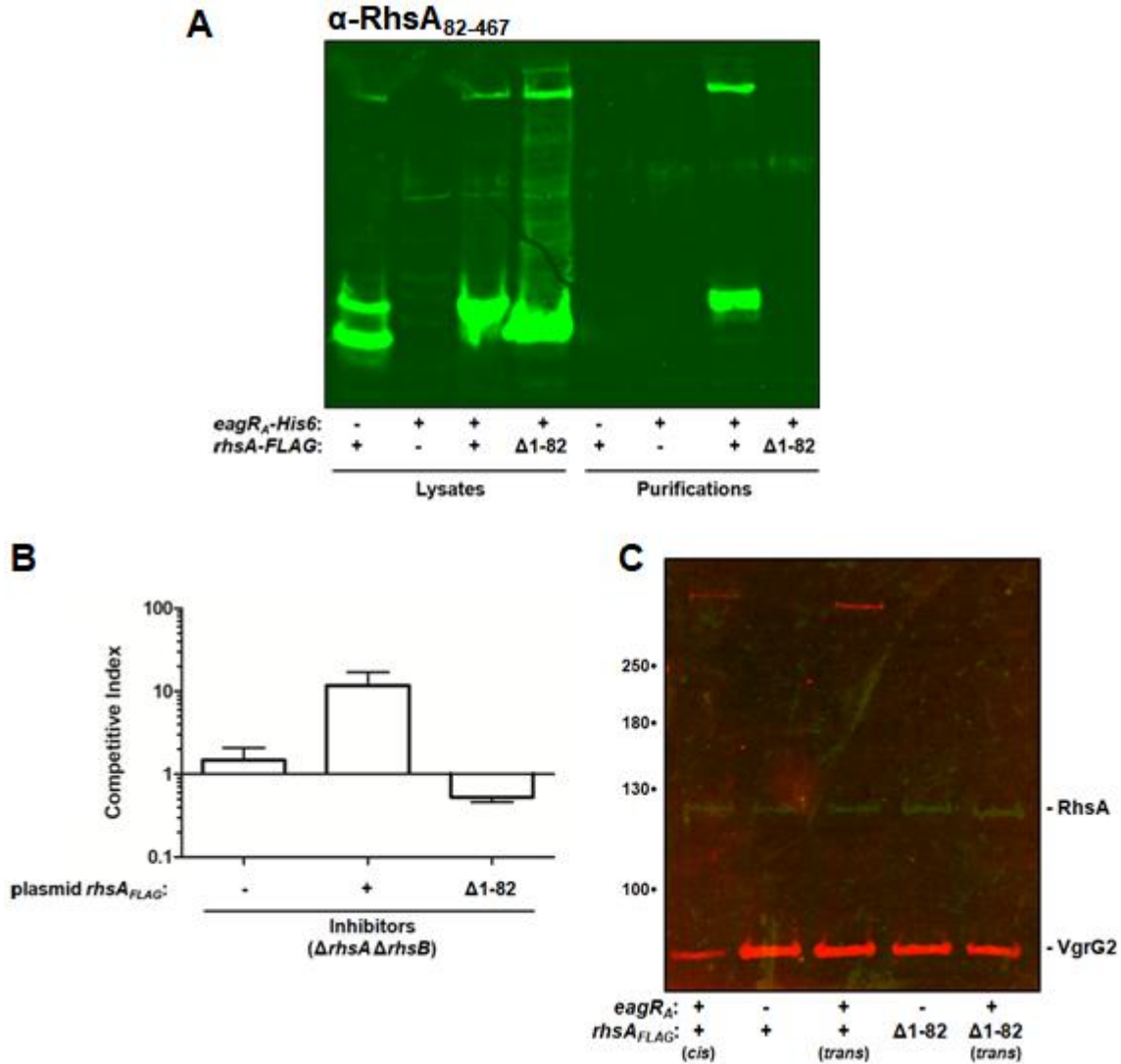


**Figure 5.3. EagR<sub>A</sub> binds the N-terminal domain of RhsA in order to support RhsA activity.** (A) Co-expression of EagR<sub>A</sub>-His6 (or empty vector) and indicated RhsA-FLAG constructs (or empty vector) in *E. coli*. Cells were lysed and subjected to Ni-NTA pulldown. Input (lysate) and bound (purification) fractions were analyzed via SDS-PAGE and  $\alpha$ -RhsA immunoblot. (B) Indicated *E. cloacae* inhibitors were incubated (without induction) at a 1:1 ratio with *E. coli* targets for 3 hours. Data represent the average and standard error of the mean for three independent experiments. (C) *E. coli* expressing plasmid-borne VgrG2-VSV and the indicated plasmid constructs were lysed and analyzed via SDS-PAGE and dual  $\alpha$ -VSV (red)  $\alpha$ -RhsA (green) immunoblot.

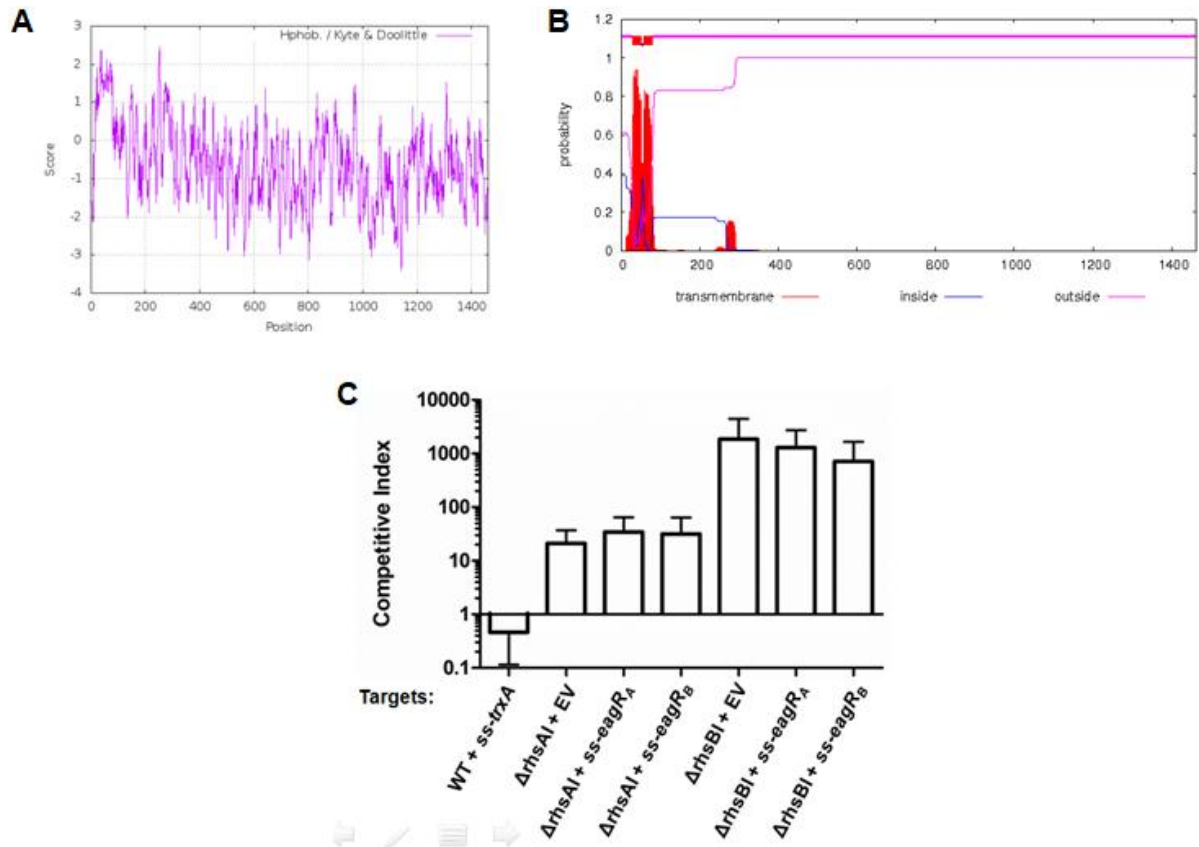


**Figure 5.4. Periplasmic EagR does not protect targets from Rhs toxins.** (A) Kyte and Doolittle hydrophobicity analysis of RhsA. (B) TMHMM transmembrane prediction analysis of RhsA. (C) Wild-type *E. cloacae* inhibitors were incubated at a 1:1 ratio with indicated *E. cloacae* targets for 3 hours. Data represent the average and standard error of the mean for three independent experiments. WT=wild-type, EV=empty vector, ss=signal sequence (from *E. coli dsbA* for the *ss-trxA* construct, or from *E. cloacae sufI* for the *eagR* constructs), *trxA*=thioredoxin A, a non-toxic control.

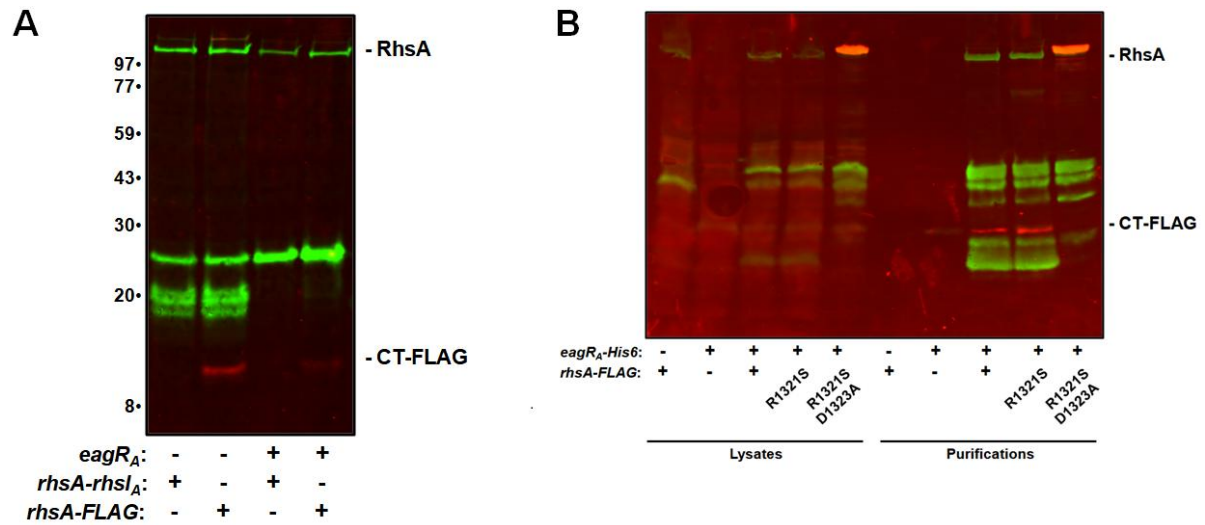


**Figure 5.5. RhsA C-terminal cleavage occurs independent of other T6SS factors, but the cleaved domain remains associated with the EagR<sub>A</sub>-RhsA complex.** (A) *E. coli* expressing the indicated plasmid-borne genes were analyzed via SDS-PAGE and dual  $\alpha$ -FLAG (red)  $\alpha$ -RhsA (green) immunoblot. (B) Co-expression of EagR<sub>A</sub>-His6 (or empty vector) and indicated RhsA-FLAG constructs (or empty vector) in *E. coli*. Cells were lysed and subjected to Ni-NTA pulldown. Input (lysate) and bound (purification) fractions were analyzed via SDS-PAGE and dual  $\alpha$ -FLAG (red)  $\alpha$ -RhsA (green) immunoblot. The R1321S mutation was used for introducing the D1323A mutation via restriction cloning.

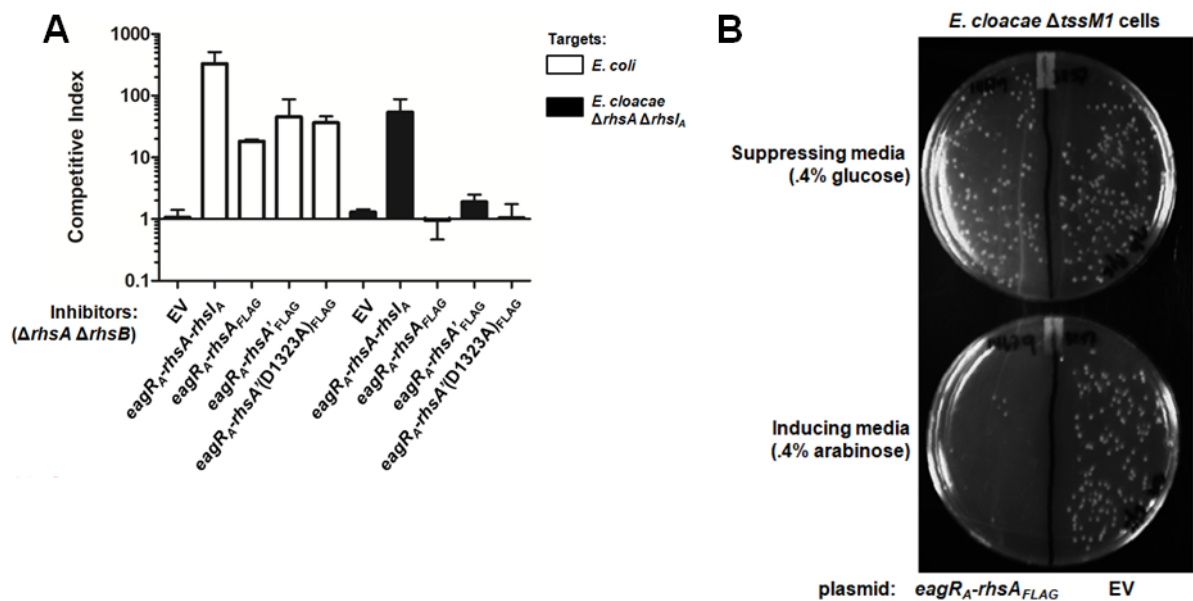


**Figure 5.6. Addition of a C-terminal FLAG tag to RhsA interferes with RhsA function.** (A) Indicated *E. cloacae* inhibitors were incubated at a 1:1 ratio with indicated targets for 4 hours. Data represent the average and standard error of the mean for two independent experiments. (B) *E. cloacae ΔtssM1* was transformed with the indicated plasmids and selected on LB-tetracycline-agar plates supplemented with either glucose or arabinose, as indicated. EV=empty vector.

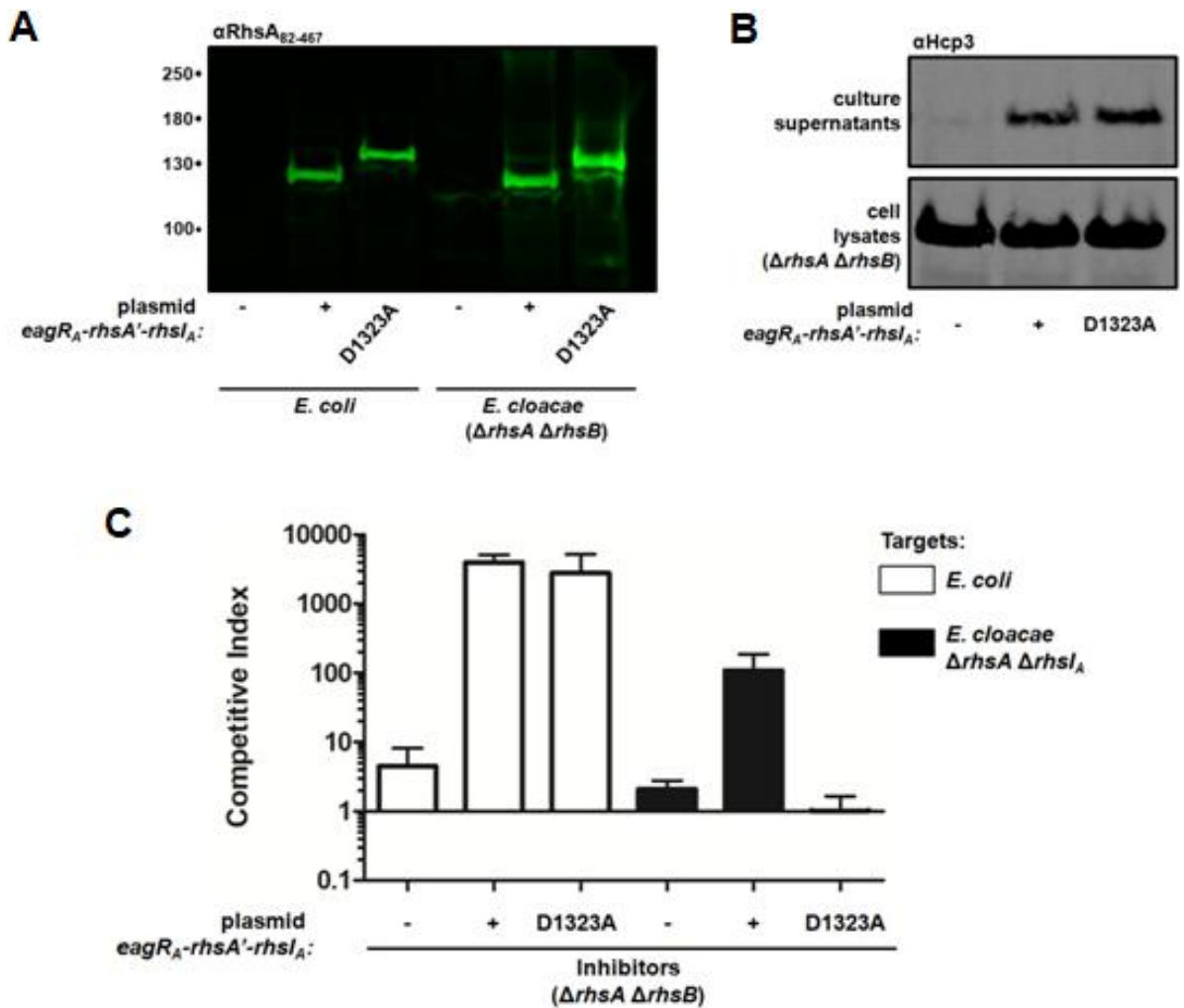


**Figure 5.7. RhsA residue D1323 is required for C-terminal cleavage.** RhsA' = R1321S mutation, used for introducing the D1323A mutation via restriction cloning. (A) Indicated plasmid constructs were induced in the indicated cell backgrounds, then cell lysates were analyzed via SDS-PAGE and  $\alpha$ -RhsA immunoblot. (B) Indicated plasmid constructs were induced in *E. cloacae*  $\Delta$ *rhsA*  $\Delta$ *rhsB*, then cell lysates and supernatants were analyzed via SDS-PAGE and  $\alpha$ -Hcp3 immunoblot. (C) Indicated *E. cloacae* inhibitors were incubated at a 1:1 ratio with indicated targets for 4 hours. Data represent the average and standard error of the mean for three independent experiments.

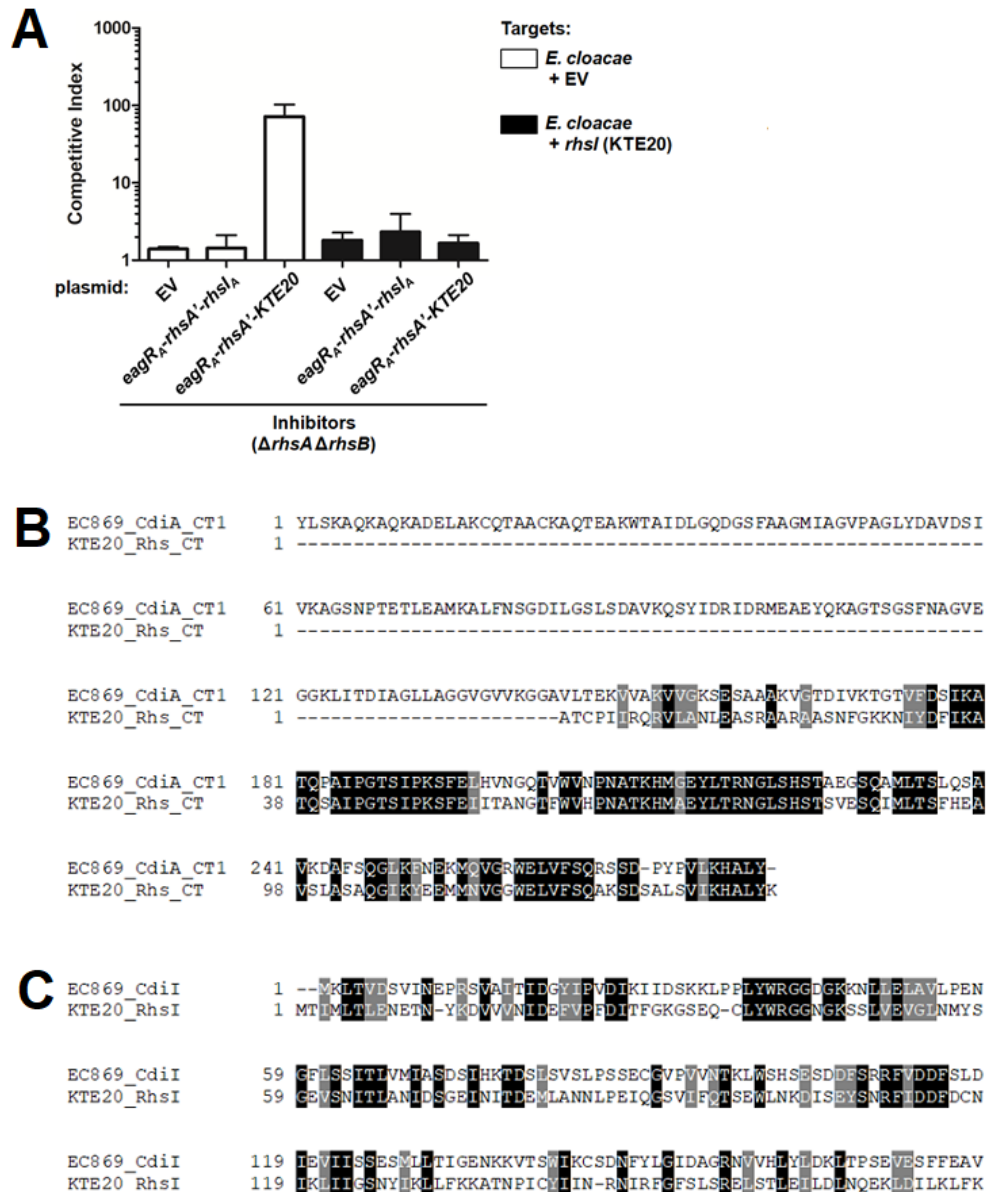


**Figure 5.8. Chimeric RhsA supports inhibition of the parental *E. cloacae* strain.** (A) Indicated *E. cloacae* inhibitors were incubated at a 1:1 ratio with the indicated target strains for 3 hours. Data represent the average and standard error of the mean for three independent experiments. EV=empty vector, RhsA'= R1321S mutation, used for introducing the C-terminal (CT) fusion via restriction cloning. (B) Multiple sequence alignment of the KTE20 Rhs CT toxin to the EC869 CdiA-CT1. CdiA-CTs are known to encode 2 distinct domains: the N-terminal domain is for toxin translocation, and the C-terminal domain encodes the toxin (159). (B) Multiple sequence alignment of the KTE20 RhsI to EC869 CdiI.

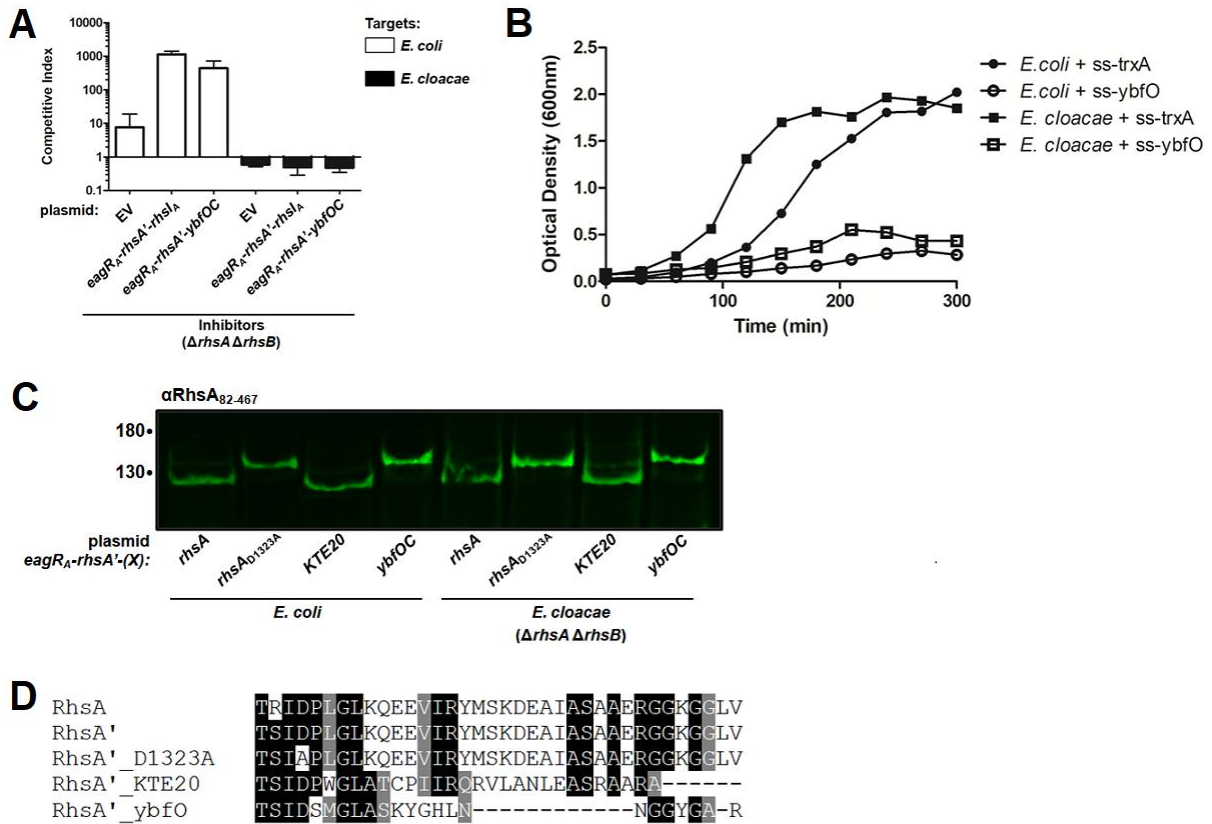


**Figure 5.9. Fusion of a periplasmic-acting toxin to RhsA does not support inhibition of the parental *E. cloacae* strain.** (A) Indicated *E. cloacae* inhibitors were incubated at a 1:1 ratio with the indicated target strains for 3 hours. Data represent the average and standard error of the mean for three independent experiments. (B) Cell densities as measured by OD600 over time. Intracellular expression of indicated constructs was induced with 0.4% L-arabinose at 0 h. ss=signal sequence (from *E. coli dsbA*), *trxA*=thioredoxin A, a non-toxic control. (C) Indicated plasmid constructs were induced in the indicated cell backgrounds, then cell lysates were analyzed via SDS-PAGE and  $\alpha$ -RhsA immunoblot. (D) Multiple sequence alignment of indicated protein sequences at the site of mutagenesis. EV=empty vector, RhsA'= R1321S mutation, used for introducing the C-terminal fusion or the D1323A mutation via restriction cloning.

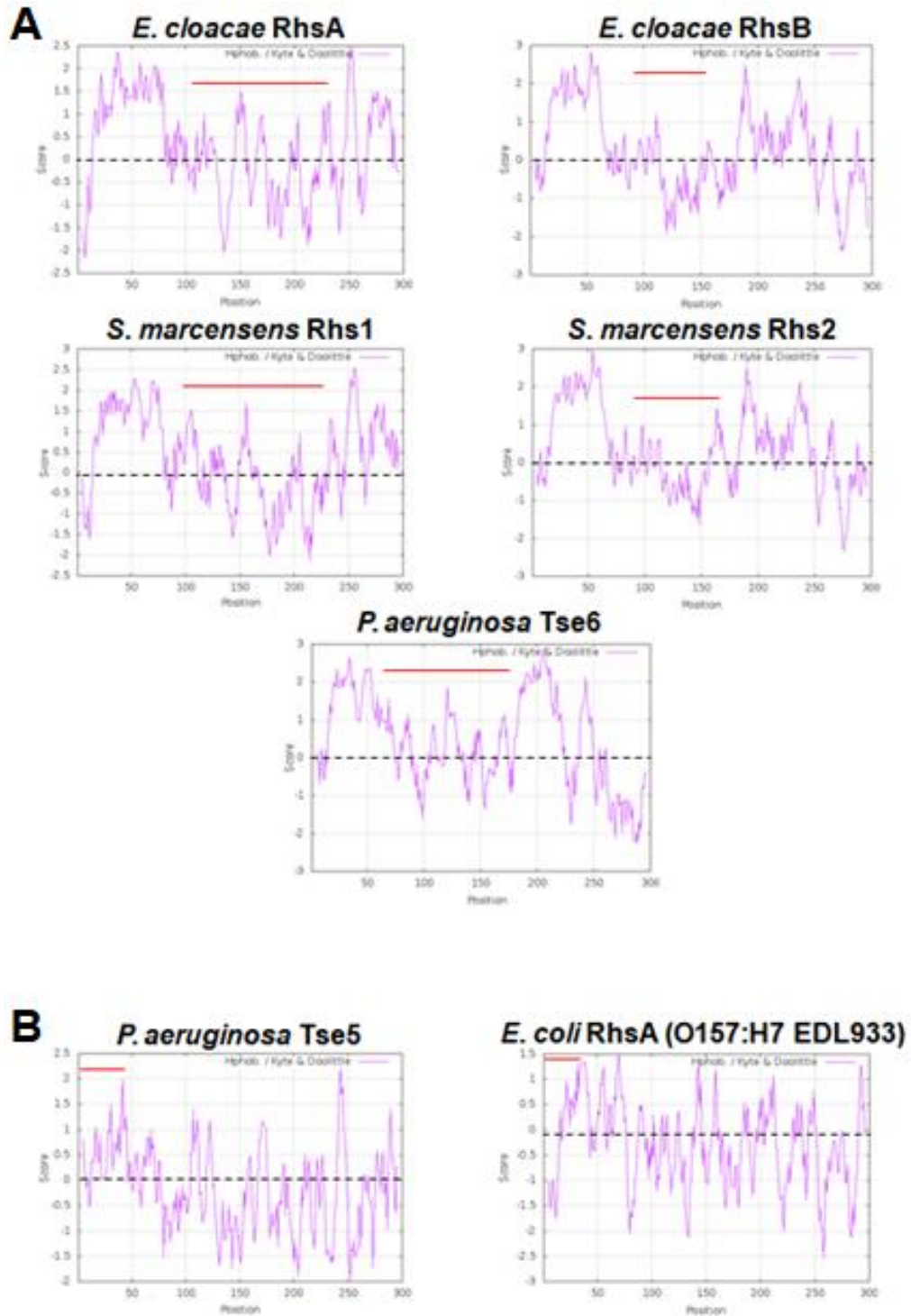


**Figure 5.10. PAAR domains of Eag-dependent effectors have unique hydrophobicity profiles.** Kyte and Doolittle hydrophobicity analyses of indicated proteins. PAAR domains are indicated with a red line. (A) Hydrophobicity analyses of known Eag-dependent effectors. (B) Hydrophobicity analyses of Eag-independent effectors.

**Table 5.1. Bacterial strains used in this study.**

<b>Strain</b>	<b>Description<sup>a</sup></b>	<b>Reference</b>
X90	<i>E. coli</i> F' <i>lacIq lac' pro'/ara</i> $\Delta(lac-pro)$ <i>nalI argE(amb) rif<sup>r</sup> thi-1</i> , Rif <sup>R</sup>	150
<i>E. cloacae</i> ATCC 13047	Type strain (ECL), Amp <sup>R</sup>	American Type Culture Collection
CH8163	ECL, Amp <sup>R</sup> Rif <sup>R</sup>	132
CH2016	X90 (DE3) $\Delta rna \Delta slyD::kan$ , Rif <sup>R</sup> Kan <sup>R</sup>	156
CH11196	ECL $\Delta tssM1::kan$ , Amp <sup>R</sup> Kan <sup>R</sup>	81
CH11178	ECL $\Delta rhsA::kan$ , Amp <sup>R</sup> Kan <sup>R</sup>	81
CH11179	ECL $\Delta rhsA$ , Amp <sup>R</sup>	81
CH11186	ECL $\Delta rhsB::kan$ , Amp <sup>R</sup> Kan <sup>R</sup>	81
CH11181	ECL $\Delta rhsA \Delta rhsI_A::kan$ , Amp <sup>R</sup> Kan <sup>R</sup>	81
CH11185	ECL $\Delta rhsA \Delta rhsI_A$ , Amp <sup>R</sup> Rif <sup>R</sup>	81
CH11188	ECL $\Delta rhsB \Delta rhsI_B::spc$ , Amp <sup>R</sup> Spec <sup>R</sup>	81
CH11223	ECL $\Delta rhsB \Delta rhsI_B::spc$ , Amp <sup>R</sup> Spec <sup>R</sup> Rif <sup>R</sup>	81
CH11733	ECL $\Delta rhsB$ , Amp <sup>R</sup>	This study
CH11748	ECL $\Delta rhsB \Delta rhsA::kan$ , Amp <sup>R</sup> Kan <sup>R</sup>	This study
CH11903	ECL $\Delta rhsB \Delta rhsA$ , Amp <sup>R</sup>	This study
CH12688	ECL $\Delta eagR_A::kan$ , Amp <sup>R</sup> Kan <sup>R</sup>	This study
CH11906	ECL $\Delta eagR_B::kan$ , Amp <sup>R</sup> Kan <sup>R</sup>	This study
CH11924	ECL $\Delta eagR_B$ , Amp <sup>R</sup>	This study
CH12689	ECL $\Delta eagR_A \Delta eagR_B::kan$ , Amp <sup>R</sup> Kan <sup>R</sup>	This study

<sup>a</sup>Abbreviations: Amp<sup>R</sup>, ampicillin-resistant; Kan<sup>R</sup>, kanamycin-resistant; Rif<sup>R</sup>, rifampicin-resistant; Spec<sup>R</sup>, spectinomycin-resistant

**Table 5.2. Plasmids used in this study.**

Number	Description <sup>a</sup>	Reference
	pCH450, Tet <sup>R</sup>	153
	pCH450kpn, Tet <sup>R</sup>	71
	pTrc99a, Amp <sup>R</sup>	GE Healthcare
	pTrc99a, Cm <sup>R</sup>	71
	pKOBEG, Cm <sup>R</sup>	144
	pCP20, Amp <sup>R</sup> , Cm <sup>R</sup>	145
pCH10524	pSCbadB2, Tp <sup>R</sup>	155
	pET21P, Amp <sup>R</sup>	Novagen
pCH70	pKAN, Kan <sup>R</sup> , Amp <sup>R</sup>	143
pCH11050	pKAN::ΔECL_01536 ( <i>tssM1</i> deletion), Kan <sup>R</sup> , Amp <sup>R</sup>	81
pCH10958	pKAN::ΔECL_01567 ( <i>rhsA</i> deletion), Kan <sup>R</sup> , Amp <sup>R</sup>	81
pCH11044	pKAN::ΔECL_03140 ( <i>rhsB</i> deletion), Kan <sup>R</sup> , Amp <sup>R</sup>	81
pCH12318	pKAN::ΔECL_01566 ( <i>eagR<sub>A</sub></i> deletion), Kan <sup>R</sup> , Amp <sup>R</sup>	This study
pCH11921	pKAN::ΔECL_03141 ( <i>eagR<sub>B</sub></i> deletion), Kan <sup>R</sup> , Amp <sup>R</sup>	This study
pCH11163	pET21P:: <i>hcp3-his6</i> , Amp <sup>R</sup> (for generation of Hcp3 antiserum)	This study
pCH11463	pET21P:: <i>rhsA(82-467)-his6</i> , Amp <sup>R</sup> (for generation of RhsA antiserum)	This study
pCH13568	pCH450:: <i>eagR<sub>A</sub></i> , Tet <sup>R</sup>	This study
pCH12033	pCH450kpn:: <i>eagR<sub>B</sub></i> , Tet <sup>R</sup>	This study
pCH13504	pTrc99a:: <i>eagR<sub>A</sub>-His6</i> , Amp <sup>R</sup>	This study
pCH14669	pCH450:: <i>rhsA-FLAG</i> , Tet <sup>R</sup>	This study
pCH14942	pCH450:: <i>rhsA<sub>83-1462</sub>-FLAG</i> , Tet <sup>R</sup>	This study
pCH14397	pBAD24:: <i>vgrG2-VSV</i> , Amp <sup>R</sup>	This study
pCH14864	pSCbadB2:: <i>eagR<sub>A</sub></i> , Tp <sup>R</sup>	This study
pCH14679	pCH450:: <i>eagR<sub>A</sub>-rhsA-FLAG</i> , Tet <sup>R</sup>	This study
pCH14640	pCH450:: <i>eagR<sub>A</sub>-rhsA-rhsI<sub>A</sub></i> , Tet <sup>R</sup>	This study
pCH14639	pCH450:: <i>rhsA-rhsI<sub>A</sub></i> , Tet <sup>R</sup>	This study
pCH4565	pCH450:: <i>rhsA<sub>R1321S</sub>-FLAG</i> , Tet <sup>R</sup>	This study
pCH15181	pCH450:: <i>eagR<sub>A</sub>-rhsA<sub>R1321S</sub>-FLAG</i> , Tet <sup>R</sup>	This study
pCH4566	pCH450:: <i>rhsA<sub>R1321S, D1323A</sub>-FLAG</i> , Tet <sup>R</sup>	This study
pCH15202	pCH450:: <i>eagR<sub>A</sub>-rhsA<sub>R1321S, D1323A</sub>-FLAG</i> , Tet <sup>R</sup>	This study
pCH15046	pCH450:: <i>eagR<sub>A</sub>-rhsA<sub>R1321S</sub>-rhsI<sub>A</sub></i> , Tet <sup>R</sup>	This study
pCH15105	pCH450:: <i>eagR<sub>A</sub>-rhsA<sub>R1321S, D1323A</sub>-rhsI<sub>A</sub></i> , Tet <sup>R</sup>	This study
pCH15086	pCH450:: <i>eagR<sub>A</sub>-rhsA<sub>R1321S</sub>-KTE20</i> , Tet <sup>R</sup>	This study
pCH15287	pTrc99a:: <i>rhsI<sub>KTE20</sub></i> , Cm <sup>R</sup>	This study
pCH15257	pCH450:: <i>eagR<sub>A</sub>-rhsA<sub>R1321S</sub>-ybfOC</i> , Tet <sup>R</sup>	This study
pCH10626	pSCbadB2:: <i>(dsbA)ss-trxA</i> , Tp <sup>R</sup>	Fernando Garza-Sánchez

pCH14919	pSCbadB2:: <i>(dsbA)ss-eagRA</i> , Tp <sup>R</sup>	This study
pCH14920	pSCbadB2:: <i>(dsbA)ss-eagRB</i> , Tp <sup>R</sup>	This study
pCH15107	pSCbadB2:: <i>(sufI)ss-eagRA</i> , Tp <sup>R</sup>	This study
pCH15136	pSCbadB2:: <i>(sufI)ss-eagRB</i> , Tp <sup>R</sup>	This study
pCH10610	pSCbadB2:: <i>(dsbA)ss-ybfO</i> , Tp <sup>R</sup>	Fernando Garza- Sánchez

<sup>a</sup>Abbreviations: Amp<sup>R</sup>, ampicillin-resistant; Kan<sup>R</sup>, kanamycin-resistant; Tet<sup>R</sup>, tetracycline-resistant; Rif<sup>R</sup>, rifampicin-resistant; Tp<sup>R</sup>, trimethoprim-resistant

**Table 5.3. Oligonucleotides used in this study.**

<b>Number</b>	<b>Name<sup>a</sup></b>	<b>Sequence<sup>b</sup></b>	<b>Reference</b>
CH2901	EagR <sub>A</sub> -KO-Sac	5'- TTT <u>GAG CTC</u> ATG CTC CGC TGC GTT ATA	This study
CH2902	EagR <sub>A</sub> -KO-Spe	5'- TTT <u>ACT AGT</u> CGT GTT ATC CTG CCA GGC	This study
CH3775	EagR <sub>A</sub> -KO-Eco	5' - GAT <u>GAA TTC</u> TAC TCT CTC GGC ACT CAG	This study
CH2904	EagR <sub>A</sub> -KO-Kpn	5'- TTT <u>GGT ACC</u> CAG AGA GCA ACA TGC CGG	This study
CH3471	EagR <sub>B</sub> -KO-Sac	5' - AAT <u>GAG CTC</u> ACT TTA TAT GGA AAT AAT CC	This study
CH3472	EagR <sub>B</sub> -KO-Bam	5' - AAA <u>GGA TCC</u> CAT TCC TTC ATT AAA CAG GCA C	This study
CH3473	EagR <sub>B</sub> -KO-Eco	5' - CTT <u>GAA TTC</u> CCA CCA TTA ACA CCA GGG	This study
CH3474	EagR <sub>B</sub> -KO-Kpn	5' - ATC <u>GGT ACC</u> GAT GAA GAC GTT GTC CGA G	This study
CH3020	Hcp3-Nco-for	5' - ATA <u>CCA TGG</u> CTA TTG ATA TGT TTC	This study
CH3022	Hcp3-Xho-rev	5' - CTA <u>CTC GAG</u> TGC TTC TTT GTT TTC TTT G	This study
CH2960	RhsA(V82)-Nco-for	5' - TGG <u>CCA TGG</u> TTA CTG ACG ATA TCA G	This study
CH2879	RhsA(A467)-Spe-rev	5' - AAA <u>ACT AGT</u> GGC AGC GGT TAC GCG CTG TGG	This study
CH4190	EagR <sub>A</sub> -Kpn-for	5'- AGT <u>GGT ACC</u> ATG AAA TAC ACC CTC CAG G	This study
CH2911	EagR <sub>A</sub> -Xho-rev	5'- TCA <u>CTC GAG</u> CCT TAC ACA TTC CGG	This study

CH2886	EagR <sub>B</sub> -Kpn-for	5'- AAT <u>GGT ACC</u> ATG ATC GCT TTT CCT GAG GG	This study
CH2887	EagR <sub>B</sub> -Xho-rev	5'- ATC <u>CCT CGA</u> GTT AAT GGT GGA AGC G	This study
CH2877	EagR <sub>A</sub> -H6-Spe-rev	5' - CAT <u>ACT AGT</u> CAC ATT CCG GTT GTC GTT AAG C	This study
CH3914	RhsA-Eco-for	5' - TTT <u>GAA TTC</u> GGC ATG AGC GAT AAC AAC	This study
CH4325	RhsA-Nco(int)-rev	5' - AGG <u>CCA TGG</u> TCG TTA TAG	This study
CH4326	RhsA-Nco(int)-for	5' - CGA <u>CCA TGG</u> CCT GAT GG	This study
CH4327	RhsA-Kpn(int)-rev	5' - CAG <u>CGG TAC</u> CAG CTG AAC	This study
CH4328	RhsA-Kpn(int)-for	5' - TTC AGC <u>TGG TAC</u> CGC TGG	This study
CH4629	rhsA-FLAG-Xho-Sbf-rev	5' - GGT <u>CCT GCA</u> GGC TCG AGT TAT TTG TCA TCA TCG TCC TTG TAG TCA GTA ATC CTC TTG CCA	This study
CH4719	RhsA-T83-Eco-for	5' - TTT <u>GAA TTC</u> ACC ATG ACT GAC GAT ATC AGT AAT ATC GCG G	This study
CH4400	EagR <sub>A</sub> -Eco-for	5' - AGT <u>GAA TTC</u> ATG AAA TAC ACC CTC CAG G	This study
CH4452	VgrG2-Eco-for	5' - ATA <u>GAA TTC</u> ATG CTC AAC CGA ATT ACC	This study
CH4453	VSV-Xho-rev	5' - TGC <u>CTC GAG</u> ATC CTT ATT TGC CAA GAC G	This study
CH4756	EagR <sub>A</sub> -Nco-for	5' - CAC <u>CCA TGG</u> AAT ACA CCC TCC AGG AAG G	This study
CH4757	EagR <sub>A</sub> -Hind-rev	5' - TGT <u>AAG CTT</u> TCA TGC CTT ACA CAT TCC G	This study

CH4329	RhsI <sub>A</sub> -Sbf-rev	5' - ACC CTC GAG <u>CCT GCA GGT</u> GTG GTC GAA CAT TAA CAT ATT AAA TCG	This study
CH4631	RhsA-R1321S- Spe-Xho-Sbf- rev	5' - GGT <u>CCT GCA GGC</u> TCG AGG GTC TAT ACT AGT TAG ACT ATT AGC ACC	This study
CH4632	RhsA-R1321S- Spe-for	5' - AGT CTA <u>ACT AGT</u> ATA GAC CCT CTG GG	This study
CH3636	RhsI <sub>A</sub> -Xho-rev	5' - GTG <u>CTC GAG</u> CAT TAA CAT ATT AAA TCG	This study
CH4898	RhsA- D1323A-Spe- for	5' - CTA <u>ACT AGT</u> ATA GCC CCT CTG GGA TTA AAA C	This study
CH4880	KTE20-RhsA- CT-Spe-for	5' - TTG <u>ACT AGT</u> ATT GAT CCG TGG GGA CTC	This study
CH4881	KTE20-RhsI- Xho-rev	5' - TTT <u>CTC GAG</u> CTA CTT AAA CAA CTT CAG AAT ATC	This study
CH4899	KTE20- RhsI- Kpn-for	5' - TCT <u>GGT ACC</u> ATG ACG ATT ATG CTT ACA TTA G	This study
CH4878	YbfO-Spe-for	5' - GTT <u>ACT AGT</u> ATA GAT TCA ATG GGA CTG GCA	This study
CH4879	YbfC-Xho-rev	5' - TTT <u>CTC GAG</u> TTA TTT CTC TTC ACT ACG AAT TAG TTC	This study
CH4758	EagR <sub>B</sub> -Nco-for	5' - AAG <u>CCA TGG</u> TCG CTT TTC CTG AGG GC	This study
CH4759	EagR <sub>B</sub> -Hind- rev	5' - TAA <u>AAG CTT</u> TCC CTG GTG TTA ATG GTG G	This study
CH4900	SufI- promoter/ss- Bam-for	5' - TGT <u>GGA TCC</u> CCT TTT TCG GCC	This study
CH4901	SufI- promoter/ss- Nco-rev	5' - AAA <u>CCA TGG</u> CGG CGC TGG CTG TCA	This study

<sup>a</sup>Abbreviations: Bam=BamHI, Eco=EcoRI, Hind=HindIII, Kpn=KpnI, Nco=NcoI, Sac=SacI, Sbf=SbfI, Spe=SpeI, Xho=XhoI

<sup>b</sup>Restriction endonuclease sites are underlined.

## Chapter 6: Concluding Remarks

Prokaryotic organisms are ubiquitous, and are essential to many of the planet's chemical processes. While plants are responsible for approximately 80% of Earth's biomass, bacteria are the next major contributors (~15% of the planet's biomass), followed by fungi contributing ~2%, and archaea ~1% (183). Given the size difference between individual plants versus individual bacteria, this finding demonstrates the abundance of bacteria on the planet. Indeed, estimates suggest there are  $\sim 10^{30}$  prokaryotic organisms globally (184). Bacteria are also the lynchpin of the Nitrogen cycle: they are the primary nitrifiers on the planet, and are therefore essential for the majority of life on Earth (185).

Bacteria exist in dense and complex microbial communities, and as such have evolved numerous growth-inhibition systems in order to out-compete neighbors. The bacterial type VI secretion system (T6SS) represents one such competition system (1, 2). First described in 2006, a significant body of work has since elaborated on the function, mechanism, diversity, regulation, and physiological significance of this apparatus. However, it is clear we do not fully understand the T6SS nor fully appreciate its role in nature (see Chapter 1).

In my thesis work, I primarily explored the genetic and molecular underpinnings of the T6SS in *Enterobacter cloacae*. Chapter 2 presented *E. cloacae* as a model system for genetic and molecular research about the T6SS, and described the known effectors deployed in this organism. I also demonstrated that while *E. cloacae* encodes two T6SS loci, the second locus has numerous genetic lesions in it that render it nonfunctional. Nevertheless, there is compelling evidence that *E. cloacae* encodes multiple effectors specific to this nonfunctional T6SS-2 locus. While

these effectors do not appear to serve any current function to the cell without an intact, functional, T6SS-2 locus, a number of questions still remain regarding the molecular specificity between structural T6SS components and the effectors they deploy.

There are 5 distinct *hcp* alleles in the *E. cloacae* genome, and all are associated with predicted effector-immunity gene pairs (Chapter 2). I was able to confirm that 3 of these 5 gene pairs do function as bona-fide effector-immunity pairs, and also that one of these effectors specifically binds its cognate Hcp, but not to the other 4 Hcps. Notably, this particular Hcp protein, Hcp3, was found to be genetically less similar to the other 4 Hcps; it is also the only Hcp protein that supports T6SS-1 activity. I surmise that the other 4 Hcps may all interact specifically with T6SS-2-encoded components. However, I have yet to test this, nor have I shown whether the other 4 Hcp-associated effectors also bind specifically to their cognate Hcp. It is also unclear what purpose there is in having 5 distinct *hcp* alleles in the genome when there are only 2 T6SS loci in the genome.

Chapter 2 also presented data suggesting *E. cloacae* deploys additional, currently unidentified, effectors. Without full knowledge of which effectors are being deployed, multiple questions still remain about the exact nature of its inter-bacterial inhibition activity, such as if all effectors inhibit various species and genera of bacteria equally. It is also not understood if these effectors behave synergistically with one another, or why the cell bothers to deploy multiple unique toxins in the first place. Given that *E. cloacae* appears to encode multiple T6SS-associated effectors that are encoded outside either T6SS locus, it remains to be seen whether these external effectors are controlled via different regulatory mechanisms than the T6SS

loci themselves. While the T6SS-1 locus appears to be constitutively active under laboratory conditions, the ancestral T6SS-2, found intact in *E. hormaechei*, appears to be suppressed under laboratory conditions. It is currently unclear what signals would promote expression of this locus, and what significance this regulation has physiologically. For example, it is possible that the T6SS-2-deployed effectors are most potent under specific environmental conditions, and are deployed only under those conditions. Alternately, the T6SS-2-deployed effectors might be favored when *E. hormaechei* encounters a particular taxon of bacteria, and that this co-occurrence only naturally occurs in specific environments.

In Chapter 3, I characterized *E. cloacae*'s putative T6SS lipase effector (Tle) protein, and described its peculiar dependency on its cognate T6SS lipase immunity (Tli) protein. I demonstrated that Tli promotes increased abundance of Tle, and is required for secretion of Tle and ultimately delivery of Tle into neighboring cells. Curiously, Tli promotes the formation of a distinct Tle variant that migrates faster than its Tli-independent form; this mobility change is observed even under reducing and denaturing conditions, suggesting this change to mobility represents a stable, potentially irreversible, biochemical change. Notably, this “converted” form of Tle is more soluble than the “unconverted” form, and *in vitro* experiments confirm the converted form retains esterase activity. Taken together, my data suggest Tli promotes biochemical modification of Tle, and this modification is required for delivery of Tle.

Many questions still remain regarding this Tle conversion phenomenon. Firstly, it is not understood what modification is occurring. Preliminary mass spectrometry data indicate the converted form of Tle is actually larger than the

unconverted form (data not shown), despite migrating faster on SDS-PAGE. This may indicate that phosphorylation or other forms of negative charge are being added to the protein, resulting in greater charge density and therefore greater mobility on SDS-PAGE. Alternately, increasing the hydrophobicity of a protein also results in increased mobility, presumably because the added hydrophobicity increases affinity to SDS, leading to an increase in charge density (177, 187). It is appealing to believe that addition of a hydrophobic modifier, perhaps a fatty acid group, onto a lipase toxin may help it interact with its membrane substrate. However, an increase in hydrophobicity would not explain why the unconverted form of Tle is largely insoluble while the converted form is significantly more soluble. Given that unconverted Tle is insoluble, it is difficult to address whether this form of Tle retains enzymatic activity. As such, I cannot currently conclude whether or not the conversion phenomenon represents a biochemical activation of the enzyme.

My data suggest that both forms of Tle associate with VgrG in a Tli-dependent fashion, but not Hcp. These experiments were performed in *Escherichia coli* K-12, which lacks any T6SS. As a result, I conclude that Tle requires Tli, but no other chaperone or adaptor, for assembly onto the T6SS apparatus, and that it associates directly with VgrG. Interestingly, it appears as though *E. cloacae* only secretes the converted form of Tle, even though both variants are capable of VgrG interaction in the heterologous *E. coli* system. Future work will hopefully elucidate where on VgrG Tle binds, and why only the converted form of Tle appears to be secreted. Given that Tle appears to have genetic association to the N-terminal region of VgrG, an attractive model for Tle binding is that it resides inside the hollow N-terminal “cup” of the VgrG trimer (92).

In Chapter 4, I presented data that demonstrate how *E. cloacae*'s Rhs proteins behave as VgrG-chaperones and thereby facilitate T6SS assembly. *E. cloacae* expresses 2 Rhs distinct proteins, and at least one is required to support T6SS activity. The N-terminal PAAR domain is insufficient in supporting this activity; instead, the Rhs  $\beta$ -encapsulation and core domains are also required for stable interaction with VgrG and ultimately T6SS activity. Moreover, I have shown that Rhs stabilizes the C-terminal  $\beta$ -spike of trimeric VgrG, independent of other T6SS factors also known to interact with VgrG. This suggests VgrG trimerization occurs prior to docking with the T6SS baseplate.

At this stage, I have not yet untangled whether this VgrG-chaperone function of Rhs is independent of the PAAR domain or not. The PAAR domain is the known VgrG-binding domain for Rhs, yet expression of PAAR alone is insufficient to support co-purification of VgrG-PAAR. It is worth noting that VgrG has been shown to bind to PAAR with VgrG<sub>3</sub>:PAAR<sub>1</sub> stoichiometry (28); this may suggest that the inability of PAAR alone to stabilize the trimeric VgrG  $\beta$ -spike leads to a VgrG molecule incapable of stable interaction with PAAR. If this is true, it may indicate that non-trimeric or mis-folded trimeric VgrG has only a weak or transient binding to Rhs through the PAAR domain. Alternately, it is possible that VgrG interacts with the Rhs  $\beta$ -encapsulation domain directly to first form a stable trimer, thereby facilitating subsequent interaction to Rhs through PAAR.

My data also suggest that while Rhs is required for T6SS activity, as assayed by growth inhibition or Hcp secretion, it is not absolutely essential for at least some T6SS sheath assembly and subsequent contraction events. I observed that the incidence of sheath contractions in *rhs*- mutants was around 4% of the incidence in

wild-type cells. It is currently unclear if these infrequent sheath assembly and contraction events are still viable firing events that simply fall below the limit of detection of my growth inhibition and secretion assays, or if the sheath contractions observed in *rhs-* cells are not able to support proper secretion for some reason. It is worth noting that I and others have observed non-canonical sheath “contraction” events where the sheath “contracts” to the distal membrane opposite of the site of T6SS assembly (195). I posit that these “bidirectional contraction” events, while counted in the assay, are not functional firing events and instead likely represent the sheath breaking, not contracting. Preliminary results indicate this “bidirectional contraction” phenotype occurs at a greater frequency in *rhs-* mutants than in wild-type (data not shown); however, given the low incidence of observed contraction events in *rhs-* cells, I therefore have a small sample size of *rhs-* contraction events to study. Additionally, I and others also observe instances where the sheath polymer extends to reach the distal membrane, then “bends” and elongates slightly more before contracting (195). Again, I preliminarily observe this more frequently in *rhs-* mutants than in wild-type cells (data not shown). It is unclear if these “bent” assemblies would have the same functionality as the canonical straight assemblies.

Additionally, I have presented evidence that Rhs is acting as a chaperone in order to increase the rate of proper VgrG folding, but that VgrG will occasionally reach the properly folded form on its own given a high enough monomer concentration. I demonstrated that over-expression of VgrG in *E. coli* leads to slight accumulation of a stable VgrG complex even in the absence of Rhs. Moreover, over-expression of VgrG in *E. cloacae* preliminarily appears to promote Hcp secretion even in the absence of Rhs. However, VgrG also appears to sometimes mis-

oligomerize and form a high-mass complex that, unlike the stable trimeric form, is sensitive to denaturation via boiling. It is possible these mis-folded complexes are sufficient to support T6SS sheath assembly in *rhs*- mutants expressing native levels of VgrG, but that these mis-folded complexes cannot ultimately support T6SS-mediated growth inhibition or Hcp secretion in the absence of Rhs.

In Chapter 5, I investigated the role of Eag proteins and how they facilitate the function of their cognate effectors. Eag proteins are encoded upstream of certain T6SS effectors, and have previously been shown to be required for growth inhibition via the cognate effector (69, 73). I demonstrated that each of *E. cloacae*'s Rhs proteins requires its cognate EagR for function, and subsequently at least one EagR protein is required to support T6SS activity in *E. cloacae*. Additionally, I confirmed that EagR<sub>A</sub> directly binds the N-terminus of RhsA, and that deletion of this binding-site on RhsA ablates RhsA function. The only Rhs function that was found to be Eag-independent was the cleavage of the C-terminal Rhs toxin domain. I found that this cleavage event is required for delivery (or activation) of the toxin, but does not affect overall Rhs-mediated T6SS activity. Furthermore, the cleaved toxin remains associated with the remaining EagR-Rhs complex, consistent with the model that the toxin remains sequestered inside the Rhs- $\beta$ -encapsulation structure.

Known Eag-binding sites are hydrophobic in nature, and the interaction between Eag and its effector can be broken through the addition of detergent, even though the effector still maintains interaction with its cognate immunity under these conditions (73, 176). Eag proteins are categorized in the DcrB Pfam, which is named after the periplasmic *E. coli* protein DcrB that is thought to be involved in the formation of membrane channels during development of bacteriophage C1 (196,

197). While the majority of DcrB Pfam entries are simply annotated as hypothetical proteins, many are annotated as protein chaperones or cell-envelope-associated proteins (198). Manually searching the Pfam list for hypothetical DcrB-homologs that are encoded upstream of putative effector-immunity gene pairs, I identified 100 putative Eag-associated T6SS effectors widespread across Gram-negative bacteria (data not shown). In all but 2 cases, the downstream effector was an Rhs protein. However, in all cases, the putative effector protein contained an N-terminal extension, followed by a PAAR domain and C-terminal extension. This follows the observed architecture of known Eag-dependent effectors: the N-terminal extension is likely a hydrophobic Eag-binding site, and the C-terminal extension is likely an effector domain.

I propose that Eag-dependent T6SS effectors evolved to require membrane association, likely for integration into or translocation across a membrane. Eag proteins then act as a chaperone for the effector in order to shield the putative transmembrane domains when integration or translocation of the effector is not desired. However, no one has yet demonstrated that Eag-dependent effectors are able to integrate into or translocate across a membrane using their putative transmembrane domains because the assembly of these effectors onto the T6SS apparatus requires Eag. Currently, it is not understood why these effectors require Eag for assembly. Given the genetic association to PAAR-containing effectors, Eag proteins may also be involved in the proper folding of the PAAR domain in order to facilitate interaction with VgrG.

It is also unclear why cleavage of Rhs toxins off the remaining polypeptide is needed in order for growth inhibition via that toxin to occur, nor why the toxin is

predicted to be encapsulated within the Rhs shell structure. The structures of the Rhs-family proteins YenC2 in *Yersinia entomophaga* and TcC in *Photobacterium luminescens* were demonstrated to form very similar  $\beta$ -encapsulation structures despite only 56% sequence identity, and both are thought to encapsulate the cleaved C-terminal toxin domain of the protein (72, 199). Additionally, eukaryotic teneurin proteins are genetically similar to bacterial Rhs proteins, and are known to be transmembrane proteins that mediate adhesion between animal cells at neural synapses (200-202). Recently, the structure of the extracellular domains of teneurins Ten2 from chicken and Ten3 from mouse were solved (203). The Rhs-like domain of these proteins form a  $\beta$ -encapsulation structure remarkably similar to the bacterial structures described previously. However, this shell structure only encapsulates a ~100-residue linker domain that threads through the shell and out in order to expose the teneurin C-terminal domain on the outside of the shell structure. While this C-terminal domain is predicted to undergo a proteolytic processing event, the cleavage site is significantly further down in teneurins than in bacterial Rhs proteins (203, 204); moreover, it is unclear why teneurins bother to fold such an elaborate shell structure only to encapsulate a linker domain.

The bacterial Rhs shell structure may simply serve as a sequestration device to physically prevent the toxin from interacting with its cognate immunity during biogenesis. While numerous other bacterial toxins do not require such sequestration prior to delivery, it is possible that Rhs toxins might have greater affinity for their immunities than other toxins and thus require physical separation from their immunities prior to delivery. Once delivered, the toxin may then separate from the shell in order to interact with substrate. The *Y. entomophaga* Rhs-family-protein

YenC2 has been shown to stably associate with its cleaved toxin domain at neutral pH, but the toxin dissociates from the shell under acidic conditions (72). YenC2 is one subunit of a much larger insecticidal toxin complex that is believed to first enter the host cell via endocytosis; upon acidification in the endosome, the complex inserts into the endosomal membrane and the YenC2 toxin domain translocates through a channel formed by the rest of the complex (205). Given that the Gram-negative periplasm is acidified by the proton gradient formed via the electron transport chain, T6SS-deployed Rhs toxins may similarly be released from the encapsulation structure once delivered into the target cell periplasm.

However, if Rhs toxins dissociate from the shell in the periplasm, then cytoplasmic toxins must still cross the target cell inner-membrane via an unknown mechanism. Additionally, this model does not explain why many T6SS-dependent Rhs proteins encode putative transmembrane domains. Perhaps a more attractive model of Rhs toxin delivery is that the entire Rhs  $\beta$ -encapsulation structure can integrate into or translocate across the inner-membrane. The N-terminus of Rhs may first integrate into the inner-membrane via its N-terminal putative transmembrane domain, leading to fusion of the shell structure into the membrane and resulting in an arrangement vaguely reminiscent of  $\beta$ -barrel membrane proteins. The shell structure may or may not fully translocate across the membrane into the cytosol, and the encapsulated toxin domain is released from the shell structure via an unknown trigger.

This thesis has focused on addressing genetic and molecular considerations regarding the T6SS, but does not address the broader significance of how the T6SS impacts ecology and human health. Recent studies have started to elucidate the

ecological impact of T6SS-wielding bacteria in their respective microbiomes. For example, it has been estimated that about a quarter of the bacteria in the human intestinal microbiome encode T6SSs (206). In 2016, Wexler *et al.* demonstrated that T6SS activity occurs throughout the murine large intestine, and calculated that over 1 billion T6SS-firing events occur per minute per gram of colonic contents (207). The colonization of T6SS-wielding commensal bacteria in murine intestines has also been shown to block the colonization of invading pathogenic strains (208). Thus, not only does the T6SS play an important role in bacterial ecology, it also suggests that T6SS-wielding commensal bacteria could be utilized as a probiotic strategy to prevent bacterial infection. However, these studies were performed in mice with simplified microbiomes; currently, it is unclear if these results will fully translate to human health.

However, T6SSs are found in both commensal and pathogenic bacteria. For example, Sana *et al.* have demonstrated that pathogenic *Salmonella enterica* serovar Typhimurium will colonize mice and kill commensal *Klebsiella oxytoca* inside the host; both the killing of commensals and the overall colonization by *S. Typhimurium* is dependent on its T6SS (209). This finding opens new avenues in animal medicine: one could specifically design vaccines against known pathogenic T6SSs in order to combat bacterial infections. Recently, this approach was tested in chickens to prevent infection by *Campylobacter jejuni*: Mallick and colleagues immunized chickens with purified recombinant Hcp from *C. jejuni*, then challenged the birds with the bacteria and found a significant reduction in the cecal load of *C. jejuni* compared to the control (210). However, any potential biomedical approaches to combat T6SS-wielding bacteria may also target beneficial resident bacteria as well.

Ultimately, any biomedical approaches involving the T6SS will require an understanding of the molecular mechanisms of toxin activity and delivery, and an understanding of how T6SSs alter the composition of bacterial microbiomes.

## References

1. Mougous, J., Cuff, M., Raunser, S., Shen, A., Zhou, M., Gifford, C., et al. (2006). A virulence locus of *Pseudomonas aeruginosa* encodes a protein secretion apparatus. *Science (New York, N.Y.)*, *312* (5779), 1526-30.
2. Pukatzki, S., Ma, A., Sturtevant, D., Krastins, B., Sarracino, D., Nelson, W., et al. (2006). Identification of a conserved bacterial protein secretion system in *Vibrio cholerae* using the *Dictyostelium* host model system. *Proceedings of the National Academy of Sciences of the United States of America*, *103* (5), 1528-33.
3. Sheahan, K.-L., Cordero, C., & Fullner Satchell, K. (2004). Identification of a domain within the multifunctional *Vibrio cholerae* RTX toxin that covalently cross-links actin. *Proceedings of the National Academy of Sciences*, *101* (26), 9798-9803.
4. Pukatzki, S., Ma, A., Revel, A., Sturtevant, D., & Mekalanos, J. (2007). Type VI secretion system translocates a phage tail spike-like protein into target cells where it cross-links actin. *Proceedings of the National Academy of Sciences*, *104* (39), 15508-15513.
5. Hood, R., Singh, P., Hsu, F., Güvener, T., Carl, M., Trinidad, R., et al. (2010). A Type VI Secretion System of *Pseudomonas aeruginosa* Targets a Toxin to Bacteria. *Cell Host & Microbe*, *7* (1), 25-37.
6. Schwarz, S., Hood, R., & Mougous, J. (2010). What is type VI secretion doing in all those bugs? *Trends in Microbiology*, *18* (12), 531-537.
7. Turnbaugh, P., Ley, R., Mahowald, M., Magrini, V., Mardis, E., & Gordon, J. (2006). An obesity-associated gut microbiome with increased capacity for energy harvest. *Nature*, *444* (7122), 1027-1031.
8. Turnbaugh, P., Hamady, M., Yatsunenko, T., Cantarel, B., Duncan, A., Ley, R., et al. (2009). A core gut microbiome in obese and lean twins. *Nature*, *457* (7228), 480-484.
9. Lakhan, S., & Kirchgessner, A. (2010). Gut inflammation in chronic fatigue syndrome. *Nutrition & Metabolism*, *7* (1), 79.
10. Frank, D., St. Amand, A., Feldman, R., Boedeker, E., Harpaz, N., & Pace, N. (2007). Molecular-phylogenetic characterization of microbial community imbalances in human inflammatory bowel diseases. *Proceedings of the National Academy of Sciences*, *104* (34), 13780-13785.
11. Marteau, P. (2009). Bacterial Flora in Inflammatory Bowel Disease. *Digestive Diseases*, *27* (1), 99-103.

12. Castellarin, M., Warren, R., Freeman, J., Dreolini, L., Krzywinski, M., Strauss, J., et al. (2012). *Fusobacterium nucleatum* infection is prevalent in human colorectal carcinoma. *Genome research*, 22 (2), 299-306.
13. Kostic, A., Gevers, D., Pedamallu, C., Michaud, M., Duke, F., Earl, A., et al. (2012). Genomic analysis identifies association of *Fusobacterium* with colorectal carcinoma. *Genome research*, 22 (2), 292-8.
14. Nano, F., Zhang, N., Cowley, S., Klose, K., Cheung, K., Roberts, M., et al. (2004). A *Francisella tularensis* pathogenicity island required for intramacrophage growth. *Journal of bacteriology*, 186 (19), 6430-6.
15. Parsons, D., & Heffron, F. (2005). *sciS*, an *icmF* homolog in *Salmonella enterica* serovar Typhimurium, limits intracellular replication and decreases virulence. *Infection and immunity*, 73 (7), 4338-45.
16. Dudley, E., Thomson, N., Parkhill, J., Morin, N., & Nataro, J. (2006). Proteomic and microarray characterization of the *AggR* regulon identifies a *pheU* pathogenicity island in enteroaggregative *Escherichia coli*. *Molecular Microbiology*, 61 (5), 1267-1282.
17. de Bruin, O., Ludu, J., & Nano, F. (2007). The *Francisella* pathogenicity island protein *IglA* localizes to the bacterial cytoplasm and is needed for intracellular growth. *BMC Microbiology*, 7 (1), 1.
18. Schell, M., Ulrich, R., Ribot, W., Brueggemann, E., Hines, H., Chen, D., et al. (2007). Type VI secretion is a major virulence determinant in *Burkholderia mallei*. *Molecular Microbiology*, 64 (6), 1466-1485.
19. Zheng, J., & Leung, K. (2007). Dissection of a type VI secretion system in *Edwardsiella tarda*. *Molecular Microbiology*, 66 (5), 1192-1206.
20. Ludu, J., de Bruin, O., Duplantis, B., Schmerk, C., Chou, A., Elkins, K., et al. (2008). The *Francisella* pathogenicity island protein *PdpD* is required for full virulence and associates with homologues of the type VI secretion system. *Journal of bacteriology*, 190 (13), 4584-95.
21. Boyer, F., Fichant, G., Berthod, J., Vandenbrouck, Y., & Attree, I. (2009). Dissecting the bacterial type VI secretion system by a genome wide in silico analysis: what can be learned from available microbial genomic resources? *BMC Genomics*, 10 (1), 104.
22. Nykyri, J., Niemi, O., Koskinen, P., Nokso-Koivisto, J., Pasanen, M., Broberg, M., et al. (2012). Revised Phylogeny and Novel Horizontally Acquired Virulence Determinants of the Model Soft Rot Phytopathogen *Pectobacterium wasabiae* SCC3193. (B. Tyler, Ed.) *PLoS Pathogens*, 8 (11), e1003013.

23. Zhang, L., Xu, J., Xu, J., Zhang, H., He, L., & Feng, J. (2014). TssB is essential for virulence and required for Type VI secretion system in *Ralstonia solanacearum*. *Microbial Pathogenesis*, *74*, 1-7.
24. Shyntum, D., Theron, J., Venter, S., Moleleki, L., Toth, I., & Coutinho, T. (2015). *Pantoea ananatis* Utilizes a Type VI Secretion System for Pathogenesis and Bacterial Competition. *Molecular Plant-Microbe Interactions*, *28* (4), 420-431.
25. Leiman, P., Basler, M., Ramagopal, U., Bonanno, J., Sauder, J., Pukatzki, S., et al. (2009). Type VI secretion apparatus and phage tail-associated protein complexes share a common evolutionary origin. *Proceedings of the National Academy of Sciences of the United States of America*, *106* (11), 4154-9.
26. Pell, L., Kanelis, V., Donaldson, L., Howell, P., & Davidson, A. (2009). The phage lambda major tail protein structure reveals a common evolution for long-tailed phages and the type VI bacterial secretion system. *Proceedings of the National Academy of Sciences of the United States of America*, *106* (11), 4160-5.
27. Lossi, N., Dajani, R., Freemont, P., & Filloux, A. (2011). Structure-function analysis of HsiF, a gp25-like component of the type VI secretion system, in *Pseudomonas aeruginosa*. *Microbiology*, *157* (12), 3292-3305.
28. Shneider, M., Buth, S., Ho, B., Basler, M., Mekalanos, J., & Leiman, P. (2013). PAAR-repeat proteins sharpen and diversify the type VI secretion system spike. *Nature*, *500* (7462), 350-353.
29. Cianfanelli, F., Alcoforado Diniz, J., Guo, M., De Cesare, V., Trost, M., & Coulthurst, S. (2016). VgrG and PAAR Proteins Define Distinct Versions of a Functional Type VI Secretion System. (E. Cascales, Ed.) *PLOS Pathogens*, *12* (6), e1005735.
30. Aschtgen, M.-S., Bernard, C., Bentzmann, S., Llobès, R., & Cascales, E. (2008). SciN Is an Outer Membrane Lipoprotein Required for Type VI Secretion in Enteroaggregative *Escherichia coli*. *Journal of Bacteriology*, *190* (22), 7523-7531.
31. Ma, L.-S., Lin, J.-S., & Lai, E.-M. (2009). An IcmF family protein, ImpLM, is an integral inner membrane protein interacting with ImpKL, and its walker a motif is required for type VI secretion system-mediated Hcp secretion in *Agrobacterium tumefaciens*. *Journal of bacteriology*, *191* (13), 4316-29.
32. Aschtgen, M.-S., Gavioli, M., Dessen, A., Llobès, R., & Cascales, E. (2010). The SciZ protein anchors the enteroaggregative *Escherichia coli* Type VI secretion system to the cell wall. *Molecular Microbiology*, *75* (4), 886-899.
33. Felisberto-Rodrigues, C., Durand, E., Aschtgen, M.-S., Blangy, S., Ortiz-Lombardia, M., Douzi, B., et al. (2011). Towards a Structural Comprehension of Bacterial Type VI

Secretion Systems: Characterization of the TssJ-TssM Complex of an Escherichia coli Pathovar. (C. Roy, Ed.) *PLoS Pathogens*, 7 (11), e1002386.

34. Ma, L.-S., Narberhaus, F., & Lai, E.-M. (2012). IcmF family protein TssM exhibits ATPase activity and energizes type VI secretion. *The Journal of biological chemistry*, 287 (19), 15610-21.

35. Durand, E., Nguyen, V., Zoued, A., Logger, L., Péhau-Arnaudet, G., Aschtgen, M.-S., et al. (2015). Biogenesis and structure of a type VI secretion membrane core complex. *Nature*, 523 (7562), 555-560.

36. Brunet, Y., Zoued, A., Boyer, F., Douzi, B., & Cascales, E. (2015). The Type VI Secretion TssEFGK-VgrG Phage-Like Baseplate Is Recruited to the TssJLM Membrane Complex via Multiple Contacts and Serves As Assembly Platform for Tail Tube/Sheath Polymerization. (P. Viollier, Ed.) *PLOS Genetics*, 11 (10), e1005545.

37. Nguyen, V., Logger, L., Spinelli, S., Legrand, P., Huyen Pham, T., Nhung Trinh, T., et al. (2017). Type VI secretion TssK baseplate protein exhibits structural similarity with phage receptor-binding proteins and evolved to bind the membrane complex. *Nature Microbiology*, 2 (9), 17103.

38. Ishikawa, T., Rompikuntal, P., Lindmark, B., Milton, D., & Wai, S. (2009). Quorum Sensing Regulation of the Two hcp Alleles in Vibrio cholerae O1 Strains. (S. Bereswill, Ed.) *PLoS ONE*, 4 (8), e6734.

39. Kapitein, N., Bönemann, G., Pietrosiuk, A., Seyffer, F., Hausser, I., Locker, J., et al. (2013). ClpV recycles VipA/VipB tubules and prevents non-productive tubule formation to ensure efficient type VI protein secretion. *Molecular Microbiology*, 87 (5), 1013-1028.

40. Kudryashev, M., Wang, R.-R., Brackmann, M., Scherer, S., Maier, T., Baker, D., et al. (2015). Structure of the Type VI Secretion System Contractile Sheath. *Cell*, 160 (5), 952-962.

41. Zoued, A., Durand, E., Brunet, Y., Spinelli, S., Douzi, B., Guzzo, M., et al. (2016). Priming and polymerization of a bacterial contractile tail structure. *Nature*, 531 (7592), 59-63.

42. Taylor, N., Prokhorov, N., Guerrero-Ferreira, R., Shneider, M., Browning, C., Goldie, K., et al. (2016). Structure of the T4 baseplate and its function in triggering sheath contraction. *Nature*, 533 (7603), 346-352.

43. Ballister, E., Lai, A., Zuckermann, R., Cheng, Y., & Mougous, J. (2008). In vitro self-assembly of tailorable nanotubes from a simple protein building block. *Proceedings of the National Academy of Sciences of the United States of America*, 105 (10), 3733-8.

44. Brunet, Y., Henin, J., Celia, H., & Cascales, E. (2014). Type VI secretion and bacteriophage tail tubes share a common assembly pathway. *EMBO reports*, *15* (3), 315-321.
45. Douzi, B., Spinelli, S., Blangy, S., Roussel, A., Durand, E., Brunet, Y., et al. (2014). Crystal Structure and Self-Interaction of the Type VI Secretion Tail-Tube Protein from Enteroaggregative Escherichia coli. (B. Kobe, Ed.) *PLoS ONE*, *9* (2), e86918.
46. Bönemann, G., Pietrosiuk, A., Diemand, A., Zentgraf, H., & Mogk, A. (2009). Remodelling of VipA/VipB tubules by ClpV-mediated threading is crucial for type VI protein secretion. *The EMBO Journal*, *28* (4), 315-325.
47. Basler, M., & Mekalanos, J. (2012). Type 6 secretion dynamics within and between bacterial cells. *Science (New York, N.Y.)*, *337* (6096), 815.
48. Basler, M., Pilhofer, M., Henderson, G., Jensen, G., & Mekalanos, J. (2012). Type VI secretion requires a dynamic contractile phage tail-like structure. *Nature*, *483* (7388), 182-186.
49. Zheng, J., Ho, B., & Mekalanos, J. (2011). Genetic Analysis of Anti-Amoebae and Anti-Bacterial Activities of the Type VI Secretion System in *Vibrio cholerae*. (P. Riggs, Ed.) *PLoS ONE*, *6* (8), e23876.
50. Basler, M. (2015). Type VI secretion system: secretion by a contractile nanomachine. *Philosophical Transactions of the Royal Society B: Biological Sciences*, *370* (1679), 20150021.
51. Durand, E., Nguyen, V., Zoued, A., Logger, L., Péhau-Arnaudet, G., Aschtgen, M.-S., et al. (2015). Biogenesis and structure of a type VI secretion membrane core complex. *Nature*, *523* (7562), 555-560.
52. Suarez, G., Sierra, J., Erova, T., Sha, J., Horneman, A., & Chopra, A. (2010). A type VI secretion system effector protein, VgrG1, from *Aeromonas hydrophila* that induces host cell toxicity by ADP ribosylation of actin. *Journal of bacteriology*, *192* (1), 155-68.
53. Sana, T., Baumann, C., Merdes, A., Soscia, C., Rattei, T., Hachani, A., et al. (2015). Internalization of *Pseudomonas aeruginosa* Strain PAO1 into Epithelial Cells Is Promoted by Interaction of a T6SS Effector with the Microtubule Network. *mBio*, *6* (3), e00712.
54. Aschtgen, M.-S., Zoued, A., Lloubès, R., Journet, L., & Cascales, E. (2012). The C-tail anchored TssL subunit, an essential protein of the enteroaggregative *Escherichia coli* Sci-1 Type VI secretion system, is inserted by YidC. *MicrobiologyOpen*, *1* (1), 71-82.

55. Zoued, A., Brunet, Y., Durand, E., Aschtgen, M.-S., Logger, L., Douzi, B., et al. (2014). Architecture and assembly of the Type VI secretion system. *Biochimica et Biophysica Acta (BBA) - Molecular Cell Research*, 1843 (8), 1664-1673.
56. Wang, T., Si, M., Song, Y., Zhu, W., Gao, F., Wang, Y., et al. (2015). Type VI Secretion System Transports Zn<sup>2+</sup> to Combat Multiple Stresses and Host Immunity. (E. Skaar, Ed.) *PLOS Pathogens*, 11 (7), e1005020.
57. Lin, J., Zhang, W., Cheng, J., Yang, X., Zhu, K., Wang, Y., et al. (2017). A Pseudomonas T6SS effector recruits PQS-containing outer membrane vesicles for iron acquisition. *Nature Communications*, 8 (1), 14888.
58. Si, M., Wang, Y., Zhang, B., Zhao, C., Kang, Y., Bai, H., et al. (2017). The Type VI Secretion System Engages a Redox-Regulated Dual-Functional Heme Transporter for Zinc Acquisition. *Cell Reports*, 20 (4), 949-959.
59. Russell, A., Hood, R., Bui, N., LeRoux, M., Vollmer, W., & Mougous, J. (2011). Type VI secretion delivers bacteriolytic effectors to target cells. *Nature*, 475 (7356), 343-347.
60. Russell, A., Singh, P., Brittnacher, M., Bui, N., Hood, R., Carl, M., et al. (2012). A Widespread Bacterial Type VI Secretion Effector Superfamily Identified Using a Heuristic Approach. *Cell Host & Microbe*, 11 (5), 538-549.
61. Whitney, J., Chou, S., Russell, A., Biboy, J., Gardiner, T., Ferrin, M., et al. (2013). Identification, structure, and function of a novel type VI secretion peptidoglycan glycoside hydrolase effector-immunity pair. *The Journal of biological chemistry*, 288 (37), 26616-24.
62. Brooks, T., Unterweger, D., Bachmann, V., Kostiuk, B., & Pukatzki, S. (2013). Lytic activity of the *Vibrio cholerae* type VI secretion toxin VgrG-3 is inhibited by the antitoxin TsaB. *The Journal of biological chemistry*, 288 (11), 7618-25.
63. Russell, A., LeRoux, M., Hathazi, K., Agnello, D., Ishikawa, T., Wiggins, P., et al. (2013). Diverse type VI secretion phospholipases are functionally plastic antibacterial effectors. *Nature*, 496 (7446), 508-512.
64. Dong, T., Ho, B., Yoder-Himes, D., & Mekalanos, J. (2013). Identification of T6SS-dependent effector and immunity proteins by Tn-seq in *Vibrio cholerae*. *Proceedings of the National Academy of Sciences of the United States of America*, 110 (7), 2623-8.
65. Jiang, F., Waterfield, N., Yang, J., Yang, G., & Jin, Q. (2014). A *Pseudomonas aeruginosa* Type VI Secretion Phospholipase D Effector Targets Both Prokaryotic and Eukaryotic Cells. *Cell Host & Microbe*, 15 (5), 600-610.

66. Miyata, S., Unterweger, D., Rudko, S., & Pukatzki, S. (2013). Dual Expression Profile of Type VI Secretion System Immunity Genes Protects Pandemic *Vibrio cholerae*. (J. Mougous, Ed.) *PLoS Pathogens*, *9* (12), e1003752.
67. Koskiniemi, S., Lamoureux, J., Nikolakakis, K., t'Kint de Roodenbeke, C., Kaplan, M., Low, D., et al. (2013). Rhs proteins from diverse bacteria mediate intercellular competition. *Proceedings of the National Academy of Sciences of the United States of America*, *110* (17), 7032-7.
68. Ma, L.-S., Hachani, A., Lin, J.-S., Filloux, A., & Lai, E.-M. (2014). *Agrobacterium tumefaciens* Deploys a Superfamily of Type VI Secretion DNase Effectors as Weapons for Interbacterial Competition In Planta. *Cell Host & Microbe*, *16* (1), 94-104.
69. Alcoforado Diniz, J., & Coulthurst, S. (2015). Intraspecies Competition in *Serratia marcescens* Is Mediated by Type VI-Secreted Rhs Effectors and a Conserved Effector-Associated Accessory Protein. *Journal of bacteriology*, *197* (14), 2350-60.
70. Li, M., Le Trong, I., Carl, M., Larson, E., Chou, S., De Leon, J., et al. (2012). Structural Basis for Type VI Secretion Effector Recognition by a Cognate Immunity Protein. (C. Roy, Ed.) *PLoS Pathogens*, *8* (4), e1002613.
71. Beck, C. M. (2015). Mechanism of toxin activity and delivery in bacterial contact-dependent competition systems. (*Unpublished doctoral dissertation*). University of California, Santa Barbara, Santa Barbara, CA.
72. Busby, J., Panjikar, S., Landsberg, M., Hurst, M., & Lott, J. (2013). The BC component of ABC toxins is an RHS-repeat-containing protein encapsulation device. *Nature*, *501* (7468), 547-550.
73. Whitney, J., Quentin, D., Sawai, S., LeRoux, M., Harding, B., Ledvina, H., et al. (2015). An interbacterial NAD(P)(+) glycohydrolase toxin requires elongation factor Tu for delivery to target cells. *Cell*, *163* (3), 607-19.
74. Ting, S.-Y., Bosch, D., Mangiameli, S., Radey, M., Huang, S., Park, Y.-J., et al. (2018). Bifunctional Immunity Proteins Protect Bacteria against FtsZ-Targeting ADP-Ribosylating Toxins. *Cell*, *175* (5), 1380-1392.e14.
75. Sana, T., Hachani, A., Bucior, I., Soscia, C., Garvis, S., Termine, E., et al. (2012). The second type VI secretion system of *Pseudomonas aeruginosa* strain PAO1 is regulated by quorum sensing and Fur and modulates internalization in epithelial cells. *The Journal of biological chemistry*, *287* (32), 27095-105.

76. Vettiger, A., & Basler, M. (2016). Type VI Secretion System Substrates Are Transferred and Reused among Sister Cells. *Cell*, *167* (1), 99-110.e12.
77. Ho, B., Fu, Y., Dong, T., & Mekalanos, J. (2017). Vibrio cholerae type 6 secretion system effector trafficking in target bacterial cells. *Proceedings of the National Academy of Sciences of the United States of America*, *114* (35), 9427-9432.
78. Nakayama, K., Takashima, K., Ishihara, H., Shinomiya, T., Kageyama, M., Kanaya, S., et al. (2000). The R-type pyocin of Pseudomonas aeruginosa is related to P2 phage, and the F-type is related to lambda phage. *Molecular Microbiology*, *38* (2), 213-231.
79. Michel-Briand, Y., & Baysse, C. (2002). The pyocins of Pseudomonas aeruginosa. *Biochimie*, *84* (5-6), 499-510.
80. Gebhart, D., Williams, S., Bishop-Lilly, K., Govoni, G., Willner, K., Butani, A., et al. (2012). Novel high-molecular-weight, R-type bacteriocins of Clostridium difficile. *Journal of bacteriology*, *194* (22), 6240-7.
81. Whitney, J., Beck, C., Goo, Y., Russell, A., Harding, B., De Leon, J., et al. (2014). Genetically distinct pathways guide effector export through the type VI secretion system. *Molecular Microbiology*, *92* (3), 529-542.
82. Schwarz, S., Singh, P., Robertson, J., LeRoux, M., Skerrett, S., Goodlett, D., et al. (2014). VgrG-5 is a Burkholderia type VI secretion system-exported protein required for multinucleated giant cell formation and virulence. *Infection and immunity*, *82* (4), 1445-52.
83. Toesca, I., French, C., & Miller, J. (2014). The Type VI secretion system spike protein VgrG5 mediates membrane fusion during intercellular spread by pseudomallei group Burkholderia species. *Infection and immunity*, *82* (4), 1436-44.
84. Blondel, C., Jiménez, J., Contreras, I., & Santiviago, C. (2009). Comparative genomic analysis uncovers 3 novel loci encoding type six secretion systems differentially distributed in Salmonella serotypes. *BMC Genomics*, *10* (1), 354.
85. Wenren, L., Sullivan, N., Cardarelli, L., Septer, A., & Gibbs, K. (2013). Two independent pathways for self-recognition in Proteus mirabilis are linked by type VI-dependent export. *mBio*, *4* (4), e00374-13.
86. Hachani, A., Allsopp, L., Oduko, Y., & Filloux, A. (2014). The VgrG proteins are 'a la carte' delivery systems for bacterial type VI effectors. *The Journal of biological chemistry*, *289* (25), 17872-84.
87. Flaugnatti, N., Le, T., Canaan, S., Aschtgen, M.-S., Nguyen, V., Blangy, S., et al. (2016). A phospholipase A1 antibacterial Type VI secretion effector interacts directly

with the C-terminal domain of the VgrG spike protein for delivery. *Molecular Microbiology*, 99 (6), 1099-1118.

88. Silverman, J., Agnello, D., Zheng, H., Andrews, B., Li, M., Catalano, C., et al. (2013). Haemolysin Coregulated Protein Is an Exported Receptor and Chaperone of Type VI Secretion Substrates. *Molecular Cell*, 51 (5), 584-593.

89. Liang, X., Moore, R., Wilton, M., Wong, M., Lam, L., & Dong, T. (2015). Identification of divergent type VI secretion effectors using a conserved chaperone domain. *Proceedings of the National Academy of Sciences of the United States of America*, 112 (29), 9106-11.

90. Unterweger, D., Kostiuk, B., Otjengerdes, R., Wilton, A., Diaz-Satizabal, L., & Pukatzki, S. (2015). Chimeric adaptor proteins translocate diverse type VI secretion system effectors in *Vibrio cholerae*. *The EMBO Journal*, 34 (16), 2198-2210.

91. Shalom, G., Shaw, J., & Thomas, M. (2007). In vivo expression technology identifies a type VI secretion system locus in *Burkholderia pseudomallei* that is induced upon invasion of macrophages. *Microbiology*, 153 (8), 2689-2699.

92. Spínola-Amilibia, M., Davó-Siguero, I., Ruiz, F., Santillana, E., Medrano, F., & Romero, A. (2016). The structure of VgrG1 from *Pseudomonas aeruginosa*, the needle tip of the bacterial type VI secretion system. *Acta Crystallographica Section D Structural Biology*, 72 (1), 22-33.

93. Poole, S., Diner, E., Aoki, S., Braaten, B., t'Kint de Roodenbeke, C., Low, D., et al. (2011). Identification of Functional Toxin/Immunity Genes Linked to Contact-Dependent Growth Inhibition (CDI) and Rearrangement Hotspot (Rhs) Systems. (M. Achtman, Ed.) *PLoS Genetics*, 7 (8), e1002217.

94. Koskiniemi, S., Garza-Sánchez, F., Sandegren, L., Webb, J., Braaten, B., Poole, S., et al. (2014). Selection of Orphan Rhs Toxin Expression in Evolved *Salmonella enterica* Serovar Typhimurium. (L. Søgaard-Andersen, Ed.) *PLoS Genetics*, 10 (3), e1004255.

95. Ma, J., Pan, Z., Huang, J., Sun, M., Lu, C., & Yao, H. (2017). The Hcp proteins fused with diverse extended-toxin domains represent a novel pattern of antibacterial effectors in type VI secretion systems. *Virulence*, 8 (7), 1189-1202.

96. Zhang, D., de Souza, R., Anantharaman, V., Iyer, L., & Aravind, L. (2012). Polymorphic toxin systems: Comprehensive characterization of trafficking modes, processing, mechanisms of action, immunity and ecology using comparative genomics. *Biology Direct*, 7 (1), 18.

97. Bondage, D., Lin, J.-S., Ma, L.-S., Kuo, C.-H., & Lai, E.-M. (2016). VgrG C terminus confers the type VI effector transport specificity and is required for binding with PAAR

and adaptor-effector complex. *Proceedings of the National Academy of Sciences of the United States of America*, 113 (27), E3931-40.

98. Salomon, D., Klimko, J., Trudgian, D., Kinch, L., Grishin, N., Mirzaei, H., et al. (2015). Type VI Secretion System Toxins Horizontally Shared between Marine Bacteria. (J. Mougous, Ed.) *PLOS Pathogens*, 11 (8), e1005128.

99. Altindis, E., Dong, T., Catalano, C., & Mekalanos, J. (2015). Secretome analysis of *Vibrio cholerae* type VI secretion system reveals a new effector-immunity pair. *mBio*, 6 (2), e00075.

100. Labbate, M., Orata, F., Petty, N., Jayatilleke, N., King, W., Kirchberger, P., et al. (2016). A genomic island in *Vibrio cholerae* with VPI-1 site-specific recombination characteristics contains CRISPR-Cas and type VI secretion modules. *Scientific Reports*, 6 (1), 36891.

101. Kirchberger, P., Unterweger, D., Provenzano, D., Pukatzki, S., & Boucher, Y. (2017). Sequential displacement of Type VI Secretion System effector genes leads to evolution of diverse immunity gene arrays in *Vibrio cholerae*. *Scientific Reports*, 7 (1), 45133.

102. Bingle, L., Bailey, C., & Pallen, M. (2008). Type VI secretion: a beginner's guide. *Current Opinion in Microbiology*, 11 (1), 3-8.

103. Coyne, M., Zitomersky, N., McGuire, A., Earl, A., & Comstock, L. (2014). Evidence of extensive DNA transfer between bacteroidales species within the human gut. *mBio*, 5 (3), e01305-14.

104. Burtnick, M., DeShazer, D., Nair, V., Gherardini, F., & Brett, P. (2010). *Burkholderia mallei* cluster 1 type VI secretion mutants exhibit growth and actin polymerization defects in RAW 264.7 murine macrophages. *Infection and immunity*, 78 (1), 88-99.

105. Chen, Y., Wong, J., Sun, G., Liu, Y., Tan, G.-Y., & Gan, Y.-H. (2011). Regulation of type VI secretion system during *Burkholderia pseudomallei* infection. *Infection and immunity*, 79 (8), 3064-73.

106. Lombardo, M.-J., Michalski, J., Martinez-Wilson, H., Morin, C., Hilton, T., Osorio, C., et al. (2007). An in vivo expression technology screen for *Vibrio cholerae* genes expressed in human volunteers. *Proceedings of the National Academy of Sciences of the United States of America*, 104 (46), 18229-34.

107. Mattinen, L., Somervuo, P., Nykyri, J., Nissinen, R., Kouvonen, P., Corthals, G., et al. (2008). Microarray profiling of host-extract-induced genes and characterization of the type VI secretion cluster in the potato pathogen *Pectobacterium atrosepticum*. *Microbiology*, 154 (8), 2387-2396.

108. Mandlik, A., Livny, J., Robins, W., Ritchie, J., Mekalanos, J., & Waldor, M. (2011). RNA-Seq-Based Monitoring of Infection-Linked Changes in *Vibrio cholerae* Gene Expression. *Cell Host & Microbe*, *10* (2), 165-174.
109. de Pace, F., Boldrin de Paiva, J., Nakazato, G., Lancellotti, M., Sircili, M., Guedes Stehling, E., et al. (2011). Characterization of IcmF of the type VI secretion system in an avian pathogenic *Escherichia coli* (APEC) strain. *Microbiology*, *157* (10), 2954-2962.
110. Southey-Pillig, C., Davies, D., & Sauer, K. (2005). Characterization of temporal protein production in *Pseudomonas aeruginosa* biofilms. *Journal of bacteriology*, *187* (23), 8114-26.
111. Chakraborty, S., Li, M., Chatterjee, C., Sivaraman, J., Leung, K., & Mok, Y.-K. (2010). Temperature and Mg<sup>2+</sup> sensing by a novel PhoP-PhoQ two-component system for regulation of virulence in *Edwardsiella tarda*. *The Journal of biological chemistry*, *285* (50), 38876-88.
112. Zhang, W., Xu, S., Li, J., Shen, X., Wang, Y., & Yuan, Z. (2011). Modulation of a thermoregulated type VI secretion system by AHL-dependent Quorum Sensing in *Yersinia pseudotuberculosis*. *Archives of Microbiology*, *193* (5), 351-363.
113. Ishikawa, T., Sabharwal, D., Bröms, J., Milton, D., Sjöstedt, A., Uhlin, B., et al. (2012). Pathoadaptive Conditional Regulation of the Type VI Secretion System in *Vibrio cholerae* O1 Strains. *Infection and Immunity*, *80* (2), 575-584.
114. Rogge, M., & Thune, R. (2011). Regulation of the *Edwardsiella ictaluri* type III secretion system by pH and phosphate concentration through EsrA, EsrB, and EsrC. *Applied and environmental microbiology*, *77* (13), 4293-302.
115. Ventre, I., Goodman, A., Vallet-Gely, I., Vasseur, P., Soscia, C., Molin, S., et al. (2006). Multiple sensors control reciprocal expression of *Pseudomonas aeruginosa* regulatory RNA and virulence genes. *Proceedings of the National Academy of Sciences of the United States of America*, *103* (1), 171-6.
116. Goodman, A., Merighi, M., Hyodo, M., Ventre, I., Filloux, A., & Lory, S. (2009). Direct interaction between sensor kinase proteins mediates acute and chronic disease phenotypes in a bacterial pathogen. *Genes & development*, *23* (2), 249-59.
117. Reimmann, C., Beyeler, M., Latifi, A., Winteler, H., Foglino, M., Lazdunski, A., et al. (1997). The global activator GacA of *Pseudomonas aeruginosa* PAO1 positively controls the production of the autoinducer N -butyryl-homoserine lactone and the formation of the virulence factors pyocyanin, cyanide, and lipase. *Molecular Microbiology*, *24* (2), 309-319.

118. Lapouge, K., Schubert, M., Allain, F.-T., & Haas, D. (2007). Gac/Rsm signal transduction pathway of  $\gamma$ -proteobacteria: from RNA recognition to regulation of social behaviour. *Molecular Microbiology*, *67* (2), 241-253.
119. LeRoux, M., Kirkpatrick, R., Montauti, E., Tran, B., Peterson, S., Harding, B., et al. (2015). Kin cell lysis is a danger signal that activates antibacterial pathways of *Pseudomonas aeruginosa*. *eLife*, *4*.
120. Mougous, J., Gifford, C., Ramsdell, T., & Mekalanos, J. (2007). Threonine phosphorylation post-translationally regulates protein secretion in *Pseudomonas aeruginosa*. *Nature Cell Biology*, *9* (7), 797-803.
121. Basler, M., Ho, B., & Mekalanos, J. (2013). Tit-for-Tat: Type VI Secretion System Counterattack during Bacterial Cell-Cell Interactions. *Cell*, *152* (4), 884-894.
122. Ho, B., Basler, M., & Mekalanos, J. (2013). Type 6 secretion system-mediated immunity to type 4 secretion system-mediated gene transfer. *Science (New York, N.Y.)*, *342* (6155), 250-3.
123. Suarez, G., Sierra, J., Sha, J., Wang, S., Erova, T., Fadl, A., et al. (2008). Molecular characterization of a functional type VI secretion system from a clinical isolate of *Aeromonas hydrophila*. *Microbial Pathogenesis*, *44* (4), 344-361.
124. Schwarz, S., West, T., Boyer, F., Chiang, W.-C., Carl, M., Hood, R., et al. (2010). Burkholderia Type VI Secretion Systems Have Distinct Roles in Eukaryotic and Bacterial Cell Interactions. (P. Christie, Ed.) *PLoS Pathogens*, *6* (8), e1001068.
125. Murdoch, S., Trunk, K., English, G., Fritsch, M., Pourkarimi, E., & Coulthurst, S. (2011). The opportunistic pathogen *Serratia marcescens* utilizes type VI secretion to target bacterial competitors. *Journal of bacteriology*, *193* (21), 6057-69.
126. Miyata, S., Bachmann, V., & Pukatzki, S. (2013). Type VI secretion system regulation as a consequence of evolutionary pressure. *Journal of Medical Microbiology*, *62* (Pt\_5), 663-676.
127. Weinstein, R., Gaynes, R., & Edwards, J. (2005). Overview of Nosocomial Infections Caused by Gram-Negative Bacilli. *Clinical Infectious Diseases*, *41* (6), 848-854.
128. Davin-Regli, A., & Pages, J.-M. (2015). Enterobacter aerogenes and Enterobacter cloacae; versatile bacterial pathogens confronting antibiotic treatment. *Frontiers in Microbiology*, *6*, 392.
129. Livermore, D., Warner, M., Mushtaq, S., Doumith, M., Zhang, J., & Woodford, N. (2011). What remains against carbapenem-resistant Enterobacteriaceae? Evaluation of

chloramphenicol, ciprofloxacin, colistin, fosfomycin, minocycline, nitrofurantoin, temocillin and tigecycline. *International Journal of Antimicrobial Agents*, 37 (5), 415-419.

130. Mezzatesta, M., Gona, F., & Stefani, S. (2012). Enterobacter cloacae complex: clinical impact and emerging antibiotic resistance. *Future Microbiology*, 7 (7), 887-902.

131. Hoffmann, H., Stindl, S., Ludwig, W., Stumpf, A., Mehlen, A., Heesemann, J., et al. (2005). Reassignment of Enterobacter dissolvens to Enterobacter cloacae as E. cloacae subspecies dissolvens comb. nov. and emended description of Enterobacter asburiae and Enterobacter kobei. *Systematic and Applied Microbiology*, 28 (3), 196-205.

132. Ruhe, Z., Wallace, A., Low, D., & Hayes, C. (2013). Receptor polymorphism restricts contact-dependent growth inhibition to members of the same species. *mBio*, 4 (4), e00480-13.

133. Beck, C., Morse, R., Cunningham, D., Iniguez, A., Low, D., Goulding, C., et al. (2014). CdiA from Enterobacter cloacae Delivers a Toxic Ribosomal RNase into Target Bacteria. *Structure*, 22 (5), 707-718.

134. Krogh, A., Larsson, B., von Heijne, G., & Sonnhammer, E. (2001). Predicting transmembrane protein topology with a hidden markov model: application to complete genomes. *Journal of Molecular Biology*, 305 (3), 567-580.

135. Hofmann, K. & Stoffel, W. (1993). TMbase - A database of membrane spanning proteins segments. *Biol. Chem. Hoppe-Seyler*, 374,166.

136. Almagro Armenteros, J., Tsirigos, K., Sønderby, C., Petersen, T., Winther, O., Brunak, S., et al. (2019). SignalP 5.0 improves signal peptide predictions using deep neural networks. *Nature Biotechnology*, 37 (4), 420-423.

137. Frank, K., & Sippl, M. (2008). High-performance signal peptide prediction based on sequence alignment techniques. *Bioinformatics*, 24 (19), 2172-2176.

138. Zhang, H., Zhang, H., Gao, Z.-Q., Wang, W.-J., Liu, G.-F., Xu, J.-H., et al. (2013). Structure of the type VI effector-immunity complex (Tae4-Tai4) provides novel insights into the inhibition mechanism of the effector by its immunity protein. *The Journal of biological chemistry*, 288 (8), 5928-39.

139. Fritsch, M., Trunk, K., Diniz, J., Guo, M., Trost, M., & Coulthurst, S. (2013). Proteomic identification of novel secreted antibacterial toxins of the Serratia marcescens type VI secretion system. *Molecular & cellular proteomics : MCP*, 12 (10), 2735-49.

140. LaCourse, K., Peterson, S., Kulasekara, H., Radey, M., Kim, J., & Mougous, J. (2018). Conditional toxicity and synergy drive diversity among antibacterial effectors. *Nature Microbiology*, 3 (4), 440-446.
141. Trunk, K., Peltier, J., Liu, Y.-C., Dill, B., Walker, L., Gow, N., et al. (2018). The type VI secretion system deploys antifungal effectors against microbial competitors. *Nature microbiology*, 3 (8), 920-931.
142. Aiyar, A., Xiang, Y., & Leis, J. (1996). Site-Directed Mutagenesis Using Overlap Extension PCR. In A. Aiyar, Y. Xiang, & J. Leis, *In Vitro Mutagenesis Protocols* (pp. 177-192). New Jersey: Humana Press.
143. Hayes, C., Bose, B., & Sauer, R. (2002). Proline residues at the C terminus of nascent chains induce SsrA tagging during translation termination. *The Journal of biological chemistry*, 277 (37), 33825-32.
144. Chaverroche, M.-K., Ghigo, J.-M., & d'Enfert, C. (2000). A rapid method for efficient gene replacement in the filamentous fungus *Aspergillus nidulans*. *Nucleic Acids Research*, 28 (22), 97e-97.
145. Cherepanov, P., & Wackernagel, W. (1995). Gene disruption in *Escherichia coli*: TcR and KmR cassettes with the option of Flp-catalyzed excision of the antibiotic-resistance determinant. *Gene*, 158 (1), 9-14.
146. Edwards, R., Keller, L., & Schifferli, D. (1998). Improved allelic exchange vectors and their use to analyze 987P fimbria gene expression. *Gene*, 207 (2), 149-157.
147. Ferrières, L., Hémerly, G., Nham, T., Guérout, A.-M., Mazel, D., Beloin, C., et al. (2010). Silent mischief: bacteriophage Mu insertions contaminate products of *Escherichia coli* random mutagenesis performed using suicidal transposon delivery plasmids mobilized by broad-host-range RP4 conjugative machinery. *Journal of bacteriology*, 192 (24), 6418-27.
148. Chung, C., Niemela, S., & Miller, R. (1989). One-step preparation of competent *Escherichia coli*: transformation and storage of bacterial cells in the same solution. *Proceedings of the National Academy of Sciences of the United States of America*, 86 (7), 2172-5.
149. Madeira, F., Park, Y., Lee, J., Buso, N., Gur, T., Madhusoodanan, N., et al. (2019). The EMBL-EBI search and sequence analysis tools APIs in 2019. *Nucleic acids research*, 47 (W1), W636-W641.
150. Beckwith, J., & Signer, E. (1966). Transposition of the lac region of *Escherichia coli*: I. Inversion of the lac operon and transduction of lac by  $\Phi 80$ . *Journal of Molecular Biology*, 19 (2), 254-265.

151. Hasegawa, M., Yada, S., Liu, M., Kamada, N., Muñoz-Planillo, R., Do, N., et al. (2014). Interleukin-22 Regulates the Complement System to Promote Resistance against Pathobionts after Pathogen-Induced Intestinal Damage. *Immunity*, *41* (4), 620-632.
152. Lutz, R., & Bujard, H. (1997). Independent and tight regulation of transcriptional units in *Escherichia coli* via the LacR/O, the TetR/O and AraC/I1-I2 regulatory elements. *Nucleic Acids Research*, *25* (6), 1203-1210.
153. Hayes, C., & Sauer, R. (2003). Cleavage of the A Site mRNA Codon during Ribosome Pausing Provides a Mechanism for Translational Quality Control. *Molecular Cell*, *12* (4), 903-911.
154. Aoki, S., Diner, E., de Roodenbeke, C., Burgess, B., Poole, S., Braaten, B., et al. (2010). A widespread family of polymorphic contact-dependent toxin delivery systems in bacteria. *Nature*, *468* (7322), 439-442.
155. Koskiniemi, S., Garza-Sánchez, F., Edman, N., Chaudhuri, S., Poole, S., Manoil, C., et al. (2015). Genetic analysis of the CDI pathway from *Burkholderia pseudomallei* 1026b. *PLoS ONE*, *10* (3).
156. Garza-Sánchez, F., Janssen, B., & Hayes, C. (2006). Prolyl-tRNA<sup>Pro</sup> in the A-site of SecM-arrested ribosomes inhibits the recruitment of transfer-messenger RNA. *Journal of Biological Chemistry*, *281* (45), 34258-34268.
157. Guzman, L., Belin, D., Carson, M., & Beckwith, J. (1995). Tight regulation, modulation, and high-level expression by vectors containing the arabinose PBAD promoter. *Journal of bacteriology*, *177* (14), 4121-30.
158. Gasteiger, E., Hoogland, C., Gattiker, A., Duvaud, S., Wilkins, M., Appel, R., & Bairoch, A. (2005). Protein Identification and Analysis Tools on the ExPASy Server. *The Proteomics Protocols Handbook*, 571-607.
159. Willett, J., Gucinski, G., Fatherree, J., Low, D., & Hayes, C. (2015). Contact-dependent growth inhibition toxins exploit multiple independent cell-entry pathways. *Proceedings of the National Academy of Sciences of the United States of America*, *112* (36), 11341-6.
160. Pradhan, B., Ranjan, M., & Chatterjee, S. (2012). XadM, a Novel Adhesin of *Xanthomonas oryzae* pv. *oryzae*, Exhibits Similarity to Rhs Family Proteins and Is Required for Optimum Attachment, Biofilm Formation, and Virulence. *Molecular Plant-Microbe Interactions*, *25* (9), 1157-1170.
161. Capage, M., & Hill, C. (1979). Preferential unequal recombination in the glyS region of the *Escherichia coli* chromosome. *Journal of Molecular Biology*, *127* (1), 73-87.

162. Lin, R.-J., Capage, M., & Hill, C. (1984). A repetitive DNA sequence, rhs, responsible for duplications within the Escherichia coli K-12 chromosome. *Journal of Molecular Biology*, 177 (1), 1-18.
163. Hill, C., Sandt, C., & Vlazny, D. (1994). Rhs elements of Escherichia coli: a family of genetic composites each encoding a large mosaic protein. *Molecular Microbiology*, 12 (6), 865-871.
164. Zhao, S., & Hill, C. (1995). Reshuffling of Rhs components to create a new element. *Journal of bacteriology*, 177 (5), 1393-8.
165. Vlazny, D., & Hill, C. (1995). A stationary-phase-dependent viability block governed by two different polypeptides from the RhsA genetic element of Escherichia coli K-12. *Journal of bacteriology*, 177 (8), 2209-13.
166. Buth, S., Menin, L., Shneider, M., Engel, J., Boudko, S., Leiman, P., et al. (2015). Structure and Biophysical Properties of a Triple-Stranded Beta-Helix Comprising the Central Spike of Bacteriophage T4. *Viruses*, 7 (8), 4676-4706.
167. Renault, M., Zamarreno Beas, J., Douzi, B., Chabaliier, M., Zoued, A., Brunet, Y., et al. (2018). The gp27-like Hub of VgrG Serves as Adaptor to Promote Hcp Tube Assembly. *Journal of Molecular Biology*, 430 (18), 3143-3156.
168. Kanamaru, S., Gassner, N., Ye, N., Takeda, S., & Arisaka, F. (1999). The C-terminal fragment of the precursor tail lysozyme of bacteriophage T4 stays as a structural component of the baseplate after cleavage. *Journal of bacteriology*, 181 (9), 2739-44.
169. Kanamaru, S., Leiman, P., Kostyuchenko, V., Chipman, P., Mesyanzhinov, V., Arisaka, F., et al. (2002). Structure of the cell-puncturing device of bacteriophage T4. *Nature*, 415 (6871), 553-557.
170. Goldenberg, D., & King, J. (1982). Trimeric intermediate in the in vivo folding and subunit assembly of the tail spike endorhamnosidase of bacteriophage P22. *Proceedings of the National Academy of Sciences of the United States of America*, 79 (11), 3403-7.
171. Fuchs, A., Seiderer, C., & Seckler, R. (1991). In vitro folding pathway of phage P22 tailspike protein. *Biochemistry*, 30 (26), 6598-6604.
172. Danner, M., & Seckler, R. (1993). Mechanism of phage P22 tailspike protein folding mutations. *Protein science: a publication of the Protein Society*, 2 (11), 1869-81.
173. Steinbacher, S., Seckler, R., Miller, S., Steipe, B., Huber, R., & Reinemer, P. (1994). Crystal structure of P22 tailspike protein: interdigitated subunits in a thermostable trimer. *Science (New York, N.Y.)*, 265 (5170), 383-6.

174. Browning, C., Shneider, M., Bowman, V., Schwarzer, D., & Leiman, P. (2012). Phage pierces the host cell membrane with the iron-loaded spike. *Structure (London, England: 1993)*, 20 (2), 326-39.
175. Uchida, K., Leiman, P., Arisaka, F., & Kanamaru, S. (2014). Structure and properties of the C-terminal  $\beta$ -helical domain of VgrG protein from *Escherichia coli* O157. *The Journal of Biochemistry*, 155 (3), 173-182.
176. Quentin, D., Ahmad, S., Shanthamoorthy, P., Mougous, J., Whitney, J., & Raunser, S. (2018). Mechanism of loading and translocation of type VI secretion system effector Tse6. *Nature Microbiology*, 3 (10), 1142-1152.
177. Shirai, A., Matsuyama, A., Yashiroda, Y., Hashimoto, A., Kawamura, Y., Arai, R., et al. (2008). Global analysis of gel mobility of proteins and its use in target identification. *The Journal of biological chemistry*, 283 (16), 10745-52.
178. Jones, A., Garza-Sánchez, F., So, J., Hayes, C., & Low, D. (2017). Activation of contact-dependent antibacterial tRNase toxins by translation elongation factors. *Proceedings of the National Academy of Sciences of the United States of America*, 114 (10), E1951-E1957.
179. Aoki, S., Webb, J., Braaten, B., & Low, D. (2009). Contact-dependent growth inhibition causes reversible metabolic downregulation in *Escherichia coli*. *Journal of bacteriology*, 191 (6), 1777-86.
180. Ruhe, Z., Nguyen, J., Beck, C., Low, D., & Hayes, C. (2014). The proton-motive force is required for translocation of CDI toxins across the inner membrane of target bacteria. *Molecular Microbiology*, 94 (2), 466-481.
181. Rakhuba, D., Kolomiets, E., Dey, E., & Novik, G. (2010). Bacteriophage receptors, mechanisms of phage adsorption and penetration into host cell. *Polish journal of microbiology*, 59 (3), 145-55.
182. Kelley, L., Mezulis, S., Yates, C., Wass, M., & Sternberg, M. (2015). The Phyre2 web portal for protein modeling, prediction and analysis. *Nature Protocols*, 10 (6), 845-858.
183. Bar-On, Y., Phillips, R., & Milo, R. (2018). The biomass distribution on Earth. *Proceedings of the National Academy of Sciences of the United States of America*, 115 (25), 6506-6511.
184. Kallmeyer, J., Pockalny, R., Adhikari, R., Smith, D., & D'Hondt, S. (2012). Global distribution of microbial abundance and biomass in subseafloor sediment. *Proceedings of the National Academy of Sciences*, 109 (40), 16213-16216.

185. Jia, Z., & Conrad, R. (2009). Bacteria rather than Archaea dominate microbial ammonia oxidation in an agricultural soil. *Environmental Microbiology*, *11* (7), 1658-1671.
186. Pissaridou, P., Allsopp, L., Wettstadt, S., Howard, S., Mavridou, D., & Filloux, A. (2018). The *Pseudomonas aeruginosa* T6SS-VgrG1b spike is topped by a PAAR protein eliciting DNA damage to bacterial competitors. *Proceedings of the National Academy of Sciences of the United States of America*, *115* (49), 12519-12524.
187. Rath, A., Glibowicka, M., Nadeau, V., Chen, G., & Deber, C. (2009). Detergent binding explains anomalous SDS-PAGE migration of membrane proteins. *Proceedings of the National Academy of Sciences of the United States of America*, *106* (6), 1760-5.
188. Burkinshaw, B., Liang, X., Wong, M., Le, A., Lam, L., & Dong, T. (2018). A type VI secretion system effector delivery mechanism dependent on PAAR and a chaperone–co-chaperone complex. *Nature Microbiology*, *3* (5), 632-640.
189. Jiang, F., Wang, X., Wang, B., Chen, L., Zhao, Z., Waterfield, N., et al. (2016). The *Pseudomonas aeruginosa* Type VI Secretion PGAP1-like Effector Induces Host Autophagy by Activating Endoplasmic Reticulum Stress. *Cell Reports*, *16* (6), 1502-1509.
190. Wilderman, P., Vasil, A., Johnson, Z., & Vasil, M. (2001). Genetic and biochemical analyses of a eukaryotic-like phospholipase D of *Pseudomonas aeruginosa* suggest horizontal acquisition and a role for persistence in a chronic pulmonary infection model. *Molecular Microbiology*, *39* (2), 291-304.
191. Barret, M., Egan, F., Fargier, E., Morrissey, J., & O'Gara, F. (2011). Genomic analysis of the type VI secretion systems in *Pseudomonas* spp.: novel clusters and putative effectors uncovered. *Microbiology*, *157* (6), 1726-1739.
192. Berni, B., Soscia, C., Djermoun, S., Ize, B., & Bleves, S. (2019). A Type VI Secretion System Trans-Kingdom Effector Is Required for the Delivery of a Novel Antibacterial Toxin in *Pseudomonas aeruginosa*. *Frontiers in Microbiology*, *10*, 1218.
193. Garza-Sánchez, F., Schaub, R., Janssen, B., & Hayes, C. (2011). tmRNA regulates synthesis of the ArfA ribosome rescue factor. *Molecular Microbiology*, *80* (5), 1204-1219.
194. Choi, K.-H., Gaynor, J., White, K., Lopez, C., Bosio, C., Karkhoff-Schweizer, R., et al. (2005). A Tn7-based broad-range bacterial cloning and expression system. *Nature Methods*, *2* (6), 443-448.
195. Szwedziak, P., & Pilhofer, M. (2019). Bidirectional contraction of a type six secretion system. *Nature Communications*, *10* (1), 1565.

196. Likhacheva, N., Samsonov, V., Samsonov, V., & Sineoky, S. (1996). Genetic control of the resistance to phage C1 of *Escherichia coli* K-12. *Journal of bacteriology*, *178* (17), 5309-15.
197. Samsonov, V., Samsonov, V., & Sineoky, S. (2002). DcrA and dcrB *Escherichia coli* genes can control DNA injection by phages specific for BtuB and FhuA receptors. *Research in Microbiology*, *153* (10), 639-646.
198. El-Gebali, S., Mistry, J., Bateman, A., Eddy, S., Luciani, A., Potter, S., et al. (2019). The Pfam protein families database in 2019. *Nucleic Acids Research*, *47* (D1), D427-D432.
199. Meusch, D., Gatsogiannis, C., Efremov, R., Lang, A., Hofnagel, O., Vetter, I., et al. (2014). Mechanism of Tc toxin action revealed in molecular detail. *Nature*, *508* (7494), 61-65.
200. Minet, A., & Chiquet-Ehrismann, R. (2000). Phylogenetic analysis of teneurin genes and comparison to the rearrangement hot spot elements of *E. coli*. *Gene*, *257* (1), 87-97.
201. Hong, W., Mosca, T., & Luo, L. (2012). Teneurins instruct synaptic partner matching in an olfactory map. *Nature*, *484* (7393), 201-207.
202. Mosca, T., Hong, W., Dani, V., Favaloro, V., & Luo, L. (2012). Trans-synaptic Teneurin signalling in neuromuscular synapse organization and target choice. *Nature*, *484* (7393), 237-241.
203. Jackson, V., Meijer, D., Carrasquero, M., van Bezouwen, L., Lowe, E., Kleanthous, C., et al. (2018). Structures of Teneurin adhesion receptors reveal an ancient fold for cell-cell interaction. *Nature Communications*, *9* (1), 1079.
204. Lovejoy, D., Chawaf, A., & Cadinouche, M. (2006). Teneurin C-terminal associated peptides: An enigmatic family of neuropeptides with structural similarity to the corticotropin-releasing factor and calcitonin families of peptides. *General and Comparative Endocrinology*, *148* (3), 299-305.
205. Gatsogiannis, C., Lang, A., Meusch, D., Pfaumann, V., Hofnagel, O., Benz, R., et al. (2013). A syringe-like injection mechanism in *Photobacterium luminescens* toxins. *Nature*, *495* (7442), 520-523.
206. Coyne, M., Roelofs, K., & Comstock, L. (2016). Type VI secretion systems of human gut Bacteroidales segregate into three genetic architectures, two of which are contained on mobile genetic elements. *BMC Genomics*, *17* (1), 58.

207. Wexler, A., Bao, Y., Whitney, J., Bobay, L.-M., Xavier, J., Schofield, W., et al. (2016, 3 8). Human symbionts inject and neutralize antibacterial toxins to persist in the gut. *Proceedings of the National Academy of Sciences*, 201525637.
208. Hecht, A., Casterline, B., Earley, Z., Goo, Y., Goodlett, D., & Bubeck-Wardenburg, J. (2016). Strain competition restricts colonization of an enteric pathogen and prevents colitis. *EMBO reports*, 17 (9), 1281-1291.
209. Sana, T., Flaughnatti, N., Lugo, K., Lam, L., Jacobson, A., Baylot, V., et al. (2016). Salmonella Typhimurium utilizes a T6SS-mediated antibacterial weapon to establish in the host gut. *Proceedings of the National Academy of Sciences of the United States of America*, 113 (34), E5044-51.
210. Singh, A., Nisaa, K., Bhattacharyya, S., & Mallick, A. (2019). Immunogenicity and protective efficacy of mucosal delivery of recombinant hcp of Campylobacter jejuni Type VI secretion system (T6SS) in chickens. *Molecular Immunology*, 111, 182-197.
211. Ma, J., Sun, M., Dong, W., Pan, Z., Lu, C., & Yao, H. (2017). PAAR-Rhs proteins harbor various C-terminal toxins to diversify the antibacterial pathways of type VI secretion systems. *Environmental Microbiology*, 19 (1), 345-360.